[redacted]

Grumman FINAL REPORT

FEASIBILITY STUDY OF UTILIZATION OF LM FOR PROJECT ABLE [redacted]

(NASA-CR-117554) FEASIBILITY STUDY OF UTILIZATION OF LM FOR PROJECT ABLE. VOLUME 2 - TECHNICAL REPORT (Grumman Aircraft Engineering Corp.) 337 p

N76-76172

[redacted]

11417

00/12

[redacted]

[redacted] Volume II

Enc 2'

[redacted]

[redacted]

C66-10110

Copy No._____

CLASSIFICATION CHANGE

To UNCLASSIFIED
By authority of GDS-EO 11652 Cat-4
Changed by C. L. Merrill Date 12/31/72
Classified Document Master Control Station, NASA
Scientific and Technical Information Facility

Grumman FINAL REPORT

FEASIBILITY STUDY OF UTILIZATION OF LM FOR PROJECT ABLE [redacted]

submitted to

NATIONAL AERONAUTICS AND SPACE ADMINISTRATION
MANNED SPACECRAFT CENTER
HOUSTON, TEXAS 77058

and

GEORGE C. MARSHALL SPACE FLIGHT CENTER
HUNTSVILLE, ALABAMA 35812

by

GRUMMAN AIRCRAFT ENGINEERING CORPORATION
BETHPAGE, NEW YORK 11714

This document contains information [redacted] national [redacted] of the U[redacted] within the meaning of the [redacted] Title 18, U.S.C., Sections 793 [redacted]. The [redacted] or the revelati[redacted] its contents in any man[redacted] an una[redacted]ized person is prohibited by law.

[redacted]

December 12, 1966
Contract NAS 9-6209

Volume II
Technical Report

[redacted]

[redacted]

PREFACE

This document completes the reporting requirements of NASA/MSC Contract NAS 9-6209, "An Effort Pertaining to Project ABLE". The study was performed under the technical direction of NASA/MSFC. The objective of the 110 day effort was to establish overall systems approaches, including technical and programatic feasibility of solar reflectors* operating in Earth orbit, supported by the LM vehicle. The work effort consisted of a 90 day technical study and program planning period and a 20 day final report preparation period. Progress reviews were held, at the request of the COR, on September 7, October 6, October 11, November 6, and November 13, 1966. In order to accommodate this increased number of reviews, a two week extension in delivery of this final report was granted by the COR.

The final report consists of three volumes, bound into four documents. The first document, "Volume I - Technical Summary", briefly outlines the objectives of the study, summarizes the results, and gives conclusions and recommendations for further study. Areas of advanced technology, wherein further effort is recommended based on the study results, are also described. The second document, "Volume II - Technical Report" is a comprehensive condensation of the work performed during the study period. The third document, "Volume III, Part 1 - Program Plan", consists of five sub-plans, covering Development and Acceptance Test, Pre-Launch Operations, Product Support, Manufacturing, and Reliability. The fourth document, "Volume III, Part 2", contains the sixth sub-plan, Cost

*The term "reflector" is properly applied to the thin membrane of metallized plastic which actually reflects the sunlight. In this report, however, the term reflector should be interpreted as either the membrane itself or including the support structure.

[redacted]

TABLE OF CONTENTS

1.0 INTRODUCTION

2.0 SUMMARY

- 2.1 Mission
- 2.2 Configuration
- 2.3 Recommendations For Future Studies

3.0 MISSION ANALYSIS

- 3.1 Illumination
- 3.2 Orbital Mechanics
- 3.3 Manned vs Unmanned
- 3.4 Radiation
- 3.5 Flight Operations
- 3.6 Weight

4.0 REFLECTOR/SUPPORT STRUCTURE

- 4.1 Structural Design
- 4.2 Structural Analysis
- 4.3 Thermal Analysis
- 4.4 Materials

5.0 ABLE LM SYSTEMS ENGINEERING

- 5.1 Thermal Analysis
- 5.2 Guidance and Control Analysis
- 5.3 Reaction Control Analysis
- 5.4 Reliability Analysis
- 5.5 Mass Properties

[redacted]

[redacted]

TABLE OF CONTENTS

6.0 ABLE LM SUBSYSTEMS ENGINEERING

6.1 Electrical Power

6.2 Environmental Control

6.3 Guidance, Navigation and Control

6.4 Reaction Control

6.5 Communications

6.6 Instrumentation

6.7 Controls and Displays

7.0 ABLE LM DESIGN AND INTEGRATION

7.1 Structural Design

7.2 Mechanical Design

7.3 Crew Provisions

APPENDIX

A. OPTICS ANALYSIS

B. STRUCTURAL ANALYSIS

B.1 Influence Coefficients

B.2 Launch and Boost Environment

B.3 Calculation of Natural Frequency

C. THERMAL ANALYSIS

C.1 Reflector Thermal Analysis

C.2 Support Structure Thermal Analysis

C.3 External Thermal Environment

C.4 ECS Performance

C.5 Reflector Inflation System

[redacted]

1.0 INTRODUCTION

The use of a large reflector in Earth orbit to illuminate selected geographical areas during the hours of darkness has been proposed. The objectives of the present study were to determine the technical feasibility of this concept, and to furnish system trade-off and design data integrating the LM spacecraft and/or its subsystems and components with the reflector. An additional objective of this study was to select a conceptual design and provide a program plan that would permit determination of the schedule and cost feasibility of the concept.

A list of the major groundrules which were supplied to Grumman by MSFC follows:

- Design emphasis shall be placed on the maximum effective utilization of existing, modified, or planned LM hardware.
- Overall technology constraints shall be based on attainment of hardware which would be operational in the 1968-69 time frame.
- The minimum illumination level which would be considered acceptable would be equivalent to a 400 ft. diameter ideal reflector at synchronous altitude.
- Illumination shall be required during all periods of darkness at the target.
- Reflector sizes ranging from 400 ft. to 3000 ft. shall be considered.
- Orbits with nominal altitudes of 6000 nm. and 24 hr. synchronous shall be of primary interest.
- The degree to which man can enhance the program by his in-space participation shall be determined.
- Single and dual Saturn V launches shall be considered.

1.0 INTRODUCTION (continued)

- The minimum operating lifetime shall be at least six months without resupply. However, an operating lifetime of 12 months is highly desirable with possible resupply.
- Useful payload weights and ambient environment data will be provided by NASA.

Using these groundrules and the assumptions listed in the various sections of the report, the technical feasibility of the Project ABLE concept was studied.

2.0 SUMMARY

2.1 MISSION

2.1.1 Altitude - Deflection Considerations

Target area illumination is extremely sensitive to deflection of the reflector surface. For example, if a 1000 ft diameter reflector could be designed which remained flat to ± 1 ft (very tight tolerance), illumination equivalent to a full moon could be achieved only by selecting an orbital altitude of 3-5000 n.mi. Higher altitudes would require tighter tolerances, large numbers of reflectors, or acceptance of less illumination.

One implication of the indication that lower altitudes are preferrable is the requirement for more than one reflector, if illumination is to be provided continuously to the target. At 3-5000 n.mi., approximately 4 reflectors are needed for continuous illumination.

2.1.2 One/Two Sides Reflective

Orbital mechanics studies indicate that changes in rotational rate can be minimized if both sides of the reflector surface have reflecting capability. The high temperatures which result, however, would eliminate Mylar from consideration. Kapton could be used, but it is a relatively new material for this application. It is suggested that additional studies be done to advance the state-of-the-art of Kapton technology. This would permit reflectorizing both sides of the membrane, and eliminate the constraints on trajectory and target choices which would result from a reflector with only one side coated.

2.1.3 Manned Vs Unmanned Mission

The evaluation of the need for man to aid in implementing the ABLE mission concept has resulted in the following preliminaries conclusions:

- Man should be considered for the first ABLE flight(s)
- Man's value on subsequent flights requires further study.

This is mainly due to the fact that some of the more intricate operational phases of the ABLE mission, such as reflector deployment, will be difficult to duplicate during the development ground test program.

2.1.3 cont'd

A program concept permitting a delayed decision on manned vs unmanned ABLE flights is therefore recommended. This would mean that the ABLE spacecraft should be designed so that it could be flown as part of either a manned or unmanned flight.

2.1.4 Radiation

The major problem in evaluating the potential radiation hazard for the ABLE mission is the uncertainity in the predicted 1968-69 environmental model. Unfortunately, it is unlikely that any new emperical data will be available early enough to provide statistical verification of any assumed model environment before major program decisions have to be made to meet a 1969 launch date. Despite the uncertainty in the radiation environment, the following preliminary conclusions have been reached:

- The use of mylar for the reflector is marginal at altitudes below synchronous
- There are no major problems while the crew is in the spacecraft
- At best, limited extra-vehicular activities may be possible.

2.1.5 Weight

The maximum ABLE payload which can be carried on a manned Saturn V launch is restricted by the maximum weight that can be supported in the SLA which is about 32,000 lbs. The estimated weight of an ABLE LM exclusive of the reflector and its support structure is 9700 lbs. This means that, for a spoke and torus reflector configuration, the maximum reflector size that can be carried with a manned ABLE LM is about 1200 ft. in diameter.

For an unmanned Saturn V launch, the maximum allowable payload is governed by the launch vehicle stack limit of 110,000 lbs. For this case, reflector diameters of 3,000 ft or greater could be carried in addition to an ABLE LM.

2.2 CONFIGURATION

2.2.1 Reflector/Support Structure

Three families of reflector/support structure were studied, with each family defined by the location of the support structure relative to the reflector surface, and by the method of deployment. After consideration of such factors as weight, ease of deployment, sensitivity to deflections, packaging efficiency, ease of resupply, and testing problems, it was felt that a two dimensional shape such as a torus with four spokes appeared most feasible.

Methods of deployment were grouped into mechanical and inflation techniques, and here the physical simplicity of inflation and its adaptability to various sizes of the support structure, made it a favored method.

There did not appear to be any greater problem in integrating the LM spacecraft with one configuration than another, because of the minimum number of interfaces between the LM and the reflector/support structure.

2.2.2 ABLE LM

The use of the basic LM vehicle and related subsystems/components, in conjunction with a large reflector, permits utilization of a developed system which offers the following advantages:

- Operational in the 1968-1969 time period
- Docking capability with the Apollo CSM
- Compatible with Saturn V launch environment
- Mounting in the spacecraft LM adapter (SLA)
- Available subsystems compatible with both manned and unmanned operation.

The ABLE version of LM is almost entirely composed of developed LM hardware. The only major new items are radiators, solar arrays and rechargeable batteries, and low-level thrusters. Major items removed from LM include the propulsion subsystems, the landing gear, and the abort guidance and radars. These changes are shown in Table 2.2-1. The functional inter-relationship between the ABLE LM subsystems is shown in Figure 2.2-1.

2.2.2 (continued)

An examination of the above changes indicates that almost all are due to the six month mission duration requirement. It is interesting that if an engineering test flight of 3 - 14 days were considered, in order to checkout deployment and flatness, an absolute minimum of new equipment would be required.

[redacted]

TABLE 2.2-1

PROGRAM PLANNING CONFIGURATION

Subsystem \ Change with respect to LM	Removed	Modified	Added
1. Structure	°Base Heat Shield °Structural support deletion as required by sub system mod.	°Thermal shielding	°Canister °Structural support addition as required by subsystem modifications, i.e., Rad. and Solar panel additons.
2. Guidance, Navigation & Control	°DECA, GDA, ASA, AEA, RGA, DEDA, AOT (GFE), LR, RR/T	°ATCA °Computer Program	°PCA (modified)* °LOTS*(GFE)
3. Crew Provisions		°Console, depending on subsystem modifications	
4. Environmental Control	°Water Sublimator °Cold Plates (RGA & ASA)	°Coolant Recirc. Assembly °Control Valves	°PCA & DCA Cold Plates °Radiator & Controls
5. Mech. Design	Landing Gear		°Solar Panel Deploy. & Align Mech. °Canister Deploy Mech. °S-Band Ant. Deploy Mech.
6. Instrumentation			°As needed for reflector and subsystem modifications
7. Electrical Power		°Power distribution section	°Solar arrays (2) (90 ft^2 ea.) °Rechargeable batteries (2) °ECAs (2) °Battery charger and voltage regulator °Solar array position control assembly

[redacted]

TABLE 2.2-1

- continued -

Subsystem \ Change with respcet to LM	Removed	Modified	Added
8. Propulsion	°Ascent propellant and tanks °Descent propellant and tanks °Ascent engine °Descent engine °Ascent helium and tank °Plumbing		
9. Reaction Control	SAME AS LM		
10. Communications	°Lunar surface TV °S-Band erectable antenna °S-Band steerable antenna	°Relocated S-Band Omnis. & EVA Antenna's	°Command Receiver °Auto. selection switch °DCA* (Modified)
11. Controls & Displays			°As needed for subsystem modifications
12. Reflector related subsystems			°Initial pressurization tanks* (2) °Peripheral thruster subsystem -thrusters (16) -helium tanks* (4) -propellant tanks* (4) °Control cables (4)

*LM developed hardware.

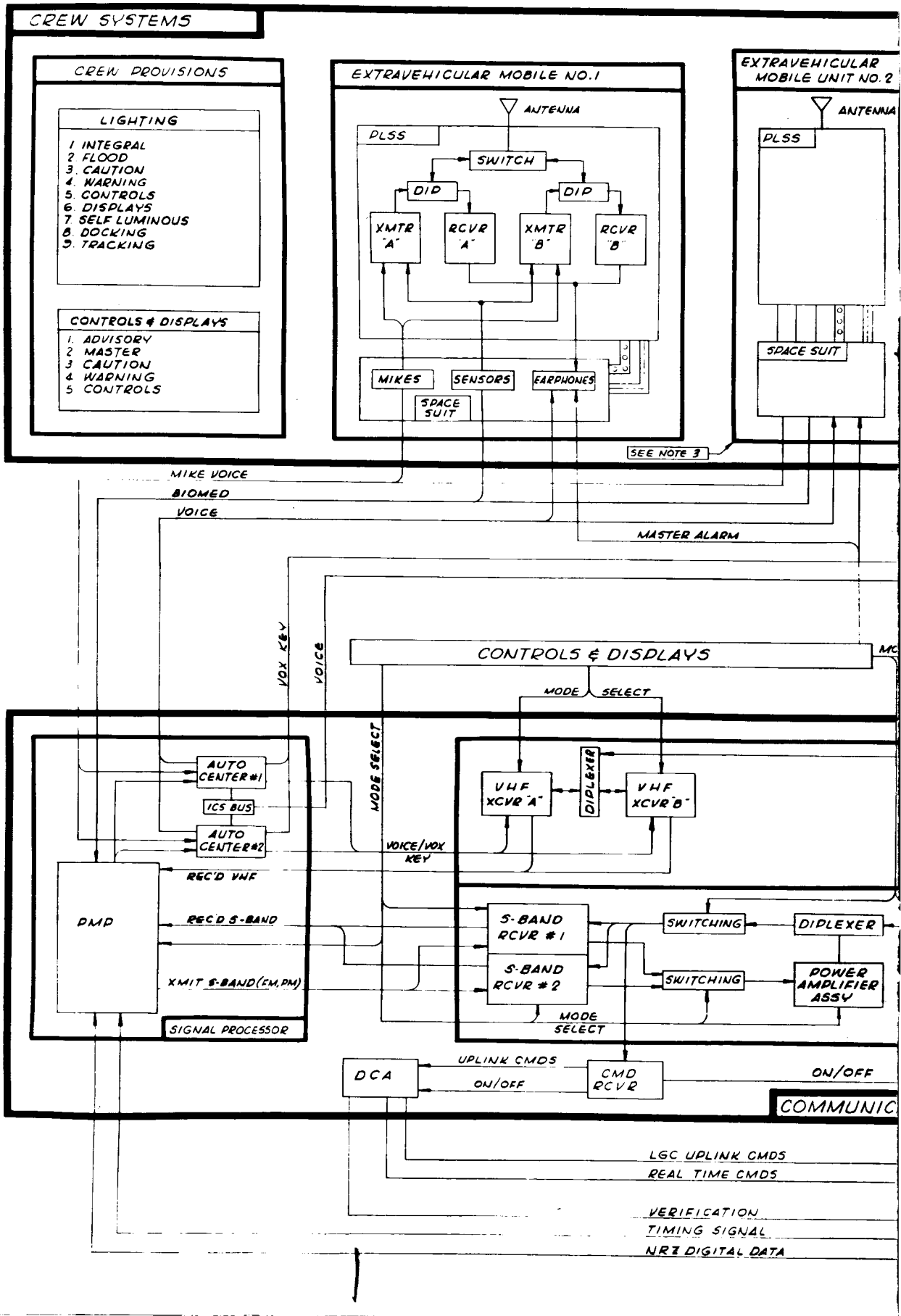
CREW SYSTEMS
CREW PROVISIONS
LIGHTING
1 INTEGRAL
2 FLOOD
3. CAUTION
4. WARNING
5. CONTROLS
6. DISPLAYS
7. SELF LUMINOUS
8. DOCKING
9. TRACKING
CONTROLS & DISPLAYS
1. ADVISORY
2 MASTER
3 CAUTION
4 WARNING
5 CONTROLS
EXTRAVEHICULAR MOBILE NO.1
ANTENNA
PLSS
SWITCH
DIP
DIP
XMTR "A"
RCVR "A"
XMTR "B"
RCVR "B"
MIKES
SENSORS
EARPHONES
SPACE SUIT
EXTRAVEHICULAR MOBILE UNIT NO. 2
ANTENNA
PLSS
SPACE SUIT
SEE NOTE 3
MIKE VOICE
BIOMED
VOICE
MASTER ALARM
VOX KEY
VOICE
CONTROLS & DISPLAYS
MODE
SELECT
MODE SELECT
AUTO CENTER #1
ICS BUS
AUTO CENTER #2
VOICE/VOX KEY
REC'D VHF
PMP
REC'D S-BAND
XMIT S-BAND (FM, PM)
SIGNAL PROCESSOR
VHF XCVR "A"
DIPLEXER
VHF XCVR "B"
S-BAND RCVR #1
S-BAND RCVR #2
SWITCHING
DIPLEXER
SWITCHING
POWER AMPLIFIER ASSY
MODE SELECT
DCA
UPLINK CMDS
ON/OFF
CMD RCVR
ON/OFF
COMMUNIC
LGC UPLINK CMDS
REAL TIME CMDS
VERIFICATION
TIMING SIGNAL
NRZ DIGITAL DATA

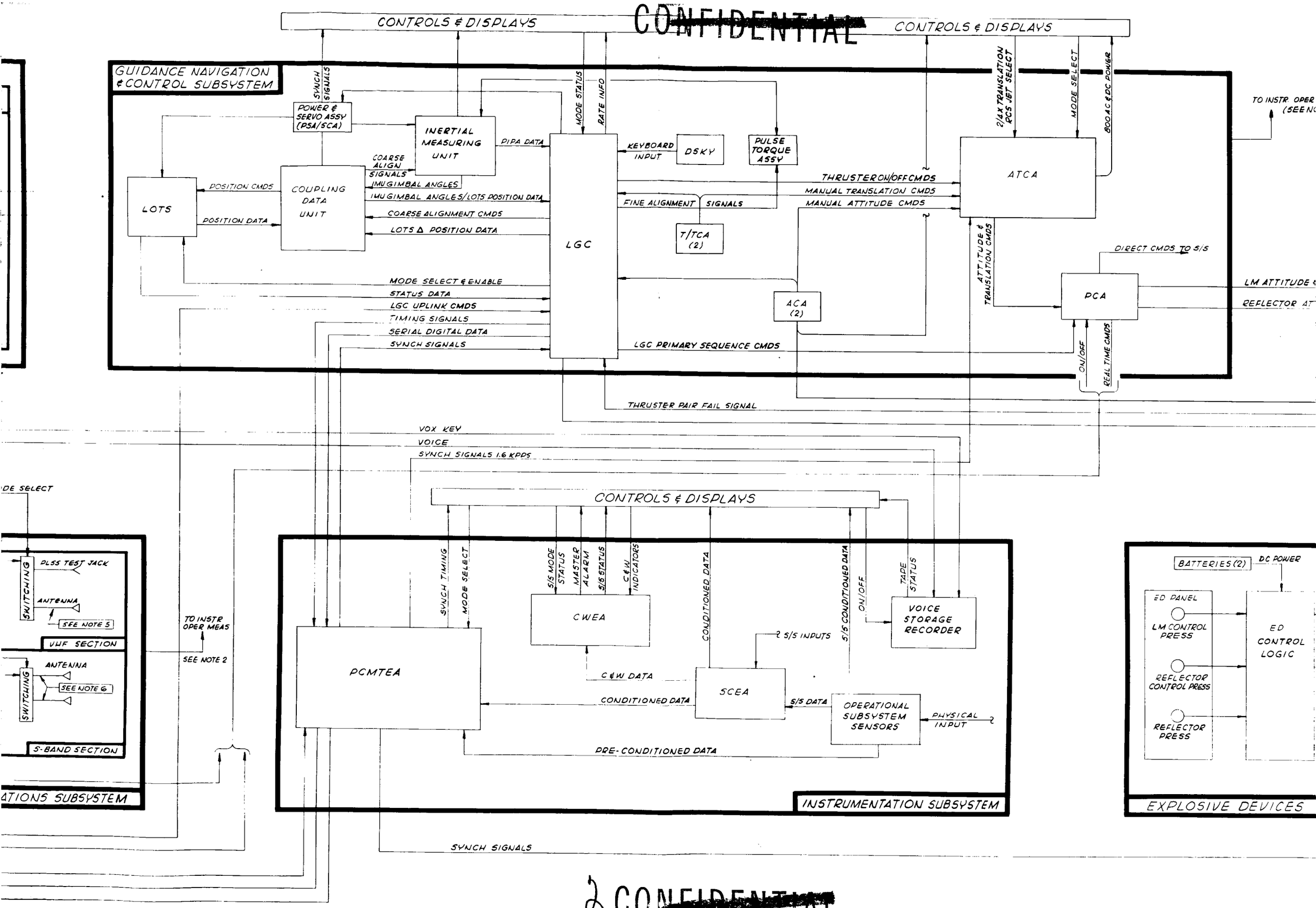
CONTROLS & DISPLAYS
CONTROLS & DISPLAYS
GUIDANCE NAVIGATION & CONTROL SUBSYSTEM
SYNCH SIGNALS
POWER & SERVO ASSY (PSA/SCA)
INERTIAL MEASURING UNIT
PIPA DATA
MODE STATUS
RATE INFO
KEYBOARD INPUT
DSKY
PULSE TORQUE ASSY
2/4X TRANSLATION RCS JET SELECT
MODE SELECT
800 AC & DC POWER
TO INSTR. OPER (SEE NO
LOTS
POSITION CMDS
POSITION DATA
COUPLING DATA UNIT
COARSE ALIGN SIGNALS
IMU GIMBAL ANGLES
IMU GIMBAL ANGLES/LOTS POSITION DATA
COARSE ALIGNMENT CMDS
LOTS Δ POSITION DATA
LGC
THRUSTER ON/OFF CMDS
MANUAL TRANSLATION CMDS
MANUAL ATTITUDE CMDS
FINE ALIGNMENT SIGNALS
T/TCA (2)
ATCA
ATTITUDE & TRANSLATION CMDS
DIRECT CMDS TO S/S
PCA
LM ATTITUDE &
REFLECTOR AT
ACA (2)
MODE SELECT & ENABLE
STATUS DATA
LGC UPLINK CMDS
TIMING SIGNALS
SERIAL DIGITAL DATA
SYNCH SIGNALS
LGC PRIMARY SEQUENCE CMDS
ON/OFF
REAL TIME CMDS
THRUSTER PAIR FAIL SIGNAL
VOX KEY
VOICE
SYNCH SIGNALS 1.6 KPDS
DE SELECT
CONTROLS & DISPLAYS
SWITCHING
PLSS TEST JACK
ANTENNA
SEE NOTE 5
VHF SECTION
ANTENNA
SWITCHING
SEE NOTE 6
S-BAND SECTION
TO INSTR OPER MEAS
SEE NOTE 2
ATIONS SUBSYSTEM
SYNCH TIMING
MODE SELECT
S/S MODE STATUS
MASTER ALARM
S/S STATUS
C&W INDICATORS
CONDITIONED DATA
S/S CONDITIONED DATA
ON/OFF
TAPE STATUS
VOICE STORAGE RECORDER
CWEA
S/S INPUTS
PCMTEA
C&W DATA
SCEA
CONDITIONED DATA
S/S DATA
OPERATIONAL SUBSYSTEM SENSORS
PHYSICAL INPUT
PRE-CONDITIONED DATA
INSTRUMENTATION SUBSYSTEM
BATTERIES (2)
DC POWER
ED PANEL
LM CONTROL PRESS
REFLECTOR CONTROL PRESS
REFLECTOR PRESS
ED CONTROL LOGIC
EXPLOSIVE DEVICES
SYNCH SIGNALS

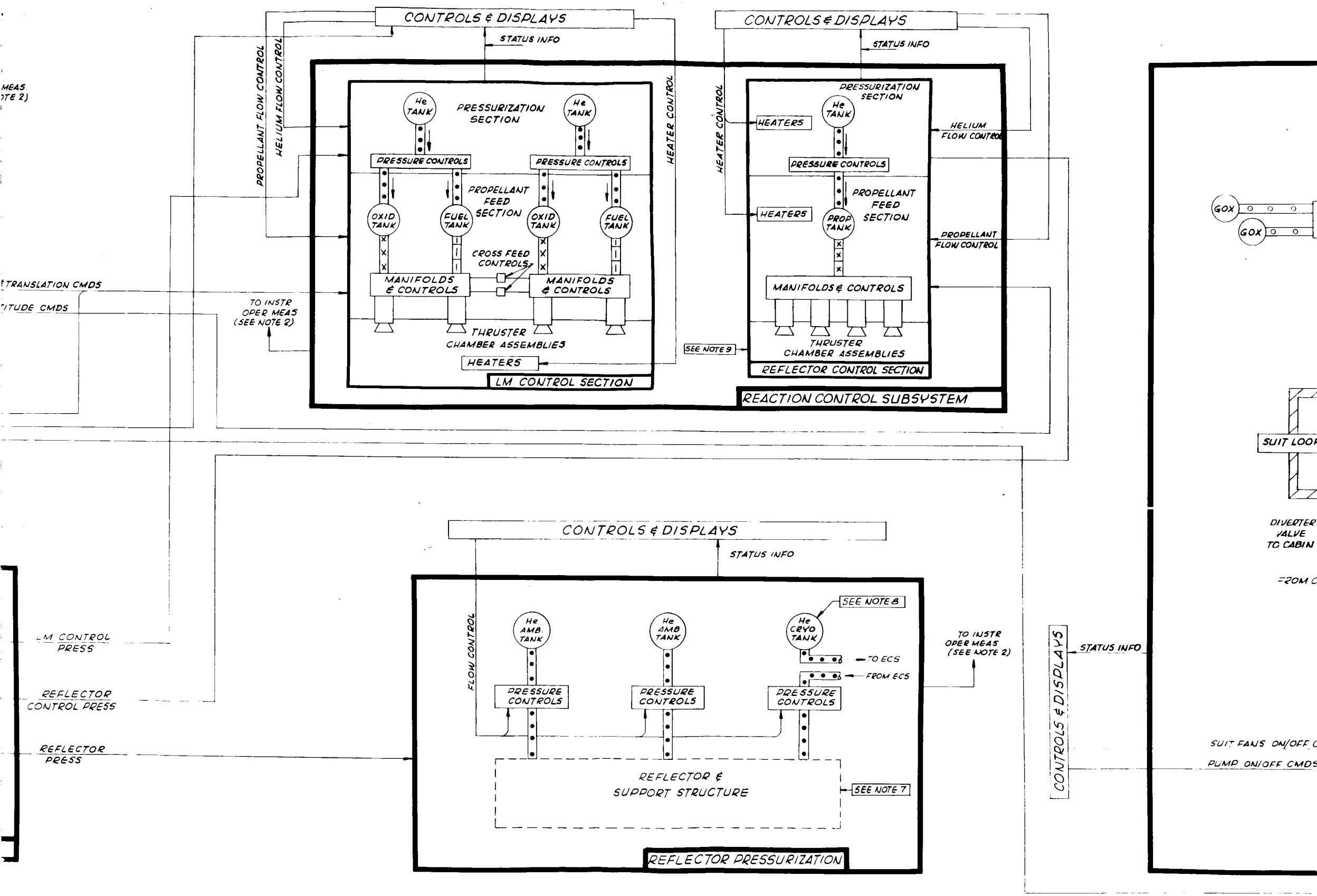
CONTROLS & DISPLAYS
STATUS INFO
PROPELLANT FLOW CONTROL
HELIUM FLOW CONTROL
HEATER CONTROL
He TANK
PRESSURIZATION SECTION
PRESSURE CONTROLS
PROPELLANT FEED SECTION
OXID TANK
FUEL TANK
CROSS FEED CONTROLS
MANIFOLDS & CONTROLS
THRUSTER CHAMBER ASSEMBLIES
HEATERS
LM CONTROL SECTION
TO INSTR OPER MEAS (SEE NOTE 2)
SEE NOTE 9
PROP TANK
REFLECTOR CONTROL SECTION
REACTION CONTROL SUBSYSTEM
MEAS. (SEE NOTE 2)
TRANSLATION CMDS
ITUDE CMDS
LM CONTROL PRESS
REFLECTOR CONTROL PRESS
REFLECTOR PRESS
He AMB. TANK
He CRYO TANK
SEE NOTE 8
TO ECS
FROM ECS
REFLECTOR & SUPPORT STRUCTURE
SEE NOTE 7
REFLECTOR PRESSURIZATION
GOX
SUIT LOOP
DIVERTER VALVE TO CABIN
FROM C
SUIT FANS ON/OFF C
PUMP ON/OFF CMDS

3

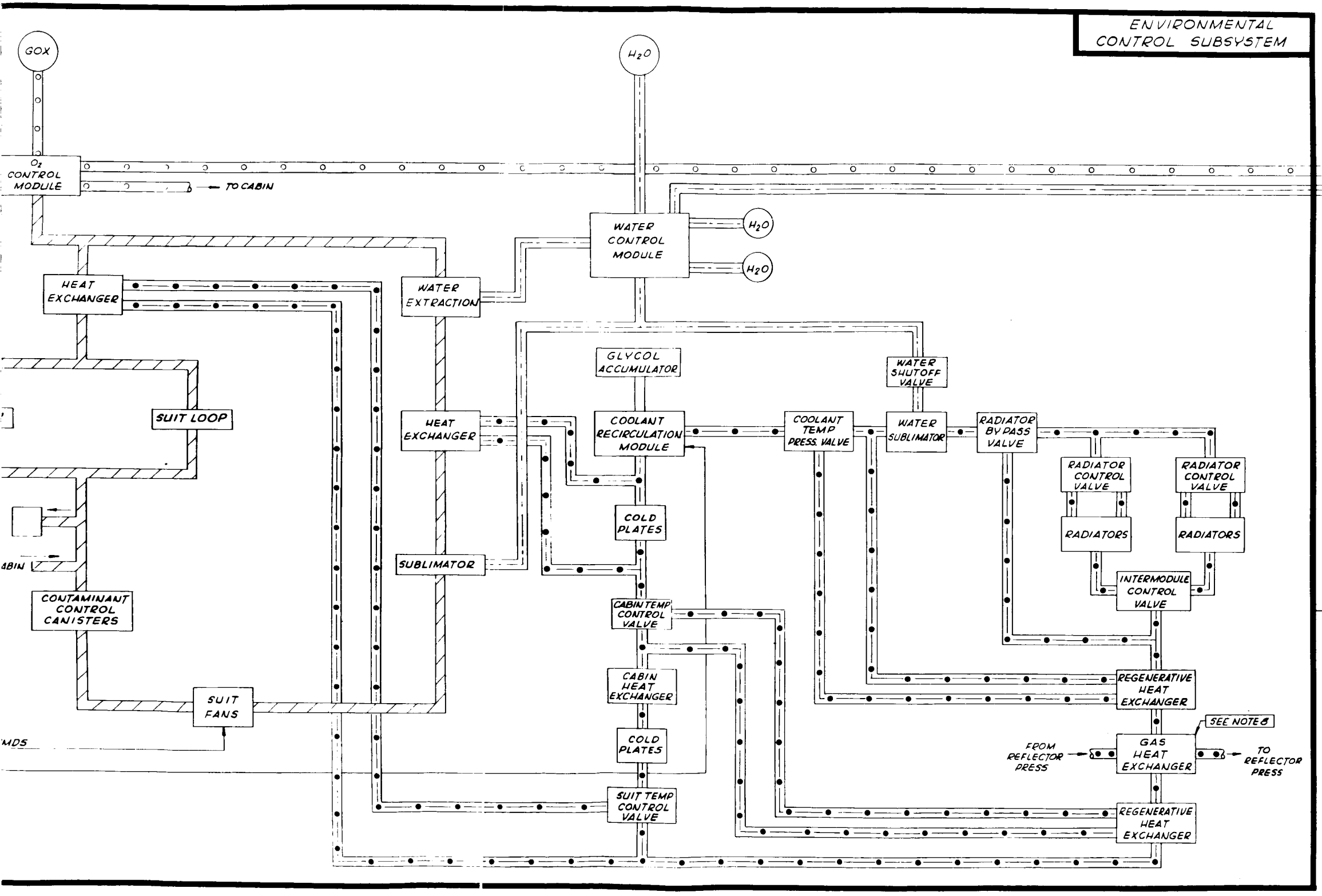
ENVIRONMENTAL CONTROL SUBSYSTEM
GOX
H_2O
O_2 CONTROL MODULE
TO CABIN
WATER CONTROL MODULE
H_2O
H_2O
HEAT EXCHANGER
WATER EXTRACTION
GLYCOL ACCUMULATOR
WATER SHUTOFF VALVE
SUIT LOOP
HEAT EXCHANGER
COOLANT RECIRCULATION MODULE
COOLANT TEMP PRESS. VALVE
WATER SUBLIMATOR
RADIATOR BY PASS VALVE
RADIATOR CONTROL VALVE
RADIATOR CONTROL VALVE
COLD PLATES
RADIATORS
RADIATORS
SUBLIMATOR
INTERMODULE CONTROL VALVE
CONTAMINANT CONTROL CANISTERS
CABIN TEMP CONTROL VALVE
CABIN HEAT EXCHANGER
REGENERATIVE HEAT EXCHANGER
SUIT FANS
SEE NOTE 8
COLD PLATES
FROM REFLECTOR PRESS
GAS HEAT EXCHANGER
TO REFLECTOR PRESS
SUIT TEMP CONTROL VALVE
REGENERATIVE HEAT EXCHANGER

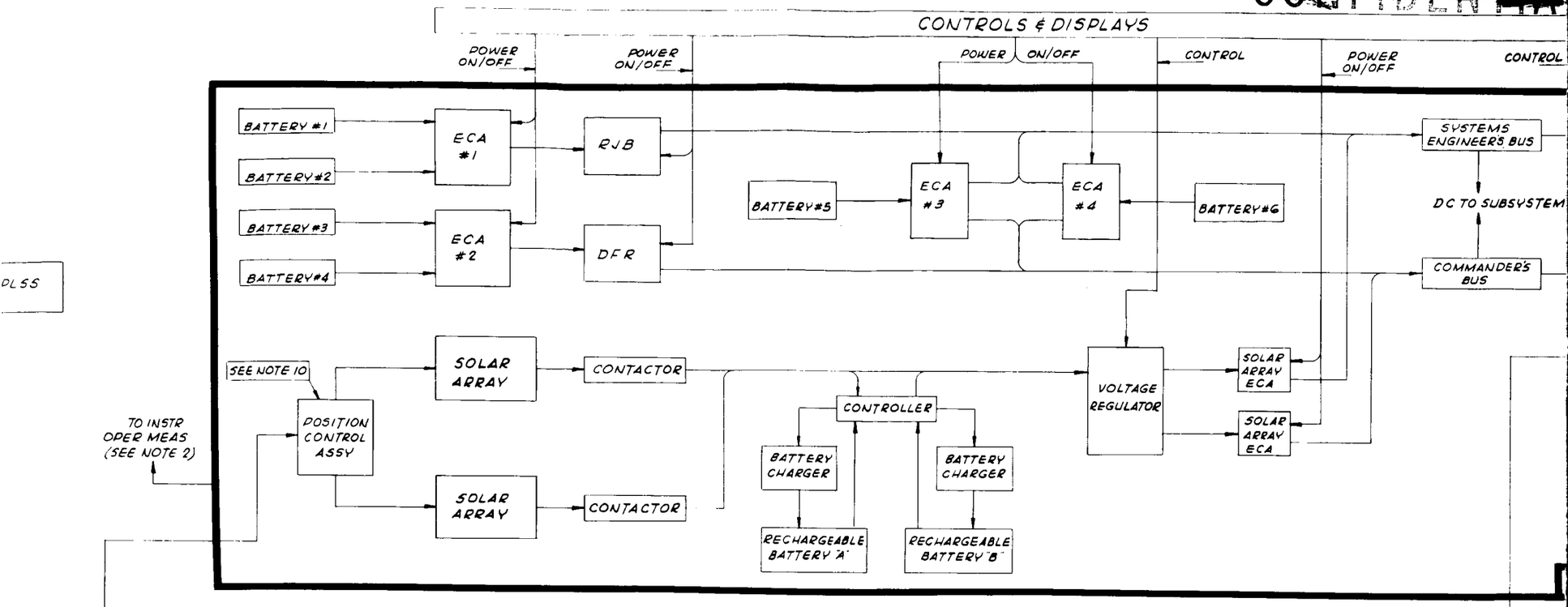
CONTROLS & DISPLAYS
POWER ON/OFF
POWER ON/OFF
POWER ON/OFF
CONTROL
POWER ON/OFF
CONTROL
BATTERY #1
BATTERY #2
BATTERY #3
BATTERY #4
ECA #1
ECA #2
RJB
DFR
BATTERY #5
ECA #3
ECA #4
BATTERY #6
SYSTEMS ENGINEERS BUS
DC TO SUBSYSTEM
COMMANDER'S BUS
SEE NOTE 10
SOLAR ARRAY
CONTACTOR
POSITION CONTROL ASSY
SOLAR ARRAY
CONTACTOR
CONTROLLER
BATTERY CHARGER
BATTERY CHARGER
RECHARGEABLE BATTERY "A"
RECHARGEABLE BATTERY "B"
VOLTAGE REGULATOR
SOLAR ARRAY ECA
SOLAR ARRAY ECA
TO INSTR OPER MEAS (SEE NOTE 2)

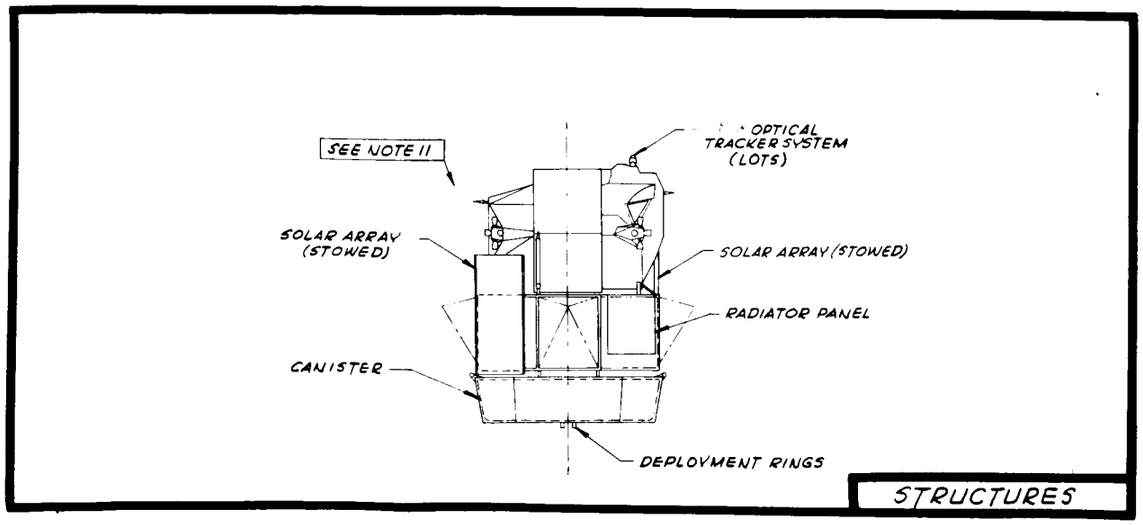
SEE NOTE 11
OPTICAL TRACKER SYSTEM (LOTS)
SOLAR ARRAY (STOWED)
SOLAR ARRAY (STOWED)
RADIATOR PANEL
CANISTER
DEPLOYMENT RINGS
STRUCTURES

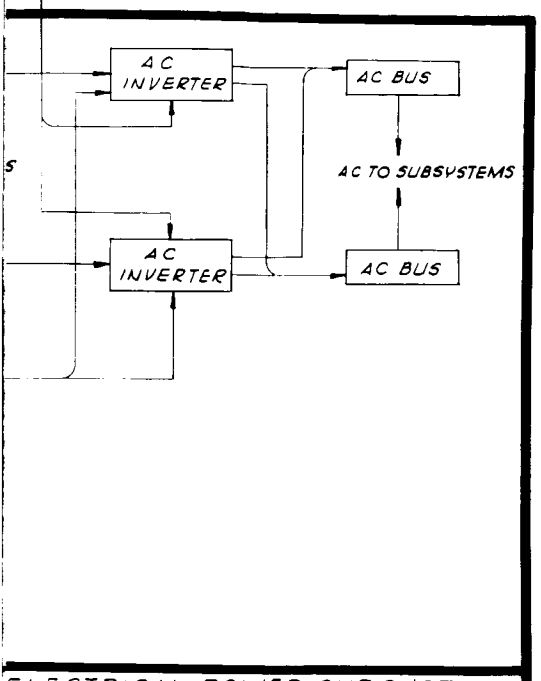

ELECTRICAL POWER SUBSYSTEM

NOTES

1. THIS IS A TENTATIVE LEVEL I, BASIC FUNCTIONAL DIAGRAM FOR THE ABLE LM.
2. MOST OPERATIONAL MEASUREMENTS ARE ROUTED TO THE INSTRUMENTATION SUBSYSTEM PRIOR TO TELEMETRY & DISPLAYS.
3. EMU #2 IS IDENTICAL TO EMU #1
4. THE ABLE LM CREW PROVISIONS WILL BE IDENTICAL TO THE LM
5. THE NUMBER OF VHF ANTENNAS WILL DEPEND UPON THE MISSION & REFLECTOR SELECTED.
6. THE NUMBER & TYPE OF S-BAND ANTENNAS WILL DEPEND UPON THE MISSION SELECTED.
7. THE REFLECTOR SIZE & SUPPORT STRUCTURE WILL DEPEND UPON THE MISSION SELECTED
8. THE GAS HEAT EXCHANGER & CRYO TANK MAY BE REMOVED IF AMBIENT STORAGE IS UTILIZED.
9. THERE ARE (4) REFLECTOR CONTROL MODULES & ARE IDENTICAL TO THE ONE SHOWN.
10. THE FINAL SOLAR ARRAY CONFIGURATION SELECTED WILL DETERMINE THE POSITION CONTROL ASSY USED.
11. THIS IS ONE TYPICAL CONFIGURATION.

ABBREVIATIONS

AC - ALTERNATING CURRENT
ACA - ATTITUDE CONTROL ASSEMBLY
ASSY - ASSEMBLY
ATCA - ATTITUDE & TRANSLATIONAL CONTROL ASSEMBLY
BIOMED - BIOMEDICAL
CES - CONTROL ELECTRONICS SECTION
CMD(S) - COMMAND(S)
COMM - COMMUNICATIONS
CRYO - CRYOGENIC
C&W - CAUTION & WARNING
CWEA - CAUTION & WARNING ELECTRONICS ASSEMBLY
DC - DIRECT CURRENT
DCA - DECODER COMMAND ASSEMBLY
DFR - DEAD FACE RELAY
DSKY - DISPLAY KEYBOARD
ECA - ELECTRICAL CONTROL ASSEMBLY
ECS - ENVIRONMENTAL CONTROL SUBSYSTEM
ED - EXPLOSIVE DEVICES
EMU - EXTRAVEHICULAR MOBILE UNIT
ENG - ENGINE
GN&C - GUIDANCE, NAVIGATION & CONTROL
GOX - GASEOUS OXYGEN
He - HELIUM
H_2O - WATER
ICS - INTERNAL COMMUNICATION SYSTEM
INFO - INFORMATION
INSTR - INSTRUMENTATION
KPPS - KILO PULSES PER SECOND
LGC - LM GUIDANCE COMPUTER
LM - LUNAR MODULE
MEAS - MEASUREMENTS
MECH - MECHANICAL
NRZ - NON RETURN TO ZERO
OPER - OPERATIONAL
O_2 - OXYGEN
PCA - PROGRAM COUPLER ASSEMBLY
PCMTEA - PULSE CODE MODULATION & TIMING ELECTRONICS ASSEMBLY
PIPA - PULSED INTEGRATED PENDULUM ACCELEROMETER
PLSS - PORTABLE LIFE SUPPORT SYSTEM
PMP - PREMODULATION PROCESSOR
PRESS - PRESSURIZATION
PROV - PROVISIONS
PSA - PULSE SERVO ASSEMBLY
PTA - PULSE TORQUE ASSEMBLY
PWR - POWER
REF - REFLECTOR
RCS - REACTION CONTROL SUBSYSTEM
RCVR - RECEIVER
RCVD - RECEIVED
RGA - RATE GYRO ASSEMBLY
RJB - RELAY JUNCTION BOX
SCEA - SIGNAL CONDITIONING - ELECTRONICS ASSEMBLY
S/S - SUBSYSTEM
SYNCH -
TCA - TRANSLATION CONTROL ASSY
TEMP - TEMPERATURE
VHF - VERY HIGH FREQUENCY
VSR - VOICE STORAGE RECORDER
XMIT - TRANSMIT
XMIT(R) - TRANSMITTER

6

PERTINENT DOCUMENTS

GROUP	DOCUMENT	NUMBER	DATE
	LM BASIC FUNCTIONAL CONFIGURATION (LEVEL I) (LM SYSTEM)	LDW 540-10025-01	3-13-65
	PROJECT ABLE DATA PACKAGE FOR PREPARATION OF PROGRAM PLAN & COST ESTIMATE.	ENG-AAP/TOM-66-351	10-26-66
	PROJECT ABLE MIDTERM REPORT		9-29-66
	ADDENDUM TO PROJECT ABLE MIDTERM REPORT		10-6-66

SYMBOLS

- OXYGEN LINE
- WATER "
- COOLANT "
- CONDITIONED OXYGEN LINE
- HELIUM LINE
- FUEL LINE
- PROPELLANT LINE
- OXIDIZER LINE

CONTRACT NO.	PRIMARY CODE	LINE NO.	DISTRIBUTION TYPE
DRAWN BY	GRUMMAN AIRCRAFT ENGINEERING CORPORATION BETHPAGE, L. I., NEW YORK		
LAYOUT BY	ABLE LM		
	BASIC FUNCTIONAL CONFIGURATION		
	LEVEL I		
SIZE	CODE IDENT NO. 26512	Fig. 2.2-1	
SCALE		SHEET OF	

2.3 RECOMMENDATIONS FOR FUTURE STUDY

2.3.1 Mission Requirements

One characteristic of a three month feasibility study is that it generally raises as many questions as it answers. In this study questions continually arose with respect to the mission requirements. In particular, the required intensity of the illumination, and the duration of time during the night that it must be provided, had major impact on the study. Better definition of the mission requirements, both with respect to the stated ABLE military objective and to other possible applications, would permit more meaningful studies to be performed in the future.

2.3.2 Deflections

Because of the major effect that reflector flatness has on illumination, and as a result of the difficulty in ground testing a full scale configuration, it is recommended that techniques for adjustment of the reflector surface in orbit, by either automatic or manual means, be given special emphasis.

2.3.3 Structural Data

Little test data exists on the behavior under load of large inflated structures. Extrapolations from existing data were used wherever possible. Parameters such as damping factors were extremely difficult to estimate. It is therefore recommended that additional data be generated, by tests of either a scale model, or of a segment of a full size configuration.

2.3.4 Kapton Technology

The characteristics of Kapton are similar to those of Mylar, except that Kapton can tolerate significantly greater thermal extremes and radiation doses than Mylar. The newness of Kapton in this ABLE application, however, make the continued study of Kapton characteristics and fabrication techniques worthwhile.

3.1 ILLUMINATION

To provide the required illumination over a particular area of interest, consideration must be given to several important factors. These factors include altitude of operation, reflector reflectivity and area, atmospheric attenuation, reflector system geometry and, most important, reflector deflection from an optically flat surface. A detailed discussion of these factors is provided in Appendix A, "Optics Analysis." In this section, only the more important conclusions, which can be drawn from Appendix A, will be discussed.

The sunlight reflected from a flat reflector in orbit is contained in a cone with approximately a 0.5 deg cone angle, which is the apparent angle of the sun seen from the earth. The illuminated area on the ground is therefore dependent only on the altitude of the spacecraft. If the reflecting surface departs from a plane, however, the reflected cone of light broadens, thus covering more ground area but with reduced average illumination. This surface deflection was quantified by defining it as the center distance between a spherical cap and the plane defining its edges.

In order to appreciate the interrelationship between these four variables (attitude, reflector diameter or area, deflection, and resulting ground illumination), Figure 3.1-1 was generated. Two values of ground illumination were selected, corresponding to "full moon" and "min. illum." (0.1 full moon). Preliminary analysis indicated that deflections of the order of 1-10 feet might be achievable, and so this range was plotted. Finally, the values of illumination were reduced by 50% to account for realistic values of reflectivity, atmospheric attenuation, and angle of incidence of the sunlight.

The great dependence of illumination on altitude, reflector diameter, and deflection is graphically shown in Figure 3.1-1. For example, if it were possible to construct a 1000 foot reflector, which deflected more than 1 foot at the center, achievement of 0.1 full moon would require orbiting at approximately 10,000 nm or lower. Achievement of full moon illumination

would similarly require orbiting at 5,000 nm or lower. One major implication of these orbits is the necessity for multiple reflectors, time-phased in the orbit, in order to provide illumination during the entire night. The problems of packaging, mounting launching and deploying 3-4 or more reflectors requires further study.

Examination of Figure 3.1-1 also reveals the difficulty of increasing illumination by increasing reflector diameter. The study indicates that the major causes of reflector deflection are due to thermal distortions and manufacturing tolerances. The nature of the thermal distortion is that it increases with the square of the reflector diameter as does the area. The rate of increase depends, among other things, on the temperature gradient in the support structure. A 10° gradient, which is about as good as can be achieved, is plotted for both full moon and minimum illumination. The horizontal nature of both curves indicates that for fixed illumination, the increases in diameter do not cause increases in allowable altitude. In other words, the advantages of increases in area which result from increasing diameter are effectively eliminated by larger deflections. Since manufacturing errors will also increase as some power of the diameter, a similar conclusion is likely.

Additional insight into the effect of thermal gradients and attitude on illumination can be gained from Figure 3.1-2, which also shows the small effect that stable orbits have on illumination. The nature of the stable orbit is such that apogee occurs during target nighttime, and so illumination from a stable elliptical orbit is always less than the equivalent circular orbit.

FIGURE 3.1-1

ALLOWABLE DEFLECTION

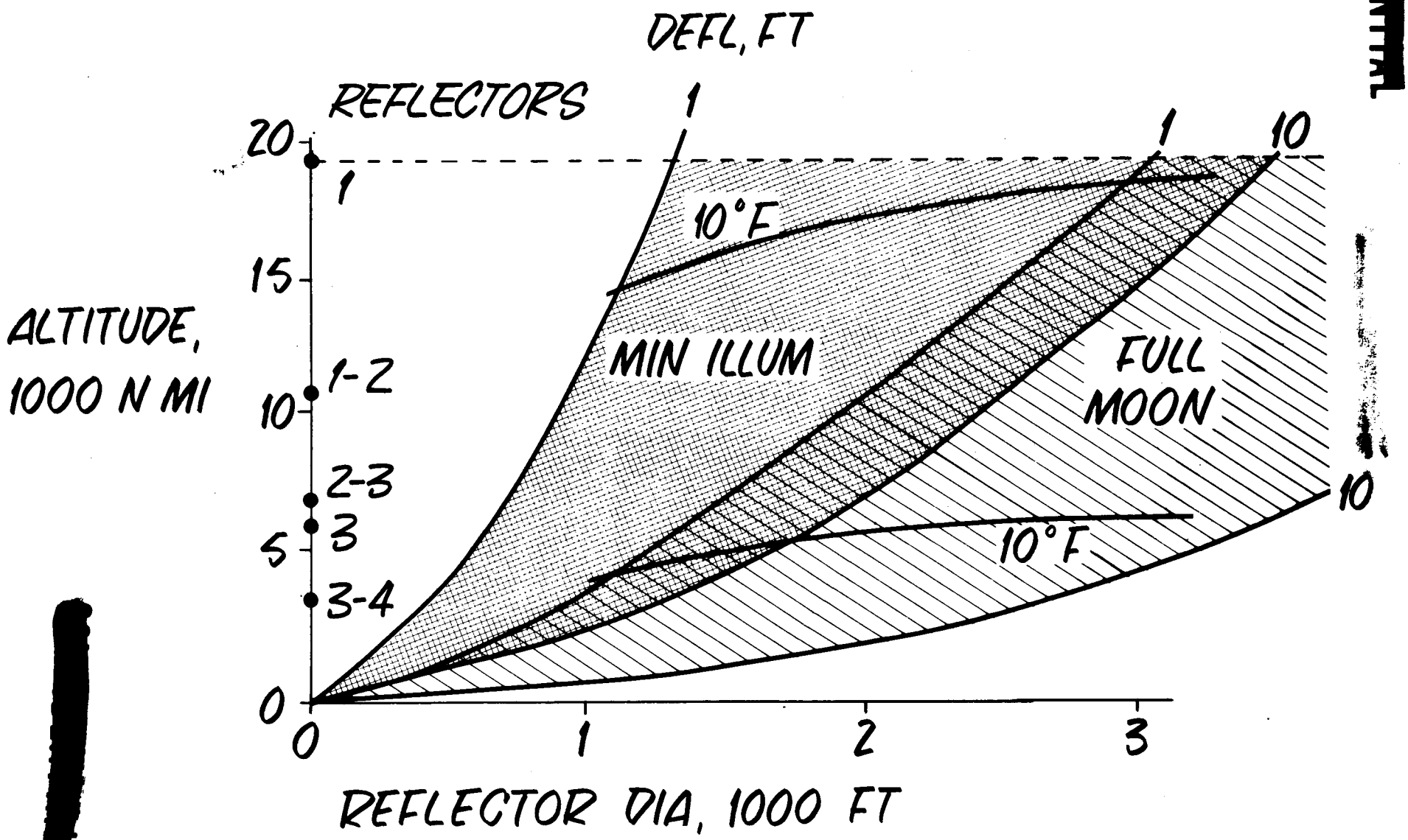

[redacted]

[redacted]

FIGURE 3.1-2

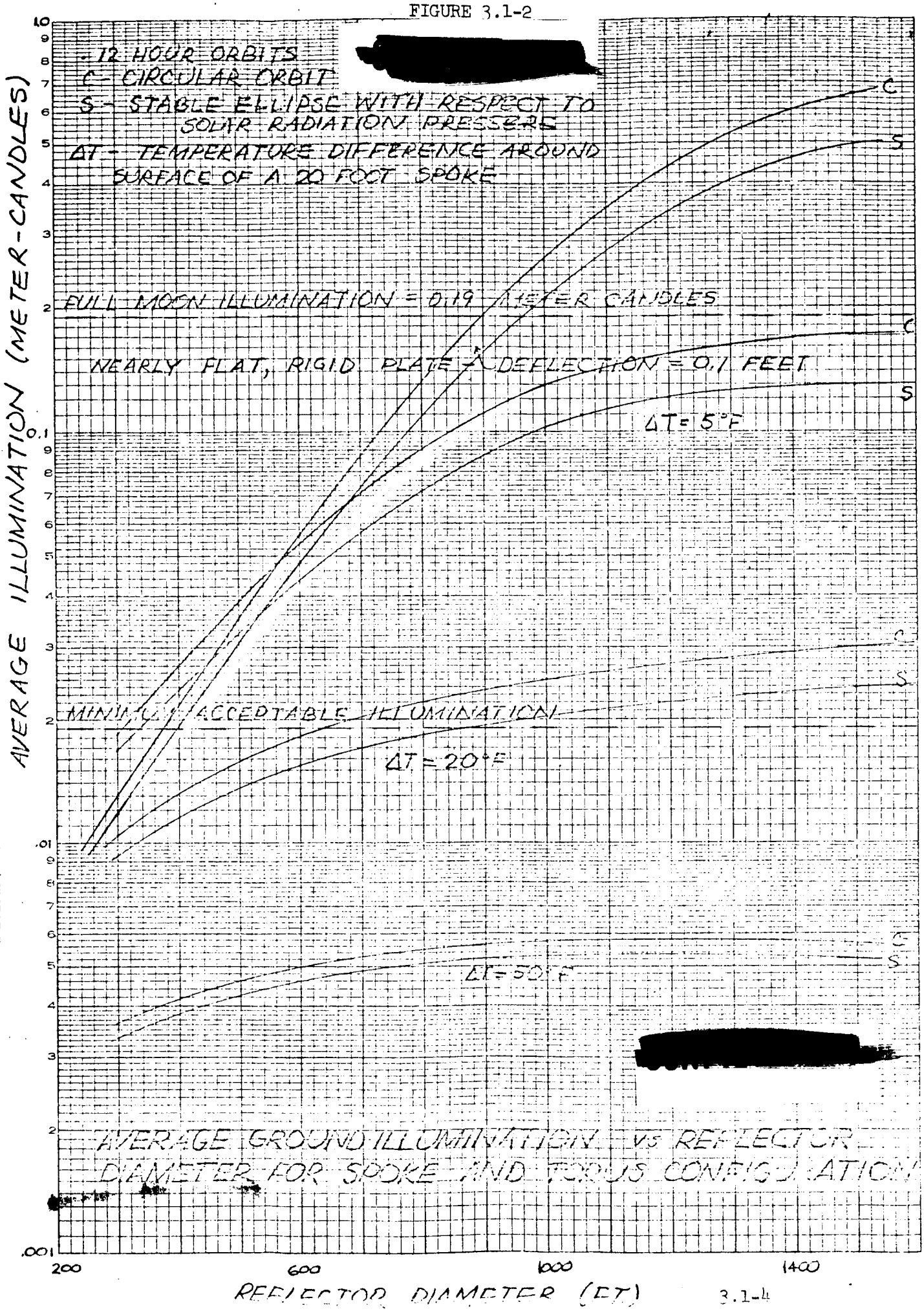

[redacted]

[redacted]

AVERAGE GROUND ILLUMINATION VS REFLECTOR DIAMETER FOR SPOKE AND TORUS CONFIGURATION

NO. 340-L31D DIETZGEN GRAPH PAPER
SEMI-LOGARITHMIC
3 CYCLES X 10 DIVISIONS PER INCH
EUGENE DIETZGEN CO.
MADE IN U. S. A.

3.2 ORBITAL MECHANICS

3.2.1 Groundrules, Assumptions and Definitions

- The Saturn V payload capabilities assumed in this study are those provided by the NASA. At present the maximum LM weight is limited by the structural capacity of the SLA.
- The period of time during which coverage is required is assumed to be between the astronomical twilights, i.e., whenever the sun is more than 18° below the horizon of the target. Coverage is assumed to exist whenever there is an unobstructed line-of-sight between reflector and target. The elapsed time between the epoch at which line-of-sight is lost and the epoch at which line-of-sight is recovered is used to slew the vehicle for coverage during the next nighttime pass over the target area.
- Occultation is determined by the cone (umbra) of the earth's shadow. The reflector is assumed to be illuminated whenever it lies outside this region.
- Orbital perturbations are assumed to arise only as a result of the earth's oblateness and the effects of solar radiation pressure. For the latter, the reflector is assumed to be a rigid, flat, perfectly reflecting plate.
- Stationkeeping maneuvers, if required, take place during the seven days each month which encompass the full moon. Stationkeeping propellant requirements have been calculated assuming that only eccentricity and apside longitude corrections were required. During these periods an inertially fixed attitude will be maintained such that the reflector plate is parallel to the sun, thus decreasing the effects of radiation pressure at these times.
- A bipropellant propulsion system, I_{sp} = 274 sec, is used for stationkeeping maneuvers, and a monopropellant system, I_{sp} = 200 sec., for all attitude control maneuvers.

[redacted]

3.2.1 (continued)

Attitude time lines are presented in terms of Right Ascension (RA), and Declination (D_e) angles which are defined in an inertial system as follows:

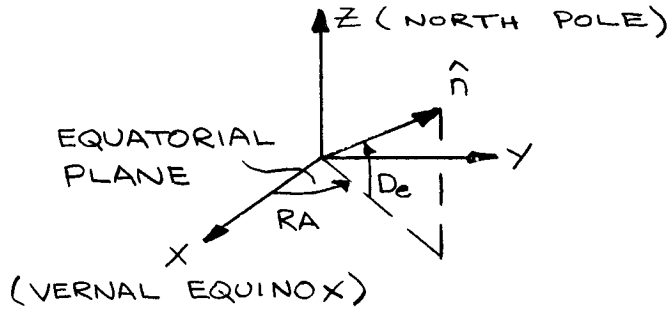

Figure 3.2-1

- The Declination is defined as the dihedral angle between the reflector's unit normal and the equatorial plane.
- The Right Ascension is the angle between the vernal equinox and the projection of the unit normal onto the equartorial plane. It is positive in a right hand sense taken about the polar axis.

All orbits considered are posigrade with 0° or 28.5° inclination. For orbits other than synchronous, orbital periods are resonant with the earth's mean solar day e.g., the orbit known as the "twelve hour orbit", is one in which the reflector is exactly over the target at midnight, on alternate passes. This in general will not result exactly in a 12 hour Keplerian Period due to the virtual motion of the sun around the earth. The 24 hour orbit, however, is resonant with earth's rotational rate.

3.2.2 Circular Orbits (Unperturbed)

Attitude Time Lines and Coverage: In order to be able to predict control system requirements for the reflector, attitude time lines have been generated, showing the Right Ascension and Declination of the unit normal of the reflector relative to the coordinate system of figure 3.2-1. (Note: Although both sides of the disc will probably be reflecting surfaces, the unit normal is arbitrarily assigned to one face. Thus, for some orientations, the target will be illuminated when the unit normal is pointing away from the target.)

[redacted]

3.2.2 (continued)

Attitude time lines are presented in figures 3.2-2 thru 3.2-4 for the "worst case" relative to control system slewing requirements. Based on analysis, the "worst case" conditions were found to occur at the winter solstice. The lines indicating morning and nightfall are the times of astronomical twilight as previously defined. When coverage of the target by the reflector beam exists, the curves are drawn with a solid line. When the target is not covered, the reflector is assumed to undergo a constant slew rate so as to be in position for the next period of coverage. This is indicated by the broken lines in the figures.

Slew rates between coverage regions were choosen on the basis of minimizing the rotational rate change requirements (and hence propellant requirements) on the control system. Reflecting surfaces on both sides of the plate are desirable for the 24 hour and 6 hour orbits for minimum control propellant expenditures, while in the 12 hour orbit it was found that the declination slews would be too great to gain any advantage by coating both sides. Based on these preliminary studies, it is concluded that each orbit condition must be analyzed separately to determine the requirement for one or two sided reflectors. However, in order to enhance flexibility in mission planning, it is recommended that the reflector be coated on both sides if the material technology permits.

Both the 12 hour and synchronous orbits (figures 3.2-3 and 3.2-2 respectively) exhibit complete coverage between evening and morning twilight, excluding periods of occultation (discussed below). Figure 3.2-4 shows that in a 6 hour orbit coverage exists for roughly one third of the required time, nightly. As a result, among the orbits whose periods were considered to most feasible, viz. whose periods are multiples or whole fractions of 24 hours, the 12 hour orbit is the lowest which provides full coverage with a single satellite. Based on the above results and supplementary calculations involving the virtual period of the satellite relative to the target, the number of satellites required for full nightly coverage as a function of orbit period is indicated in Table 3.2-1. Where it was considered that purely geometrical coverage would not provide sufficient illumination, an additional satellite is added to the "No. of Satellites" required column. For example, although one 12 hour satellite will provide coverage between the astronomical twilights, the illumination at the horizons may not be acceptable, therefore, a potential requirement for a second satellite is indicated.

3.2.2 (continued)

TABLE 3.2-1

Number of Satellites Required for Full Coverage

Orbit Period (Hrs.)	No. of Satellites
24	1
12	1-2
8	2-3
6	3
4	3-4

The required slew rates during daylight hours from figures 3.2-2 thru 3.2-4 are tabulated below (Table 3.2-2). These slew rates ensure that the reflector will be at the proper attitude for the next period of coverage. The required torques resulting from the varying slew rates during coverage periods are presented in Section 3.2.5.

TABLE 3.2-2

Slewing Requirement Between Coverage Phases

Time of Year	Orbit	R.A. rate deg/hr	D_e rate deg/hr
Winter	synchronous	+ 4.6	$\mp$ 1.7
Winter	12 hour	+11.7	arbitrary for propellant optimization
Winter	6 hour	+35.6	$\mp$ 1.3

Occultation: The period of occultation is dependent upon orbit altitude, inclination, nodal drift rate and time of launch. Figure 3.2-5 shows the percentage of time per orbital pass during which the reflector is occulted for equatorial orbits with 24, 12 and 6 hour periods as a function of the angle between vernal equinox and the earth-sun line. (Note, on the first day of spring this angle is 0°, and at the winter solstice

3.2.2 (continued)

it is 270°.) In figure 3.2-6 the percentage time in occultation is presented for the same three orbits with inclinations of 28.5°. For each orbit presented, the line of nodes is assumed fixed, 90° from the vernal equinox.

From these figures, it is seen that as the orbital period is increased the percentage occultation time per orbit decreases, however, the actual time in occultation increases. For the 24 hour orbits this occultation time is 1.18 hr. per orbit compared to .94 hr. for the 12 hour orbits. These numbers represent the maximum occultation time for the orbits over an operational period of one year. The effect of orbit inclination is to reduce the range angle between earth-sun line and vernal equinox (θ) during which occultation of the satellite occurs, and to shift the semi-annual occultation periods relative to the vernal equinox. For the 12 hour orbits, the 28.5° inclination results in a 32.5 day reduction in the length of the occultation period.

For the inclined orbits considered, given any arbitrary launch date, a six month mission will never be completely free of occultation. For the 12 hour inclined orbit the maximum mission duration free of occultation will be 129.86 days.

3.2.3 Effects of Perturbations on Circular Orbits

Qualitative Description of Perturbing Forces: The effects of perturbing forces on the elements of an orbit may be represented most conveniently by resolving the forces into the three rectangular coordinates of an orbit-fixed system, components $\vec{S}$, $\vec{T}$, and $\vec{N}$:

- $\vec{S}$, the orthogonal component, is perpendicular to the plane of the orbit. It is positive in the direction of the north pole of the ecliptic.
- $\vec{T}$, the tangential component is directed tangent to the orbit at the same point, and is positive when it is parallel to the direction of the motion.
- $\vec{N}$, the normal component, is defined perpendicular to both $\vec{S}$ and $\vec{T}$ and is positive when directed inward.

The instaneous effects of the perturbing forces on each of the orbit elements are summarized in figure 3.2-7. These effects are given for positive values of $\vec{S}$, $\vec{T}$ and $\vec{N}$.

[redacted]

Fig. 3.2-7

Perturbations on Orbital Elements

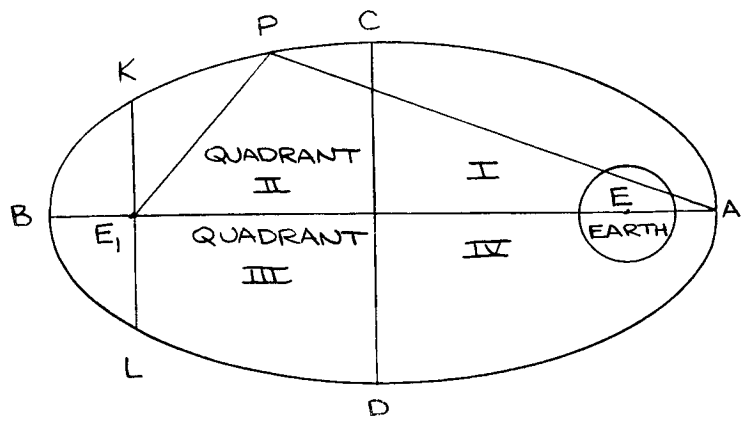

	S	T	N
NODES	Advance in first and second quadrants; Regress in third and fourth quadrants.	None	None
INCLINATION	Increases in first and fourth quadrants; Decreases in second and third quadrants	None	None
SEMI-MAJOR AXIS	None	Always Increases	None
LINE OF APSIDES	No effect if ω is measured from fixed point rather than from Ω_0	Advances in interval ACB; Regresses in interval BDA	Advances in interval LAK; Regresses in interval KBL
ECCENTRICITY	None	Increases in interval DAC; Decreases in interval CBD	Increases in interval BDA; Decreases in interval ACB

Figure 3.2-7 is presented exactly as it appears in reference 3.2-1. To illustrate the use of the figure, consider the solar pressure perturbations. Available data on the effects of solar radiation pressure on circular orbits indicates that after a short time in orbit, a well defined line of apsides forms 90° from the earth sun line. This condition is represented by positioning the sun below the arc BDA in figure 3.2-7. For this example, it is assumed that the reflector unit normal bisects the angle between the vehicle-sun-line and the vehicle line-of-sight to the geocenter, E. Hence, the direction of the solar force will be opposite in direction to the

[redacted]

3.2.3 (continued)

reflector unit normal. Since the $\vec{T}$ component of the perturbation force is defined positive counter-clockwise, figure 3.2-7 shows that $\vec{T}$ is negative along CBD and positive along DAC. (Note that for near circular orbits, E and E_1 approach coincidance at the center of revolution). Similarly, $\vec{N}$ is negative along ACB and positive along BDA. Thus, by comparison with figure 3.2-7, it is seen that due to $\vec{T}$, the eccentricity increases at all times whereas the line of apsides advances in quadrants I and III and regresses in quadrants II and IV. Due to $\vec{N}$, the eccentricity also increases at all times, and the line of apsides advances in quadrants II and IV and regresses in quadrants I and III.

The results of a digital simulation of these forces, using an Enke technique for orbit determination, show that when the above conditions pertain, the eccentricity does increase continually. In addition, a slow advance of the line of apsides is found, reflecting the fact that when the satellite is in the half of its orbit nearest the sun, the line of apsides advances for the majority of the time, whereas the line of apsides regresses in the other half of its orbit. The digital simulation, which contained only solar pressure perturbations, showed that for approximately six months the eccentricity increased, and the line of apsides advanced a total of 90°. But in this same time duration, the sun has moved 180° so that the instantaneous location relative to the orbit is now to the right of point A in figure 3.2-7, and henceforth will be located above arc ACB. Thus for the next six months the perturbing forces have the opposite effect and at the end of one year the orbit returns to the original circular orbit. In addition, the simulation showed that out-of-plane effects were small, while the semi-major axis, and therefore the orbital period, remained virtually unchanged.

Effects of the earth's oblateness were later added. Results for an 1100 foot reflector initially in a 12 hour circular orbit are shown in figures 3.2-8, -9 and -10. Figure 3.2-8 shows time-histories of apogee and perigee radii and orbit eccentricity for 190 days in orbit. The large scale effects of solar pressure discussed above are still apparent in this simulation, but the effects of oblateness are seen as well. The eccentricity increases for the entire 190 days but appears to be leveling off at the end of this period. The orbital period, which is found from apogee and perigee radii, is seen to increase from 11.98 to 12.01 hours over the entire 190 days. Contained in figure 3.2-9 are time histories of inclination and the longitude of the node. Over 190° of apparant sun motion along the ecliptic,

3.2.3 (continued)

the orbit's inclination increases from 28.5° to 28.85°; the node is seen to precess at an essentially constant rate, from 90° to 78.43° over 190 days. The angle between the sun and the line of apsides is initially near 90°, and precesses a total of 72° over 190 days.

Figure 3.2-10 shows that coverage is maintained for the first 78 days of the mission, at which time a rapid increase in T_{NC}, the time during which there is no coverage, is observed. Therefore, stationkeeping would be required to maintain the operational status of a circular orbit at least on a bimonthly basis. Included in figure 3.2-10 are the central angles, $\Delta\sigma_T$(P.M.) and $\Delta\sigma_T$(A.M.), between the target and the satellite at the astronomical twilights of the target. The parameter $\Delta\sigma_P$, figure 3.2-10, is the longitude difference between the sun and the orbit perigee vectors.

Stationkeeping Requirements

The flight plan assumed for stationkeeping was as follows:

- The satellite is initially in a circular orbit
- The reflector is allowed to drift from station under the influence of the perturbing forces for 23 days of each month when the target is receiving little or no lunar illumination
- During the $6\frac{1}{2}$ day full moon period, stationkeeping maneuvers are performed. Thus at the end of the average lunar month, $29\frac{1}{2}$ days, the reflector is always back on station.
- During $6\frac{1}{2}$ day stationkeeping period the reflector maintains an inertially fixed attitude showing its minimum cross-section to the sun to decrease solar perturbations during this time.

The ΔV required for stationkeeping each month was found to vary almost linearly with the parameter A/M, the area to mass ratio of the reflector. Values of ΔV calculated from this parameter are conservative, however, since the reflector is assumed to have a reflectivity of unity. The dependence on A/M reflects the fact that this ratio is proportional to the total impulse absorbed from the sun. The equations used to compute stationkeeping ΔV are summarized below, for the most economical means of performing each correction:

3.2.3 (continued)

- Inclination i - thrust normal to the orbit plane at either the ascending or descending node:

$$|\Delta V_N| = \Delta i \; v_o \qquad (3.2\text{-}1)$$

where v_o is the orbital velocity at the point of correction

- Period, T - thrusting circumferentially at perigee:

$$T = 2\pi \sqrt{\frac{1}{\mu}\left(\frac{\mu r_p}{2\mu - r_p v_p^2}\right)^3}$$

$$\Delta V = \left(\frac{2\mu - r_p v_p^2}{3 r_p v_p}\right) v_p \frac{\Delta T}{T} \qquad (3.2\text{-}2)$$

for eccentricity > 0

and $\Delta V = -\frac{V}{3}\frac{\Delta T}{T}$ for circular orbits, where μ is the gravitational constant, and r_p and v_p are the radius and velocity at perigee.

- Eccentricity, e - thrusting circumferentially at apogee, removing e/2 and then at perigee removing e/2:

$$v_a = \sqrt{\frac{\mu}{r_a}(1-e)}$$

$$v_p = \sqrt{\frac{\mu}{r_p}\left(1+\frac{e}{2}\right)}$$

$$|\Delta V| = \frac{1}{4} e (v_p + v_a) \qquad (3.2\text{-}3)$$

where v_a and r_a are velocity and radius at apogee.

Application of the above equation to data obtained from references 3.2-2 and 3.2-3 on the decay of orbit elements due to solar pressure, indicates that the Δ V required for stationkeeping is due almost entirely to the eccentricity correction. Period corrections were very small, and it was found after performing a linear analysis that apsidal corrections could be contained in eccentricity corrections at no additional Δ V cost.

3.2.3 (continued)

Figures 3.2-11, -12 and -13 summarize the results of this analysis. Eccentricity perturbations are shown in figures 3.2-11 and 3.2-12. Figure 3.2-11 shows how the eccentricity increases with time in orbit for different values of A/M. It was found that, within the accuracy of the available data, curves for constant A/M are straight lines independent of orbital altitude. The accuracy of this assumption is illustrated in figure 3.2-12 which is drawn for 23 days in orbit and on which are shown specific data points. The ΔV required to correct the eccentricity after 23 days in orbit is shown in figure 3.2-13 as a function of orbit altitude. This dependence on altitude can be inferred from equation 3.2-3 which contains apogee and perigee velocities on the right hand side. (It should be noted that the largest values of A/M probably will not exceed 4000 slug/ft^2).

For 12 hour and synchronous orbits, the data in figures 3.2-12 and 3.2-13 were used to calculate the total stationkeeping propellant weight and total impulse required over the full 180 day proposed mission. These quantities were calculated assuming five stationkeeping maneuvers; i.e. no stationkeeping maneuver is performed at the end of the sixth month when the mission nominally terminates. If the mission is to continue any further it is assumed that the CSM will perform stationkeeping for the sixth month. After each thrusting maneuver, the weight of the reflector decreases, thus the value of A/M increases. For this reason, the propellant and total impulse requirements include what is used for attitude control.

Figure 3.2-14 shows the total ΔV required for stationkeeping for a 180 day mission, under the above assumptions. Note that except for small reflectors ($d <$ 1000 feet) the ΔV per month is not constant, but increasing each month. The total ΔV is shown for varying reflector diameters and orbital periods. Higher orbits, which have lower orbital velocities, require smaller ΔV.

The total stationkeeping propellant weight (solid lines) is shown in figure 3.2-15 as a function of reflector diameter. The dashed lines show the total propellant used for stationkeeping and attitude control. The propellant weight per month is a slowly decreasing function but may be assumed constant for $d <$ 2000 feet. As in figure 3.2-14, highest values of propellant weight are found in lower orbits.

3.2.3 (continued)

In figure 3.2-16 the total impulse is shown in the same format as was the propellant weight in figure 3.2-15. These values of total impulse are used to find the required total propulsion system weight from figure 3.2-17. The total impulse capacity is shown to be increased by adding sets of LM tanks (i.e. two oxidizer, two fuel and two helium tanks) as required.

3.2.4 Stable Orbits

In section 3.2.3 the perturbations of circular orbits were described, and it was seen that the two most important perturbations, eccentricity and apside location, exhibited cyclic behavior. After 180 days the eccentricity reached a maximum value and after one year returned to zero. Similarly the line of apsides advanced for the first half year and regressed back to the initial value during the second half. It seems probable, then, that some value of eccentricity yields an orbit which remains unchanged relative to the target at midnight under the influence of the perturbing forces considered. If such stable orbits do indeed exist, stationkeeping requirements could be greatly reduced, yielding significant savings in propulsion system redesign and total system weight.

The existance of numerous near-stable orbits was established in reference 3.2-3. Therefore, an attempt was made to determine the elements of a stable 12 hour orbit for an 1100 foot reflector based on an initial value for A/M of 1153.8 ft^2/slug. It was not possible to determine this orbit exactly in the time available, but a near-stable orbit was computed with apogee and perigee altitudes of 11726 and 10086 nautical miles respectively.

Time histories of the parameters of this orbit are given in figures 3.2-18, -19 and -20, for 180 days in orbit. Figure 3.2-20 indicates that the near stable orbit yields favorable coverage for nearly 6 months. Plotted are the central angles between the target and the salellite at the astronomical twilights, $\Delta\sigma_T$ (P.M.) and $\Delta\sigma_T$ (A.M.). Also included is a time history of time, T_{NC}, during which there is no coverage. It can be seen that from the 130th day, a significant increase in loss of coverage appears, resulting in a 1.1 hr maximum coverage loss on the 180th day. Improved definition of the initial elements of the stable orbit should improve the coverage toward the end of the 6 month period.

3.2.4 (continued)

LM Stationkeeping Capability

Due to the apparent sensitivity of the stable orbits to initial conditions and vehicle parameters, the capability of the LM RCS system to perform stationkeeping maneuvers was evaluated. After deployment of the reflector it is estimated that the LM RCS would have 500 lb of propellant available for stationkeeping maneuvers. This would then provide a ΔV capability of 162 ft/sec. Using equations 3.2-1, -2, and -3, upper limits on the amount by which the parameters inclination, period and eccentricity may be corrected can be found. As indicated in section 3.2.3 apside corrections can be included in the eccentricity corrections at no additional ΔV cost . The results are shown below.

Parameter	i	T	e
Maximum Correction	0.72°	0.48 hr	.024

These values compare favorably with the six month perturbations found in the near stable orbit discussed above.

Attitude Time Line: To establish the control system slewing requirement for the 12 hour, 28.5° inclined stable orbit discussed above, the attitude time line, in terms of Right Ascension and Declination of the reflector unit normal, was generated. Figure 3.2-21 is a typical attitude profile for 2 days of operation following the vernal equinox. It became evident that the control system propellant quantities computed for circular equatorial orbits would be satisfactory for preliminary sizing of the system. Therefore, the trade-off studies discussed in Section 3.2-4 involving control system requirements and satellite orbit altitude for circular equatorial orbits apply to the stable inclined orbit.

3.2.5 Torque Environment

External Torques - The primary sources of external torques acting on the vehicle are gravity gradient and solar pressure effects.

The gravity gradient torques acting on the vehicle were determined from the following expressions:

[redacted]

3.2.5 (continued)

$$M_y = 1.605 \times 10^{-8} \frac{a_{11}\, a_{13}}{K^3} (I_{xx} - I_{yy}) \quad \text{(ft-lb)}$$

$a_{11} = \cos\theta \cos\psi$

$a_{13} = \sin\theta \cos\phi + \cos\theta \sin\phi \sin\psi$

where $\psi = -De$, $\theta = RA - \sqrt{\frac{\mu}{(R_{ORBIT})^3}}\, t$, $\phi = 0$

$K = R_{orbit}/R_{synch}$

R_{orbit} = orbit radius (ft)

R_{synch} = synchronous orbit radius (ft)

I_{xx} and I_{yy} = Inertias about the x and y axes respectively (slug-ft^2)

$$M_Z = 1.605 \times 10^{-8} \frac{a_{11}\, a_{12}}{K^3} (I_{xx} - I_{zz})$$

$a_{12} = \sin\theta \sin\phi - \cos\theta \cos\phi \sin\psi$

I_{zz} = Inertia about the z axis (slug-ft^2)

M_x is assumed zero since $I_{yy} \approx I_{zz}$

The attitude angles from the attitude time lines presented in Section 3.2.2 were substituted into the above expressions to derive the time history of the gravity gradient torques. These time histories are shown in figures 3.2-22 through 3.2-27 for 24, 12 and 6 hour circular orbits respectively. The 12 hour stable orbit torques will be similar to those shown for the 12 hour circular orbit.

The solar pressure torque acting on the reflector was approximated by the equation:

$$T_s = PL_{cp} \frac{d^2\pi}{4} \cos^2\theta \quad (\text{sgn} \cos\theta)$$

where

T_s is the solar torque (ft lb)

L_{cp} is the distance between center of gravity and center of pressure (ft)

d is the reflector diameter (ft)

[redacted]

3.2.5 (continued)

θ is the pitch angle

and P = solar pressure, 1.88×10^{-7} lb/ft^2

The time variation of this torque for the orbits considered is essentially dependent on the orbit period because the pitch angle derived from the attitude time lines can be approximated by a straight line. Plots of solar torque versus time are presented in Figure 3.2-28.

Rotational Maneuvering Requirements

The slewing torque requirements are generated by the maneuvers necessary to orient the reflector to direct the beam to the target. These slewing maneuvers are also required when the target is not illuminated to ensure that the correct orientation exists at the time the target is reaquired.

The time histories of the angular rates required to accomplish these orientations are shown in figures 3.2-29 through 3.2-31 for the 24, 12 and 6 hour orbits respectively.

The peak slewing torque requirements were derived from the rate change requirements by determining the largest rate change required in the shortest period of time. The peak torque obtained is summarized in the table below.

24 hr.	$3.2 \times 10^{-9}\ I_{yy}$ ft-lb
12 hr.	$5.6 \times 10^{-8}\ I_{zz}$ ft-lb
6 hr.	$1.7 \times 10^{-8}\ I_{zz}$ ft-lb

Peak Maneuvering Torques

Peak Total Torques

The attitude control torquer must generate torques which can offset the gravity gradient, solar pressure, and maneuvering torques. Hence, the minimum control torque required for attitude control is:

$$T_p = T_{G\ max} + T_{S\ max} + T_{M\ max}$$

3.2.5 (continued)

where

T_p	= minimum required control torque	ft. lb.
$T_{G\ max}$	= peak gravity gradient torque	ft. lb.
$T_{S\ max}$	= peak solar torque	ft. lb.
$T_{M\ max}$	= peak maneuver torque	ft. lb.

The minimum control torque, T_p , is presented as a function of reflector diameter in Figure 3.2-32 for the 24, 12 and 6 hour circular orbits.

Total Angular Impulse Requirements

In order to size the control torquer capacity, the total angular impulse was computed in the following manner. The gravity gradient and solar torque time histories were integrated over the duration of the mission (180 days) and the slewing angular impulse was obtained from the expression:

$$I_m = I \sum_{i=1}^{n} (\Delta \dot{\theta})_i$$

where

I_m	is the maneuver angular impulse -	ft lb sec.
I	is the moment of inertia -	slug ft^2
$(\Delta \dot{\theta})_i$	is the th rate change -	rad/sec
n	is the total rate changes for the mission (180 days)	

The total angular impulse required is shown in figure 3.2-33 for the 24, 12 and 6 hour orbits.

3.2.6 Conclusions and Recommendations

Based on the above parametric studies, the following conclusions pertinent to the Able mission are cited:

- The minimum altitude at which one satellite provides full nightly coverage is approximately 11,000 n.mi. (12 hr orbit)
- Inclined orbits reduce the percentage time of the year in which loss of coverage due to occultation by the earth's umbra exists.

3.2.6 (continued)

- The length of time per orbit in which the reflector is occulted increases with increased orbit altitude
- Stationkeeping requirements associated with maintaining a favorable circular orbit decreases with increased altitude.
- Stable orbits exist which theoretically eliminate the requirements for stationkeeping
- Circular orbits will yield slightly higher illumination than stable orbits of equal period.

Although a 12 hr orbit yields coverage from night to morning twilight, illumination levels during the early and late periods of the night will be severely degraded. Hence, the liklihood of a multiple reflector system for orbits with resonent periods other than synchronous is high. In addition, the certain occultation of the reflector at all altitudes supports the requirement for multiple satellites. For a 12 hour orbit inclined 28.5 degrees, occultation periods of up to .94 hrs/orbit for up to 52 days is possible.

The stationkeeping requirements for maintaining an effective circular orbit was found to be large. Additional LM RCS tankage or use of the LM ascent propulsion tanks would be necessary. Hence, it is recommended that the stable orbit concept be adopted for the Able mission. Further study to determine the effects of off-nominal characteristics of the reflector (i.e. degradation in reflectivity) on maintaining the orbit should be performed to accurately determine the extent of stationkeeping required.

3.2.7 References

3.2-1 Moulton, F.R. "An Introduction to Celestial Mechanics", The Macmillan Company, 1914.

3.2-2 Perrine, B. "Perturbations to an Equatorial Synchronous Orbit Due to Solar Pressure (U), R- Aero - Dap-36-66, 3 May 1966

3.2-3 Perrine, B. "Documentation of Solar Pressure Perturbations to Earth Orbits", R-Aero - Dap - 71-66, 18 August 1966

ATTITUDE TIME LINE

SYNCHRONOUS EQUATORIAL ORBIT
WINTER SOLSTICE
TARGET LATITUDE - 17°

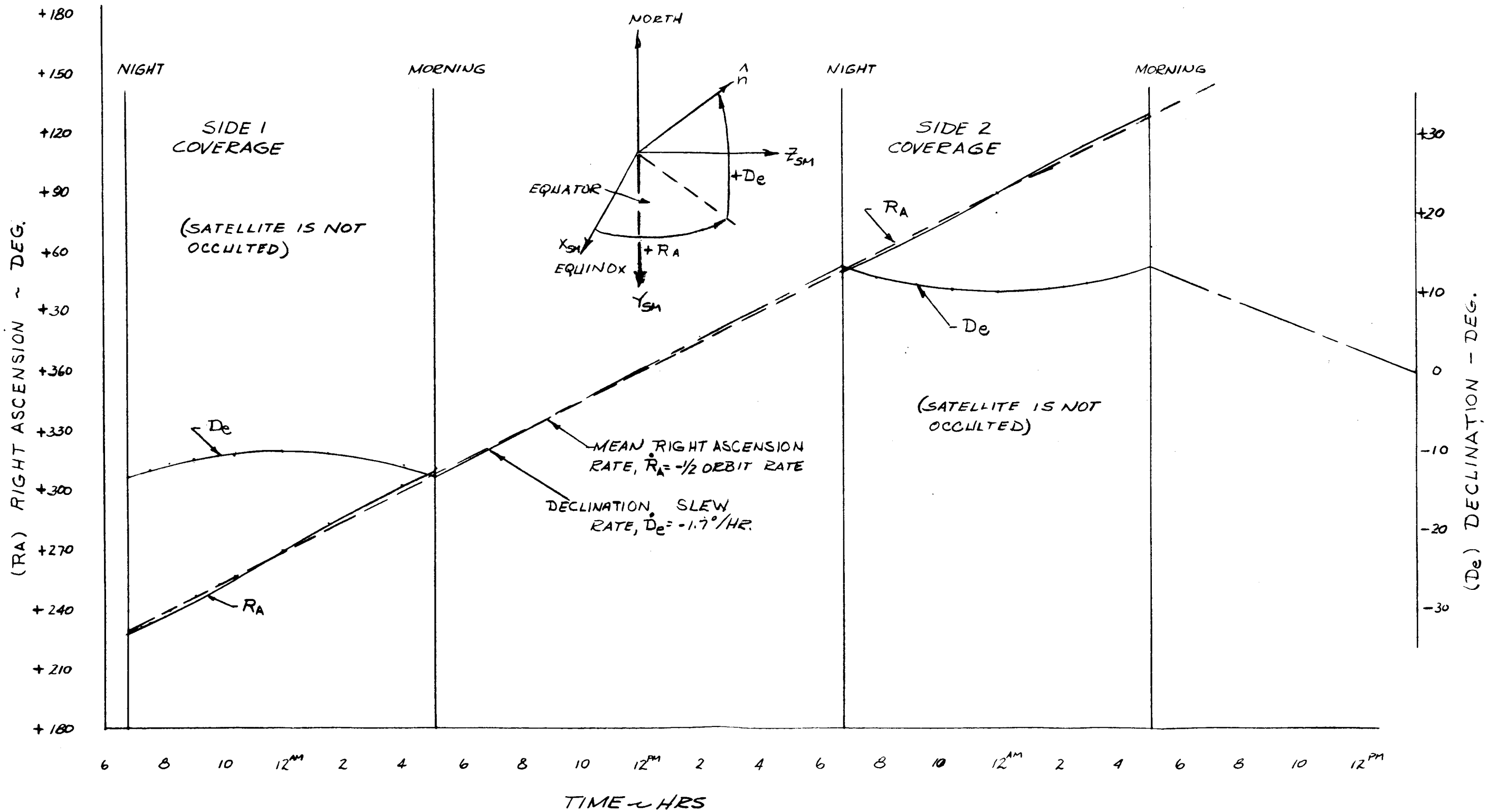

FIGURE 3.2-2

[redacted]

ATTITUDE TIME LINE

12 HOUR ORBIT (EQUATORIAL)
WINTER SOLSTICE
TARGET LATITUDE = 17°

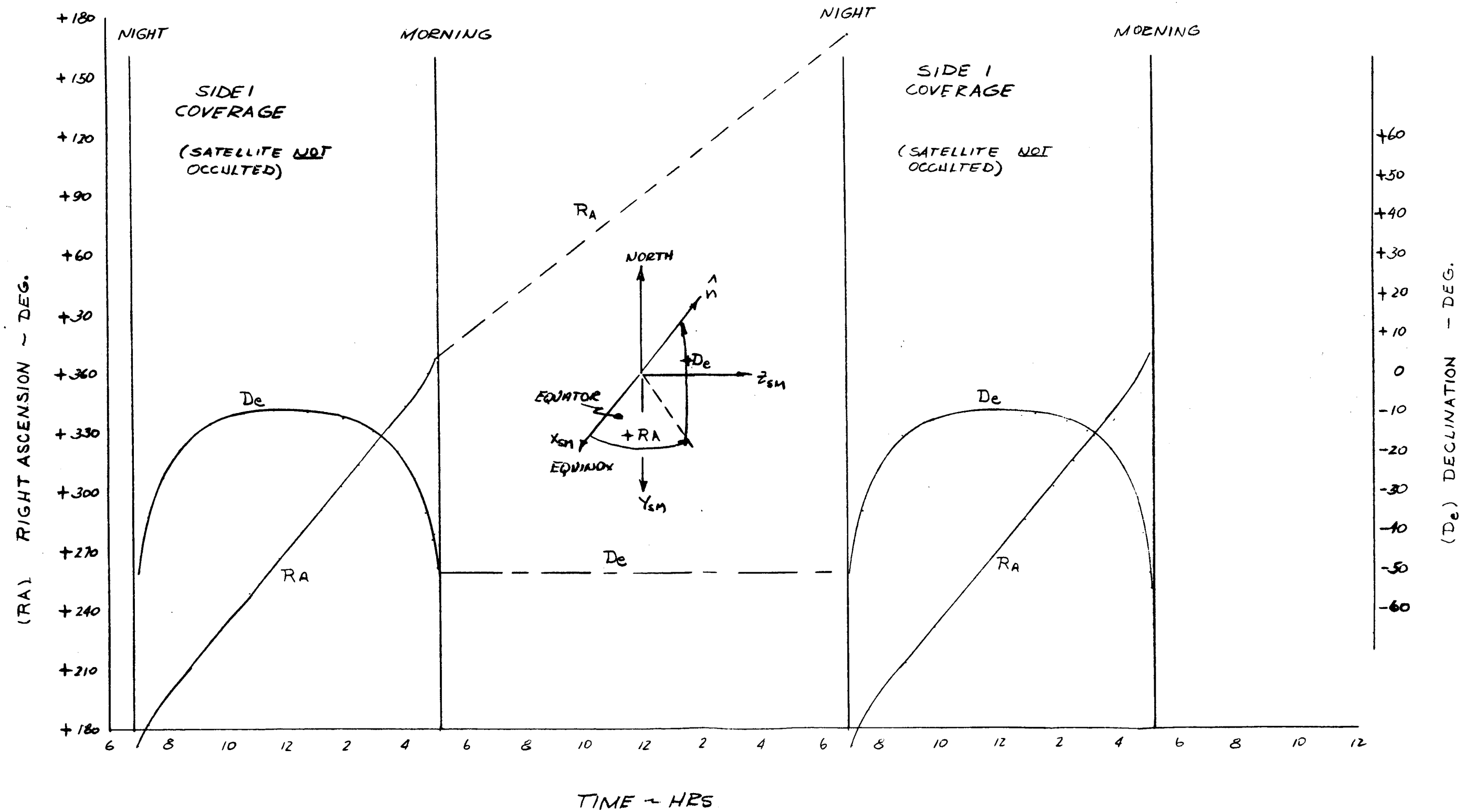

[redacted]

FIGURE 3.2-3

[redacted]

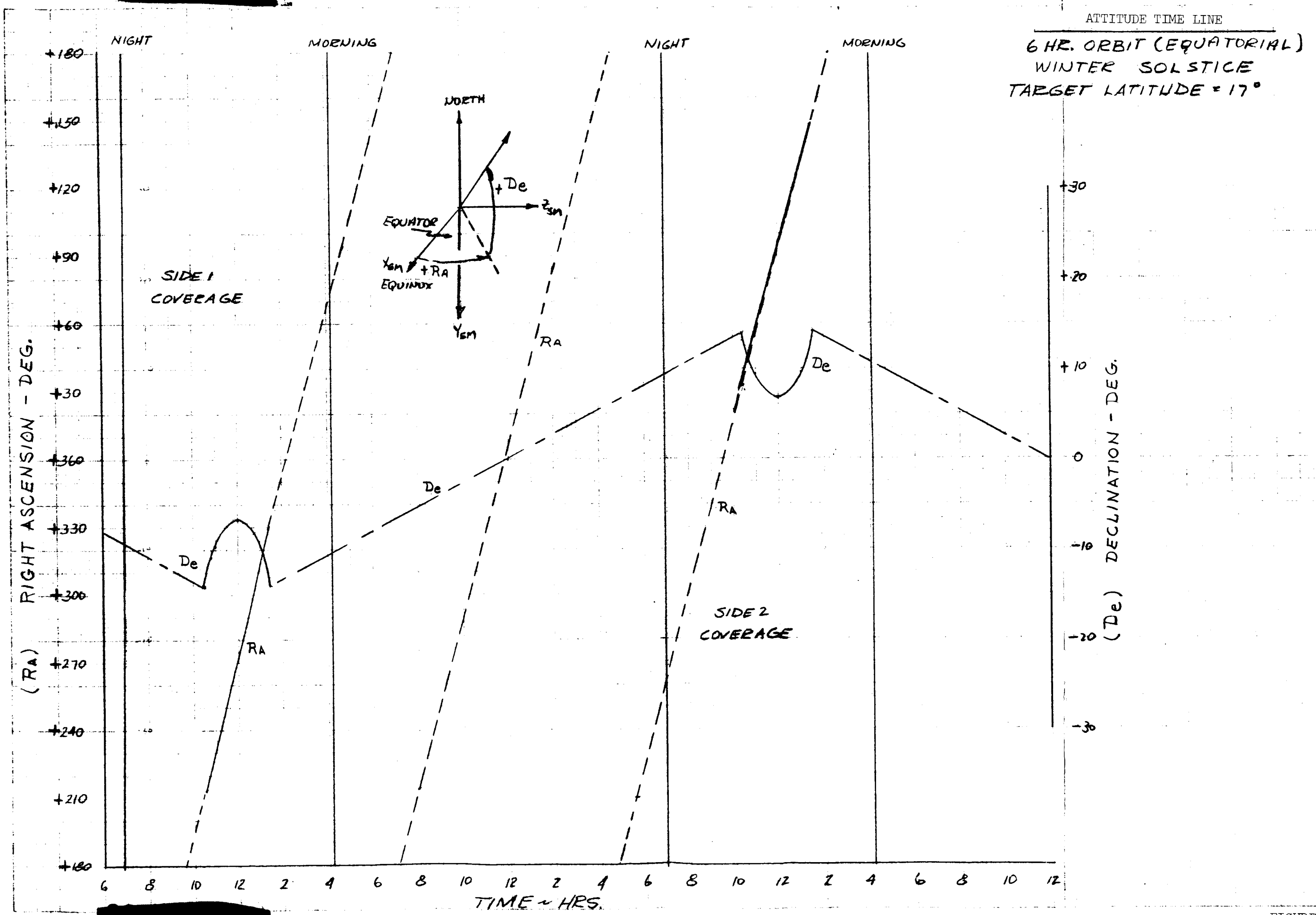

[redacted]

FIGURE 3.2-4

[redacted]

OCCULATION OF SIX, TWELVE,
TWENTY-FOUR HOUR ORBITS

THETA θ - ANGLE BETWEEN VERNAL EQUINOX AND EARTH SUN LINE.

ORBIT INCLINATION = 0.0 DEG.

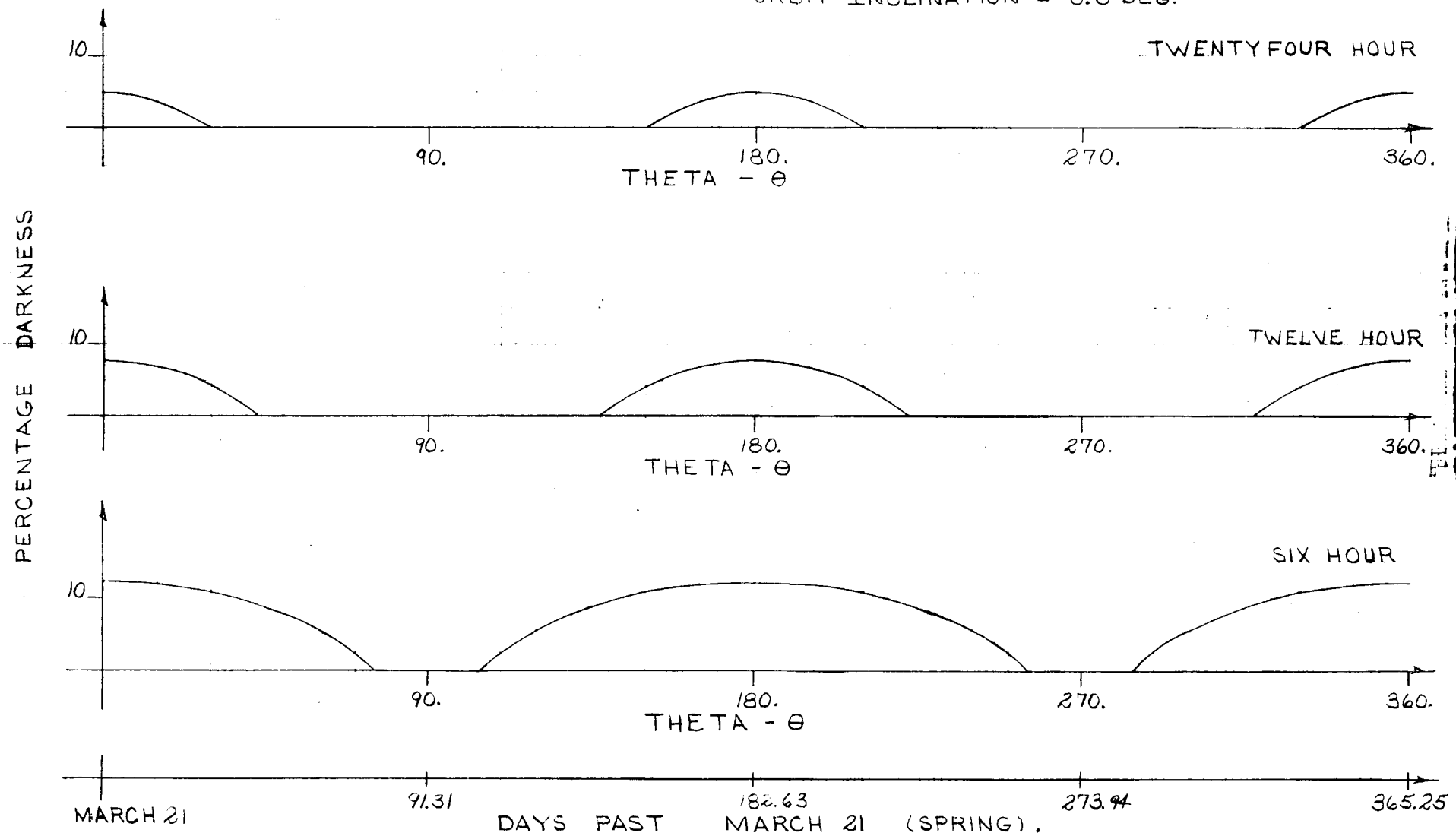

[redacted]

FIGURE 3.2-5

[redacted]

OCCULATION OF SIX, TWELVE,
TWENTY-FOUR HOUR ORBITS

THETA-θ ANGLE BETWEEN VERNAL EQUINOX AND EARTH SUN LINE.

ORBIT INCLINATION = 28.5 DEG.

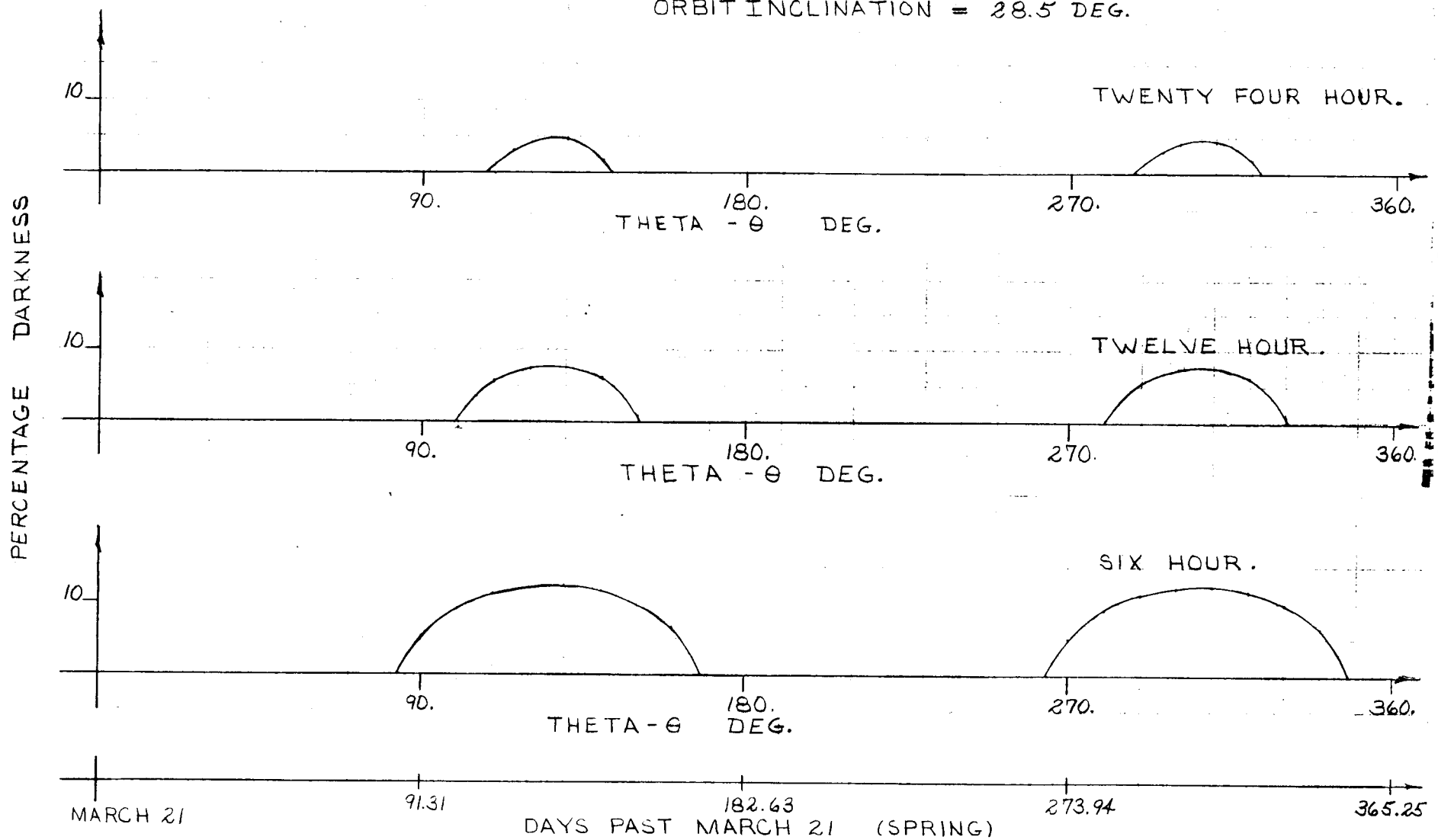

[redacted]

FIGURE 3.2-6

PERTURBED CIRCULAR ORBIT

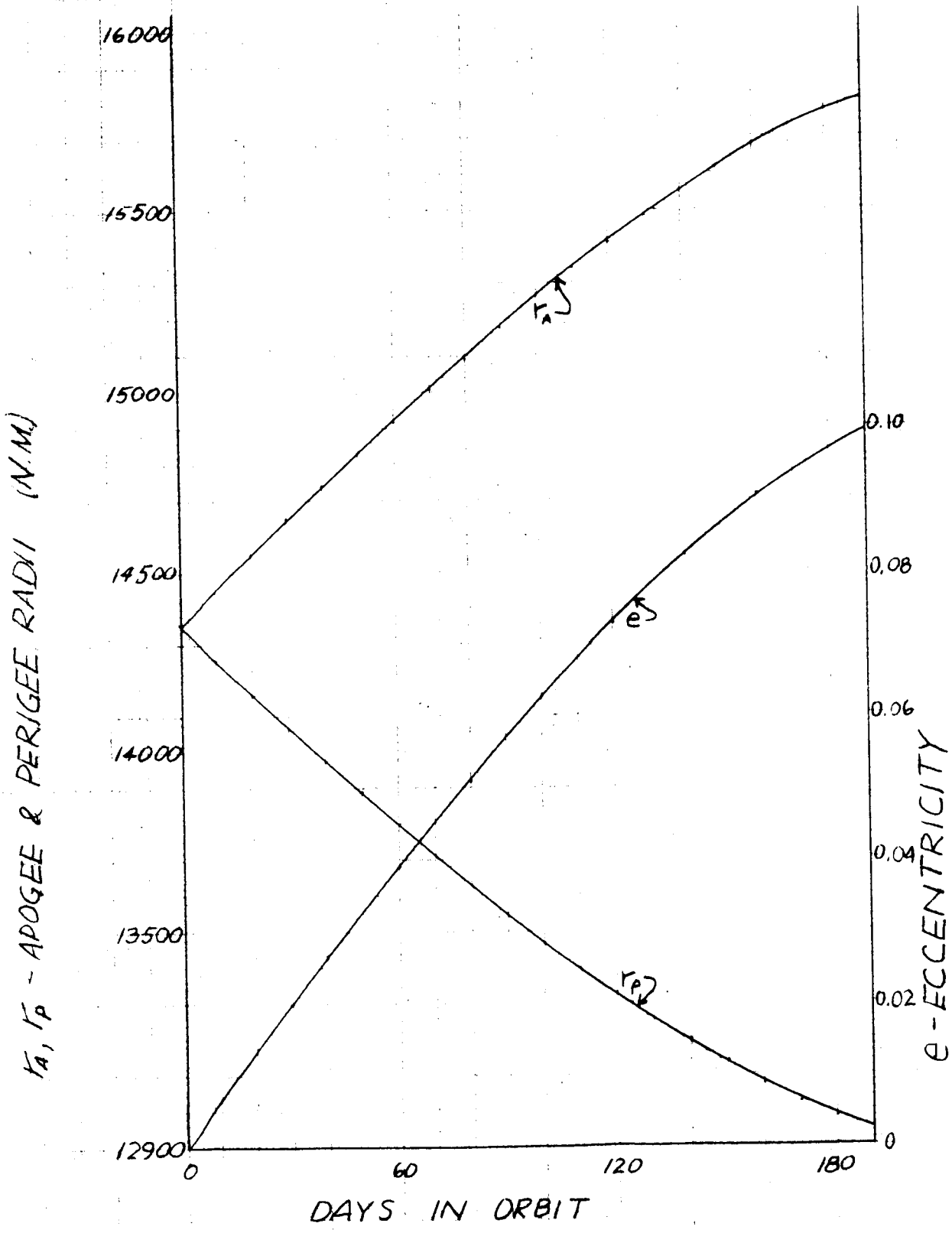

FIGURE 3.2-8

PERTURBED CIRCULAR ORBIT

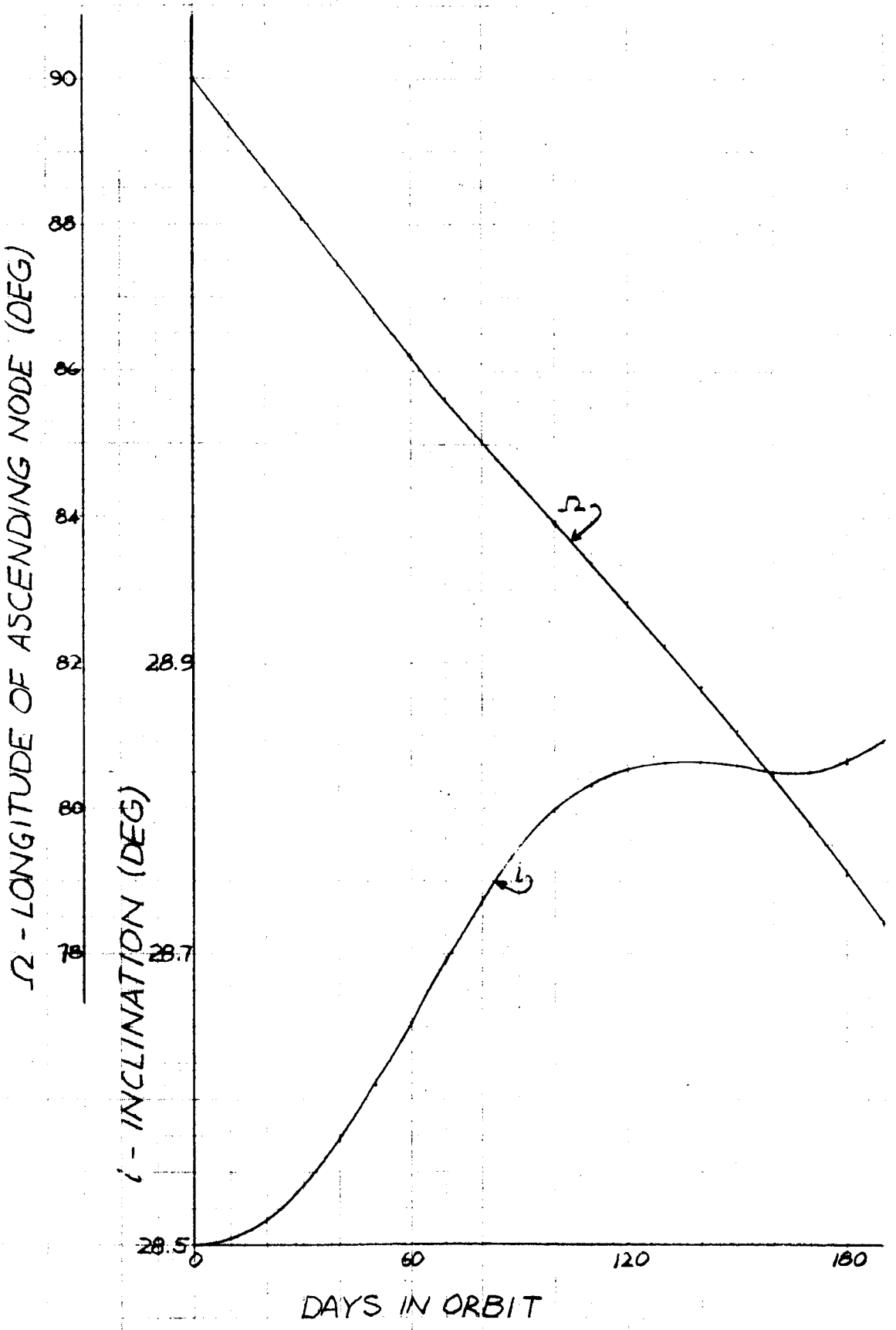

FIGURE 3.2-9

PERTURBED CIRCULAR ORBIT

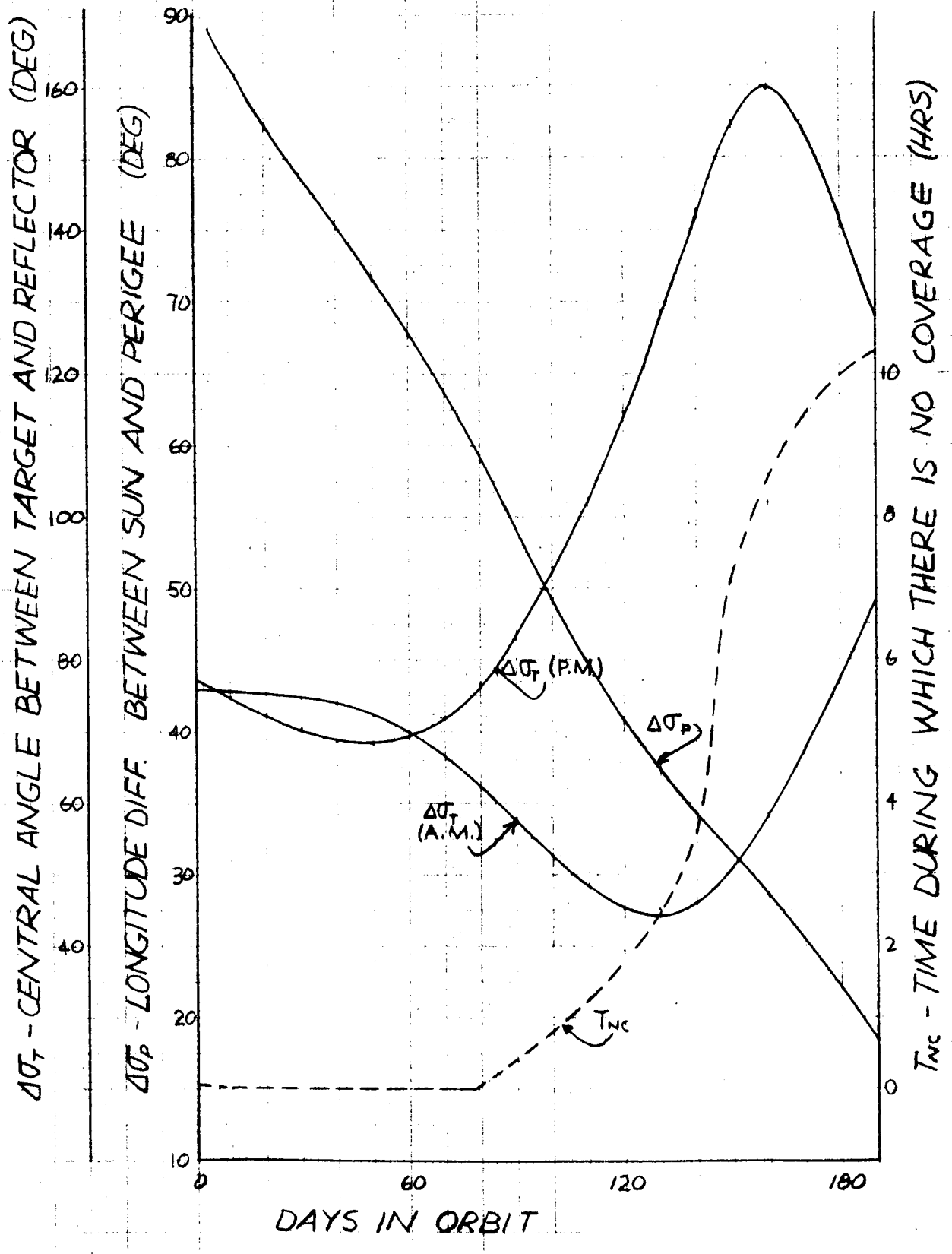

FIGURE 3.2-10

SOLAR ECCENTRICITY PERTURBATIONS DURING ONE MONTH

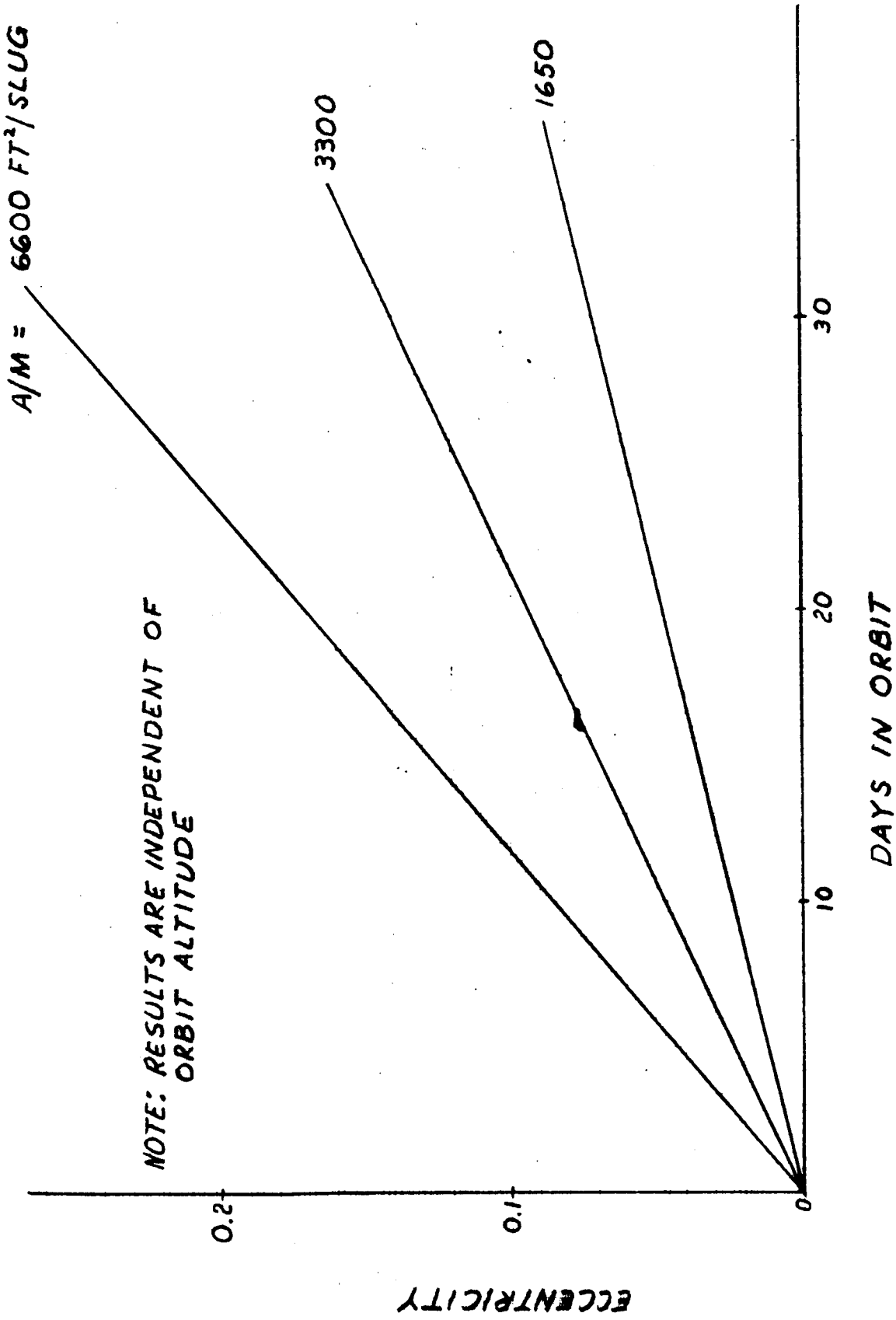

FIGURE 3.2-11

ECCENTRICITY PERTURBATIONS DUE TO SOLAR PRESSURE
(AFTER 23 DAYS IN ORBIT)

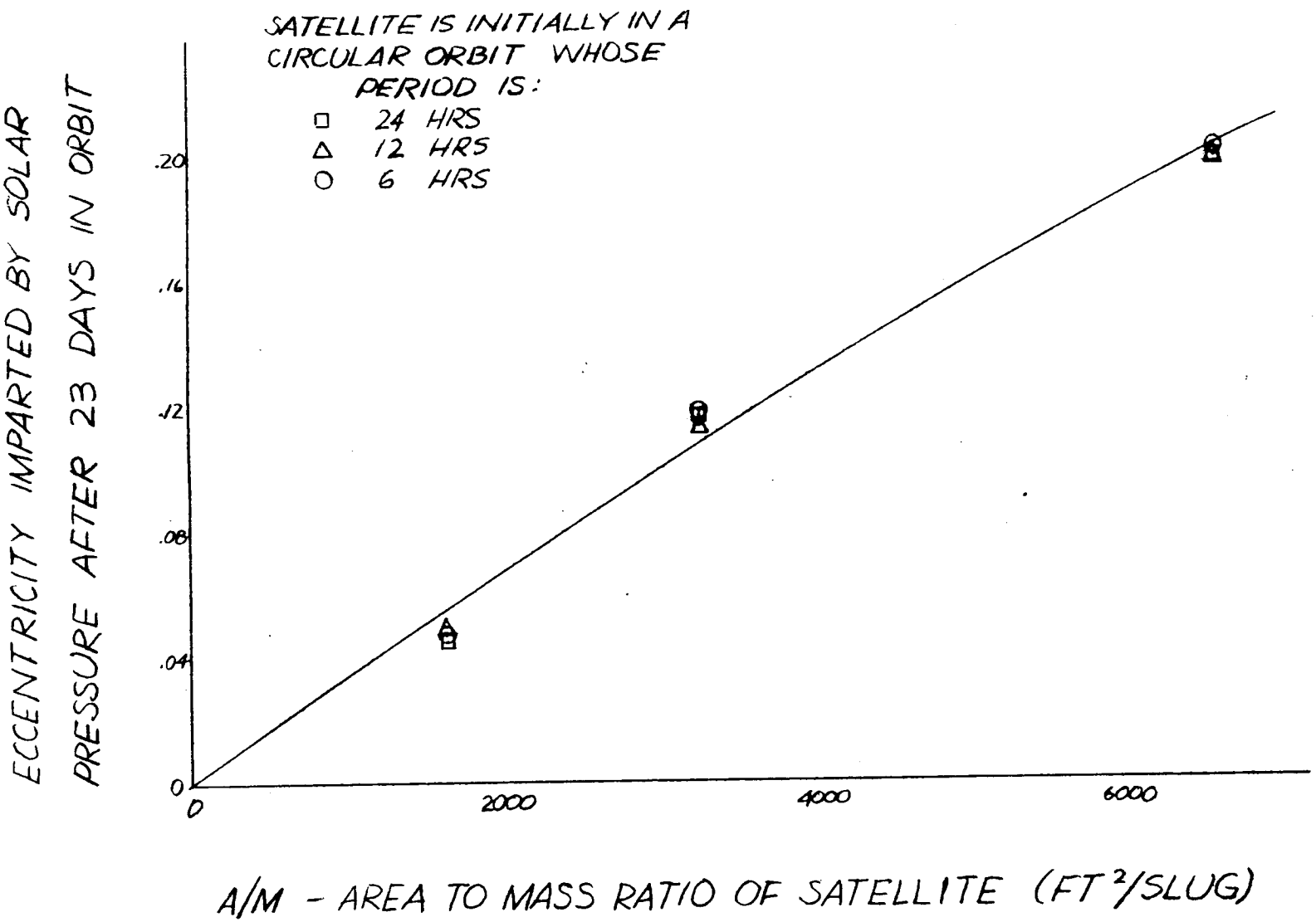

AZ 9/22/66

[redacted]

FIGURE 3.2-12

[redacted]

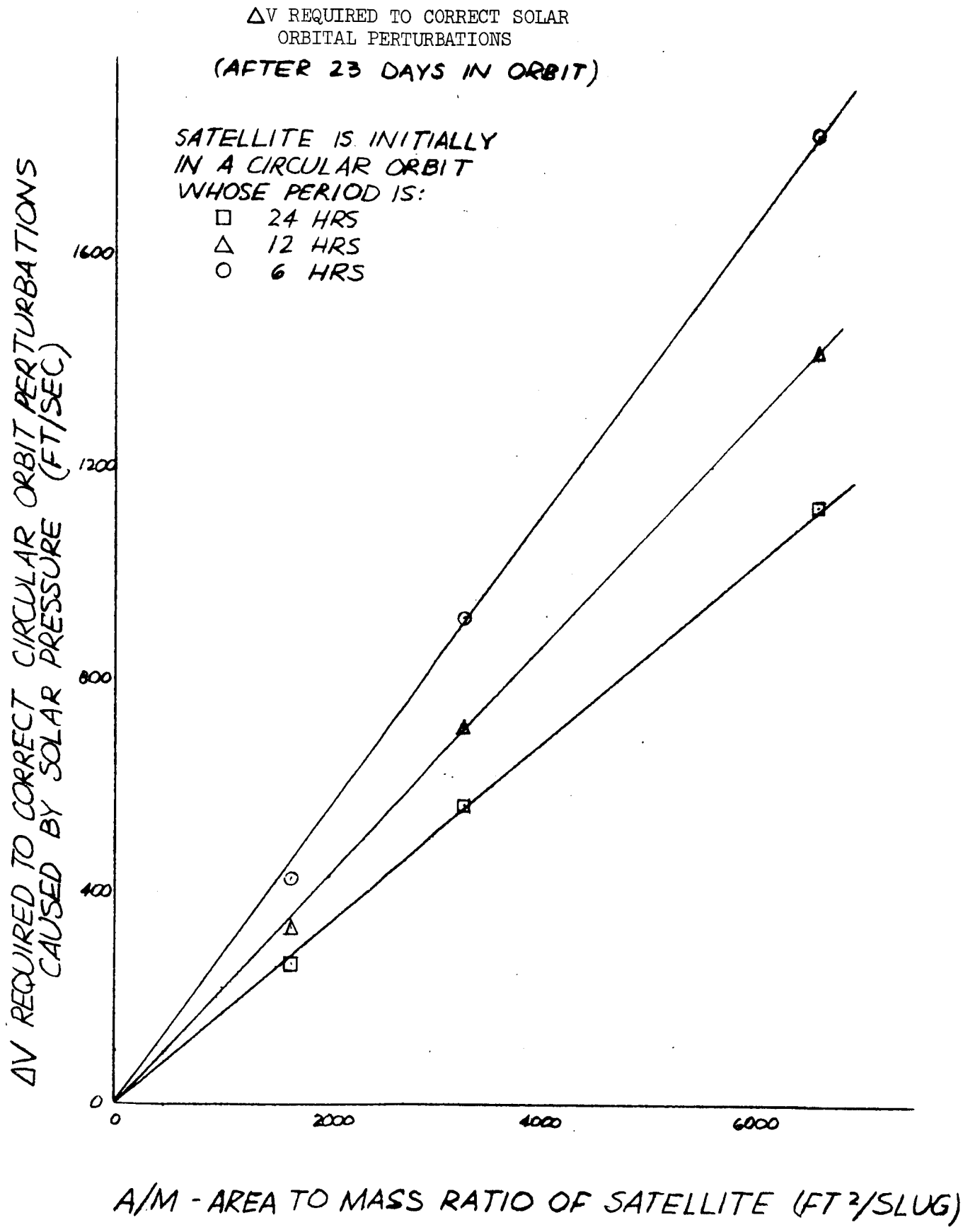

AE 9/22/66

FIGURE 3.2-13

[redacted]

[redacted]

STATIONKEEPING ΔV (SIX MONTH TOTAL)

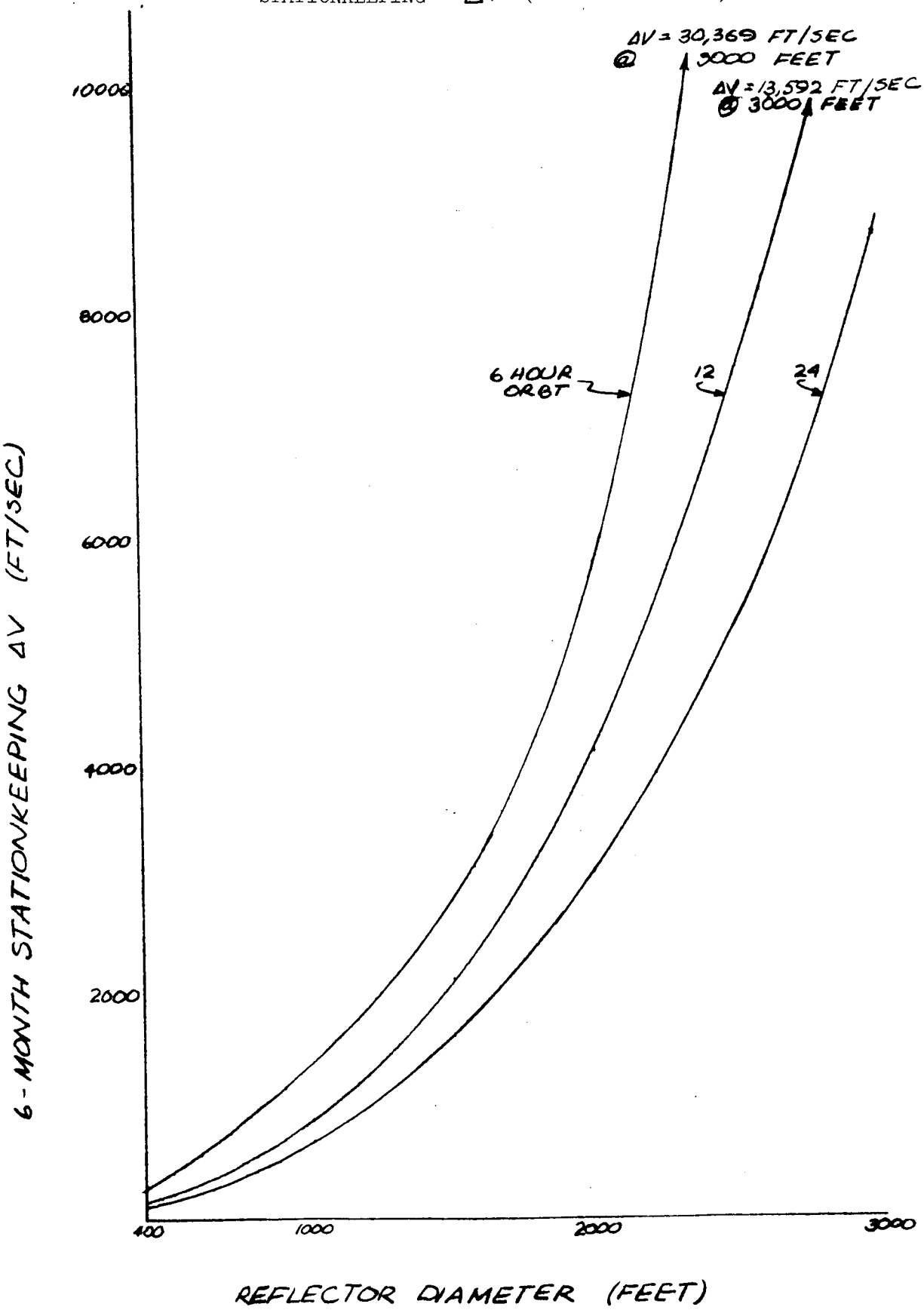

[redacted]

FIGURE 3.2-14

[redacted]

PROPELLANT WEIGHT REQUIREMENTS

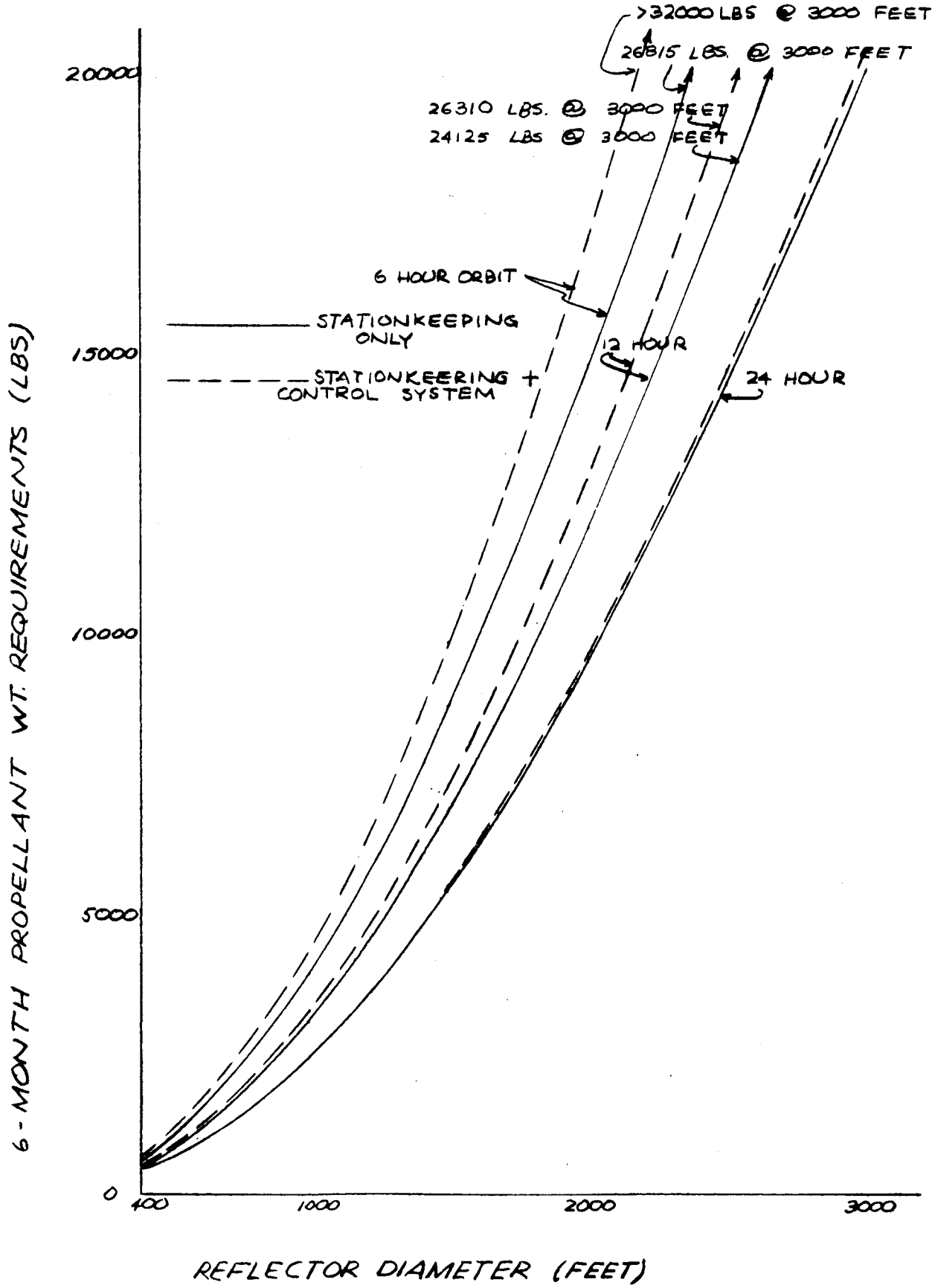

[redacted]

FIGURE 3.2-15

[redacted]

SIX MONTH TOTAL IMPULSE
REQUIREMENTS

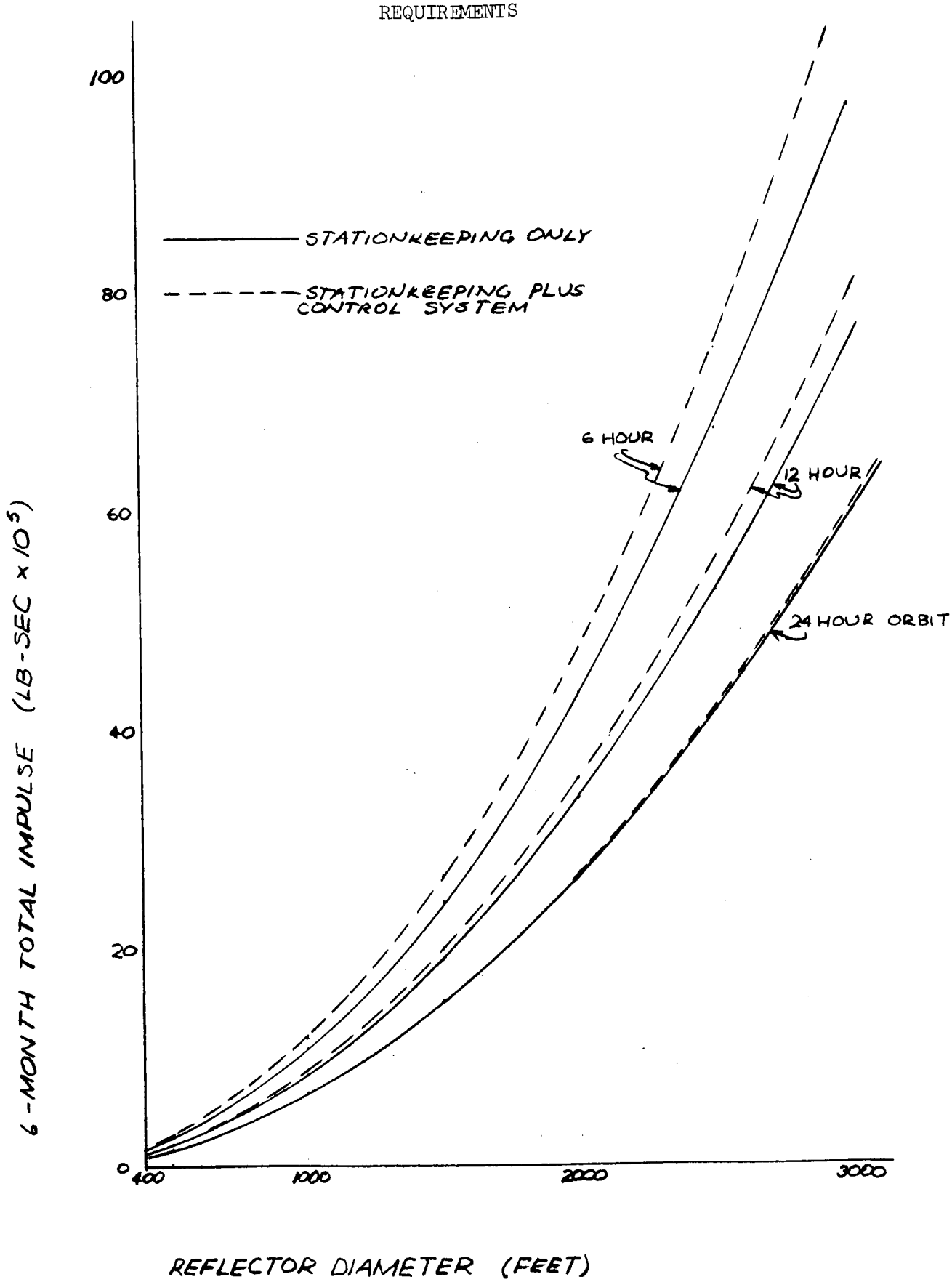

FIGURE 3.2-16

[redacted]

FIGURE 3.2-17

PROPULSION SYSTEM WEIGHT

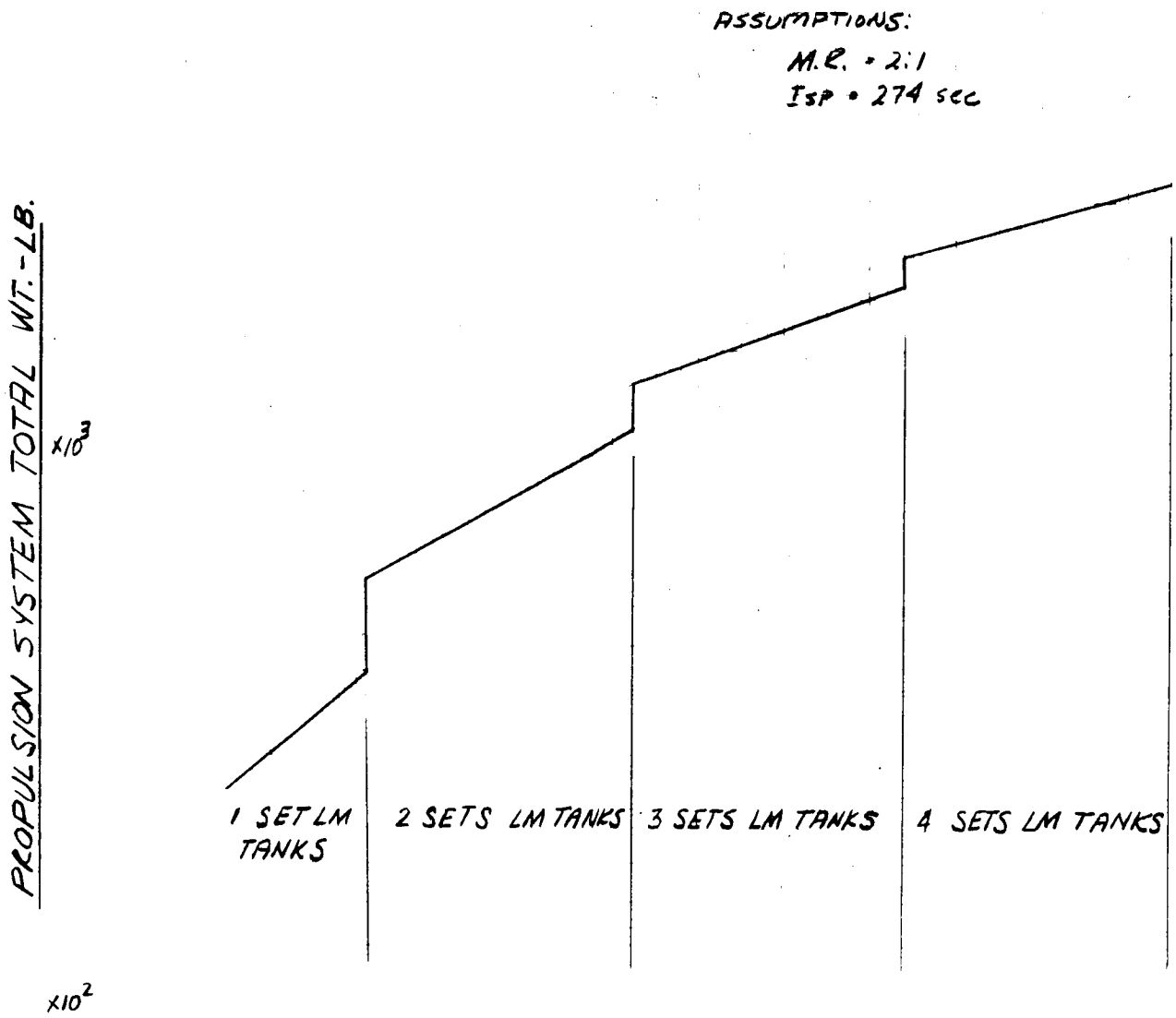

HS 10/19/66

[redacted]

PERTURBED "STABLE" ORBIT

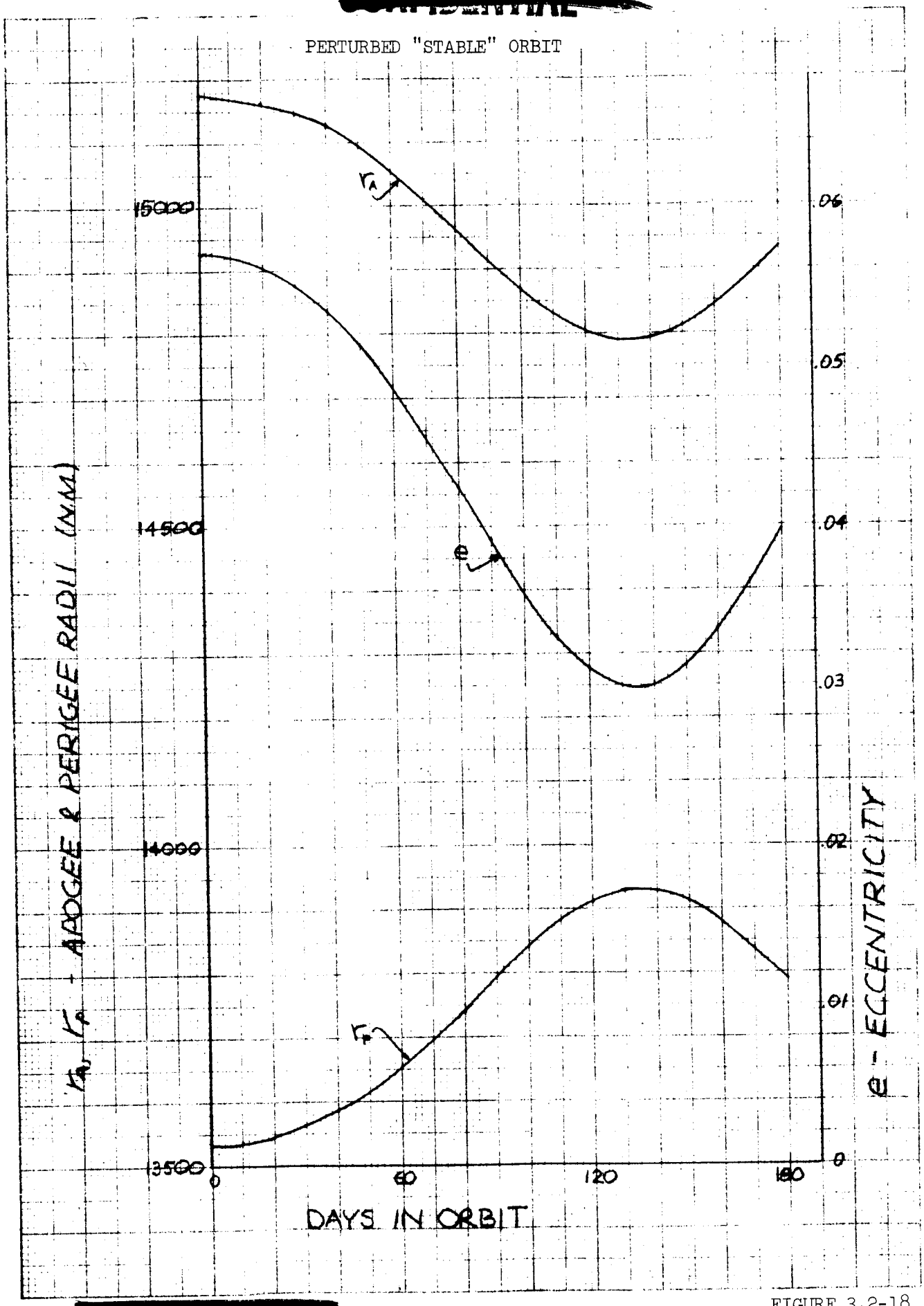

FIGURE 3.2-18

[redacted]

[redacted]

PERTURBED "STABLE" ORBIT

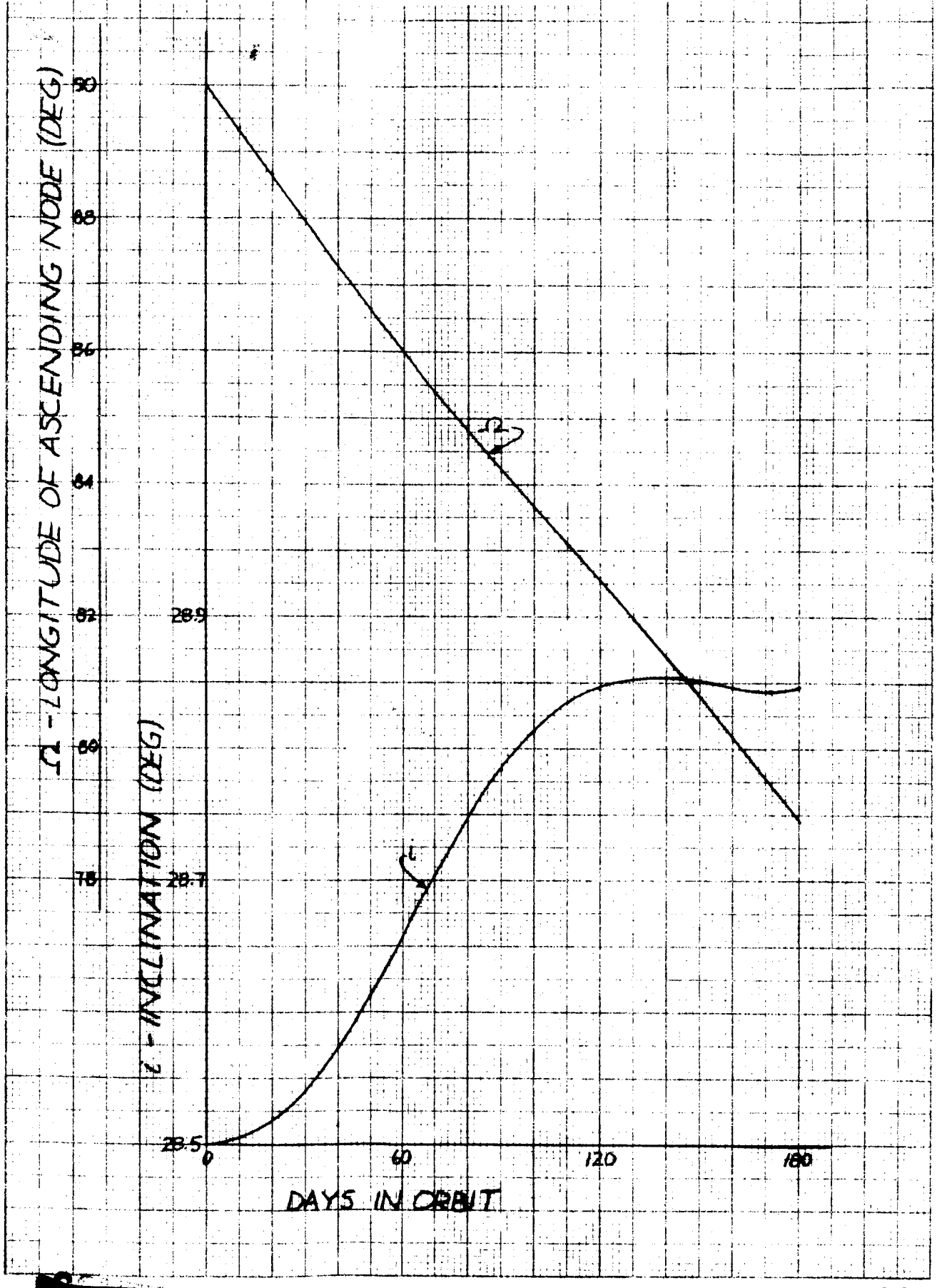

[redacted]

FIGURE 3.2-19

[redacted]

PERTURBED "STABLE" ORBIT

[redacted]

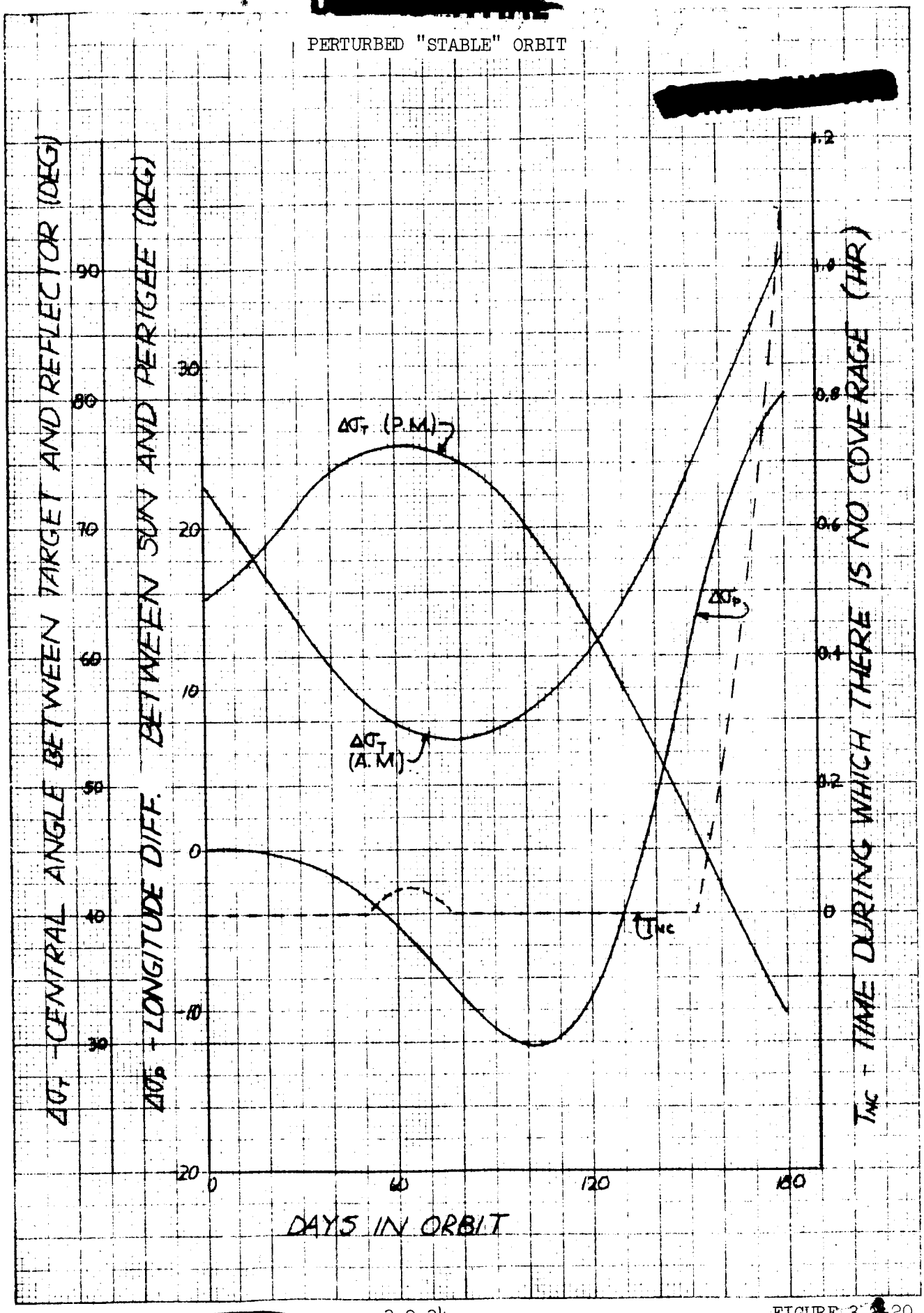

[redacted]

FIGURE 3.2-20

CONFIDENTIAL

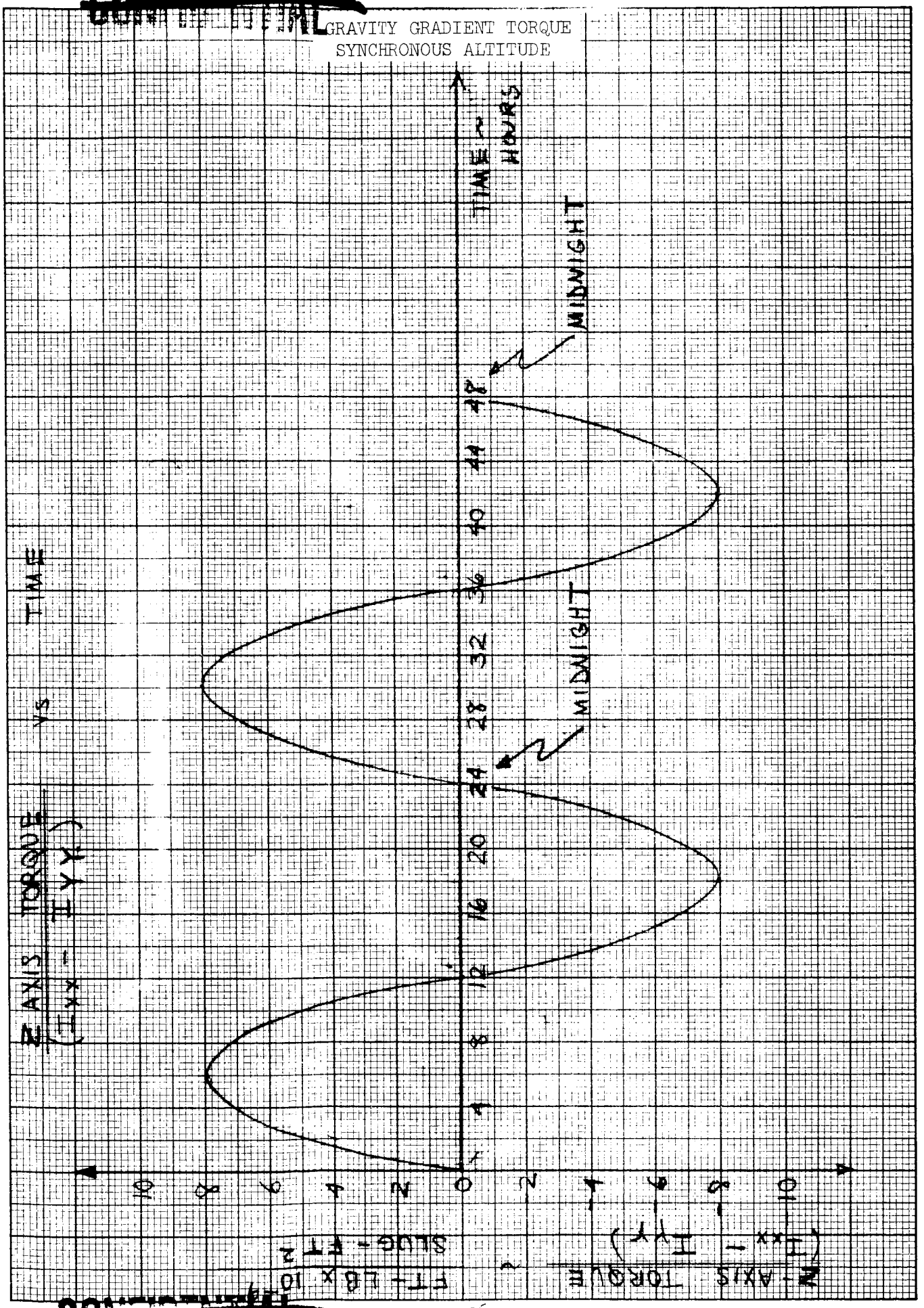

CONFIDENTIAL

FIGURE 3.2-22

[redacted]

ATTITUDE TIME LINE

12 HOUR STABLE ORBIT
INCLINATION = 28.5°
A/M = 1154 FT²/SLUG

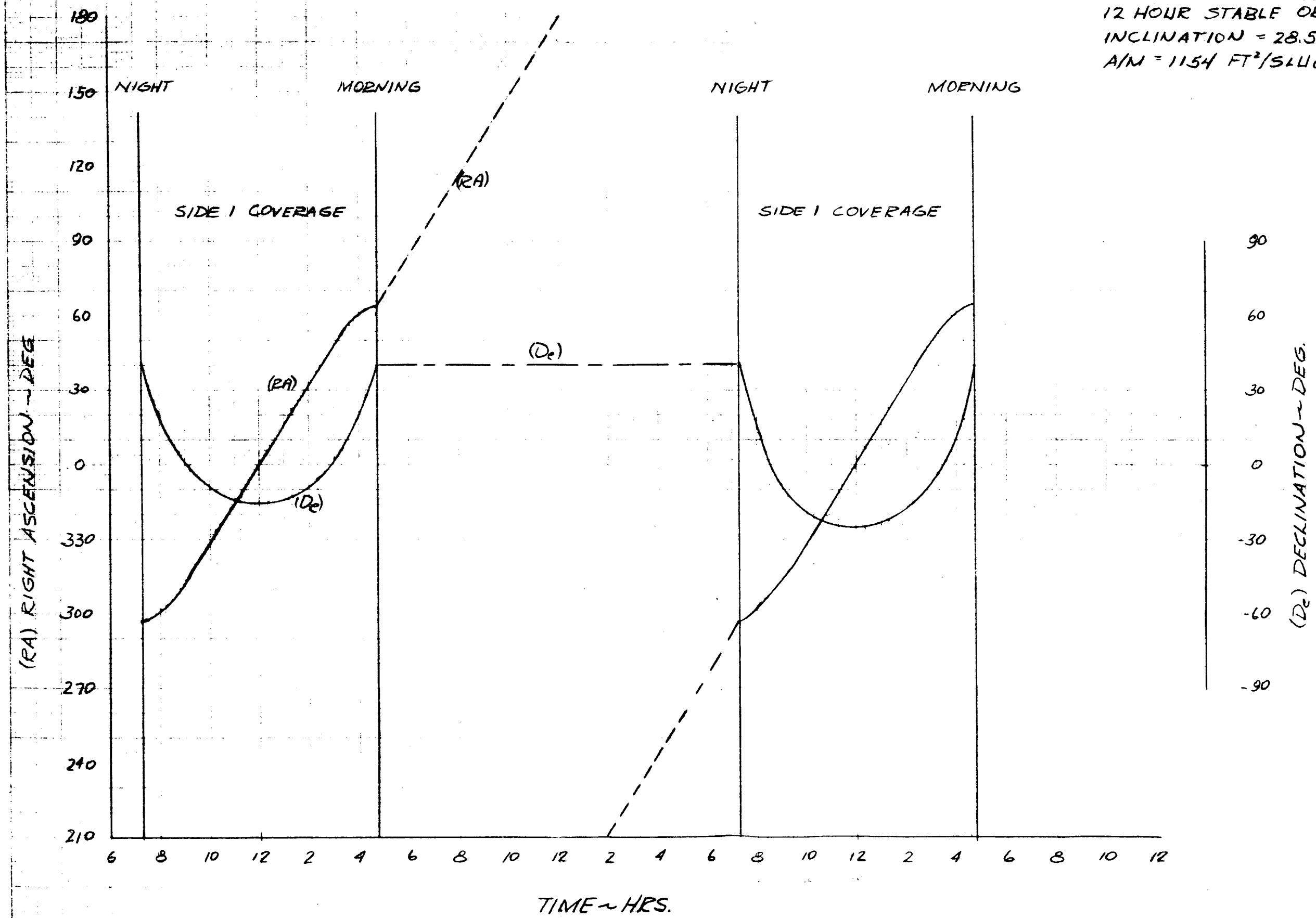

[redacted]

FIGURE 3.2-21

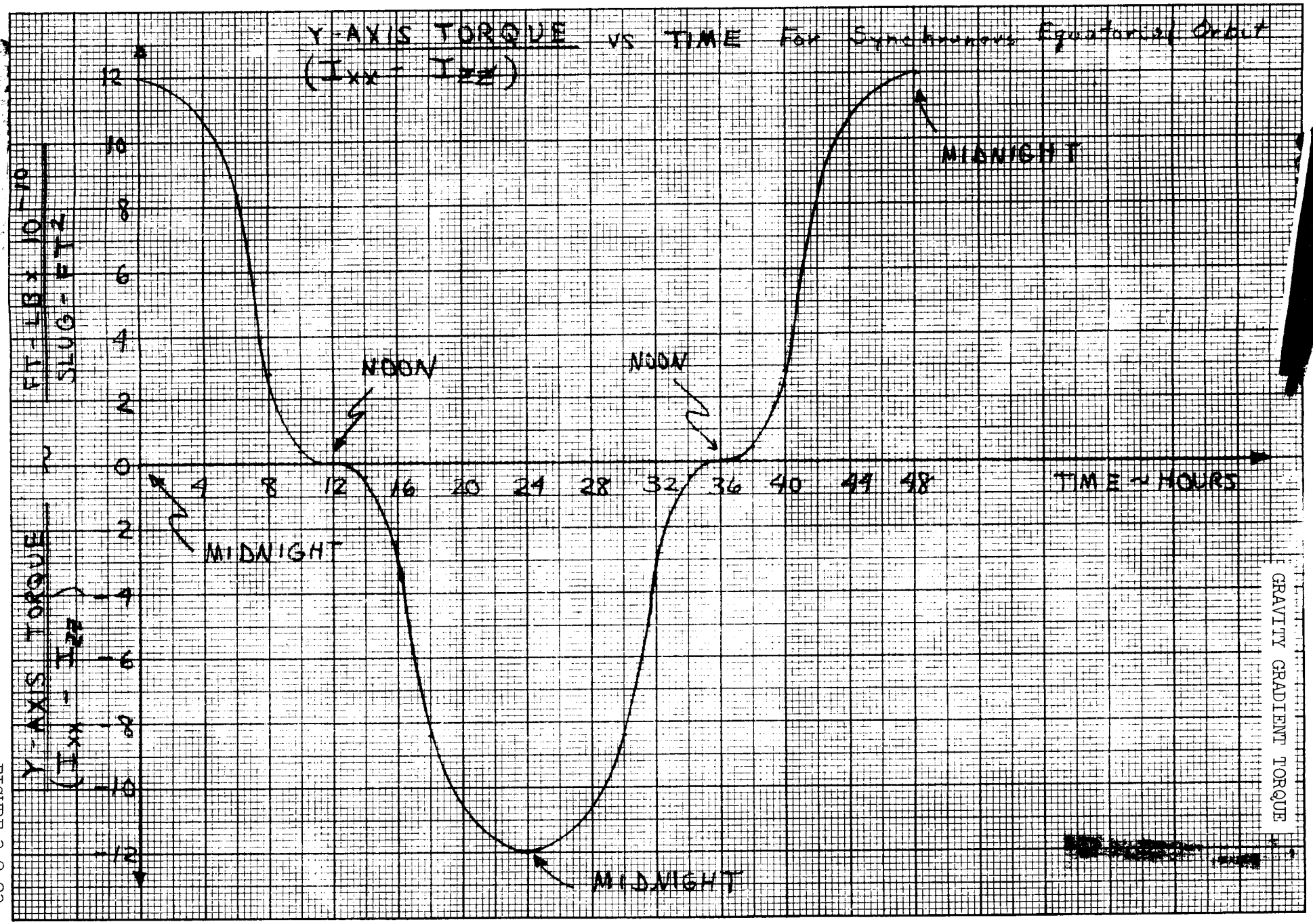

GRAVITY GRADIENT TORQUE

FIGURE 3.2-23

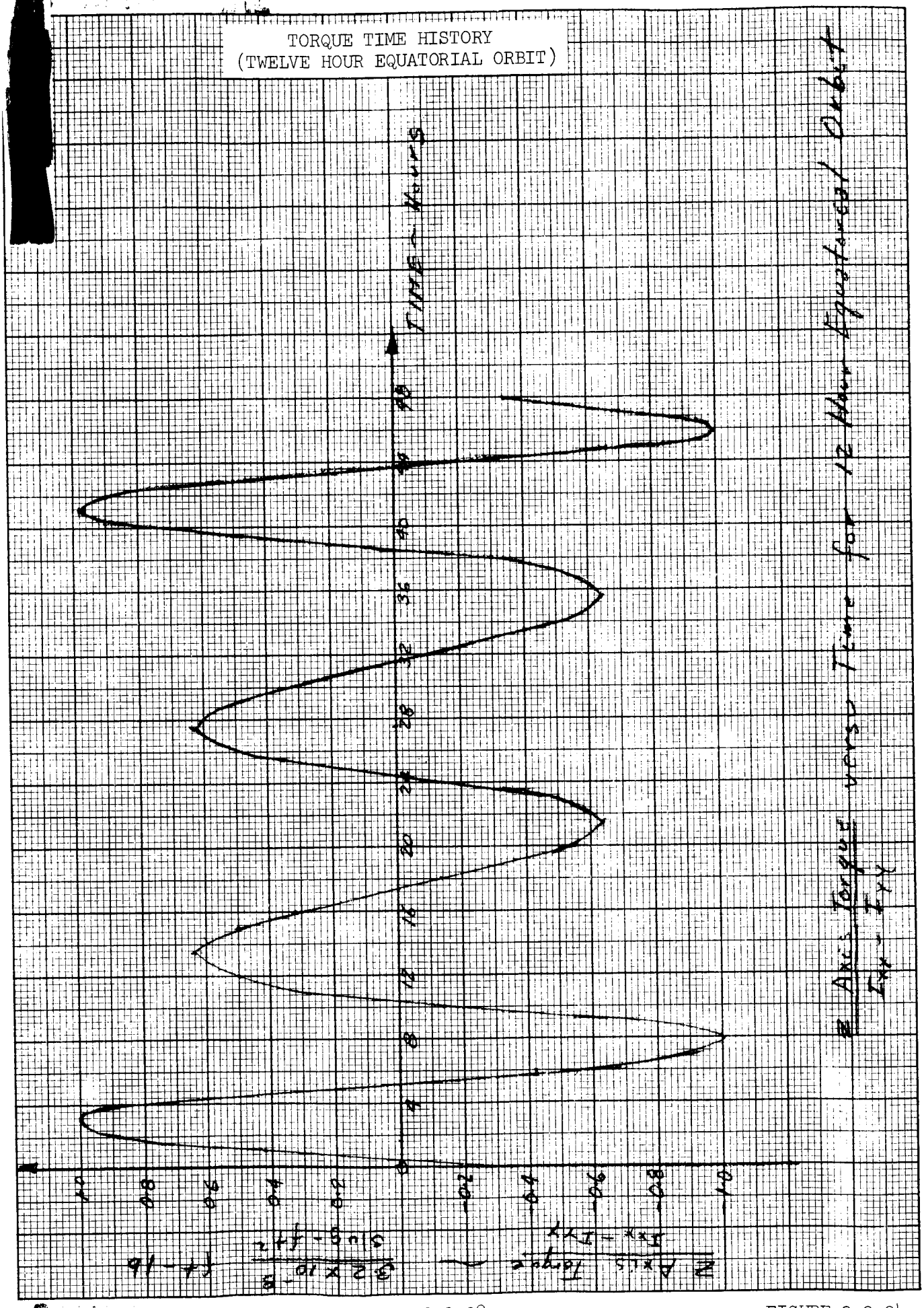
TORQUE TIME HISTORY
(TWELVE HOUR EQUATORIAL ORBIT)
Time - Hours
Z Axis Torque versus Time for 12 Hour Equatorial Orbit
Ext = Exx
Z Axis Torque ~ 9.2 x 10^-8 Ft-lb
Ixx - Iyy
9.2 x 10^-8 Ft-lb

FIGURE 3.2-24

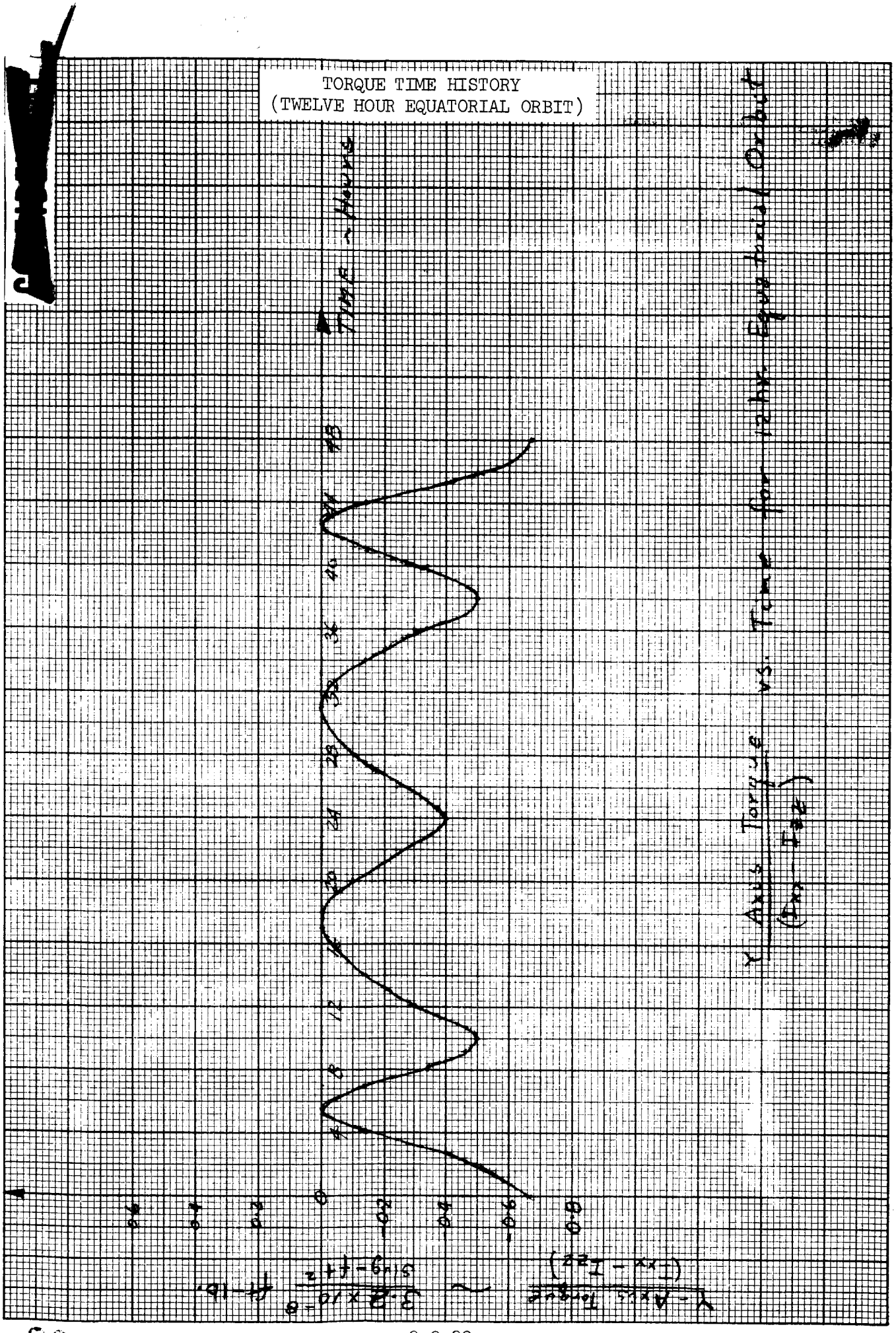
TORQUE TIME HISTORY
(TWELVE HOUR EQUATORIAL ORBIT)
Y Axis Torque vs. Time for 12 hr. Equatorial Orbit
(Ex - Ezz)
Time ~ Hours
0.8
0.6
0.4
0.2
0
-0.2
-0.4
-0.6
-0.8
4
8
12
16
20
24
28
32
36
40
44
48

FIGURE 3.2-25

[redacted]

TORQUE TIME HISTORY
(SIX HOUR EQUATORIAL ORBIT)

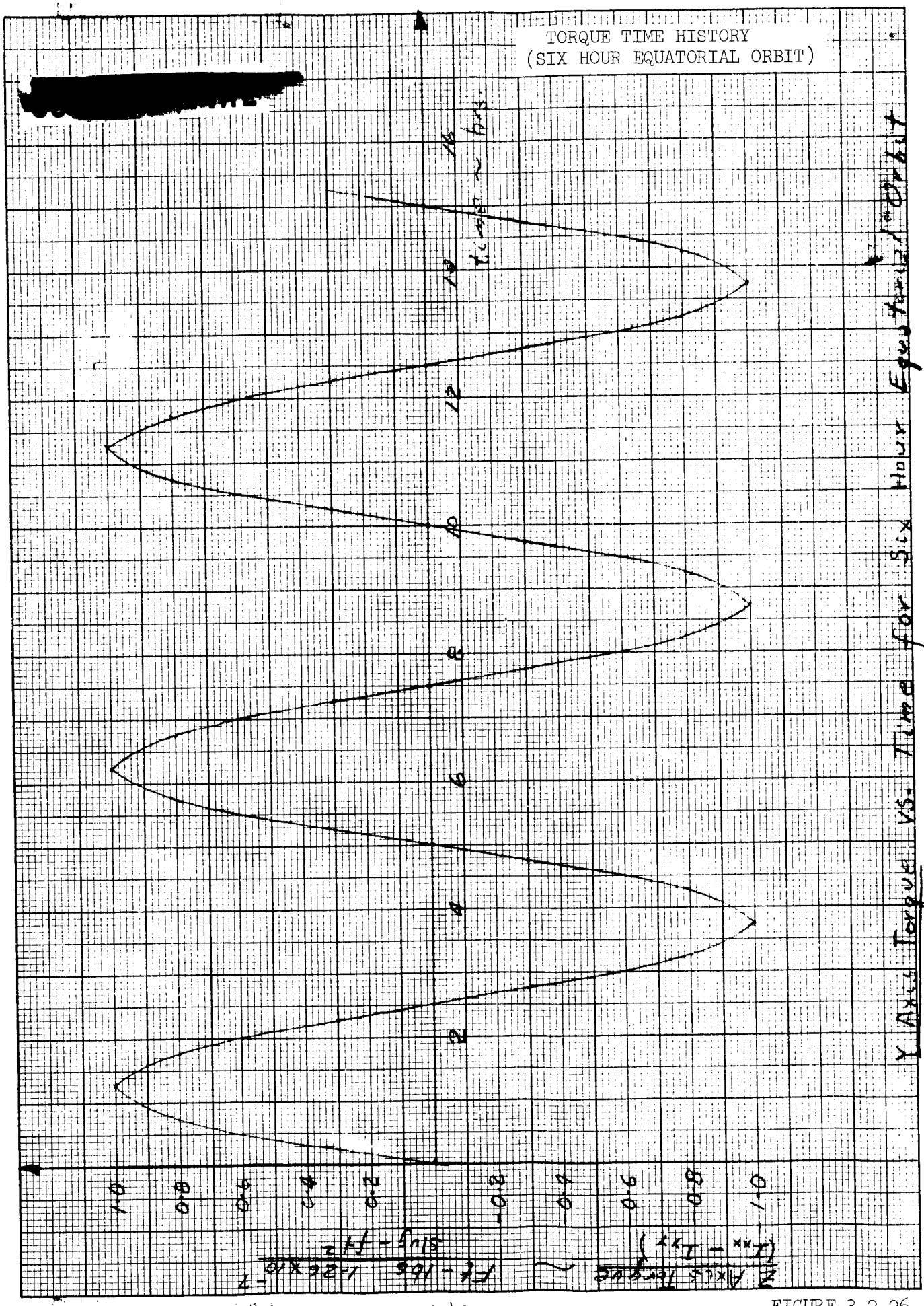

Y Axis Torque vs. Time for Six Hour Equatorial Orbit

$(I_{xx} - I_{yy})$

3.2-40

FIGURE 3.2-26

[redacted]

TORQUE TIME HISTORY
(SIX HOUR EQUATORIAL ORBIT)

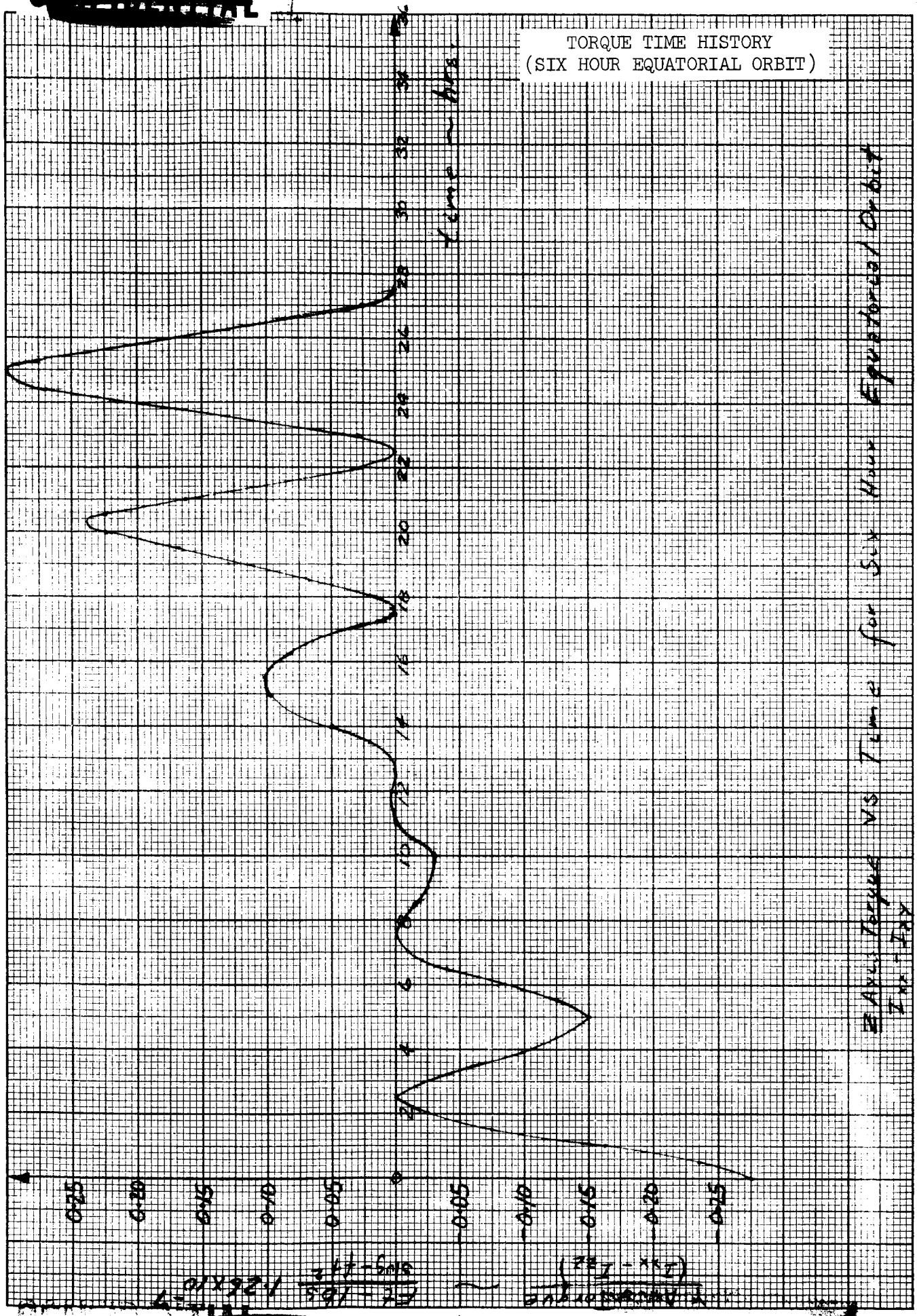

[redacted]

FIGURE 3.2-27

[redacted]

SOLAR TORQUE TIME HISTORY

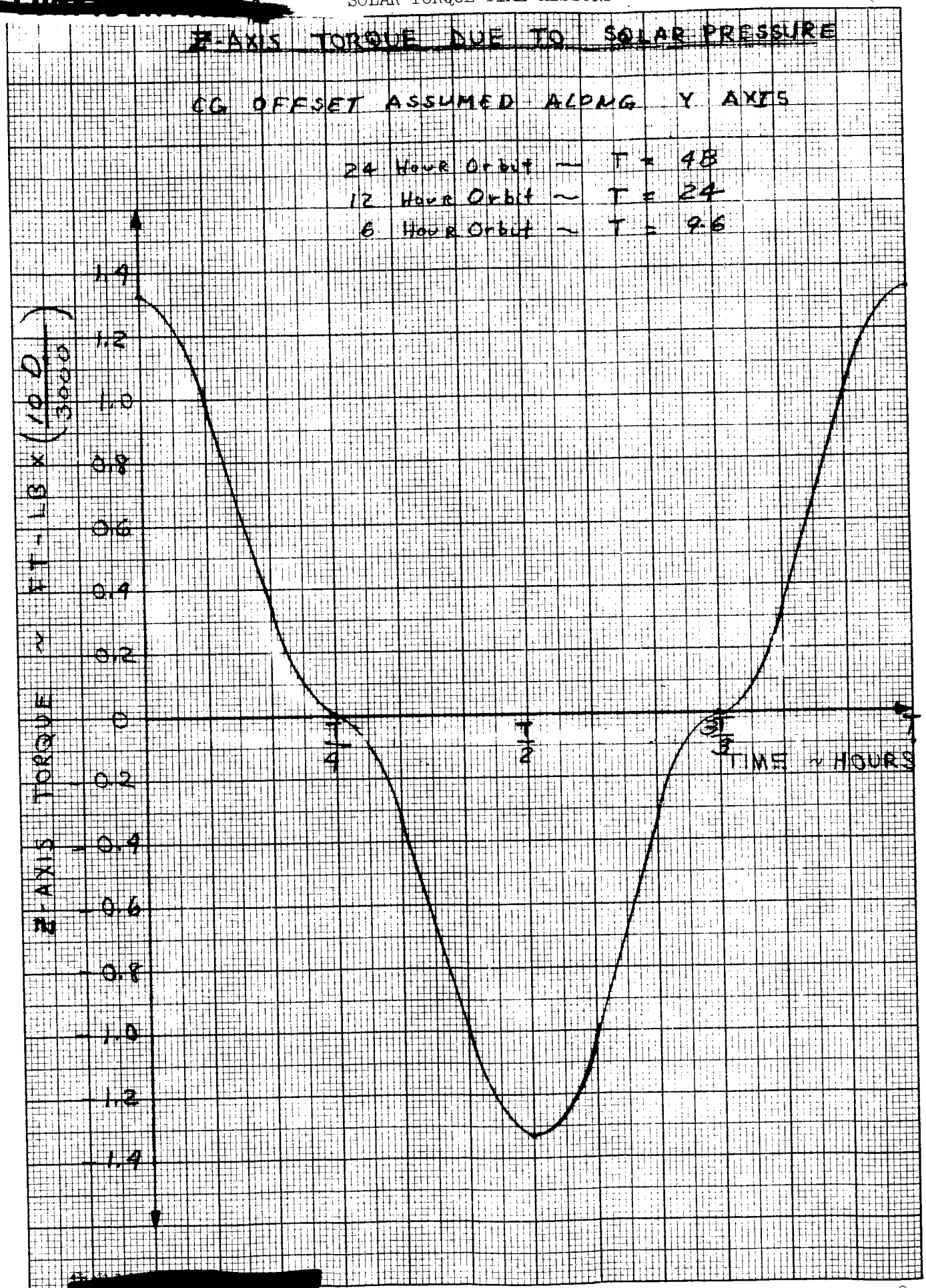

[redacted]

FIGURE 3.2-28

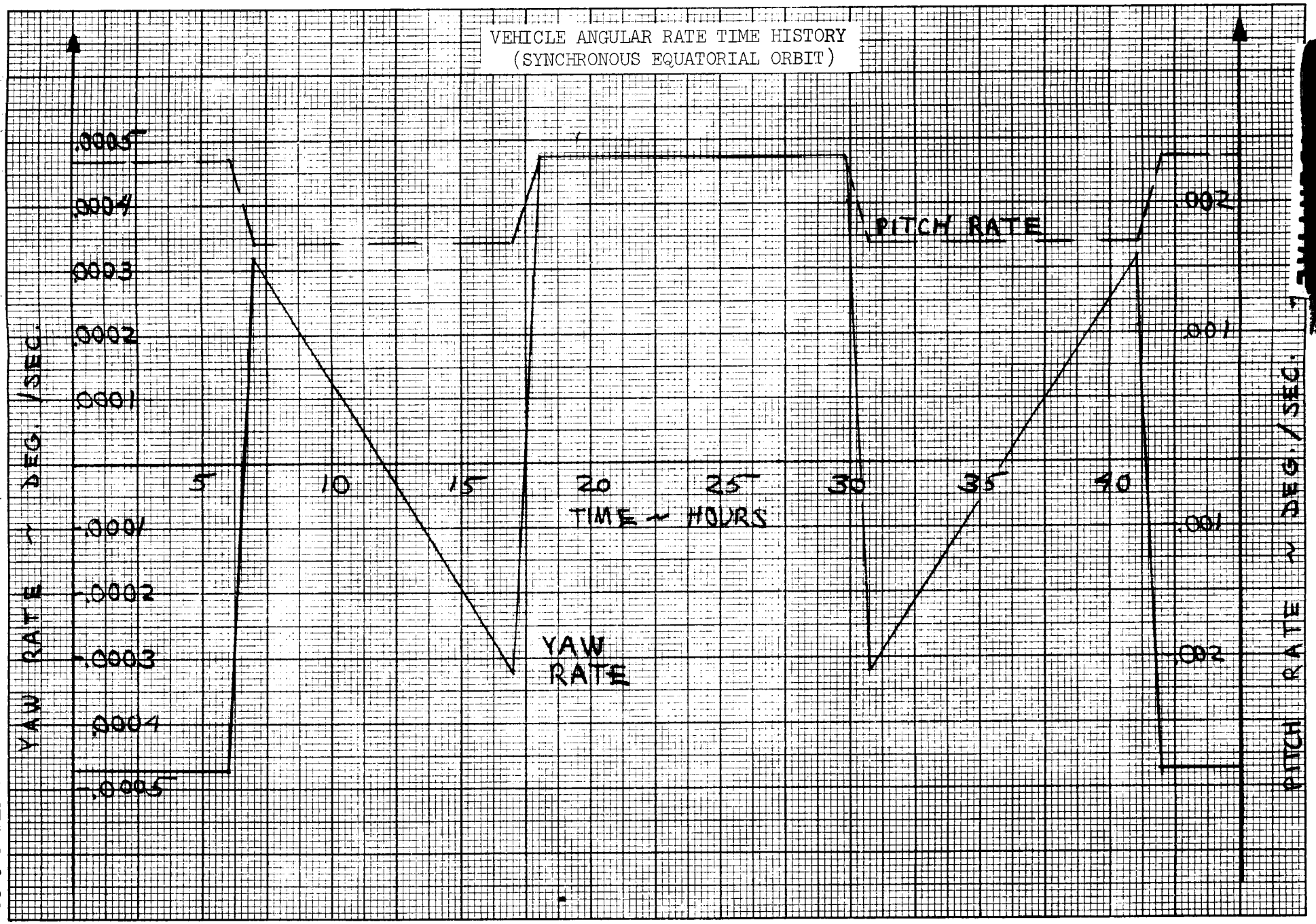
VEHICLE ANGULAR RATE TIME HISTORY
(SYNCHRONOUS EQUATORIAL ORBIT)
YAW RATE ~ DEG./SEC.
.0005
.0004
.0003
.0002
.0001
-.0001
-.0002
-.0003
-.0004
-.0005
5
10
15
20
25
30
35
40
TIME ~ HOURS
YAW RATE
PITCH RATE
PITCH RATE ~ DEG./SEC.
.002
.001
-.001
-.002

FIGURE 3.2-29

VEHICLE ANGULAR RATE TIME HISTORY
(TWELVE HOUR EQUATORIAL ORBIT)

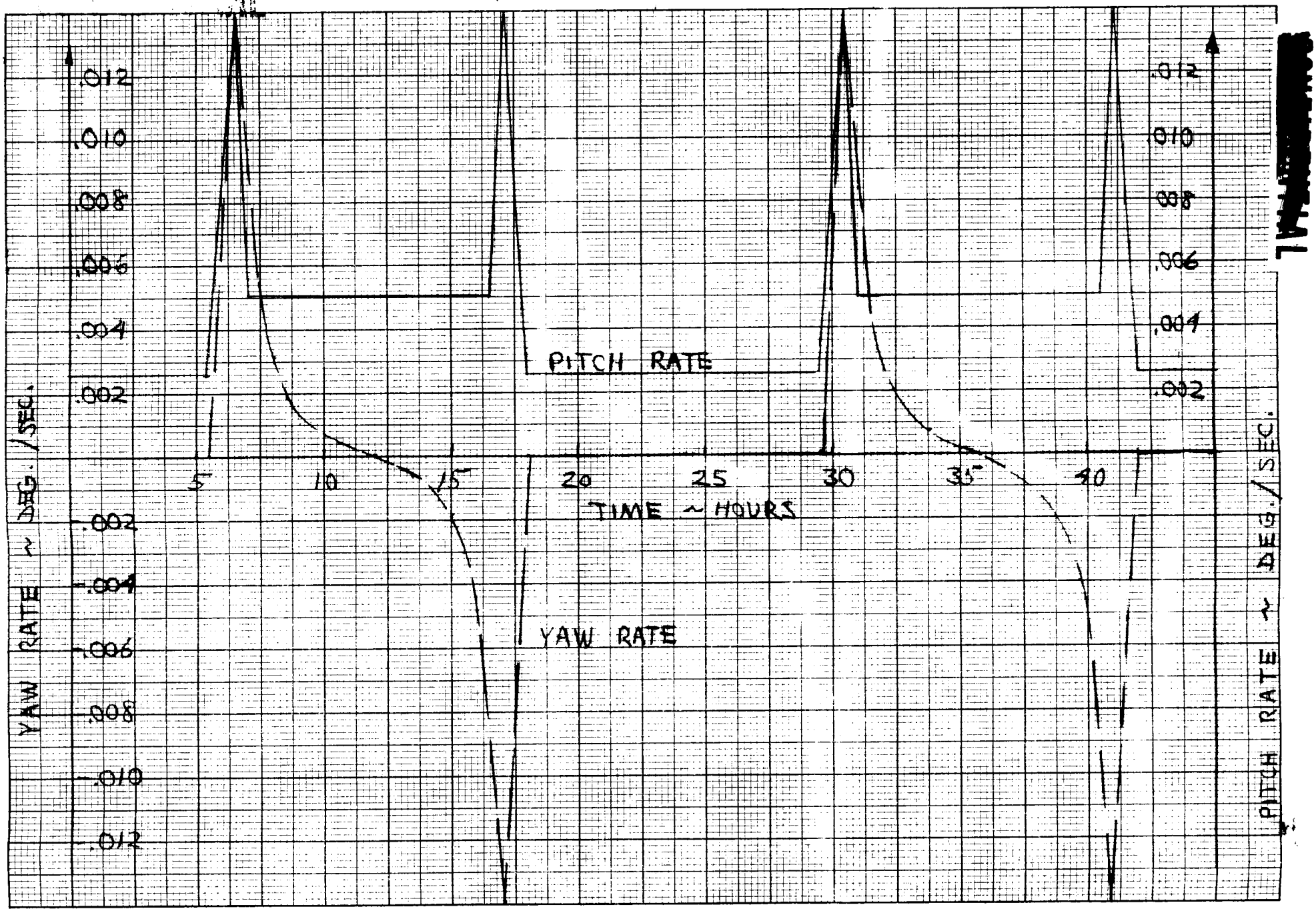

FIGURE 3.2-30

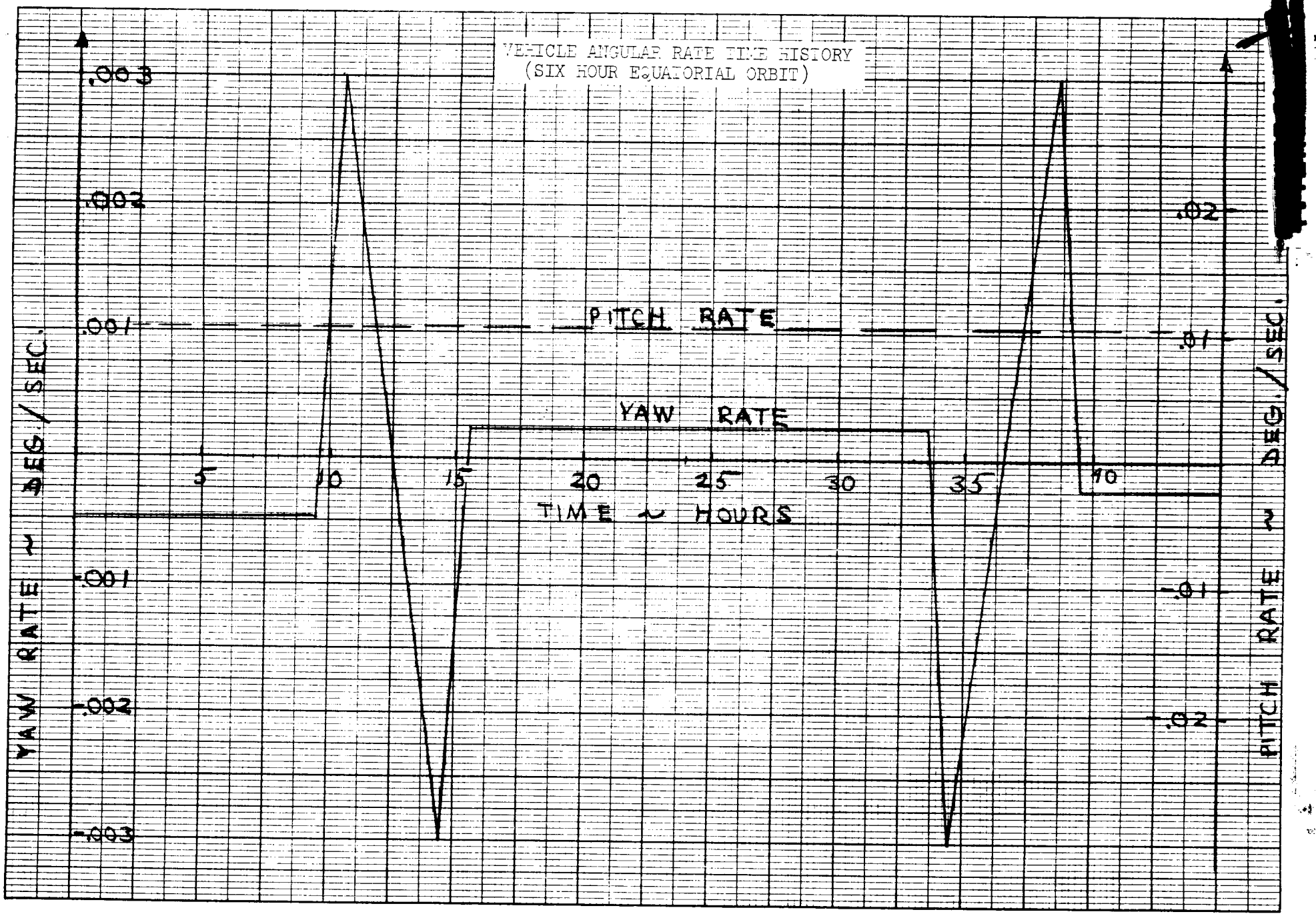
VEHICLE ANGULAR RATE TIME HISTORY
(SIX HOUR EQUATORIAL ORBIT)
PITCH RATE
YAW RATE
TIME ~ HOURS
YAW RATE ~ DEG./SEC.
PITCH RATE ~ DEG./SEC.
.003
.002
.001
-.001
-.002
-.003
.02
.01
-.01
-.02
5
10
15
20
25
30
35
40

FIGURE 3.2-31

FIGURE 3.2-32

MINIMUM CONTROL TORQUE REQUIREMENTS
FOR EQUATORIAL ORBITS

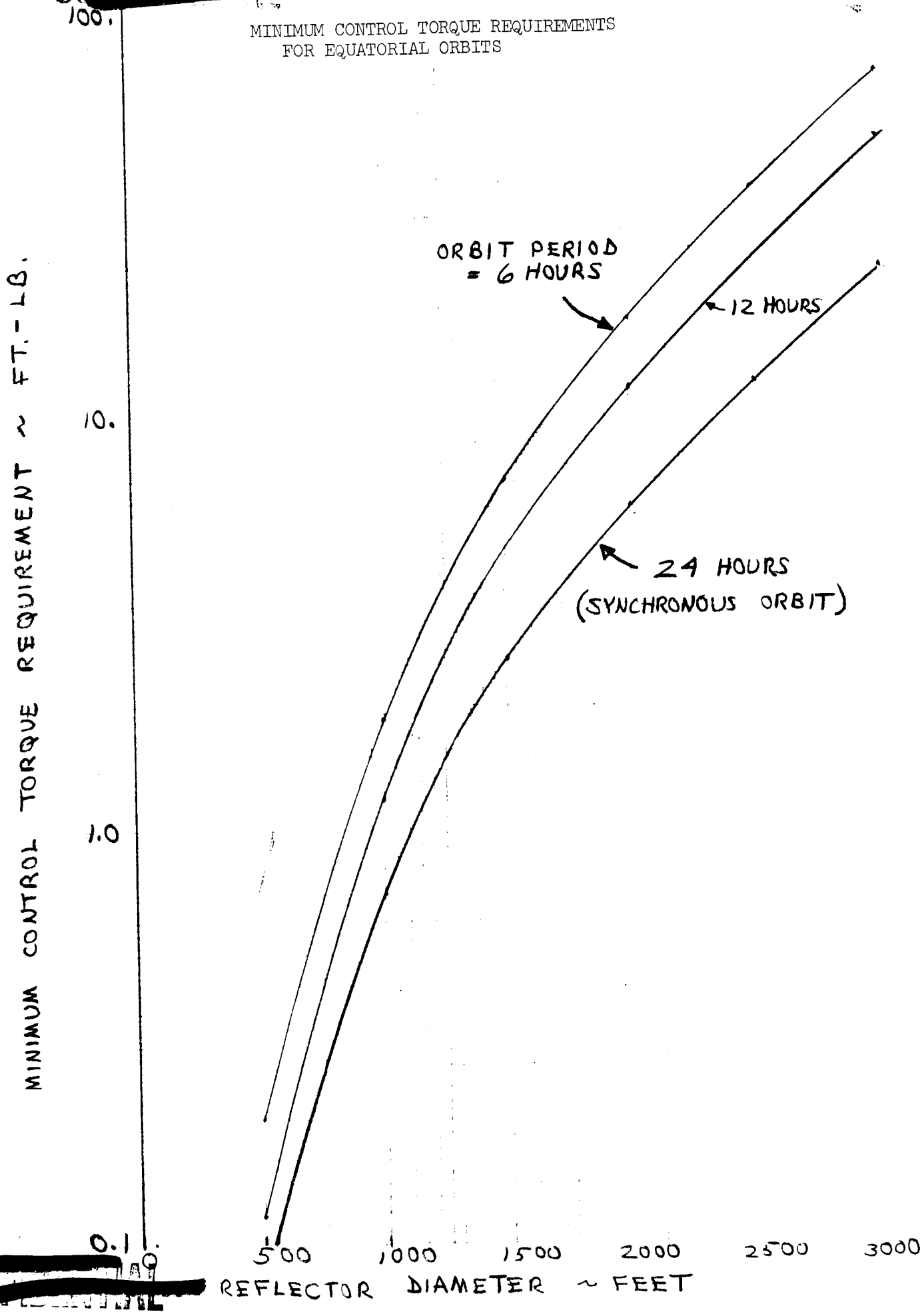

[redacted]

FIGURE 3.2-33

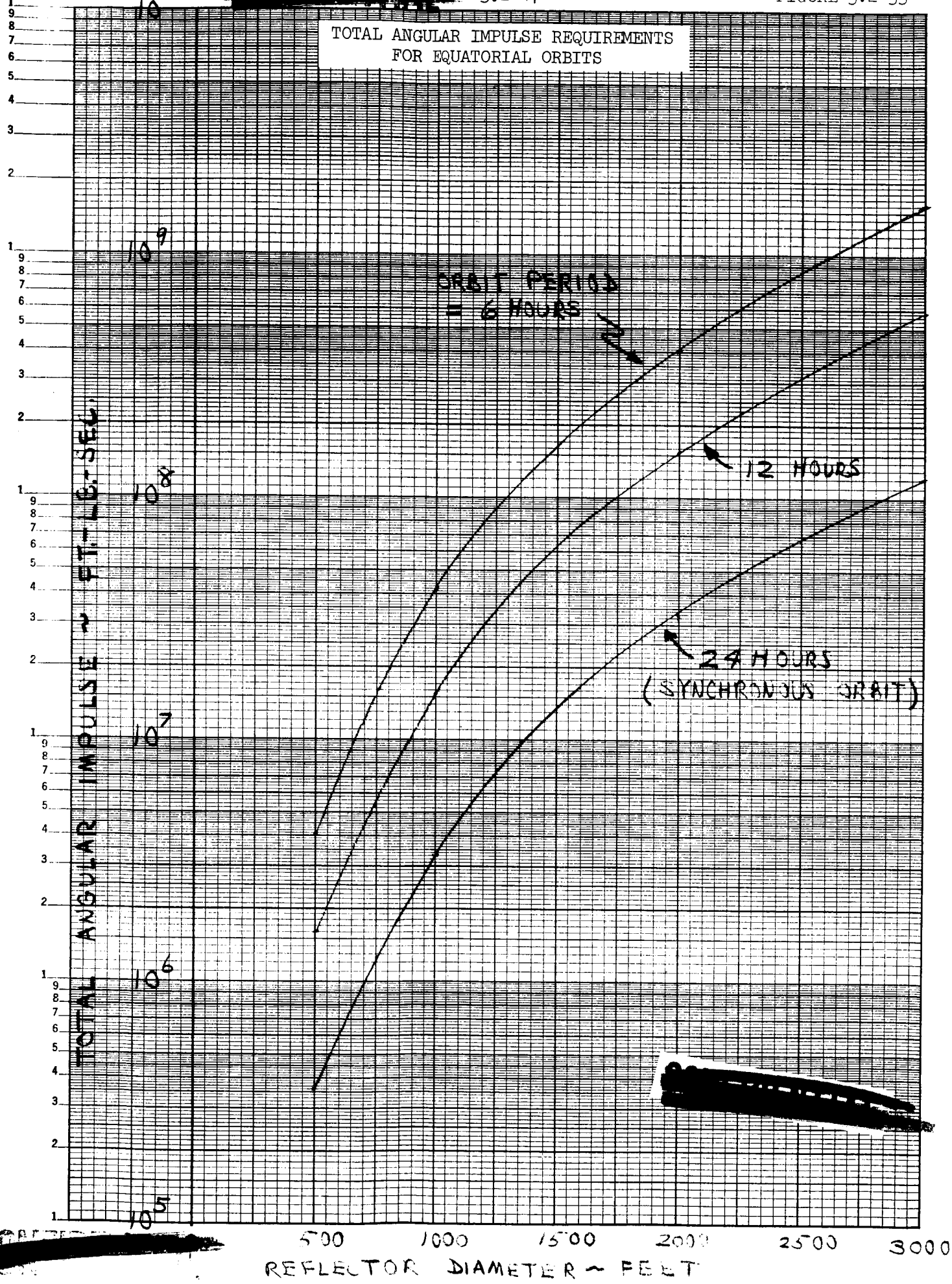

[redacted]

[redacted]

3.3 MANNED VERSUS UNMANNED MISSION

3.3.1 Mission Comparison

The differences between a manned and an unmanned mission start with the launch configuration and terminate with the monitoring of the initial operational phases of the ABLE mission. The six month operational phase would be unmanned, even for a manned flight. A comparison of manned versus unmanned mission parameters is summarized in Table 3.3-1.

There are actually two manned mission configurations, single Saturn V launch and dual Saturn V launch, as discussed in Section 3.5. The dual Saturn V launch would actually be a combination of the features described in Table 3.3-1, for both manned and unmanned missions, during the launch and orbital achievement phases. Of course, rendezvous and docking would also be required. Subsequent to spacecraft docking in orbit, the rest of the dual launch mission would be identical to the manned Saturn V launch conditions listed in Table 3.3-1.

3.3.2 Potential Uses of Man

In "flying" a manned mission, one can take advantage of the greater flexibility of having a "man in the loop", plus the increased overall reliability of the manned mission (Section 5.4). In particular, for the ABLE mission, man's visual observation and monitoring capability could be especially valuable since some of the flight operational procedures, such as reflector deployment, would probably never have previously been ground tested.

The major potential uses/advantages of man would be in the areas of:

- Control of reflector deployment and rigidization
- Checkout of ABLE LM subsystems
- Alignment of reflector and adjustment of tension
- Monitoring of intial operational phases
- Correcting failures, or reducing their effects
- General verification of operations in areas difficult to ground test

[redacted]

3.3.2 (Continued)

Man has the unique capability to provide on-the-spot analysis and decision making, in-flight schedule change, and "trouble-shooting" and maintenance. It has been found that the most reliable systems are those which incorporate both a man-machine interraction together with redundant modes of operation.

3.3.3 Preliminary Conclusions

The evaluation of the need for man to aid in implementing the ABLE mission concept has resulted in the following preliminary conclusions:

- Man should be considered for the first ABLE flight(s)
- Man's value on subsequent flights requires further study

A program concept permitting a late discussion on manned versus unmanned ABLE flights is therfore recommended. This would mean that the ABLE spacecraft should be designed so that it could be flown on either a manned or unmanned flight.

TABLE 3.3-1

ABLE MISSION COMPARISON

Mission Type Parameters	Unmanned Saturn V Launch	Manned Saturn V Launch
Launch Conditions	Could utilize direct ascent method to orbit; greater payload capability.	Requires parking orbit concept and multiple (3) burn capability of SIVB stage; lower orbital payload capability.
Orbital Achievement	Direct ascent or earth parking orbit feasible (less payload for direct ascent method); no rendezvous required.	Earth parking orbit concept to orbital altitude more economical with greater payload capability. No rendezvous but transposition required.
System Check-out	Automatic systems check-out required. Monitoring required by ground control.	Manned systems check-out feasible and more simplified procedures available.
Reflector Deployment	Automatic reflector deployment system required, monitored by ground	Man-assisted reflector deployment sys. feasible. Less complex deploy system required. Filming of deployment by 3-man crew.
Reflector Check-out	Automatic alignment, calibration & check-out system required, monitored by ground through closed loop TV system and other instrumentation.	Semi-automatic and man-assisted procedures can be utilized and simplified to checkout reflector system. Data on checkout acquired by crew.
Reflector Positioning/ Pointing	Automatic means to position/point reflector required, monitored by ground control	Man-assisted capability exists for greater accuracy. May be subjected to more disturbance torques (man-made).
Data Acquisition	Automated (preprogrammed) data acquisition and storage capability required. TV and other instrumentation required, monitored by ground control.	Vital man inputs/outputs & on site data capability exists through direct voice communication. Minimum data storage required during manned portion direct filming of reflector sys. (Deployment, etc.) by crew exists.
Communications	Automated uplink-downlink system required for continuous monitoring by ground control	Direct voice communications with crew available, not required on continuous basis, during manned portion of mission.

TABLE 3.3-1

ABLE MISSION COMPARISON

(Continued)

Mission Type Parameters	Unmanned Saturn V Launch	Manned Saturn V Launch
Initial Operational	Automated operational checkout and status monitoring required by ground control.	Crew monitoring capability exists with further adjustments to reflector system as necessary.
Mission Support	Staging of reflector deployment and operation required if continuous communications not available; modifications to reflector system and ground support operations required.	Availability of crew, during manned portion deletes continuous communications requirement existing MSFN ground support operations network utilized.

[redacted]

3.4 RADIATION CONSIDERATIONS

3.4.1 Environment

The radiation environment that was used for this study came from two different sources. One was the MSFC specified election and proton spectra for both 6,000 nautical mile and synchronous altitude near equatorial orbits.

The other was a projected 1968 environment for 30° inclination orbits at altitudes from 6,000 to 18,000 nautical miles (Ref. 3.4-1) which was chosen in order to evaluate the potential radiation hazard at altitudes between 6,000 nautical miles and synchronous. The radiation spectra of Ref. 3.4-1 yielded dose rates from one to two orders of magnitude higher than the above mentioned MSFC environment at the 6,000 nautical mile altitude. No direct comparison was possible at synchronous altitude. The major reason for the difference is the difficulty in predicting the environmental model for the 1968 time period since the environment varies drastically around solar maximum.

Dose rate calculations were performed and evaluated from both spectra at 6,000 nautical miles, for the spectra of Ref. 3.4-1 between 6,000 and 18,000 nautical miles and for the MSFC spectrum at synchronous altitude. The effect of solar flare radiation was ignored since, relative to the dose rates from the natural environment, it resulted in both:

- A low probability of receiving greater doses during the relatively short duration of any manned portion of the ABLE mission and
- Much lower total accummulated doses averaged over a six month unmanned mission.

3.4.2 Protection Criteria

The effects of the radiation environment on the crew, spacecraft equipment, and materials located exterior to the spacecraft were considered in this evaluation.

[redacted]

3.4.2 (continued)

There are three possible locations for a crewman, on an ABLE LM mission, from the point of view of having different equivalent protection from the space radiation. They are, in oder of increasing protection afforded, extra-vehicular activity (EVA), inside the LM, and inside the CM. The estimated equivalent protection afforded a crewman in each location is summarized in Table 3.4-1. The equivalent shielding is defined

Table 3.4-1

Equivalent Protection

Location	Equivalent Shielding (gm/cm^2 of Aluminum)
EVA	0.2
inside LM	0.6 (includes spacesuit)
inside CM	4.0

as that thickness of material, spread over a spherical shell, that yields the same dose rate at the center of the sphere as would be encountered inside the actual vehicle or spacesuit. The value of 0.6 g/cm^2 inside the ABLE LM cabin is believed to be a representative value for a suited astronaut. A value of 0.4 gm/cm^2 would be more appropriate if the astronaut were in a shirt-sleeve environment.

The safe radiation exposure limit for the crew was taken as the average allowable yearly dose which is summarized in Table 3.4-2 for the critical organs of interest.

Table 3.4-2

Radiation Exposure Limits

Critical Organ	Average Yearly Dose (Rads)
Skin of Whole Body	250
Blood Forming (BFO)	55
Eyes	27

3.4.2 (continued)

Dose rates for the skin and eyes were calculated using the equivalent protection summarized in Table 3.4-1. Dose rates at the blood forming organs (BFO) were calculated by adding 5 gm/cm^2 of tissue equivalent shielding to the nominal thicknesses listed in Table 3.4-1.

The potential degradation of ABLE LM equipment due to the radiation environment was considered by choosing the class of low frequency silicon transistors as being representative of the most radiation sensitive equipment onboard the spacecraft. Any calculation of radiation damage must be performed on an individual component basis. A specific transistor must be located inside its package within the spacecraft and the equivalent shielding afforded it evaluated. Then the particular application of the transistor within its electrical circuit and the margin available for its particular application must all be evaluated to establish the critical radiation dose for damage. Based on LM experience, a damage dose of 10^5 rad behind an equivalent shield of one gm/cm^2 was chosen as being representative of the most radiation-sensitive electronic components onboard the ABLE LM.

The most radiation sensitive materials directly exposed to the space environment are mylar for the reflector system, and the external thermal control coatings of the spacecraft. A total accummulated dose of 10^8 rad was chosen as the threshold for damage to the mechanical properties of mylar. The effects of radiation on the spacecraft thermal control coatings is not well known at the present time.

3.4.3 Calculation Procedure

Dose rates behind aluminum shielding were computed for the various charged particle environments (Section 3.4.1) at altitudes from 6,000 n.mi. to synchronous orbit.

The assumed shield configuration was a spherical shell of aluminum with the dose point at the center of the sphere. Electrons and protons were assumed to be incident isotropically.

[redacted]

3.4.3 (continued)

The results are shown in Figs. 3.4-1 through 3.4-3 for the projected 1968 environment (Ref. 3.4-1) and in Figs. 3.4-4 and 3.4-5 for the MSFC specified environment. Dose rates received by the crew, or by equipment, from electrons and protons can be estimated from the curves by applying a factor of 0.5 to account for self-shielding. The self-shielding factor is taken as one for the bremsstrahlung contributions.

A summary of the radiation dose rates for the shield thicknesses of interest in evaluating the effects on the crew, electronic equipment, and reflector material is shown in Table 3.4-3. The self-shielding factor of 0.5 was applied to the electron and proton dose rates shown in the table.

Table 3.4-3

Radiation Summary

Altitude (naut. mi.)		Dose Rates (rad/day							
		0.2 gm/cm^2		0.6 gm/cm^2		4.0 gm/cm^2		1 gm/cm^2	0 gm/cm^2
		Skin	BFO	Skin	BFO	Skin	BFO		
(1)	6,000	3×10^4	4.1	5×10^3	4.1	4.5	3.4	1.2×10^3	4×10^5
(1)	11,000	2.5×10^4	2.7	3×10^3	2.7	3	2.2	300	4×10^5
(1)	15,000	7×10^3	0.4	3×10^2	0.4	0.4	0.3	20	1×10^5
(2)	6,000	500	.04	65	.04	0.1	.05	15	4×10^5
(2)	Synchronous	2×10^3	1.6	90	1.6	1.8	1.3	4	6×10^4

(1) Ref. 3.4-1

(2) MSFC Specified Environment

The addition of 0.5 gm/cm^2 of shielding to the eyes when the crew is either in the ABLE LM or EVA would reduce the dose rate at the eye by an order of magnitude and make the skin dose the controlling factor.

[redacted]

[redacted]

3.4.4 Evaluation of Radiation Hazard

It was assumed that the equivalent of 0.5 gm/cm^2 of eye protection would be added so that the radiation exposure limit to the eyes would not be a controlling factor in limiting the maximum crew time on the ABLE LM or for EVA.

The evaluation of the potential radiation hazards were based on the results listed in Table 3.4-3 and the protection criteria of Section 3.4.2. The results are summarized in Table 3.4-4. The maximum exposure limits in the ABLE LM and during EVA were constrained by the allowable skin dose. The maximum exposure limit in the CM was governed by the allowable dose to the eyes. The major conclusions that can be reached at this time is dependent to a certain extent on which, of the two radiation environment models used in this evaluation, is employed. In either case it must be recognized that the results are "order of magnitude" estimates.

Table 3.4-4

Maximum Exposure Limits

	Altitude (naut. mi.)	Maximum Exposure Times				
		Crew Operations			Sensitive	
		EVA (hours)	inside LM (hours)	inside CM (days)	Electronics (days)	Mylar (days)
(1)	6,000	0.2	1.2	6.6	80	250
	11,000	0.2	2	10	330	250
	15,000	0.9	20	67	5000	1000
(2)	6,000	12	92	270	6700	250
	Synchronous	3	67	17	25000	1700

(1) Ref. 3.4-1

(2) MSFC Specified Environment

[redacted]

3.4.4 (continued)

The major conclusions that are common to both environmental models are:

- o The use of mylar is marginal at altitudes below synchronous
- o There is no problem for the crew while in the CM

The MSFC specified environment, alone, leads to the conclusions that:

- o There is no problem for the crew while in the ABLE LM at any altitude
- o Limited EVA's are possible
- o There is no radiation damage problem to equipment.

The major problem in evaluating the potential radiation hazard for the ABLE mission is the uncertainty in the predicted 1968-69 environmental model. Unfortunately, it is unlikely that any new emperical data will be available early enough to provide statistical verification of any assumed model environment before major program decisions have to be made to meet a 1969 launch date.

3.4.5 References

3.4-1 Vette, J., et al, NASA SP-3024, Vol. II, 1966.

[redacted]

MODEL DATE

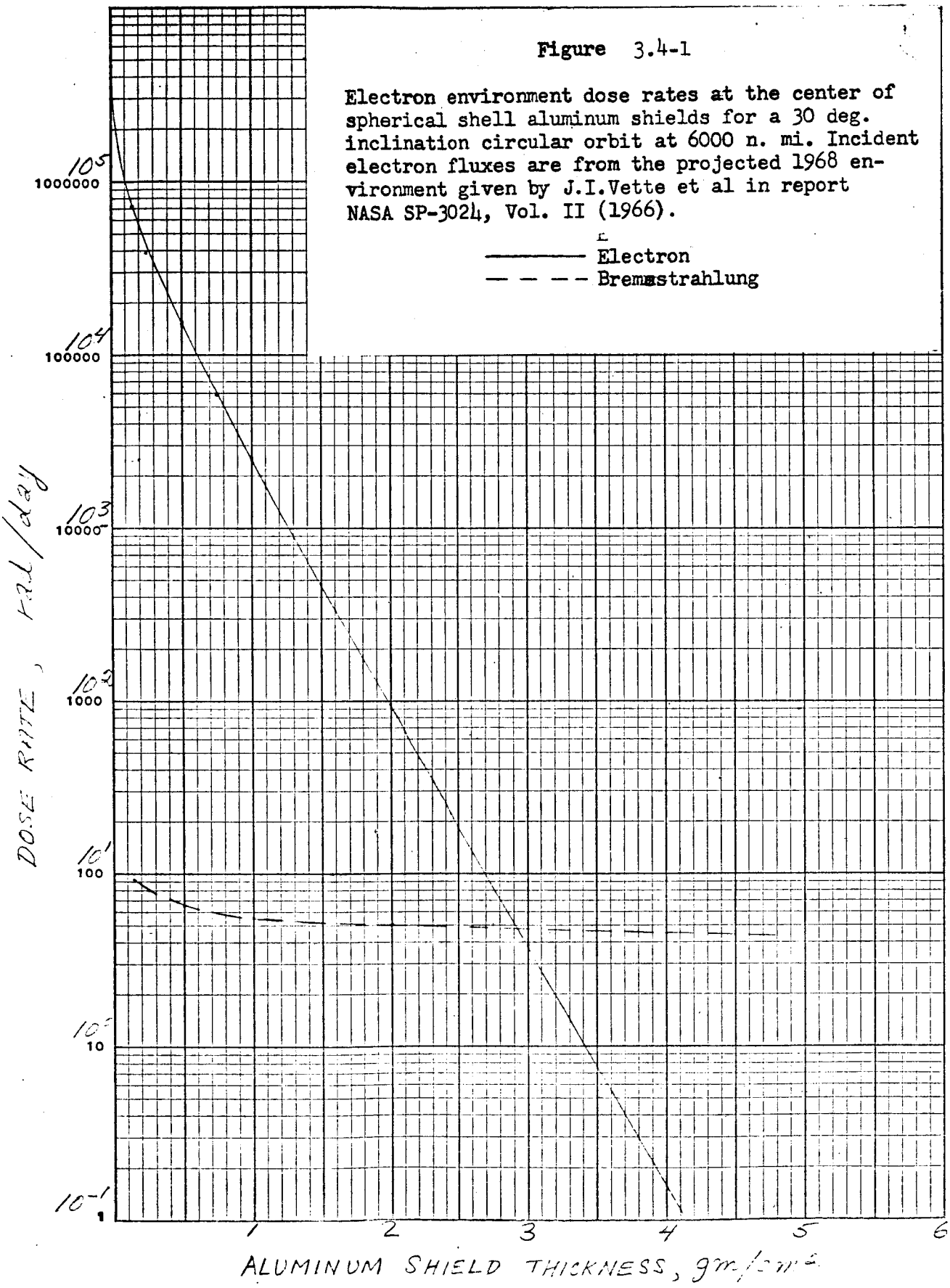

Figure 3.4-1

Electron environment dose rates at the center of spherical shell aluminum shields for a 30 deg. inclination circular orbit at 6000 n. mi. Incident electron fluxes are from the projected 1968 environment given by J.I.Vette et al in report NASA SP-3024, Vol. II (1966).

[redacted]

[redacted]

MODEL DATE

Figure 3.4-2

Electron environment dose rates at the center of spherical shell aluminum shields for 30 deg. inclination circular orbits. Incident electron fluxes are from the projected 1968 environment given by J. I. Vette et al. in NASA SP-3024, Vol. II (1966).

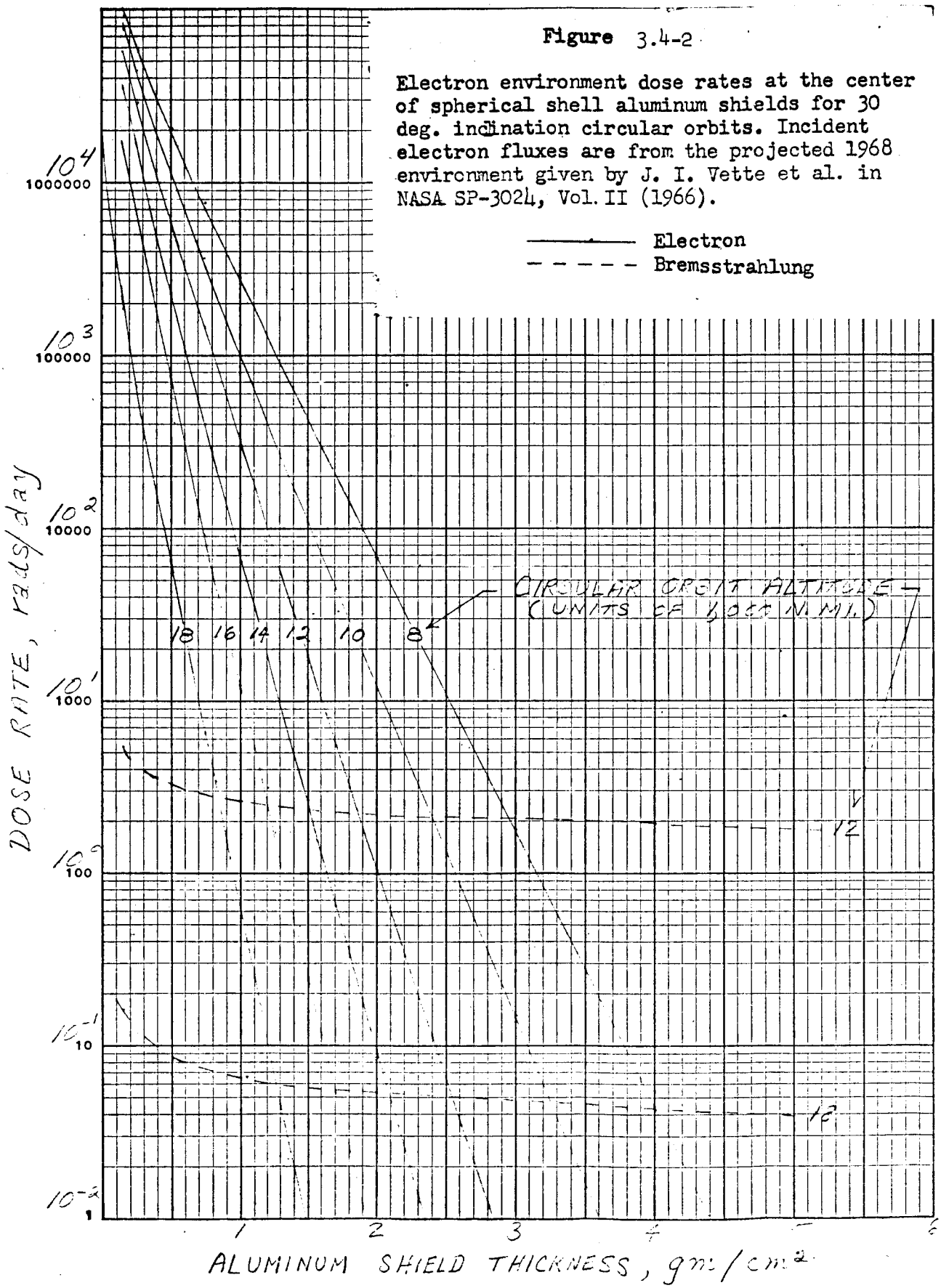

[redacted]

[redacted]

MODEL DATE

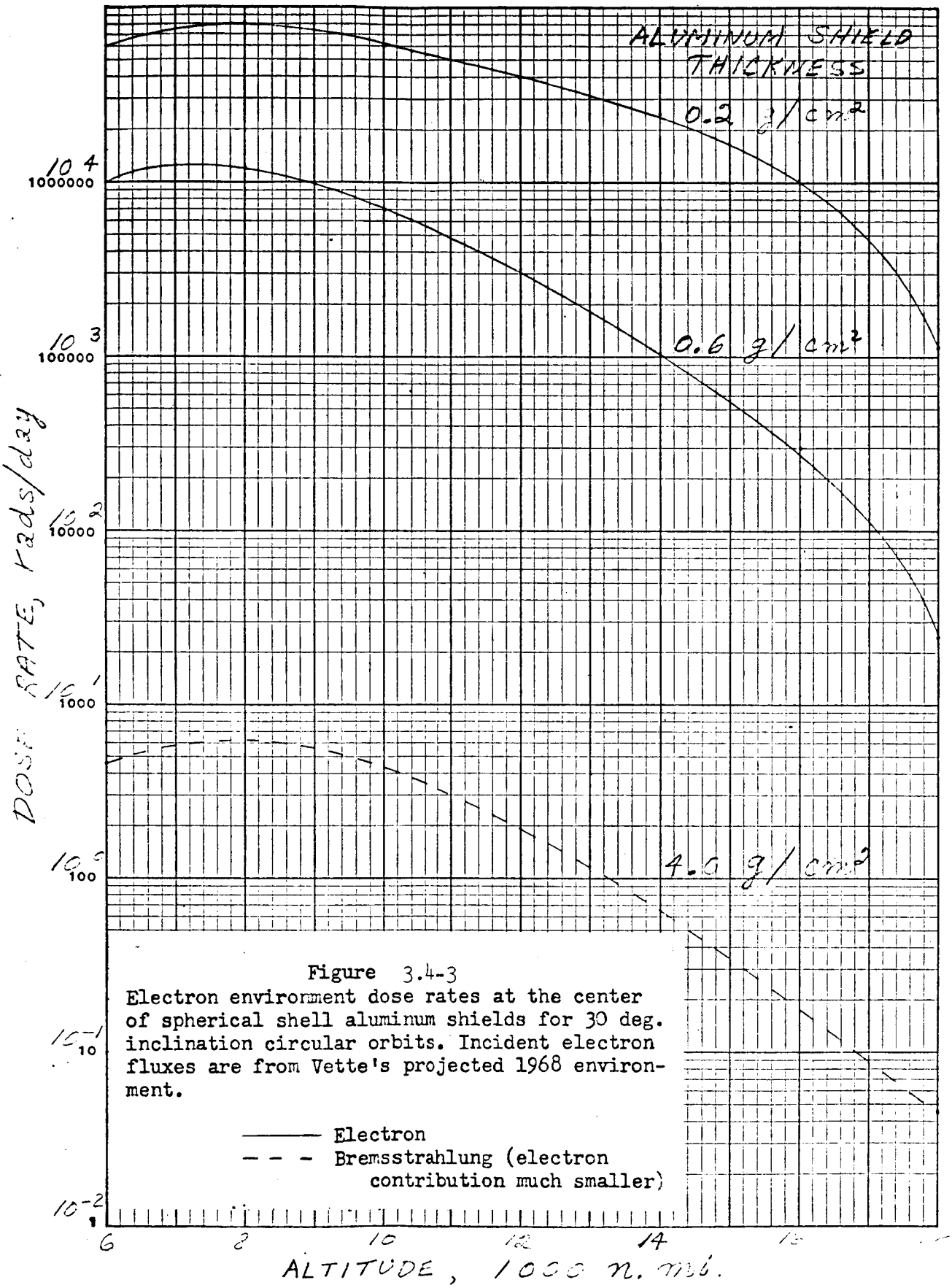

Figure 3.4-3
Electron environment dose rates at the center of spherical shell aluminum shields for 30 deg. inclination circular orbits. Incident electron fluxes are from Vette's projected 1968 environment.

——— Electron
– – – Bremsstrahlung (electron contribution much smaller)

[redacted]

[redacted]

MODEL

DATE

Figure 3.4-4

Dose rates at the center of spherical shell aluminum shields for the MSFC environment at a 6,000 n. mi. orbit near the equator.

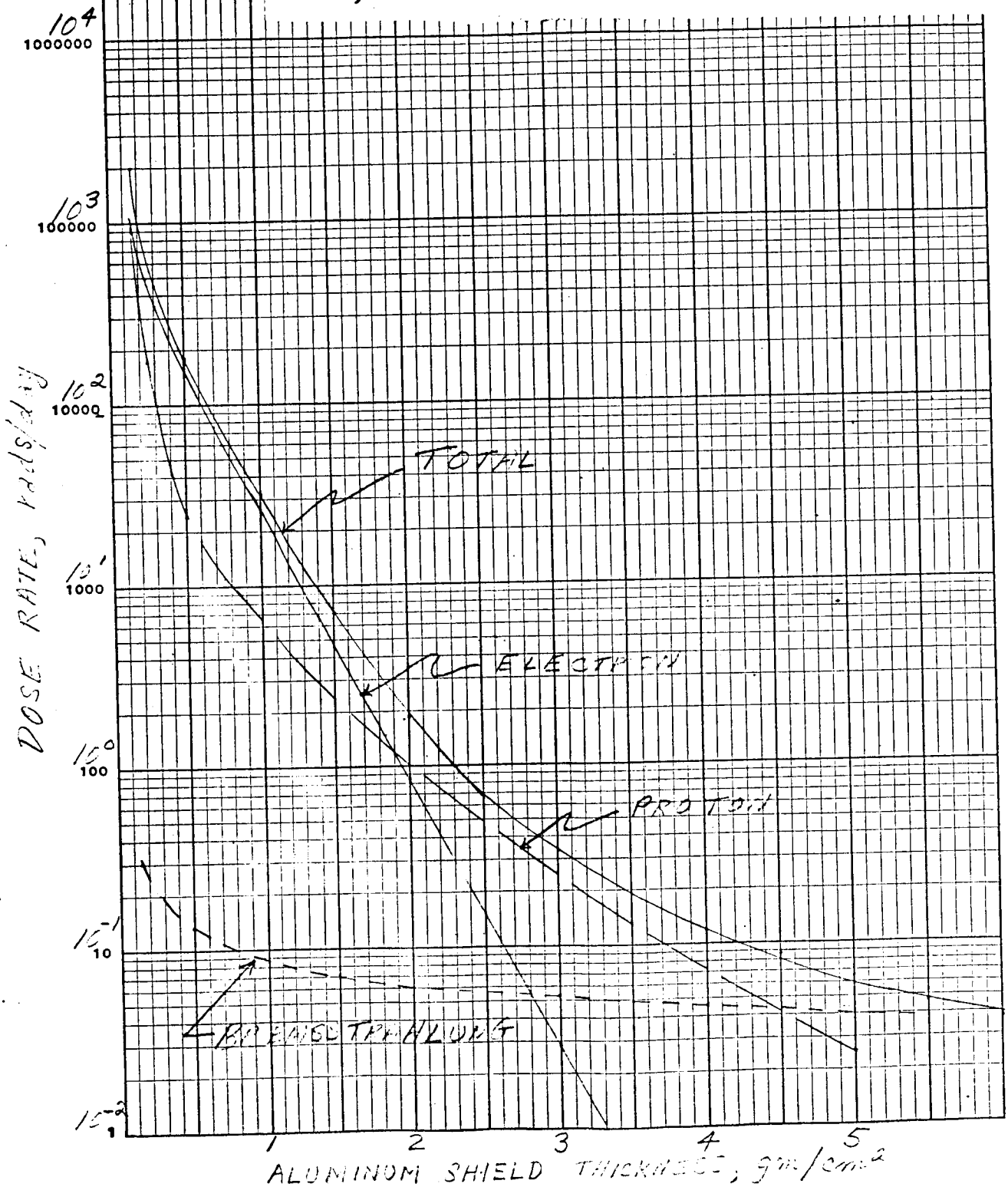

[redacted]

[redacted]

MODEL DATE

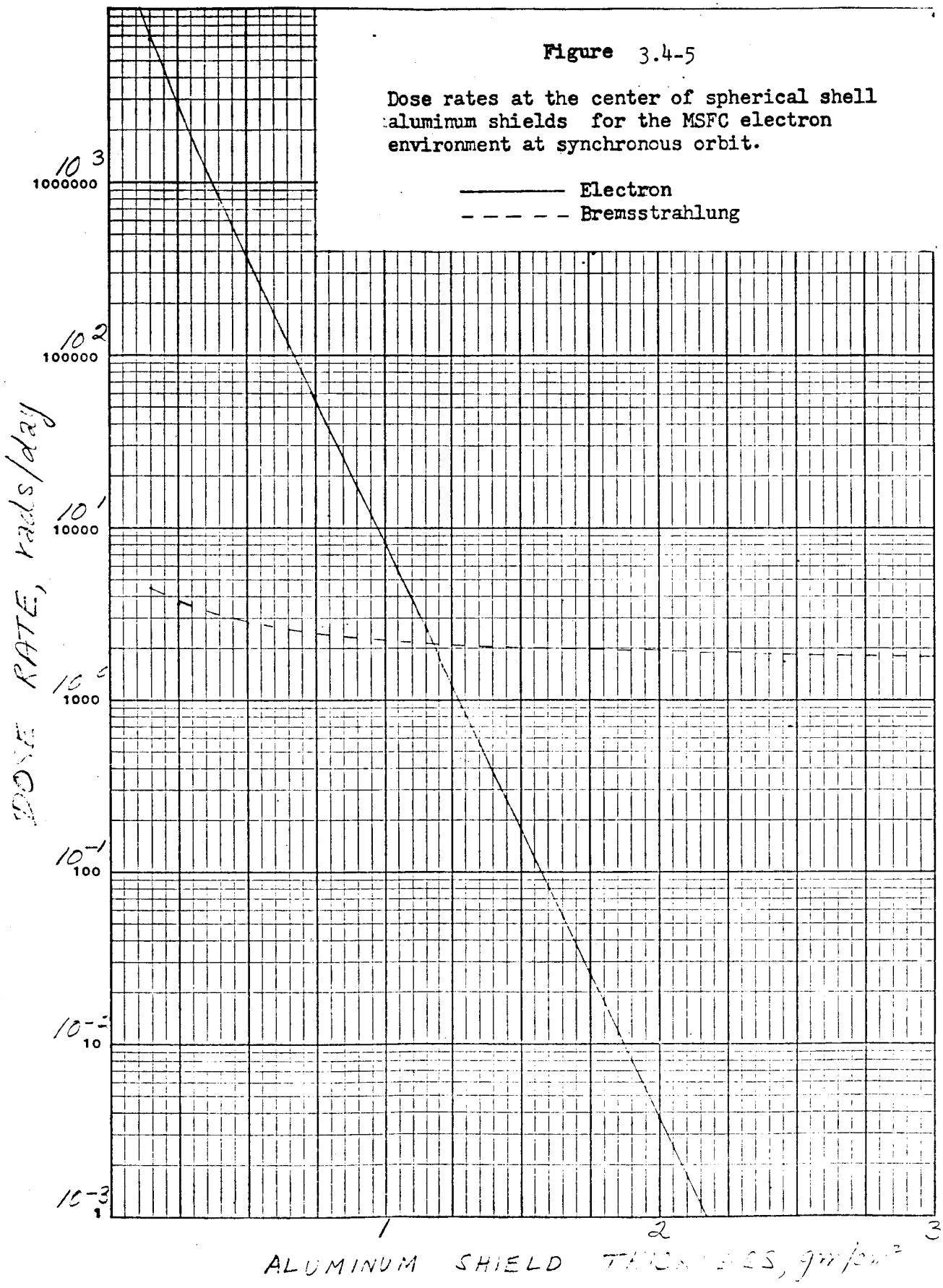

Figure 3.4-5

Dose rates at the center of spherical shell aluminum shields for the MSFC electron environment at synchronous orbit.

——— Electron
- - - - - Bremsstrahlung

[redacted]

[redacted]

3.5 FLIGHT OPERATIONS

3.5.1 Ground Communication Coverage

For initial planning purposes, the Apollo Manned Space Flight Network (MSFN) has been investigated for fulfilling the primary ground communications and tracking requirements for Project ABLE. The basic Manned Space Flight Network (MSFN) is described and the ground station communication coverage available for a 28.5 degree inclination orbit of altitude 6,000 n.mi. or greater is presented. In addition, the possiblity of using the Satellite Control Facility (SCF) as a secondary network is considered. The SCF support capability is based on the defense objective of the ABLE mission and the proposed incorporation of the Space Ground Link Sub-system (SGLS) into the SCF sites.

In identifying[1] the USAF Satellite Control Facility (SCF), the present sites are categorized with respect to "single" or "dual" spacecraft support capability; where "dual" refers to two "single" stations co-located. It is assumed that upon Space Ground Link Sub-system (SGLS) implementation, the SCF/SGLS stations will retain their previous "single" or "dual" capability.

3.5.1.1 Network Configuration and Capabilities

The primary MSFN configuration consists of fourteen stations which utilize the unified S-band (USB) mode of communications. Nine of these stations are characterized by "dual" capabilities, which provide for tracking and communications support of two vehicles within the antenna beamwidth. The "dual" sites are capable of receiving and recording four distinct S-band signals, two of which may be processed in real-time. The remaining five stations, designated as having "single" capabilities, provide tracking and communications support for one vehicle and may receive, record and process two distinct S-band signals. Table 3.5-1 identifies the stations comprising the MSFN and their respective capabilities.

The Air Force SCF network consists of seven Remote Tracking Sites (RTS), identified in Table 3.5-2. Currently, the RTS are being augmented with the Space Ground Link Sub-system (SGLS) which operates on the same principle as the NASA/USBS, ie., ground/satellite communications utilize a pair of coherently related, multiplexed uplink

1 Dept. of the Air Force, AFRDDC; NASA Request for USAF Satellite Control Facility Network Information, 24 August 1966

[redacted]

3.5.1.1 cont'd

and downlink RF carriers. The SGLS coherent RF carriers will retain the basic USBS baseband structure.

Table 3.5-3 lists several of the SGLS site parameters and indicates the corresponding USBS characteristics. As indicated in Table 3.5-2 the SGLS "A" station is comparable to the "single" USBS stations, ie., tracking support of one spacecraft tracking and communications support, similar to that provided by "dual" USBS sites, is possible at the co-located sites ("B" stations) specified in Table 3.5-2.

The SGLS is marked by a high degree of similarity to the USBS; however, notable differences are:

- Uplink carrier frequency
  - USBS 2100-2110 MHz
  - SGLS 1760-1840 MHz
- Digital Uplink Command Mode
  - USBS Phase shift keying (PSK)
  - SGLS Frequency shift keying (FSK)
- Downlink non-coherent carrier
  - USBS FM with multiplexing of data on carrier
  - SGLS PM with PCM data directly modulated on carrier

3.5.1.2 Network Visibilities and Communication Coverage

During the initial phase of study, the visibility and communication coverage available for orbits of 6,000 n.mi. and 19,350 n.mi. altitudes with inclinations of 28.5° or less were examined. Subsequent planning considered that the ABLE reference orbit may be elliptical with an apogee of 11,700 n.mi., a perigee of 10,100 n.mi. and a inclination of 28.5°. Satisfactory ground station visibility and communication coverage for 6,000 n.mi. altitude orbit will assure even greater visibility and coverage for the elliptical reference orbit.

Figure 3.5-1 illustrates the approximate composite plot of the MSFN visibility for a 6,000 n.mi. altitude orbit. (For the elliptical reference orbit, this visibility contour would be expanded appreciably). It is apparent that continuous coverage exists for a 28.5° inclination orbit of 6,000 n.mi. altitude or greater. The small area exhibiting no-coverage (shown shaded) is considered negligible. The

3.5.1.2 cont'd

MSFN stations capable of affording continuous coverage in the Southeast Asia area include Guam, Carnarvon and Canberra.

As a result of the orbiting reflector's high altitude, full MSFN ground communications are possible; thus providing full time command capability if required. In the event that rendezvous and resupply with a second vehicle is required, ground coverage, in conjunction with the MSFN capabilities, permit adequate support of both vehicles.

An approximate composite plot of SCF visibility is shown in Fig. 3.5-2 for a 6,000 n.mi. altitude orbit. The no-coverage area for the 28.5° inclination is shown shaded. As indicated, continuous visibility is not available; however, the no-coverage area presented to the 28.5° inclination orbit is considered to be tolerable. For the ABLE elliptical reference orbit, continuous coverage is possible in the vicinity of Southeast Asia.

The "Dual" SCF support in the Southeast Asia area, accomplished by two sites affording simultaneous coverage (Guam and Mahe Seychelles), is marginal at 6,000 n.mi. altitude. For the elliptical reference orbit, the visibility becomes greatly expanded so that multiple SCF site support is assumed.

In comparing the SCF composite visibility to that of the MSFN, the latter appears to have only a slight advantage. The significant feature of the MSFN network however, is the general increase in operational capability produced by the greater number of stations.

[redacted]

TABLE 3.5-1

MSFN CONFIGURATION

MSFN Station	Dual (D) or Single (S)
Cape Kennedy	D
Grand Bahama Is.	S
Bermuda	S
Antigua	S
Ascension	D
Canary Island	S
Madrid	D
Cararvon	D
Canberra	D
Guam	D
Hawaii	D
Goldstone	D
Guaymas	S
Corpus Christi	S

[redacted]

TABLE 3.5-2

SCF CONFIGURATION

SCF Station	"A" or "B" Station *
Kodiak, Alaska	A
Thule, Greenland	A
Anderson AFB, Guam	A
Mahe Seychelles Island	A
Vandenberg AFB, California	B
New Boston, N. H.	B
Kaena Point, Hawaii	B

* An "A" Station is capable of tracking one spacecraft. A "B" station is essentially a dual station, i.e., two "A" stations co-located. A "B" station is capable of tracking two spacecraft simultaneously.

[redacted]

TABLE 3.5-3

SGLS/USBS Station Summary

Parameter		SGLS	USBS Near-Earth Station	USBS Deep-Space Station
Antenna	Dia	60'	30'	85'
Operating Frequency	XMIT Rec	1760-1840 MHZ 2200-2300 MHZ	2100-2110 MHZ	2100-2110 MHZ
Output Power		10 KW Max.	1-10 KW or 2 KW/channel for dual freq.operation	10 KW
Uplink Command Mode		FSK	PSK	PSK
Antenna Gain	XMIT Rec.	48.4 db 50.2 db	42 db 43 db	51 db 52 db
Max. Tracking Rates	Vel. Acc.	10°/sec (1) 5°/sec^2 (1)	4°/sec 5°/sec^2	3°/sec 5°/sec^2
Max. R. F. Carriers Rec.		"A" Station: 1-coherent PM carrier and 1-non-coherent PM carrier "B" Station: 2-coherent PM carriers & 2-non-coherent PM carriers	"Single" Site: 1-coherent PM carrier and 1-non-coherent FM carrier "Dual"Site: 2-coherent PM carriers and 2-non-coherent FM carriers	
Multiple S/C Tracking Capability		"A" Station: 1-S/C with 1 min. turn-around time "B" Station: 2-S/C	"Single" Site: 1-S/C "Dual" Site: 2-S/C	

(1) These tracking rates are design values

[redacted]

3.5.2 Operation Launch Vehicle Consideration

The feasibility and operational capabilities of single and dual launch Saturn vehicles were investigated. The following Saturn V and uprated Saturn (IB) configuration alternatives were considered:

- Single Saturn V Launch
  - Direct ascent method
  - Earth parking orbit method
- Dual Saturn V Launch
  - Rendezvous in synchronous orbit
- Saturn V - Saturn IB Dual Launch
  - Rendezvous in nominal low attitude parking orbit

The single Saturn V launch configuration using a parking orbit technique has subsequently been selected for ABLE design reference purposes. The dual launch alternative involving an uprated Saturn led to further consideration of the uprated Saturn as an economical developmental flight test vehicle for early investigation of the basic reflector deployment and flight control characteristics. The reflector flight test aspect is presented in Section 3.5.3.

3.5.2.1 Single Saturn V Launch

Direct Ascent - This alternative, for synchronous altitude, offers the advantage of economics since only one launch vehicle is required with virtually no equipment modification. In addition, launch pad activities are the same as those for Apollo, and orbital operations are simplified since rendezvous is not required. The major drawback, however, is low orbital payload (Table 3.5-4), the maximum being 62,400 lbs for a 28.5 degree inclination orbit hovering at 108 degrees east longitude. This allows 22,300 lbs for the LM/reflector/support structure.

Earth Parking Orbit - This alternative offers the same advantages as the direct ascent method, plus the added advantage of orbital operations similar to Apollo. Payload capability is also a drawback, however, maximum payload is 70,100 lbs for a 28.5 degree inclination, synchronous altitude orbit, hovering at 105.5 degrees east longitude (Table 3.5-4). LM/reflector/support structure allowable weight is 30,000 lbs.

3.5.2.2 Dual Saturn V Launch

The major advantage of this mission is payload capability. The maximum payload is 70,000 lbs per vehicle for a 28.5 degree inclination orbit hovering at 105.5 degrees east longitude. (Table 3.5-4). These profiles are similar to Apollo except for the synchronous orbit rendezvous.

However, this alternative has several drawbacks. The first is economics, ie. two Saturn V's are required. In addition to the launch vehicles, the costs associated with the support of two Saturn V launches launched close together must be considered. The other drawback is time between launches. This time for Launch Comples 39 (Saturn V launches) is approximately 15 days because of the need to move the Mobile Service Structure (MSS) from Pad A to Pad B; however, some relief may be obtained by MSS schedule manipulation.

This mission requires orbital storage of the first vehicle for as much as 15 days because of the above Launch Complex 39 turn-around time. During this period, the LM/Reflector can be left in the S-IVB SLA and gravity gradient stabilized. This would eliminate the need of mechanizing a system to remove the unmanned LM/Reflector from the SLA. The various subsystem requirements are the same as those for a single launch with the exception that the LM/Reflector may require equipment to be activated during this period; i.e., fluid system heaters, power supply, battery cooling.

A potential problem may arise from the two spent S-IVB stages which are left in orbit in the vicinity of the LM/Reflector, since these vehicles could collide with the reflector.

Earth Parking Orbit Rendezvous - This alternative offers simpler launch complex activities than the dual Saturn V launch. It also utilizes the existing Apollo prelaunch, launch and mission operation experience gained during the Saturn IB (as well as Saturn V) missions. The Saturn IB and Saturn V combination can place a larger payload into a 100 n.mi. Earth Orbit; however, the Saturn V's capability to place this combined payload into a higher altitude orbit is limited. Further study may be warranted to determine gain with respect to payload over a single Saturn V's capability.

The major advantages and disadvantages associated with each single Saturn and dual Saturn launch alternative are summarized in Table 3.5-5.

TABLE 3.5-4

Orbital Payload Summary

~~CONFIDENTIAL~~

	Synchronous Altitude Hover Point (Deg. Longitude)	Inclination (Deg.)	Payload (lbs.) (1)
Single Saturn V			
o Direct Ascent to Synch. Orbit	80.5 E 108.0 E 108.0 E	0 0 28.5	54,700 59,600 62,400
o Earth Parking Orbit Before Transfer	105.5 E 105.5 E	0 28.5	63,400 70,100
Dual Launch Saturn V			
o Earth Parking Orbit	105.5 E 105.5	0 28.5	63,400/vehicle 70,100/vehicle
Dual Launch Saturn V and Saturn IB with Earth Orbit Rendezvous	105.5 E 105.5 E	0 28.5	63,400 + 70,100 +

Notes: (1) 40,100 lbs. for CSM weight must be subtracted from this figure to obtain allowable LM/Reflector/Support Structure weight.

~~CONFIDENTIAL~~

[redacted]

TABLE 3.5-5

Summary of Alternative Saturn Launch Vehicle Advantages and Disadvantages

	Single Saturn V Direct Ascent	Single Saturn V Parking Orbit	Dual Launch Saturn V	Dual Launch Saturn V & IB Parking Orbit Rendezvous
Economical	x	x		
Large Orbital Payload (1)		x	x	x
Simplified Launch Pad Activities	x	x		x
Orbital Operations Similar to Apollo		x	x	
S-IVB Present Restart Capability Sufficient	x			
Orbital Operations Simplified	x	x		
CSM Not Required to Inject	x	x	x	x

Notes: (1) See Table 1

x -- Advantage

[redacted]

[redacted]

3.5.3 LM/Reflector Test Flight

Consideration has been given to conducting an early Saturn IB launched LM/Reflector test flight to demonstrate basic Reflector deployment and flight operational capability. The purpose of this mission, an orbital test of the LM/Reflector, could be achieved with minor modifications to a basic LM and with little impact to the present NASA launch schedule. This mission would be similar to the currently planned Apollo mission "258", a dual Saturn IB launch of an unmanned LM and manned CSM.

The short duration, low-altitude flight to test Reflector deployment and operation could be flown using a LM Reflector and S-IB launch vehicle for an unmanned LM/Reflector launch into earth orbit. This launch would be planned in conjunction with an Apollo Applications mission so that the CSM and crew could then rendezvous with the LM/Reflector for the deployment check. The manned CSM would be utilized only after its main mission was completed.

The results of the mission would demonstrate the Reflector deployment and rigidization systems in the space environment as well as the control capabilities of the Reflector subsystem. The atmospheric environment in low earth orbit is different from high altitude orbits in terms of disturbances. However, the basic

- deployment and rigidization method,
- control characteristics under orbital space conditions,
- applicability of man to support initial operations of large deployable structure

can be evaluated either directly or with well founded extrapolation. Furthermore, the presence of crewmen in monitoring the first deployment and operations will provide first hand substantiation of ABLE design practice or enable design modification of subsequent operational missions.

3.5.4 Manned Mission Operations

The prime responsibilities of the crew with regard to the ABLE mission is to insure satisfactory deployment and initiation of the Reflector System. The flight vehicle will have undergone a prelaunch checkout (as described in the

[redacted]

[redacted]

3.5.4 cont'd

prelaunch operations sub-plan of Volume III) and have been subjected to the launch-through orbital insertion/stabilization environments prior to the manned inflight checkout.

3.5.4.1 Post-Launch Checkout

After canister outgassing, the LM will be manned for system and subsystem operational checkout. Prior to manning, the CSM will pressurize the LM cabin. The first crewman enters the LM cabin to conduct a LM subsystem status check. The second crewman follows and assists in the LM/Reflector subsystem checkout.

The mated CSM/LM Reflector checkout will confirm post-launch subsystem operation before unmanned LM/Reflector separation and deployment. The crew will exercise the LM/Reflector control and maneuvering systems and monitor them in conjunction with the ground command mode (through the LM's PCA and LGC.). This test is to verify remote operations prior to Reflector deployment.

After subsystem checkout, the LM is prepared for unmanned deployment operations. The ground uplink command section is activated. The IMU is coarse aligned using the CSM as reference and then fine aligned by orienting the vehicle to reference stars. The crew then puts the LM/Reflector in an attitude hold mode before returning to the CSM.

3.5.4.2 Deployment and Rigidization

The deployment phase starts after the outgassing period has been completed; the LM has been activated, checked out, and is on attitude hold. The two-man crew has returned to the CSM and the CSM has undocked from the LM/Reflector. The sequence of events of the deployment phase is described in the following paragraphs and is illustrated in Figure 3.5-3.

[redacted]

3.5.4.2 cont'd

1) The CSM transposes to the canister, which is attached to the bottom of the LM descent stage. CSM approaches the canister and attaches a line to the Reflector rings from the CSM. (The line is designed to snap under tension before the Reflector material tears).

2) The CSM then backs away from the canister to approximately 100-150 feet (until the line is almost taut) and initiates canister deployment by automatic means. The canister opens like a clam shell, which is hinged to the bottom of the LM descent stage. The Reflector material springs out slightly and is fully extended outward by the CSM slowly backing away with the line attached to the Reflector. During this period, pressurized helium gas from a tank in the LM descent stage is commanded to flow into the extending spokes of the Reflector to provide some torsional rigidity during this partial deployment. The CSM then releases the line from one of the two Reflector rings.

3) The CSM maneuvers one end of the structure which is still attached to the line, through 180 degrees to fully extend the structure. At this point, the CSM releases the remaining line and backs off to observe and monitor the remaining initial deployment while station keeping in the vicinity of the LM.

4) Additional helium gas from peripheral tanks is commanded to slowly deploy the structure outward to its maximum diameter by flowing through the remaining two spokes.

5) After this deployment, the CSM docks with the LM, two crewmen transfer into the LM in order to rigidize, align, and checkout the system. The CSM remains docked to the LM during this phase, if CSM thermal constraints permit. Approximately 24-hours are allocated to accomplish this complete phase. Final rigidization is done by using additional helium gas from the tank in the LM descent stage to rigidize the Reflector support structure to the yield point. This may require approximately 2-hours. After rigidization, the remaining time is utilized to align and checkout the system for unmanned operation.

[redacted]

3.5.4.3 Post-Deployment LM/Reflector Checkout

This phase of flight marks the first point where the ABLE system i.e., the Reflector, the onboard supporting subsystems and the ground control network can perform an end-to-end system checkout.

The chief elements of this manned operation checkout, i.e., those which contribute to increasing the success of the nominal six-month unmanned operational phase are:

- Reflector structural alignment and C/O
- Solar Panel Deployment and C/O
- LM/Reflector Position Alignment
- ABLE System Monitoring and Manned Final Adjustment.

Each of these post-deployment checkout elements are described in the following paragraphs:

- Structural Alignment and Checkout - The alignment and checkout of the Reflector for initial operation is accomplished by the crew through visual sightings, instrumentation monitoring and communication between the LM, CSM and the MSFN. The procedure is as follows:
  - Visual sightings are made by the crew to check the structural alignment of the Reflector and the results are transmitted to MSFN
  - Visual checks of sections of Reflector material are then made to observe the degree of Reflector smoothness and to assess the effects of micrometeoroid impact. This assessment is repeated at intervals through this phase. The resulting data are transmitted to MSFN.
  - Alignment of the peripheral thruster clusters is then checked. This is accomplished by pulsing each thruster and transmitting the results of each test firing to MSFN.
  - During the entire alignment and checkout procedure transducers are utilized throughout the system to monitor the inflation gas pressure, stress, strain and other parameters.

3.5.4.3 (continued)

- Solar Panel Deployment and Checkout - Prior to separation of the LM and the CSM, the LM solar panels are deployed. The crew monitors the deployment. The checkout procedure consists of verifying proper EPS operation while varying the position of the Reflector with respect to sun angle.

- Position Alignment - With the LM/Reflector re-docked to the CSM, the LM control modes are used in conjunction with the Reflector thrusters to check for position alignment as follows: The LM control modes include automatic and attitude hold. The automatic mode provides the ability to maintain the vehicle in an inertially-fixxed attitude, once that attitude has been attained. The attitude hold mode of operation enables the crew to manually maneuver and provide attitude-hold capability during non-maneuvering periods. The positioning initialization and check includes:

  - Manually maneuvering the LM/Reflector combination to check Reflector's attitude or position/keeping ability.
  - Verification of automatic control mode in position keeping
  - Evaluation of the effects of environment and disturbances on attitude hold mode

  Using the LM to finalize the Reflector for the unmanned operational phase contributes positively to increasing manned mission safety. Using the LM's maneuvering capability instead of the CSM conserves the CSM's reaction controls and crew support expendables for orbital return and re-entry.

- Monitor and Final Adjust LM/Reflector Operations - After deployment, alignment and checkout of the LM/Reflector for unmanned operation, the crewmen in the LM return to the CM; the CSM separates and station keeps within the vicinity of the LM/Reflector for a period of up to eighty hours. This period includes ten hours contingency for docking and re-entering the LM in the event that further adjustments of the Reflector are required.

[redacted]

3.5.4.3 cont'd

During this phase of operation, the crew in the CSM will observe, monitor and verify the satisfactory response of the LM/Reflector to ground command control. Additionally, the effects of solar pressure, gravity gradient, and thermal gradients may be evaluated by maneuvering the LM/Reflector system as required and determining the resulting effects from CSM observations (by the crew) and ground station monitoring.

After successful initial operation of the LM/Reflector, the CM and crew return to earth and the LM/Reflector system continues unmanned operation for six months. During this period, ground stations periodically monitor the LM/Reflector status telemetry, obtain LM/Reflector tracking data and control the Vehicle's attitude via uplink/downlink RF communications.

FIGURE 4.2-2 SCF VISIBILITY FOR 6,000 n.m. ALTITUDE ORBITS

[redacted]

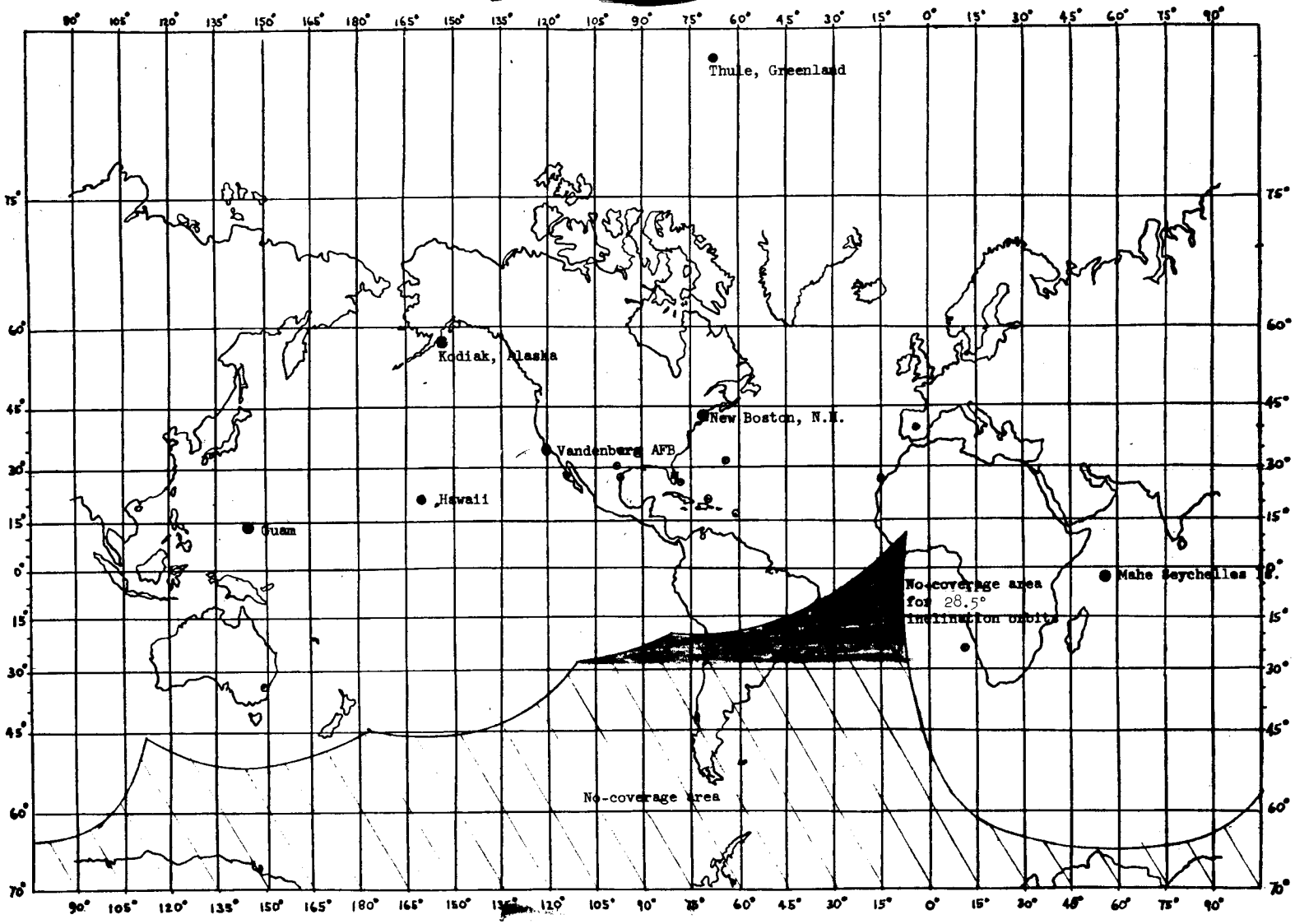

[redacted]

FIGURE 4.2-1 MSFN VISIBILITY FOR 6000 N.MI. ALTITUDE ORBIT

[redacted]

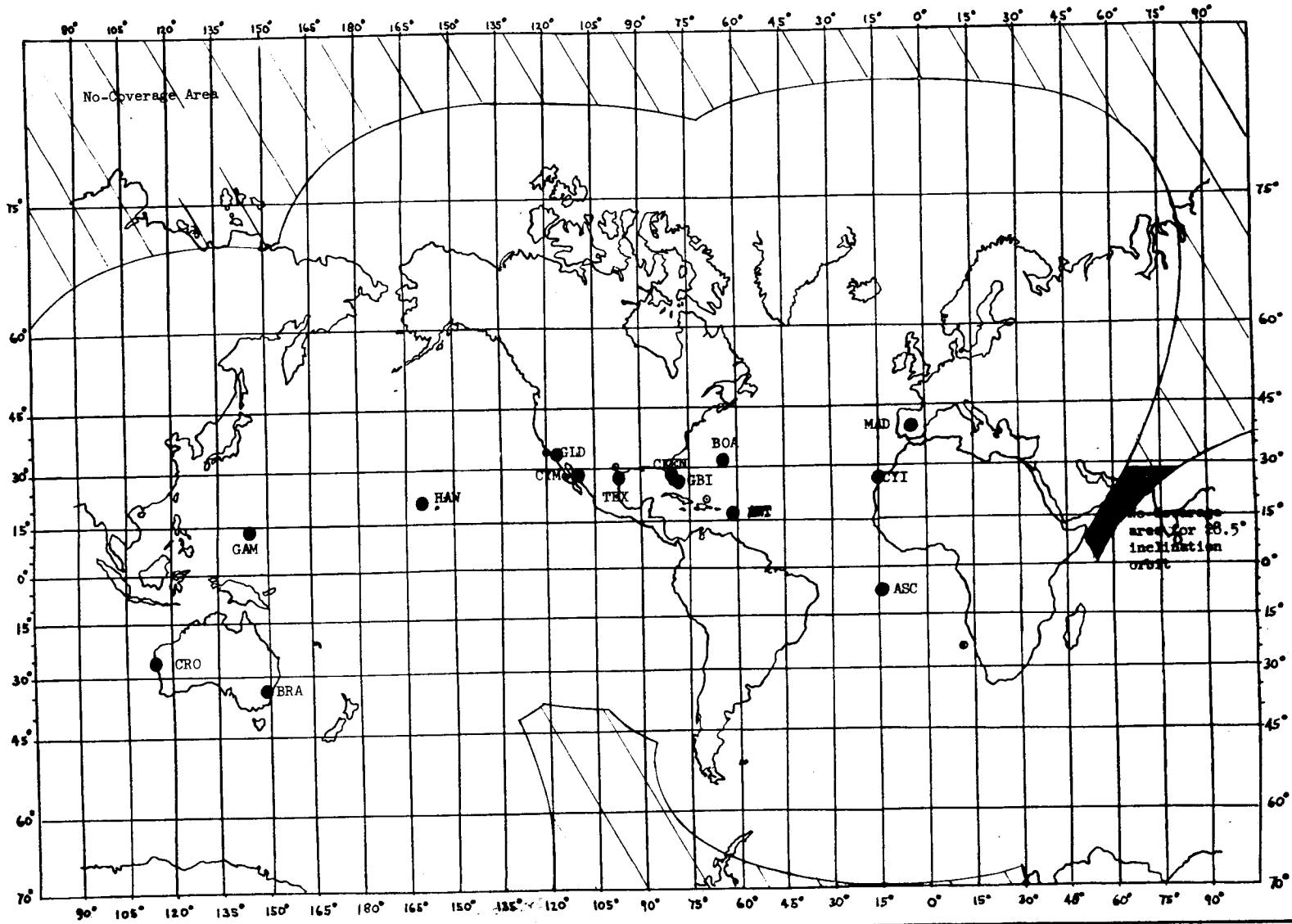

FORM G332 5-63 (ENG 72)

[redacted]

[redacted]

FIGURE 3.5-3
ABLE LM DEPLOYMENT CONCEPT

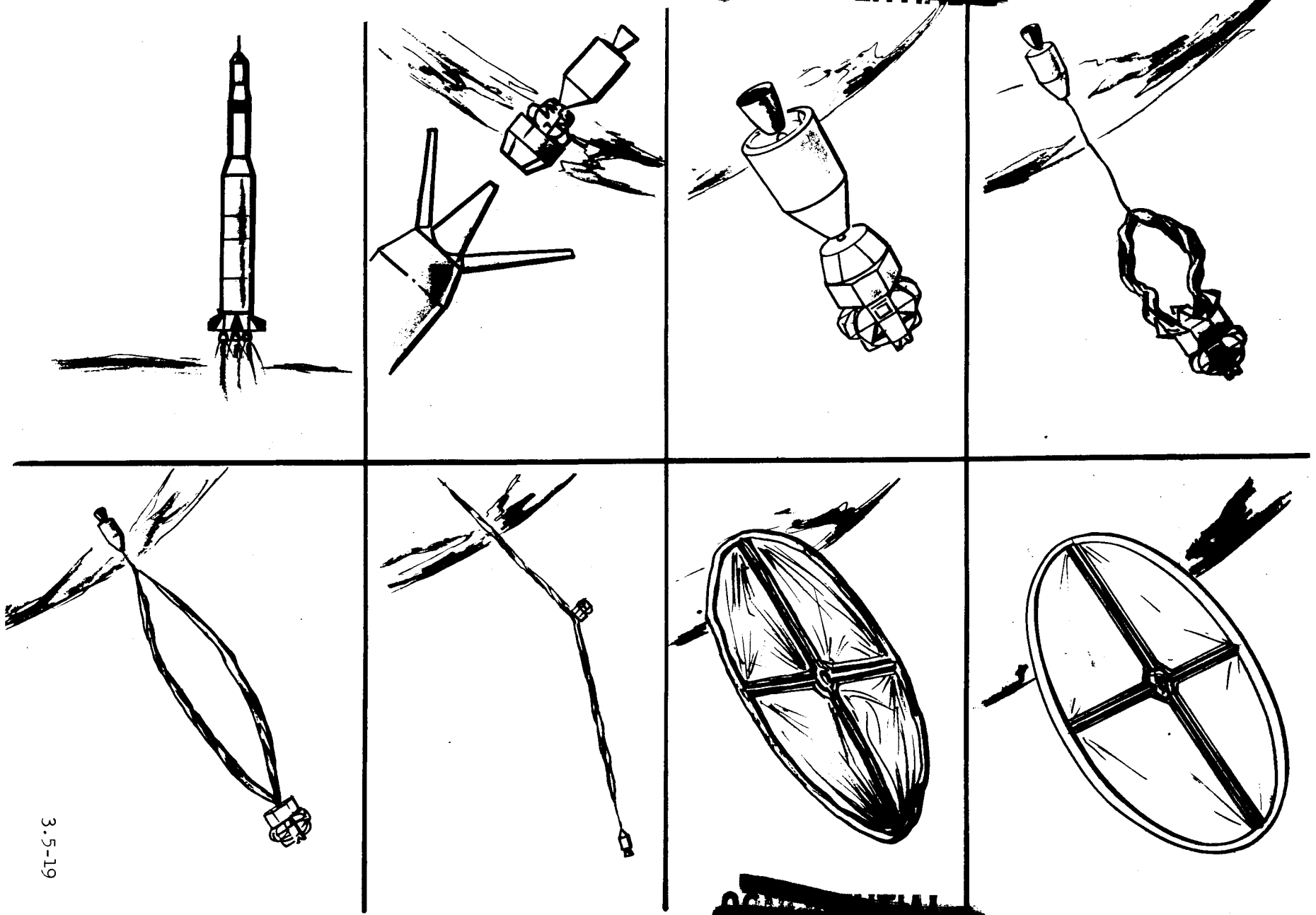

[redacted]

3.6 WEIGHT

3.6.1 Weight Limitations

The maximum allowable Saturn V launch weight forward of the Instrument Unit (IU) is 110,000 lbs. The maximum payload that can be supported in the SLA is approximately the earth launch control weight for the LM of 32,000 lbs. The change in the c.g. of the ABLE LM with respect to the Apollo LM will influence the allowable earth launch weight, but this is expected to amount to a negligible change.

The effect of these constraints on an ABLE LM with an inflatable spoke and torus reflector configuration is shown in Fig. 3.6-1. The estimated weight of 9700 lbs. for an ABLE LM exclusive of the reflector system is shown as the horizontal line in the figure. A detailed weight statement for the ABLE LM appears in Section 5.5. The curve in Fig. 3.6-1 shows the increase in total ABLE LM weight with reflector diameter. For an ABLE LM/CSM single launch the maximum allowable payload weight is governed by the SLA limit. This established the maximum diameter reflector for the spoke and torus configuration. A weight statement for a sample 1100 ft. diameter reflector is shown in Table 3.6-1.

Table 3.6-1

WEIGHT STATEMENT FOR 1100 FT. DIAMETER REFLECTOR

Torus & Spokes	7080 lbs.
Stringer & Ribs	4180
Spoke Insulation (to minimize temperature gradient)	1280
Reflector	3650
Negator Spings (8)	120
Peripheral Attitude Control Thruster Installation (Propellant 552 lbs., system 158 lbs.)	710
Wiring (from LM to periphery)	100
Gas Bottle Installation (2 LM RCS Helium Tanks, Valves, plumbing, etc.)	30
Misc. - ABLE LM attachments, thruster and gas bottle installations, Local structural beef-up	250
TOTAL REFLECTOR	17,400 lbs.

[redacted]

3.6.1 (continued)

For a Saturn V unmanned ABLE LM launch, the maximum allowable payload weight is now governed by the launch vehicle stock limit of 110,000 lbs. This means that reflector diameters of 3,000 ft. or greater could be accommodated.

An alternate tripod configuration, sized to give a reflector of equal surface area to a torus configuration, was found to be about 24% lighter. This would yield proportionately larger allowable reflector sizes for the manned ABLE LM/CSM configuration.

[redacted]

[redacted]

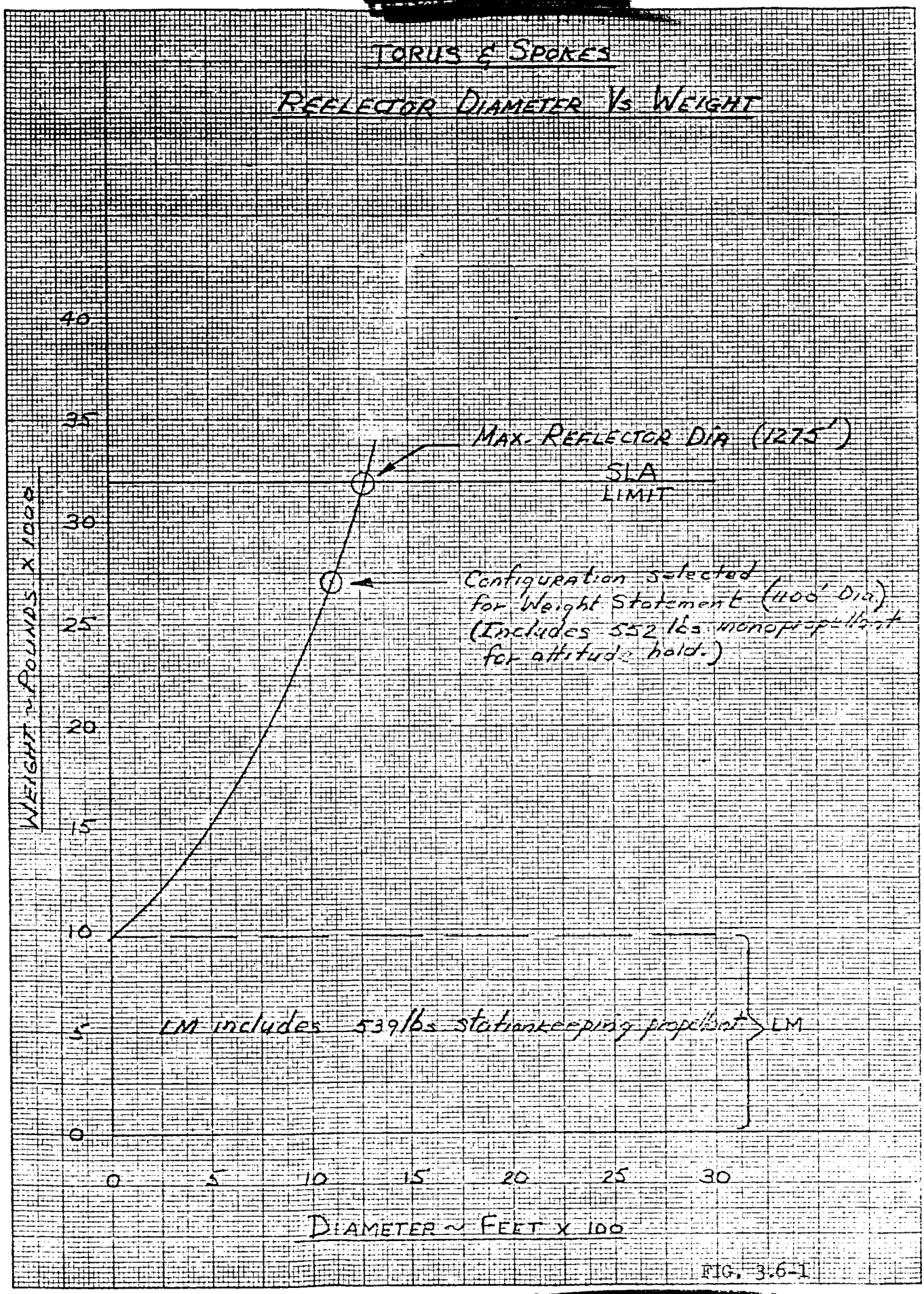

FIG. 3.6-1

[redacted]

4.0 REFLECTOR/SUPPORT STRUCTURE

4.1 STRUCTURAL DESIGN

A number of configurations (see Figure 4.1-1) were studied and categorized under three family types as either disc, sphere, or hemisphere.

The disc configurations have a structural support system in the same plane as the reflective surface. This results in large differences in moment of inertia. The spherical configurations were studied in an attempt to negate the resulting gravity gradient problem. The solution of this problem was accomplished at the price of greatly increasing the gross weight. The hemispherical family designation is used to denote configurations where the supporting sturcture is on one side of the reflective surface. These configurations were initiated to achieve a compromise to the "high weight/high gravity gradient" problem.

The disc family has several advantages relative to the sphere or hemisphere. These include:

- large diameters (greater than 400 ft) are feasible
- ease of resupply
- ease of deployment
- testing simplicity

The disc configuration is such that diameters as large as 3000 ft appear to be feasible. In both the sphere and hemisphere, weight and the physical size of the support members would probably become prohibitively large for reflectors of this magnitude. In the disc configuration, the consumables would be located at the center of the disc and access by a resupply vehicle could easily be accomplished. The disc shape also simplifies deployment, as compared with hemisphere, because of the absence of large structural members normal to the plane of the reflector. The inherent two dimensional shape of the reflector and structure would simplify the testing of the configuration, either on a scale model or on the full scale vehicle

Two disc configurations in particular were studied in more depth. They were referred to as the "torus and spoke" and the "star".

4.1.1 Torus and Spokes

This configuration shown in Figure 4.1-2a consists of an external torus, internal torus (HUB), a number of spokes extending radially between the torii, and reflective surfaces between the spokes. The spokes are the structural elements that carry the bending moments due to control forces. One approach to the structural configuration of the spokes and torus, is a composite "Aluminum Kapton-Aluminum". This material would be rigidized by pressurizing to the yield stress of the aluminum. Another approach might be the "stringer-frame" concept, where small diameter frames and stringers would be judiciously located on the spokes and torus. These frames and stringers would than be rigidized by pressurization. Inflatable type support structures were chosen over other rigid types for several reasons. These include:

- structural efficiency
- packaging efficiency
- length of straight members not limited
- existing state of the art (Echo)
- physical simplicity of deployment

4.1.2 "Star"

This configuration shown in Figure 4.1-2b is similar to the torus-spokes except that the external torus is deleted. One advantage of this concept over the "torus-spokes" is that the reflector must be joined to two edges of the torus-spokes rather than three.

Study of the two configurations above indicated a major problem of thermal distortions. One solution, appropriate isulation, is discussed in Section 4.3. Another approach to its solution is the triangular configuration shown in Figure 4.1-2c. Utilizing the theorem of three points defining a plane, and applying a load to the corners, the reflective surface will theoretically be in plane, regardless of the thermal deflections. There appear to be structural and mechanical problems created by this configuration, however. No in-depth study was made at this time to quantitatively evaluate them.

REFLECTOR CONFIGURATIONS

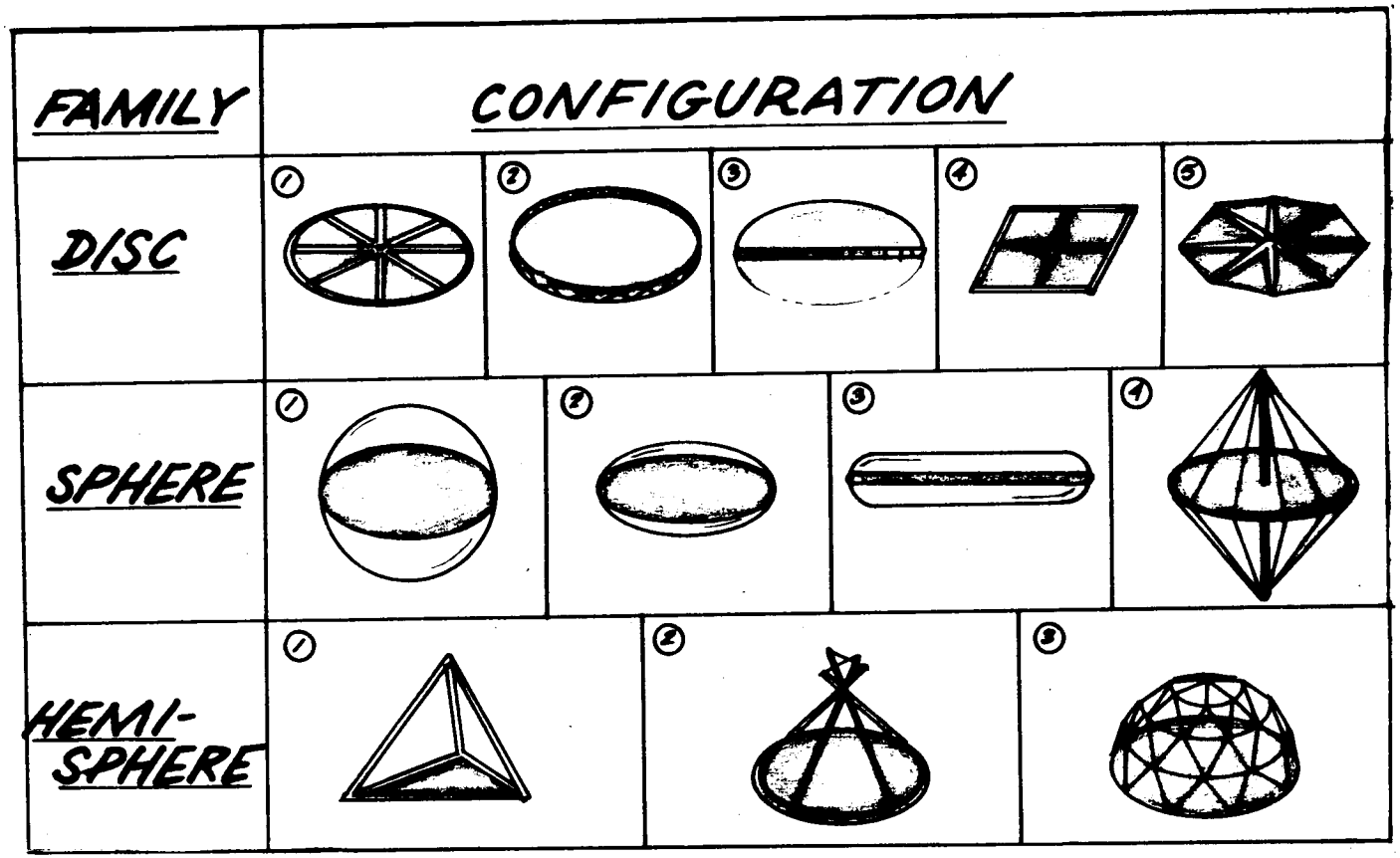

FIGURE 4.1-1

[redacted]

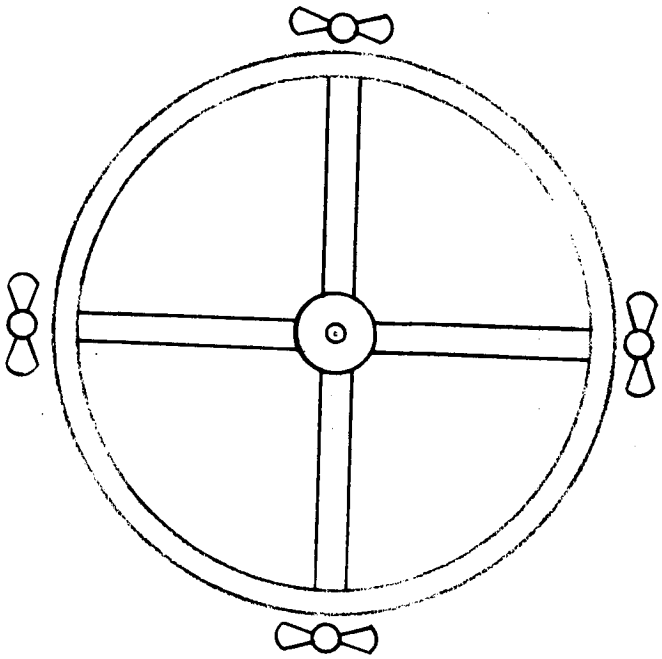

TORUS AND SPOKES
(a)

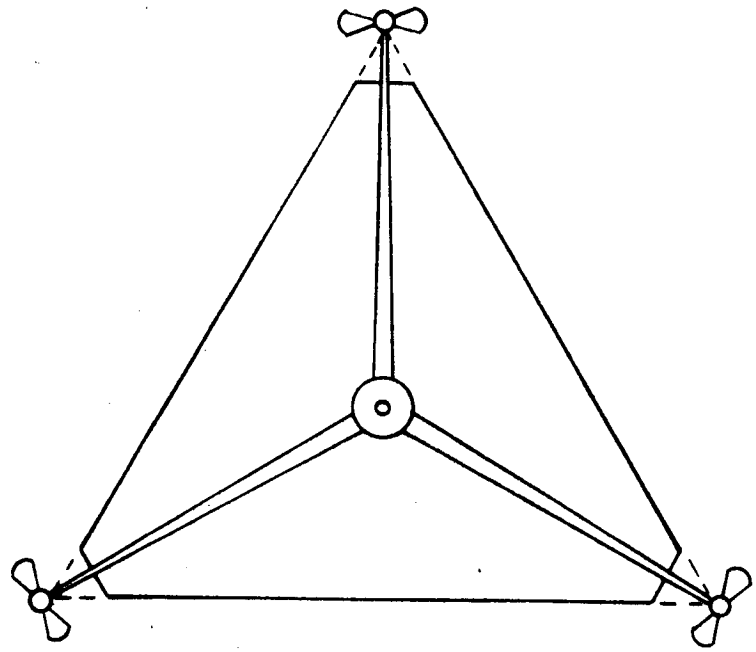

TRIANGLE
(c)

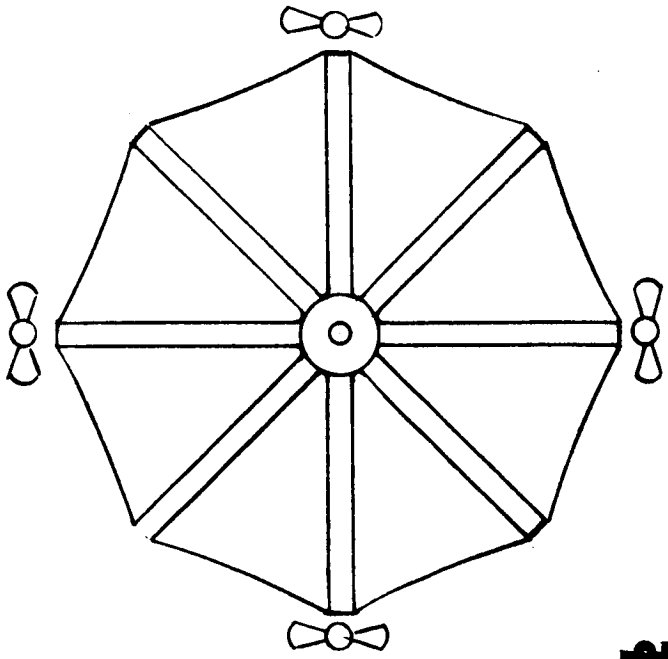

STAR
(b)

[redacted]

FIGURE 4.1-2 REFLECTOR CONFIGURATIONS

[redacted]

4.2 STRUCTURAL ANALYSIS

This section presents structural analyses of two general configurations:

- o a circular reflector membrane supported by a torus with four spokes
- o a triangular reflector of equivalent area supported by three spokes intersecting at the center of area

The basic material used for the structural supports for the above configurations is aluminum-mylar laminate, which is stressed above the yield during erection to obtain rigidization of the material. The aluminum layers are each 0.0005 in. bonded to a layer of 0.00035 in. mylar. The structural supports are twenty foot cylindrical tubes made of the above material stiffended by 5 inch diameter rigidized tubes in the form of stringers and frames. The reflector membrane is made of aluminized Kapton with a thickness of .00035 inches.

The effects of gravity gradient loads, solar pressure, thermal gradients, membrane tension forces, membrane deflections, natural frequencies and creep were studied. The results of this analysis indicate that the deflection of the overall system is primarily due to thermal gradients in the spokes, in addition to manufacturing tolerances. The effect of solar pressure and gravity gradients on deflections is small. The analysis also indicates that reflector membrane tensile loads are strongly influenced by the manufacturing tolerances; large tolerances can induce high tensile stresses.

In addition to the structural cross sectional arrangement mentioned above this investigation also included a study of a stabilized structure utilizing internal pressure. If a pressure of 2 psi could be maintained in the reflector support structure, the allowable bending moment in the torus and spokes for the twenty foot diameter section can be increased by a factor of 1.5 over the unpressurized structure. However, consideration must be given to the weight of gas necessary to carried to maintain pressure lost due to meteoroid penetration. A study of this effect was made for the one year life requirement. The results of the calculation showed that approximately 1.5×10^6 lbs of pressurization gas would be necessary in order to maintain the required pressure. In view of the excessive weight, this structural system was not considered feasible.

[redacted]

[redacted]

4.2 (continued)

A structural efficiency study was also conducted on a photolyzable film wire mesh concept for a rigidized structure. A comparison using published compression data was made for a photolyzed wire mesh cylinder and an aluminum foil cylinder. The result showed that the aluminum cylinder was capable of carrying a larger compression load than the wire mesh structure.

Finally, early consideration was also given to a support structure consisting of aluminum mylar laminate cylinders without internal pressure. However, this structure results in extremely large r/t values giving negligible values of bending stress allowables.

It is concluded from the analyses and studies carried out under this program that it appears structurally feasible to design and fabricate an expandable structure to carry out the assigned mission. The more promising structural arrangements are analyzed in the remainder of this report, i.e. the torus-spoke configuration and the tripod configuration. It must be noted, however, that problem areas still remain for further study. These include the following:

- bending and compression buckling test data
- more accurate analyses of the effects of manufacturing tolerances
- detail static and dynamic analyses of the effects of load and thermal disturbances
- materials creep data and creep deformations.

4.2.1 Basic Structural Cross Section Properties

A typical structural support system for the reflector membrane consists of a 20 foot diameter aluminum-mylar laminate stiffended by 5 inch diameter aluminum-mylar laminate tubular stiffener. The 20 ft. diameter was selected after preliminary analyses showed a good ratio of buckling stress to weight. Five inch diameter tubular frames are also incorporated circumferentially around the 20 foot tube to provide stiffener and shell stability to the structure. For rigidization, separate pressures will be required for the 5 inch diameter tubes. The laminate section used throughout this analysis is two external layers of .0005 inch aluminum bonded to a core of .00035 inch mylar. A cross section is shown in figure 4.2-1.

[redacted]

[redacted]

4.2.1 (continued)

A stress-strain curve for the Echo II laminate, which was .18 mil aluminum layers with the 0.00035 mil ylar, is shown in figure 4.2-2 as taken from the indicated reference.

Also taken from the same reference is a curve of compression buckling stress versus the r/t of the cylinder figure 4.2-3. These data have been used in this analysis to substantiate the structure of the vehicle. Future studies will be required to show that data taken from the references can be verified by additional development testing.

Properties of Cross Section of Torus and Spoke Members

The basic structural material consists of an aluminum mylar laminate with the following thicknesses:

Material:

0.0005 aluminum
0.00035 mylar
0.0005 aluminum

0.00135 total thickness

For purposes of this analysis it is assumed that the structural material thickness is 0.0010 since only the aluminum thickness is considered for structural purposes. This is a conservative approach.

The stringer is a 5 in. diameter tube of the same material as above with an area of 0.0157 inches square.

In order to compute the allowable bending moment, the following calculations were performed:

Member	Area	y	Ay	$\bar{y}$	$A\bar{y}$	$A\bar{y}^2$
1	.0078	120	.94	117	.91	107
2	.0157	112	1.76	109	1.71	186
3	.0157	93	1.46	90	1.41	127
4	.0157	64	1.00	61	.96	59
5	.0157	27	.42	24	.38	9

[redacted]

4.2.1 (continued)

Member	Area	y	Ay	$\bar{y}$	$A\bar{y}$	$A\bar{y}^2$
6	.0157	-13	-.204	-16	-.25	4
7	.0157	-51	-.80	-54	-.85	46
8	.0157	-84	-1.32	-87	-1.37	119
9	.0157	-117	-1.84	-120	-1.88	225
10	.0078	-119	-.93	-121	-.95	115
	.1413		.45			997

$$\bar{y} = 3$$

Area of skin = $2\pi rt = 6.28 \times 120 \times .001 = .754 \text{ in}^2$

Total Section Area = 1.04 in^2 including all skin

Total Section Area = $.282 \text{ in}^2$ without skin

Inertia of skin = $\pi r^3 t = 3.14\ (120)^3\ \ .001 = 5430 \text{ in}^4$

Total Section Inertia = 7424 in^4 including skin

Total Section Inertia = 1994 in^4 without skin

Using these section properties, the allowable moment which can be carried by the spoke or torus can be computed as follows:

Allowable stress for $\frac{r}{t} = \frac{2.5}{.001} = 2500$

F_c = 1000 psi from buckling stress vs r/t curve figure 4.2-3

$$F_c = \frac{Mc}{I}$$

$$M = \frac{1000 \times 1994}{121} = 16500 \text{ in. lb or } 1375 \text{ ft. lbs.}$$

using safety factor of 1.35 M = 1020 ft. lbs.

4.2.2 Investigation of Torus-Spoke Supported Reflector

The torus spoke configuration consists of the torus outer ring, four spokes and the reflector membrane as shown in the sketch. The selected diameter for this investigation is 1100 ft.

[redacted]

4.2.2 (continued)

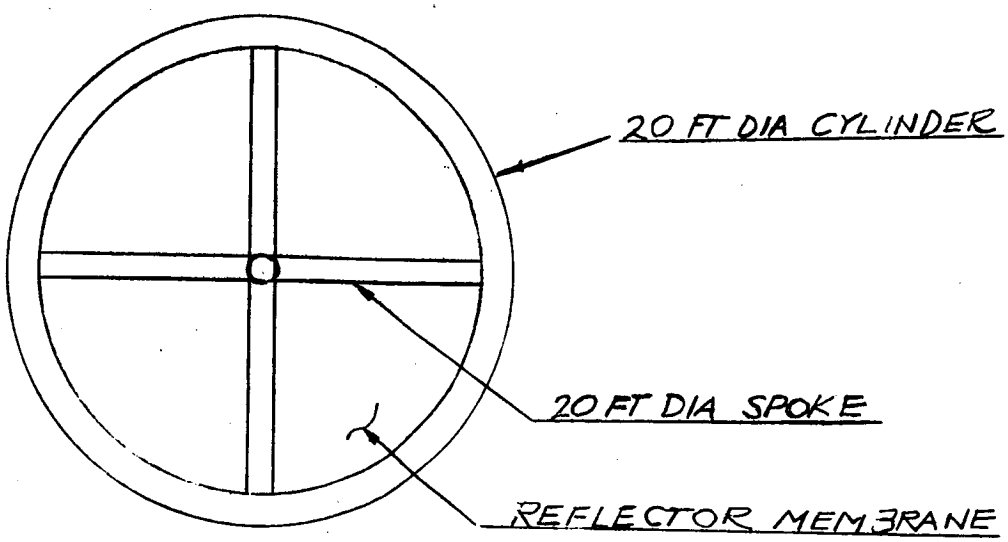

This configuration is analyzed for deflections and stresses due to:

1. Reflector membrane tension load
2. Gravity gradients
3. Solar pressure
4. Thermal gradients
5. Natural frequencies
6. Creep

The analyses shows that critical stress conditions are predominant under action of the membrane tension load while the major contribution to deflections is caused by thermal gradients through the twenty foot diameter cross section.

4.2.2.1 Influence Coefficients and Deflections

In this study the torus spoke configuration was analyzed to obtain the structural influence coefficients and to determine the deflections due to gravity gradient forces.

The structural model used was a 3000 ft. four spoke torus with a constant circular cross-section of 30 ft. diameter. While the latest investigation is for a 1100 ft. diameter torus with a 20 foot diameter cross-section, the results of this analysis show that deflections due to gravity gradients would not be significant in either case. A synchronous orbit was chosen for the example. The magnitude of the gravity gradient at 45° to the orbit tangent was then defined and resultant deflections obtained.

[redacted]

4.2.2.1 (continued)

From the matrix analyses shown in the Appendix for complex structures, a mathematical model was chosen with 16 node points representing the torus and 13 node points representing the 4 spokes. Since both torus and spokes have identical cross sections, the element areas are constant. Thus,

$$A_{x\text{-sect.}} = \pi Dt = \pi(30 \times 12)\ (.0006) = .678 \text{ in.}^2$$

The model is assumed to be fixed at the center node of the structure in six degrees of freedom. The remaining nodes are assumed free in six degrees of freedom. A unit normal load matrix was then applied to the torus and resulting deflections were obtained. The typical deflection pattern due to a unit load discreetly applied is 25.4 inches. It should be noted that there is no applied load of this magnitude applied to the end of a spoke due to any design condition.

A load matrix representing gravity gradient forces was then applied to the structure. The deflections due to this loading conditions is 0.093 inches.

4.2.2.2 Analysis of Membrane Preload Effect On Support Structure

The solution for a pressure stabilized torus and membrane is given in section 3.4.2.2.8 of USAF ASD-TDR-63-4275 Part II.

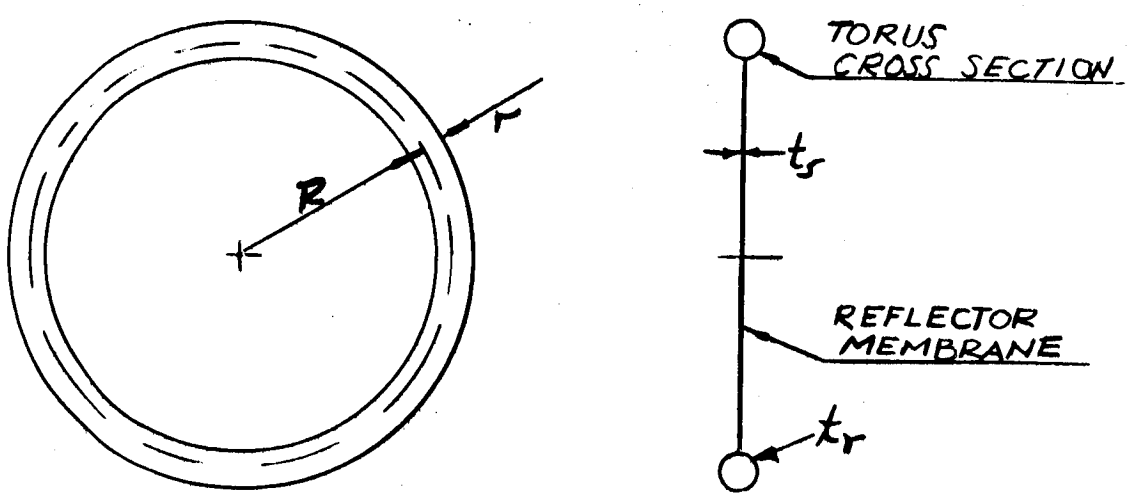

The initial radius differences between membrane and inner torus is given by t_o.

The constant prestretching force in the membrane is N_s.

[redacted]

4.2.2.2 (continued)

The degree of prestretching in the membrane is given by:

$$\frac{N_s}{R}\left[\frac{1}{\pi}\frac{R}{r} + 2\frac{Er}{Es}(1-\mu)\right]\frac{tr}{t_s} = 2\,Ert_o\,\frac{tr}{R^2} + p\,(1-2\mu)\,\frac{r}{R}$$

were: $Er = 2.6 \times 10^6$ psi

$Es = 5 \times 10^5$ psi

$tr = .001$ inches

$ts = .00035$ inches

$\mu = .3$

$R = 6600$ inches

$r = 120$ inches

For this analysis it was assumed that the torus pressure was maintained at a value to give a torus skin stress level of 5000 psi.

Substitution into the equation gives the relation between the membrane load and the initial radius difference

$$N_s = .0206\,t_o + .0593$$

This is plotted in the figure 4.2-4.

Since pressure is maintained in the above analysis, an approximate solution for the membrane load versus radius dimension difference without torus pressurization is given by the following solution

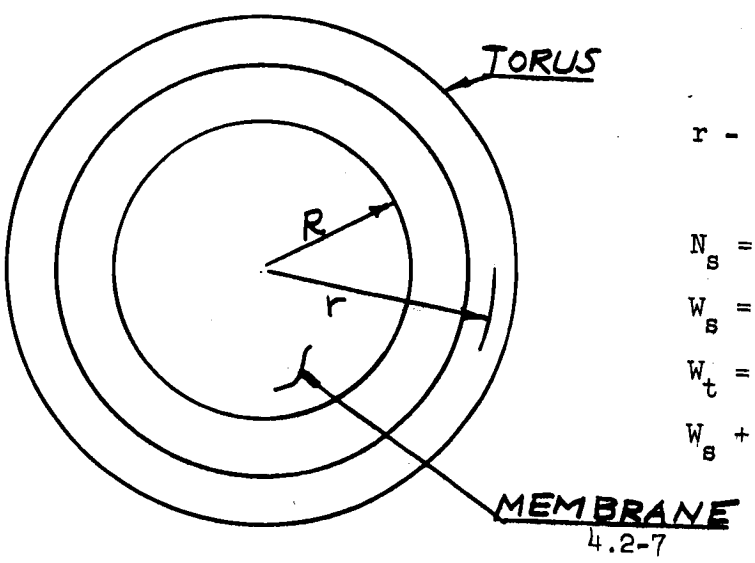

$r - R = t_o$ = initial difference in radii dimension of sheet and torus, inches

N_s = uniform load in sheet lbs/in

W_s = deflection in sheet, radial inches

W_t = deflection torus, radial inches

$W_s + W_t = 2\,t_o$

[redacted]

4.2.2.2 (continued)

Using the standard deflection equations:

$$W_s = \frac{N_s\ 2R}{t_s\ E_s} \qquad W_t = \frac{2\ N_s\ r^2}{A_t\ E_t}$$

$$\frac{N_s\ R}{t_s E_s} + \frac{N_s r^2}{A_t\ E_t} = t_o$$

$$N_s \left[\frac{r + t_o}{t_s\ E_s} + \frac{r^2}{A_t\ E_t} \right] = t_o$$

$$N_s \left[\frac{r}{t_s\ E_s} + \frac{t_o}{t_s\ E_s} + \frac{r^2}{A_t\ E_t} \right] = t_o$$

$$N_s \left[\frac{6600}{.00035x5x10^5} + \frac{t_o}{.00035x5x10^5} + \frac{(6600)^2}{1x2.5\ x10^6} \right] = t_o$$

$$N_s \left[37.8 + \frac{t_o}{175} + 17.4 \right] = t_o$$

$$N_s\ \frac{t_o}{175} + 55.2\ N_s = t_o$$

$$N_s\ t_o + 9670\ N_s = 175\ t_o$$

The results of this equation are very close to the values plotted in the figure 4.2-4. It should be noted that high membrane load can be induced by a relatively low fabrication difference in radius.

The effects of creep deflections have not been included in this analysis due to the lack of adequate creep test data for extended periods of time and in biaxial directions. Additional studies must be carried out to determine the effect of creep on deformations of the reflective membrane.

[redacted]

[redacted]

4.2.2.3 Combined Bending and Axial Loads In The Torus Spoke Configuration

The permissible tensile stress in the membrane sheet will be limited by the stresses induced in both the torus shell and the spoke shell. The tensile load in the sheet induces bending moments and axial forces in the torus as well as axial loads in the spoke member. Following is an analysis of the stresses induced in the torus due to the hoop compression caused by sheet tension. The sheet tension is assumed to be 100 psi or an axial load of approximately 0.030 lbs per inch.

Because of the presence of the spokes, the torus undergoes not only compression but also bending. Take as a free body a portion of the torus which includes one of the spokes:

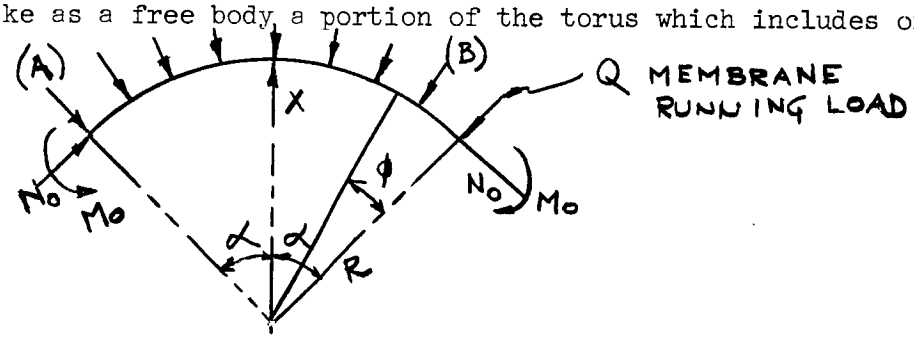

From Timoshenko "Strength of Materials" Part I, there can be no shearing stresses over the cross sections A & B because of symmetry. The longitudinal force N at any cross section is given by:

$$N = N_o \cos \phi + 2\, QR \sin^2 \frac{\phi}{2} = QR - \frac{X \cos \phi}{2 \sin \alpha} \qquad (1)$$

The bending moment for the same cross section is given by:

$$M = M_o - N_o R\,(1 - \cos \phi) + 2QR^2 \sin^2 \phi/2$$

$$= M_o + \frac{XR}{\sin \alpha} \sin^2 \frac{\phi}{2} \qquad (2)$$

Assuming identical spoke and torus cross sections it can be shown by strain energy methods similar to those given in the above reference that:

$$X = \frac{QR}{(A/I)\, R^2 f_2(\alpha) + 1 + f_1(\alpha)} \qquad (3)$$

$$M_o = -\frac{XR}{2} f_3(\alpha) \qquad (4)$$

[redacted]

[redacted]

4.2.2.3 (continued)

$$f_1(\alpha) = \frac{1}{2\sin^2\alpha}\left(\frac{\sin 2\alpha}{4} + \frac{\alpha}{2}\right) \qquad (5)$$

$$f_2(\alpha) = \frac{1}{2\sin^2\alpha}\left(\frac{\sin 2\alpha}{4} + \frac{\alpha}{2}\right) - \frac{1}{2\alpha} \qquad (6)$$

$$f_3(\alpha) = \frac{1}{\sin\alpha} - \frac{1}{\alpha} \qquad (7)$$

For a value of $\frac{I}{A} = 7160\ in^2$ the compressive force can be approximated by $N = QR$ with an error of 2% or less for reflectors 1,000 feet in diameter or greater. For the following configuration:

R = reflector radius = 550 ft.

α = 45 degrees (4 spokes)

$\frac{I}{A}$ = Inertia/area = 7160 in^2

Q = membrane running load = 0.03 lb/in

$f_1(\alpha) = 0.643$

$f_2(\alpha) = 0.00608$

$f_3(\alpha) = 0.141$

The reaction on the spoke is from (3)

$$X = \frac{.03\ (550 \times 12)}{\frac{(550 \times 12)^2}{7160} \times .00608 + 1 + .643} = \frac{198}{36.9 + 1.643} = 5.14 \text{ lbs.}$$

The bending moment at center span from (4)

$$M_o = -\frac{5.14 \times (550 \times 12) \times .141}{2} = -2390 \text{ in - lbs.}$$

[redacted]

[redacted]

4.2.2.3 (continued)

The compressive force at center span is from (1)

$$N_o = (.03 \times 550 \times 12) - \frac{5.14\ (\cos)}{2 \sin 45°} = 198 - 3.6 = 194.4 \text{ lbs.}$$

The bending moment at the spoke is from (2)

$$M_s = -2390 + \frac{5.14\ (550 \times 12)}{\sin (45°)} \sin^2 (22.5°) = -2390 + 7050 = 4660 \text{ in - lbs.}$$

The compressive force at the spoke intersection is from (1)

$$N_s = (.03 \times 550 \times 12) - \frac{5.14 \cos (45°)}{2 \sin 45°} = 198 - 2.6 = 195.4 \text{ lbs.}$$

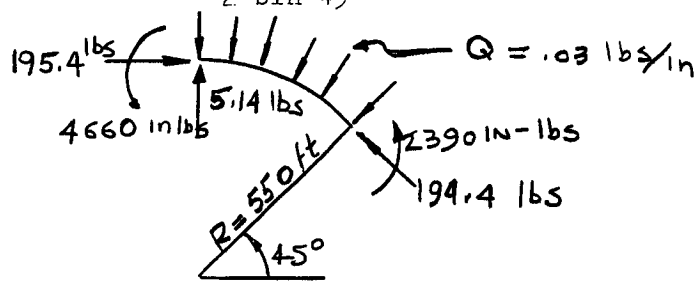

The member internal forces as given by the above analysis are shown on the free-body diagram and the resulting stresses are given below.

Stresses in Torus Cross Section

M_s = 4660 in -lbs. moment in torus at spoke intersection

N_s = 195 lbs. axial load in torus at spoke intersection

The bending and axial stresses induced by the above are:

$$f_b = \frac{4660 \times 121}{1994} = -283 \text{ psi}$$

$$f_c = \frac{195}{0.2826} = \begin{array}{l} -690 \text{ psi} \\ -973 \text{ psi compression total} \end{array}$$

The allowable compression stress:

$$r/t = \frac{2.5}{0.001} = 2500$$

f_c = 1000 psi from Schjeldahl data (figure 4.2-3)

[redacted]

[redacted]

4.2.2.4 Deflections Of The Reflector Sheet Due To Gravity Gradient And Solar Pressure

An investigation of the deflections of the four spoke-torus reflector was made in order to obtain an estimate of required membrane tensions. It was assumed that the spoke and torus were relatively stiff in comparison with the reflector.

The deflections, Z, perpendicular to the plane of a membrane are given in polar coordinates (ρ , θ) by:

$$\frac{\partial^2 z}{\partial \rho^2} + \frac{1}{\rho}\frac{\partial z}{\partial \rho} + \frac{1}{\rho^2}\frac{\partial^2 z}{\partial \theta^2} = -\frac{w}{s}(\rho, \theta)$$

where w = applied load - lbs/ft^2

s = membrane running load lbs/ft.

For a one-quarter segment (see Figure below) influence coefficients for 9 points were obtained using the finite difference operator of "Numerical Methods in Engineering", Salvadori and Barron, with unit applied load about each point. Multiplication of the influence coefficient matrix by the appropriate load matrix gives deflections due to gravity gradient and solar pressure. These values are 2.15 x 10^{-5} ft. and 7.25 x 10^{-4} ft. respectively.

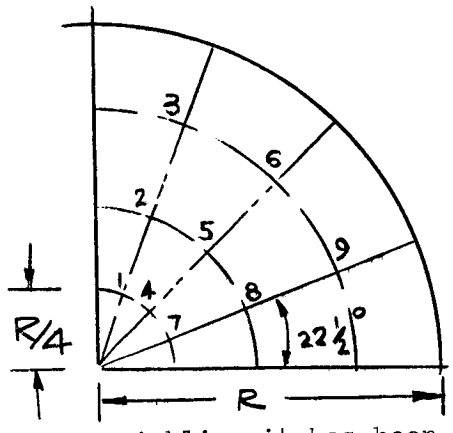

REFLECTOR DEFLECTION POINTS

In order to remove wrinkling it has been estimated that a membrane running load of 0.035 lbs/in is required. For a 1100 ft. diameter, 1/3 mil Kapton reflector;

R = Radius of reflector = 550 ft.

m = Reflector density = $\frac{0.0026}{32.2}$ = .807 x 10^{-4} slugs/ft^2

S = Membrane running load = 0.035 x 12 = 0.420 lbs/ft.

w = orbital frequency = $\frac{2}{12 \times 60 \times 60}$ = 1.45 x 10^{-4} rad/sec^2 (12 hr. orbit)

[redacted]

4.2.2.4 (continued)

The maximum deflection due to gravity gradient is:

$$\text{defl}_{\max_{g.g.}} = 0.0321 \times .807 \times 10^{-4} (550)^3 \times (1.45 \times 10^{-4})^2/.420 = 2.15 \times 10^{-5} \text{ ft.}$$

The maximum deflection due to a solar pressure of 13.12×10^{-10} psi is:

$$\text{defl}_{\max_{s.p.}} = .0.0533 \times 13.12 \times 10^{-10} \times 144 \times \frac{(550)^2}{.420} = 7.25 \times 10^{-4} \text{ ft.}$$

These results indicate that the membrane tension requirement will primarily be determined by the tension necessary to remove initial wrinkling. This requirement could be lowered several orders of magnitude before deflections of the reflector sheet due to gravity gradient and solar pressure begin to approach those due to temperature gradient and manufacturing tolerances.

4.2.2.5 Deflection In Spoke Beams Due To Thermal Gradients

The thermal gradient through the cylindrical spoke members will induce deflections which will degrade the reflective capability of the reflector surface. For this analysis it is assumed that the LM is attached at the center of the support structure. The analysis may be considered applicable for either the star or torus configuration inasmuch as it is assumed that the torus does not provide resistance to the spoke deflection. The thermal gradient is assumed linear from which it is concluded that thermal stresses do not exist since the deflection is unrestrained. The spoke is assumed to be a twenty foot diameter circular cylinder of rigidized aluminum-mylar laminate.

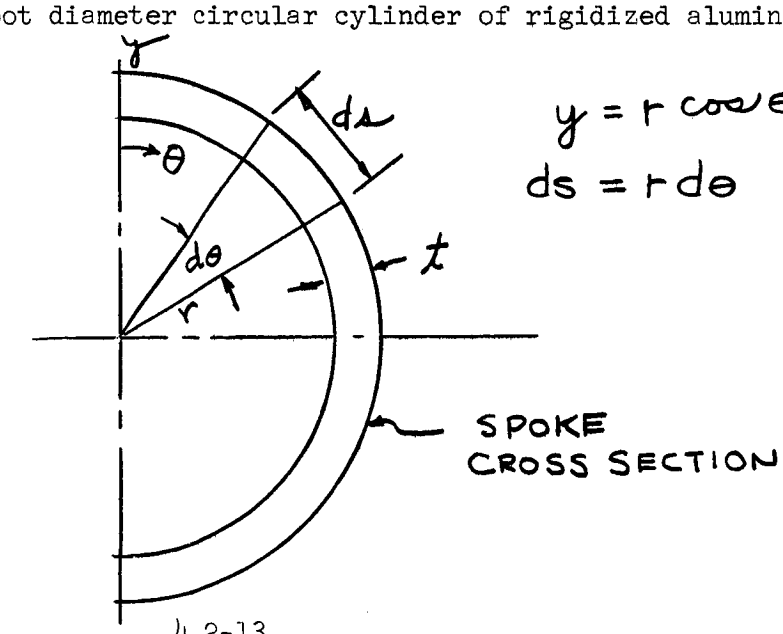

4.2.2.5 (continued)

Moment due to the thermal gradient about the centroid of the section:

$$M = \alpha E \int_0^{\ell} T(y)\, t\, ds\, y$$

$$M = \alpha E \int_0^{\pi} T(\theta)\, t\, r\, d\theta\, r \cos\theta = \alpha E t r^2 \int_0^{\pi} T(\theta) \cos\theta\, d\theta$$

Temperature distribution across the beam section:

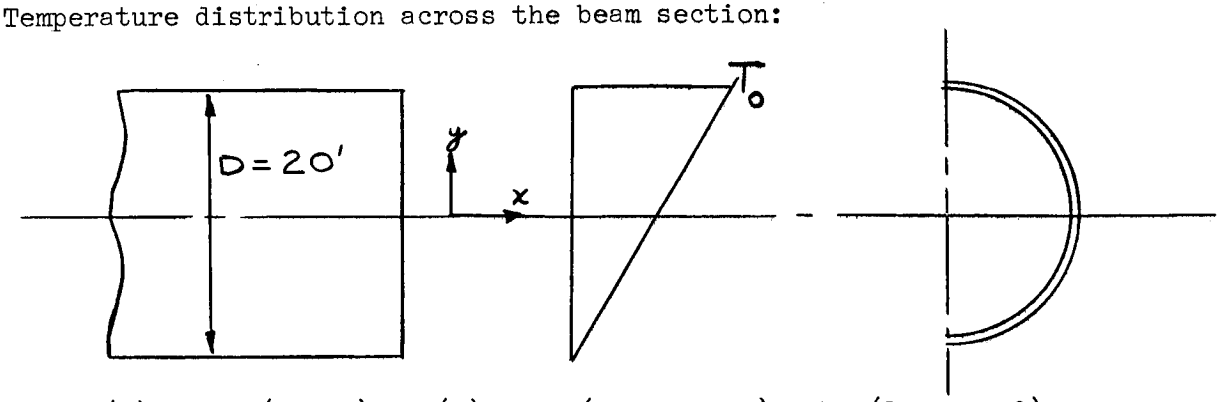

$$T(y) = \frac{To}{2}\left(1 + \frac{y}{r}\right) ; \quad T(\theta) = \frac{To}{2}\left(1 + \frac{r\cos\theta}{r}\right) = \frac{To}{2}(1 + \cos\theta)$$

$$M = 2\alpha E t r^2 \int_0^{\pi} \frac{To}{2}(1 + \cos\theta)\cos\theta\, d\theta = \alpha E t r^2 T_o \left[\int_0^{\pi} \cos\theta d\theta + \int_0^{\pi} \cos^2\theta d\theta\right.$$

$$M = \frac{\pi}{2}\alpha E t r^2 T_o \; ; \text{ Moment of inertia} = \pi r^3 t$$

The deflection of an unrestrained beam heated by a linear thermal gradient is equivalent to a simply supported beam loaded by equal and opposite end couples, where the moment is given by above.

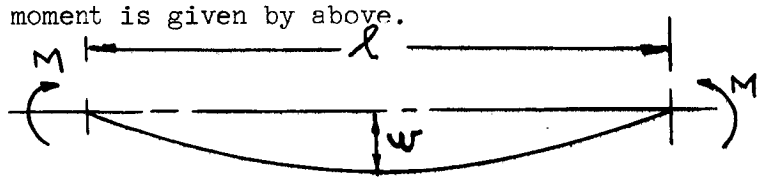

$$w = \frac{M\, l^2}{8\, EI}$$

$$w = \frac{\pi}{2}\alpha \frac{E\, t\, r^2\, T_o\, l^2}{8\, \pi\, r^3\, t\, E}$$

$$w = \frac{\alpha}{8}\, \frac{To}{D}\, l^2$$

[redacted]

4.2.2.5 (continued)

The results of this equation are plotted in figure 4.2-5. A ten degree thermal gradient is maintained in the structure through the use of "super insulation" wrapped around the support structures. The insulation consists of layers of mylar 0.125 mil thick aluminized on both sides.

4.2.2.6 Loads Due To Station Keeping With LM RCS Engines

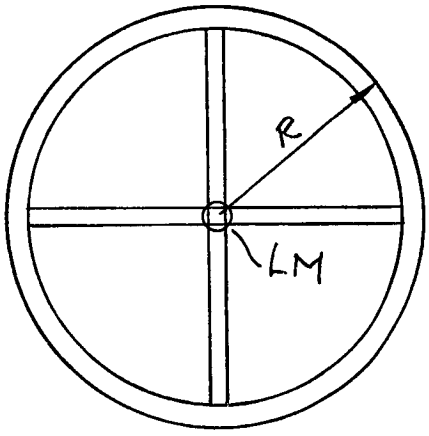

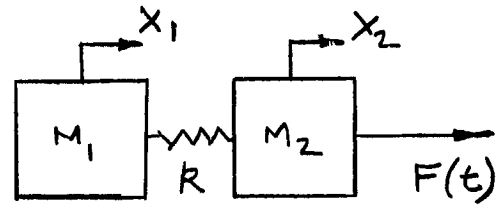

In order to determine preliminary loads due to LM RCS firing, the LM-Reflector combination of figure 1a was represented by the mathematical model of Figure 1b. This model will give an approximation of behavior due to first in-plane bending mode.

If $Y = X_2 - X_1$ is the relative displacement between the masses it can be shown that due to a unit impulse that:

$$Y = \frac{1}{M_2 w} \sin wt \qquad (1)$$

$$\text{where } w = \frac{K}{(M_1 M_2/(M_1 + M_2))}$$

With the use of Duhamels Integral the response to a force as shown in Figure is:

$$Y_1 = \frac{Fo}{M_2 w^2} \left(1 - \cos w t \right) \text{ for } t < T_o \qquad (2)$$

$$Y_2 = \frac{Fo}{M_2 w^2} \sqrt{2(1 - \cos w T o)} \cos (w t - \alpha) \text{ for } t > t o \qquad (3)$$

[redacted]

[redacted]

4.2.2.6 (continued)

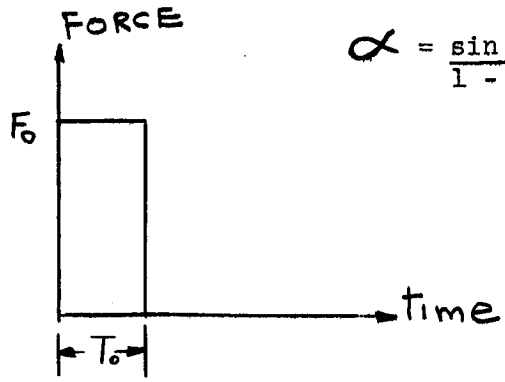

$$\alpha = \frac{\sin w\,To}{1 - \cos w\,To}$$

as $w\,To \rightarrow 0$) (e.g., $wTo < .1\pi$)

$$Y_1 = \frac{Fo}{M_2 w^2} \quad \frac{w^2 To^2}{2} = \frac{Fo\,To^2}{2M_2} \qquad (4)$$

$$Y_2 \cong \frac{Fo\,To}{M_2 w} \sin w\,t \qquad (5)$$

Assuming a fixed end condition between the torus and spokes and assuming a rigid torus

$$k = \frac{48EI}{R^3} \qquad (6)$$

and

$$m = \text{max bending moment} = \frac{6EIY}{R^2}\max \qquad (7)$$

For the following parameters:

R = Reflector Radius = 550 ft.

E = Modulus of elasticity of spoke = 2.6×10^6 psi

I = Moment of inertia of spoke = 2000 in^4

$$M_1 = \frac{10{,}000}{386} = 41.5 \ \frac{\#\text{-sec}^2}{in}$$

$$M_2 = \frac{10{,}000}{386} = 25.9 \ \frac{\#\text{-sec}^2}{in}$$

Fo = 100 lbs = RCS thrust

[redacted]

4.2.2.6 (continued)

The natural frequency is from (1a) and (6)

$$w = \sqrt{\frac{48 \times 2000 \times 2.6 \times 10^6}{(550 \times 12)^3} \times \frac{1}{\frac{25.9 \times 41.5}{67.4}}}$$

$$= \sqrt{\frac{.870}{16}}$$

$$= .233 \text{ rad/sec}$$

$$f_n = \frac{.233}{2\pi} = .0370 \text{ cps}$$

The maximum moment is by (7)

$$M_{max} = \frac{6 \times 2000 \times 2.6 \times 10^6}{(550 \times 12)^2} (16.6 \text{ To}) = 11{,}900 \text{ To in-lbs.}$$

The maximum deflection is by (5)

$$Y_{max} \cong \frac{100 \text{ To}}{25.9(.233)} = 16.6 \text{ To inches}$$

Using an allowable bending moment for the spoke of 12,240 in-lbs., the allowable RCS firing time for the assumed configuration is:

$$\text{To} = \frac{12{,}240}{11{,}900} = 1.03 \text{ sec.}$$

For smaller reflectors, the firing time increases. By comparison, the mimimum engine firing time is 0.040 seconds. Further analysis of firing frequency effects is recommended when total impulse requirements for near stable orbits are obtained.

4.2.2.7 Deflection Due To Solar Pressure

The solar pressure is a result of the momentum of the proton stream from the solar radiation with its magnitude depending on the surface angle of incidence and reflectivity. It is assumed for this analysis that the low linear momentum of the other solar particles, such as protons and electrons are insignificant and will not be considered. The load per square inch of surface for the solar pressure is taken as:

$$P = 13.12 \times 10^{-10} \text{ lbs. per square inch.}$$

4.2.2.7 (continued)

For this preliminary analysis, it is assumed that each spoke supports one quarter of the total pressure applied at the centroid of the circular sector.

The force per quarter area is:

$$F = \frac{1}{4} \quad (13.12 \times 10^{-10} \times \pi (6600)^2) \quad = .045 \text{ lbs.}$$

The distance from the center of pressure to the center is:

$$l = \frac{2}{3} \frac{r}{\pi/2} = 2800''$$

$$p = \frac{P\, l^3}{3\, EI} = \frac{.045 \times (2800)^3}{3 \times 2.67 \times 10^6 \times 2000} = 0.062 \text{ inches at load}$$

$$\text{deflection at tip} = \frac{6600}{2800} \times 0.062 = 0.146 \text{ inches}$$

The deflection due to solar pressure is therefore negligible.

4.2.2.8 Total Deflection Of Support Structure

Deflection of the support structure due to gravity gradient is approximately 0.09 inches, due to solar pressure about 0.15 inches, but 12 inches deflection due to thermal gradient of 10°F for insulated structure.

The deflection of the membrane due to gravity gradient and solar pressure is respectively 2.15×10^{-5} ft and 7.25×10^{-4} ft.

The above results show that the major consideration for deflection is the thermal gradient.

4.2.2.9 Creep

The basic support structure and reflector membrane should be analyzed for creep deformation. The time temperature and stress level for each component must be evaluated to arrive at rational value of creep deflection. In the case of the reflector membrane the tensile stress assumed to provide good reflective qualities is 100 psi with a temperature of approximately 350°F. Material creep data will have to be obtained for the total mission life for proper evaluation of design conditions. Data at these conditions does not currently exist for the planned materials applications.

[redacted]

4.2.4 Tripod Configuration

The tripod configuration assumed for this analysis is based on a three-spoke support structure which provides support for an equilateral triangular reflector membrane at the tips of the triangle. The plane of the membrane will be determined by the plane defined by the tips of the three spokes.

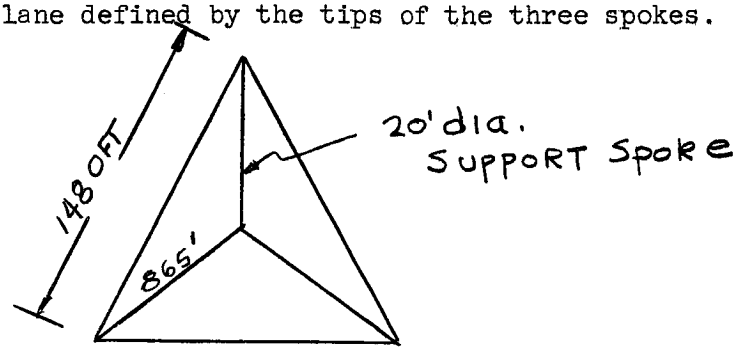

area = 949,850 sq. ft. equivalent to area of 1100 ft. diameter circle.

A radial load of 434 pounds is required at each corner to maintain 100 psi membrane tensile stress in the reflective surface. The 100 psi stress is assumed necessary near the center of the triangle (at maximum cross section).

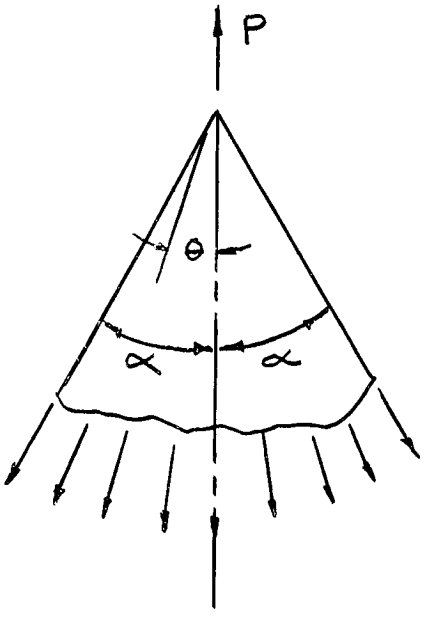

The solution given in Timoshenko "Theory of Elasticity"

$$r = \frac{P \cos \theta}{tr\,(\alpha + \frac{1}{2} \sin 2\alpha)}$$

since σ_r is a minimum at

$$\theta = \alpha$$

$$\sigma_r = \frac{P \cos}{tr\,(\alpha + \frac{1}{2} \sin 2\alpha)}$$

for $\alpha = 30°$ $\sigma_r = 100$ psi

$$P = \frac{100\ tr}{\cos \alpha} (\alpha + \tfrac{1}{2} \sin 2\alpha)$$

$$= 434 \text{ lbs.}$$

[redacted]

4.2.4 (continued)

To determine the section properties, assume the five inch diameter stiffeners are 0.001 inch aluminum bonded to either side of the 0.00035 inch mylar. The section area is then 2 x .282 = .564 in.^{2} and the moment of inertia is 2 x 1994 = 3988 in.^{4}

To determine the stresses due to membrane tension forces, the axial load in the tubular members is 434 lbs. For an eccentricity of 36 inches, the moment is 36 x 434 = 15650.

$$\sigma_c = -\frac{15650 \times 120}{3988} - \frac{434}{.564} = -472 - 770$$
$$= -1242 \text{ psi}$$

The allowable compression stress is:

$$\frac{r}{t} = \frac{2.5}{.002} = 1250$$

$$F_c = -1700 \text{ psi}$$

The results of the deflection analysis of the torus configuration indicated that the most significant contribution to the total deflection is due to the thermal gradient; the effects of gravity gradients and solar pressure are negligible. In this case, it may be assumed that the deflection due to temperature gradient is given by the curve presented in the analysis for the torus using the lengths given for the triangular support structure. It should be noticed that in-plane motions of the spoke tips do cause deflections in the reflector surface. For example, if the distance between tips is reduced from 1480 ft. to 1478 ft., the reflector edge can "sag" as much as 38 ft.!

[redacted]

STIFFENED CYLINDER CROSS SECTION

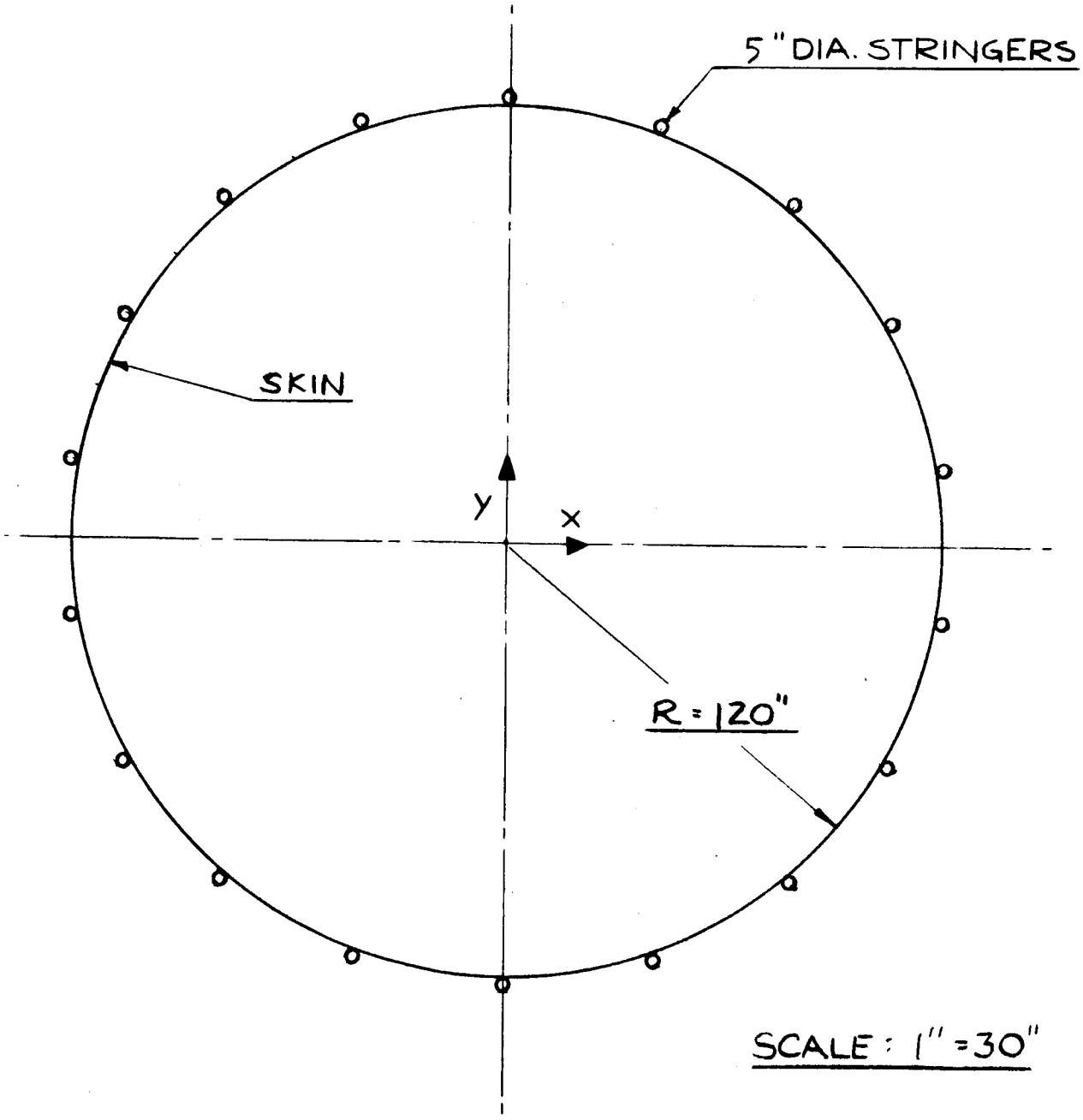

FIGURE 4.2-1

[redacted]

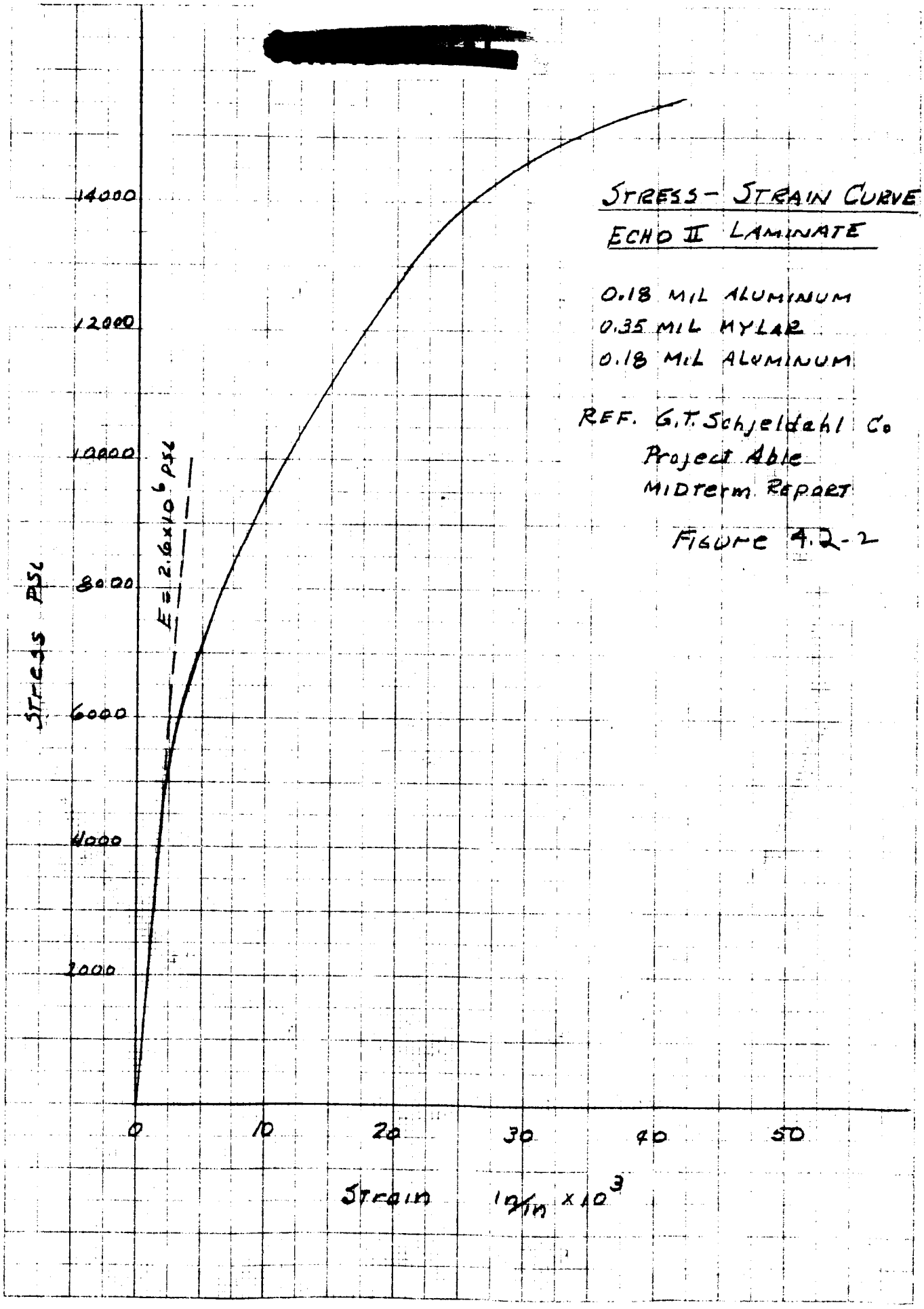
STRESS - STRAIN CURVE
ECHO II LAMINATE
0.18 MIL ALUMINUM
0.35 MIL MYLAR
0.18 MIL ALUMINUM
REF. G.T. Schjeldahl Co
Project Able
MIDterm Report
FIGURE 4.2-2
14000
12000
10000
8000
6000
4000
2000
STRESS PSI
E = 2.6x10^6 PSI
0
10
20
30
40
50
STRAIN in/in x10^3

[redacted]

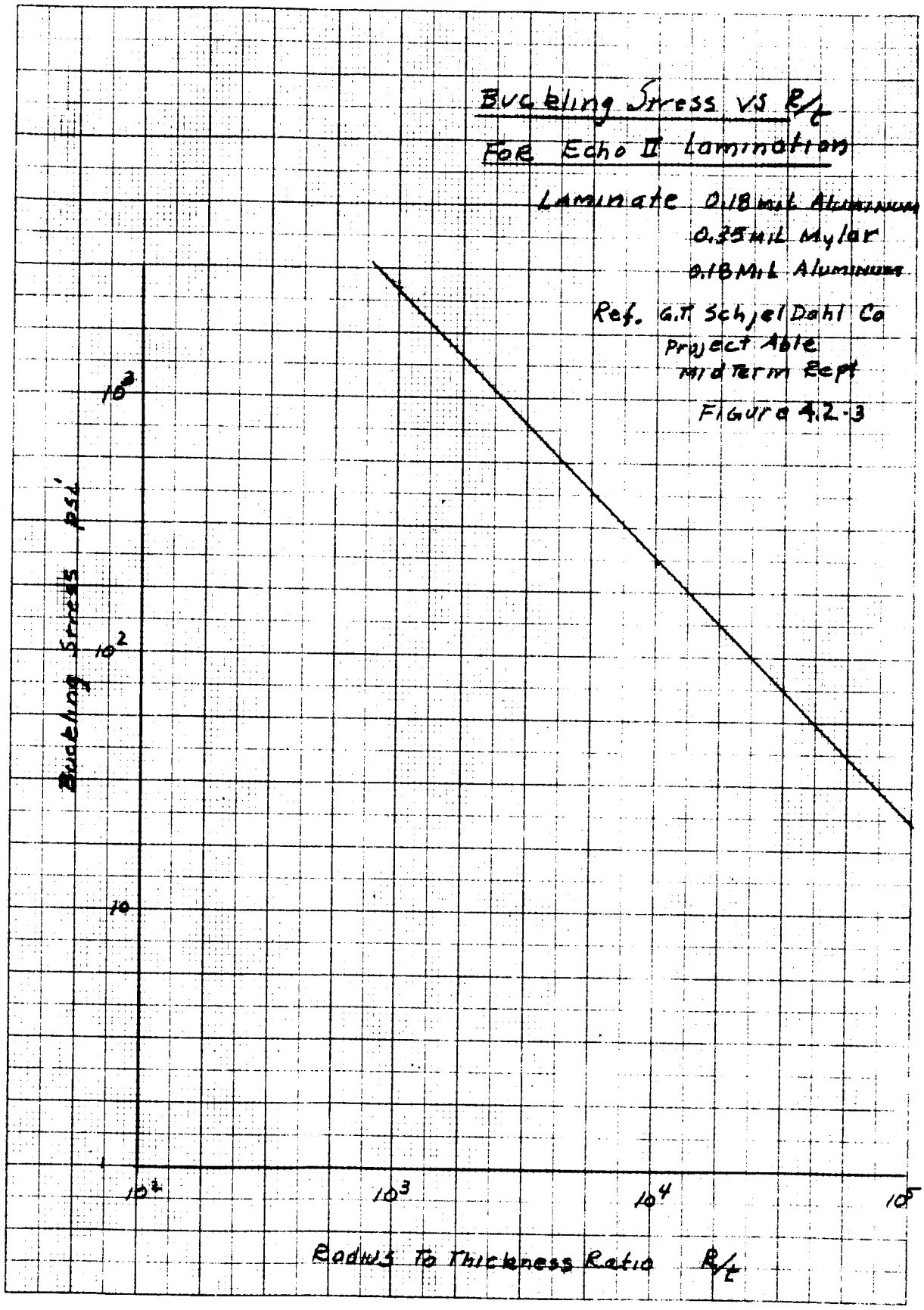

[redacted]

[redacted]

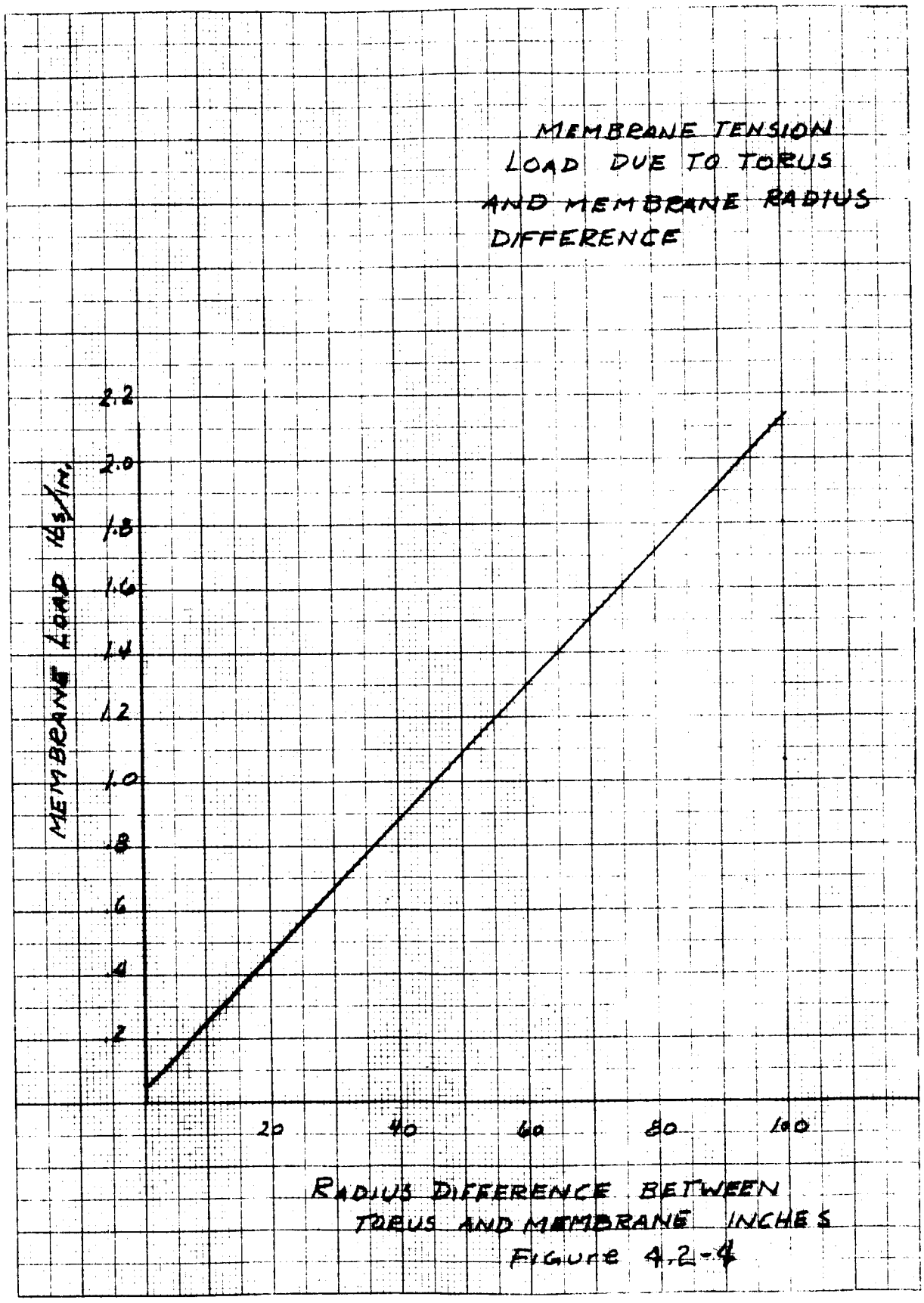

FIGURE 4.2-4

[redacted]

K+E 10 X 10 TO ½ INCH 46 1327
7 X 10 IN. • ALBANENE® MADE IN U.S.A.
KEUFFEL & ESSER CO.

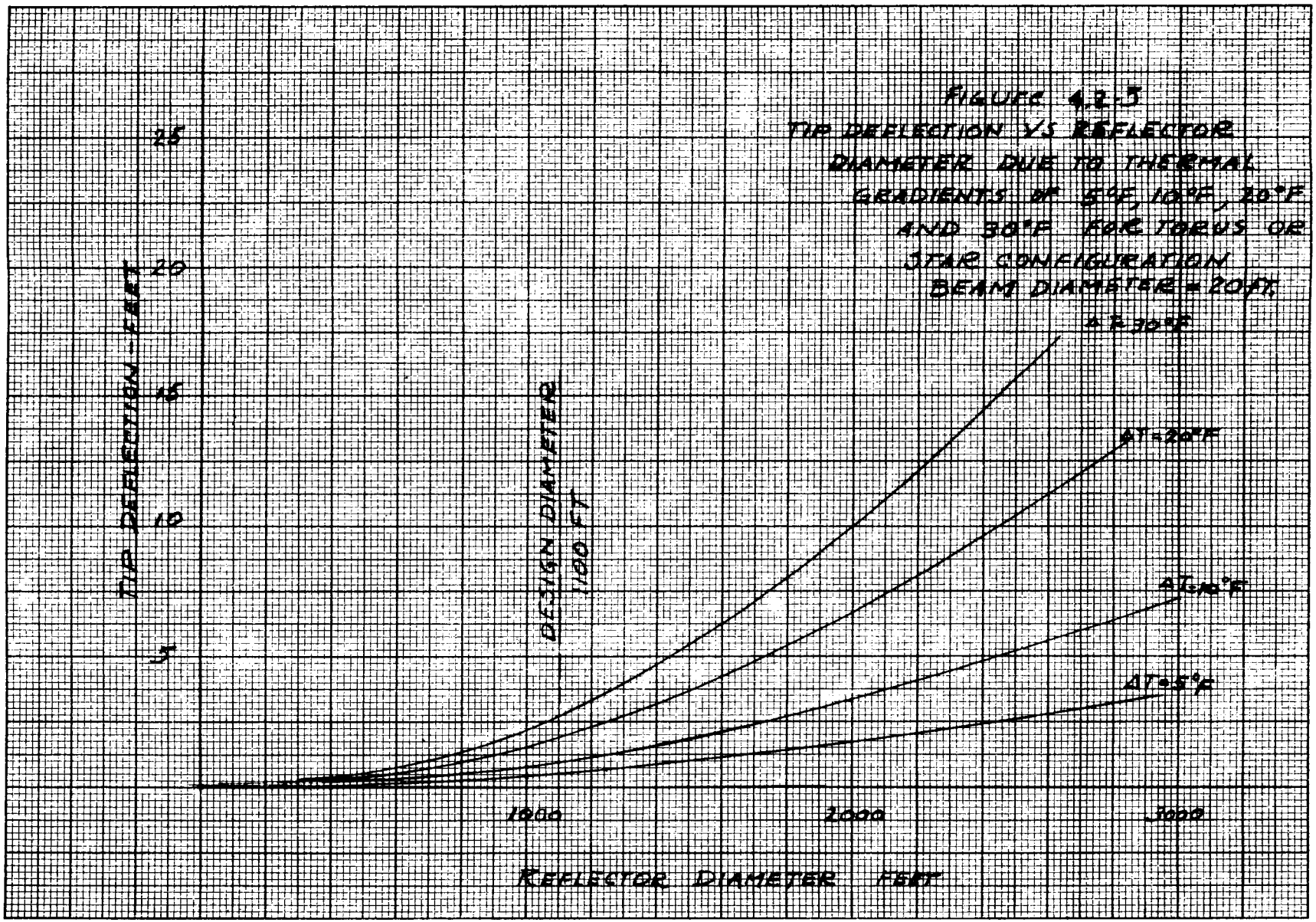

FIGURE 4.2-5
TIP DEFLECTION VS REFLECTOR DIAMETER DUE TO THERMAL GRADIENTS OF 5°F, 10°F, 20°F AND 30°F FOR TORUS OR STAR CONFIGURATION
BEAM DIAMETER = 20 FT.

K+E 10 X 10 TO ½ INCH 46 1327
7 X 10 IN. • ALBANENE MADE IN U.S.A.
KEUFFEL & ESSER CO.

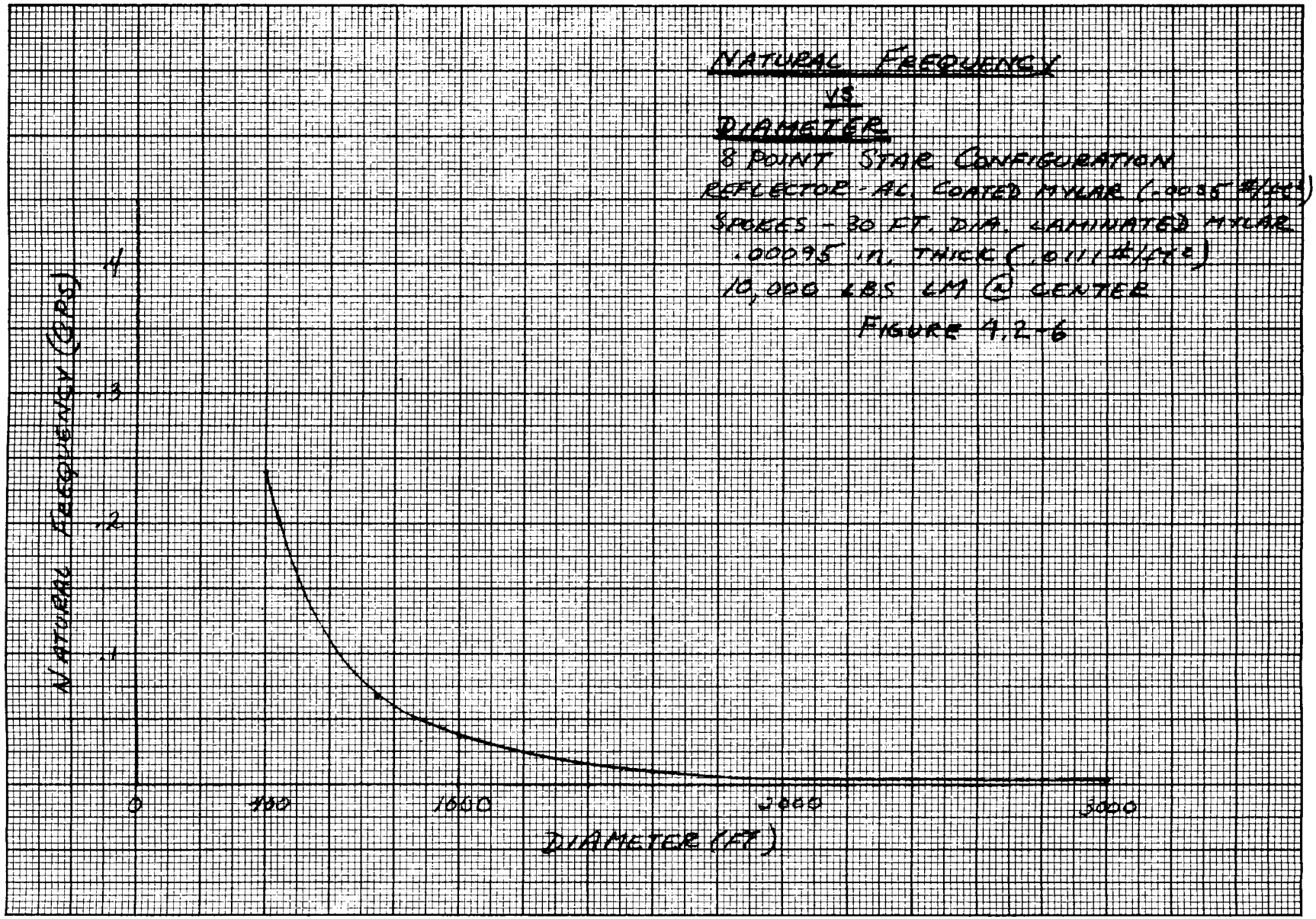

[redacted]

4.3 THERMAL ANALYSIS

4.3.1 Reflector

The choice of a reflector material is dependent on the temperature extremes that will be encountered. Reflector temperatures are dependent on the material thermal properties and on mission orbital parameters. A detailed discussion of the reflector thermal analysis is contained in Appendix C.1

The reflector thermal design concept consists of aluminum vapor deposited on both sides of a Kapton sheet (nominal surface $\alpha/\epsilon = 4.0$). This coating results in a nominal maximum reflector temperature of 395°F. This temperature is within the working range of Kapton (see Section 4.4).

4.3.2 Support Structure

For any given orbital position of the spacecraft, the heat flux distribution around a cross-section of the support structure will be non-uniform. This will lead to temperature differences within the structure and possible thermal distortion problems. The structural thermal design must be directed toward reduction of these temperature differences within the cylindrical cross-sections of the structure. A feasible thermal design concept follows. A more detailed discussion of the support structure thermal analysis is contained in Appendix C.2.

The interior surfaces of the inflatable structure are coated with a "black" material having an emittance of 0.9. The spoke protion of the structure is wrapped with a super insulation blanket consisting of a number of layers of aluminized mylar to provide isolation from the external non-uniform environmental heat flux. For example, an insulation blanket consisting of a total of six layers of crinkled aluminized mylar used in conjunction with an internal surface emittance of 0.9 will reduce the temperature difference within the structure to a nominal value of 5°F with a range approximating ±2°F depending on factors such as handling, uniformity of material properties, etc. Fig. 4.3-1 shows the temperature difference within the structure as a function of insulation effective emittance. The particular value of effective insulation emittance can be obtained by varying either the number of shields, the surface properties, or a

[redacted]

combination of both. Fig. 4.3-2 provides information enabling selection of a particular combination. Curves I and II provide the effective emittance values for ideal thermal shields having the surface properties associated with the materials described on the figure. Curves III and IV present a more realistic approach by including a wrap factor of 2.0 to account for additional heat leaks resulting from outgassing orifices, conduction at insulation contact points, etc. Fig. 4.3-3 shows the insulation weight as a function of the insulation requirements for an example, 1,100 ft. reflector. In addition to the above thermal control concepts, an external control coating on the external layer of insulation ($\alpha / \epsilon = 1.0$) will maintain maximum structural temperatures at approximately 75°F.

An alternate method of reducing temperature differences within the structure has been suggested by the Goodyear Aerospace Corporation of Akron, Ohio. This method consists of a composite of wire bonded to a cylindrical photolyzable film tube. After inflation, the film is decomposed by solar radiation, thus leaving only the wire mesh. This permits a more uniform heating of the structure since the mesh is relatively transparent. No attempt has been made at GAEC to determine temperature differences in this type of structure because of lack of available information on structure construction, material properties, etc. However, the concept of a photolyzable film structure is presented here as a possible solution to the structural temperature difference problem.

4.3.3 Peripheral Thruster Impingement

In order to prevent the RCS peripheral jet plume from impinging upon the reflector structure and subjecting the structure to localized high heating rates, various protective methods have been investigated.

It is estimated that the peripheral jets may continuiously fire for as long as 30 minutes. Therefore, it is necessary to design the reflector structure protective system for a steady state condition.

The simplest solution is to locate the jets far enough away from the reflector structure so that the local structure temperature will be below 250°F, which is in the upper temperature limit of mylar used for the reflector structure, thus requiring no additional heat shield or insulation. Fig. 4.3-4 shows local reflector

structure temperature as a function of jet location (distance from the reflector structure). The data presented in Fig. 4.3-4 should be considered as a conservative approximation of the actual conditions. The exhaust plume profile used for the analyses was based on the LM RCS plume profile modified for the expected combustion chamber thermodynamics properties. The heating rates were also extrapolated from data compiled for the LM RCS engine plume heating.

If no restriction is placed upon the locations of the jets, a heat shield comprised of 25 layers of 1/3 mil nickel foil covering a 10 ft^2 area in the region adjacent to the jet is recommended. This heat shield can be collapsible and would weight approximately 5.1 lbs per engine.

4.3.4 Peripheral Thruster Temperatures

During off periods the temperature of the peripheral thruster units can be maintained within the limits of 40°F to 100°F throughout the orbit without the use of auxiliary heaters. The maximum temperature can be held below 100°F as long as the external surface has a thermal control coating with an absorptance/emittance ratio below approximately 0.7. The minimum temperature can be maintained above 40°F by utilizing the heat capacity of the thruster equipment and further insulating it with approximately 3/4 inch of aluminized mylar super insulation (100 layers/inch).

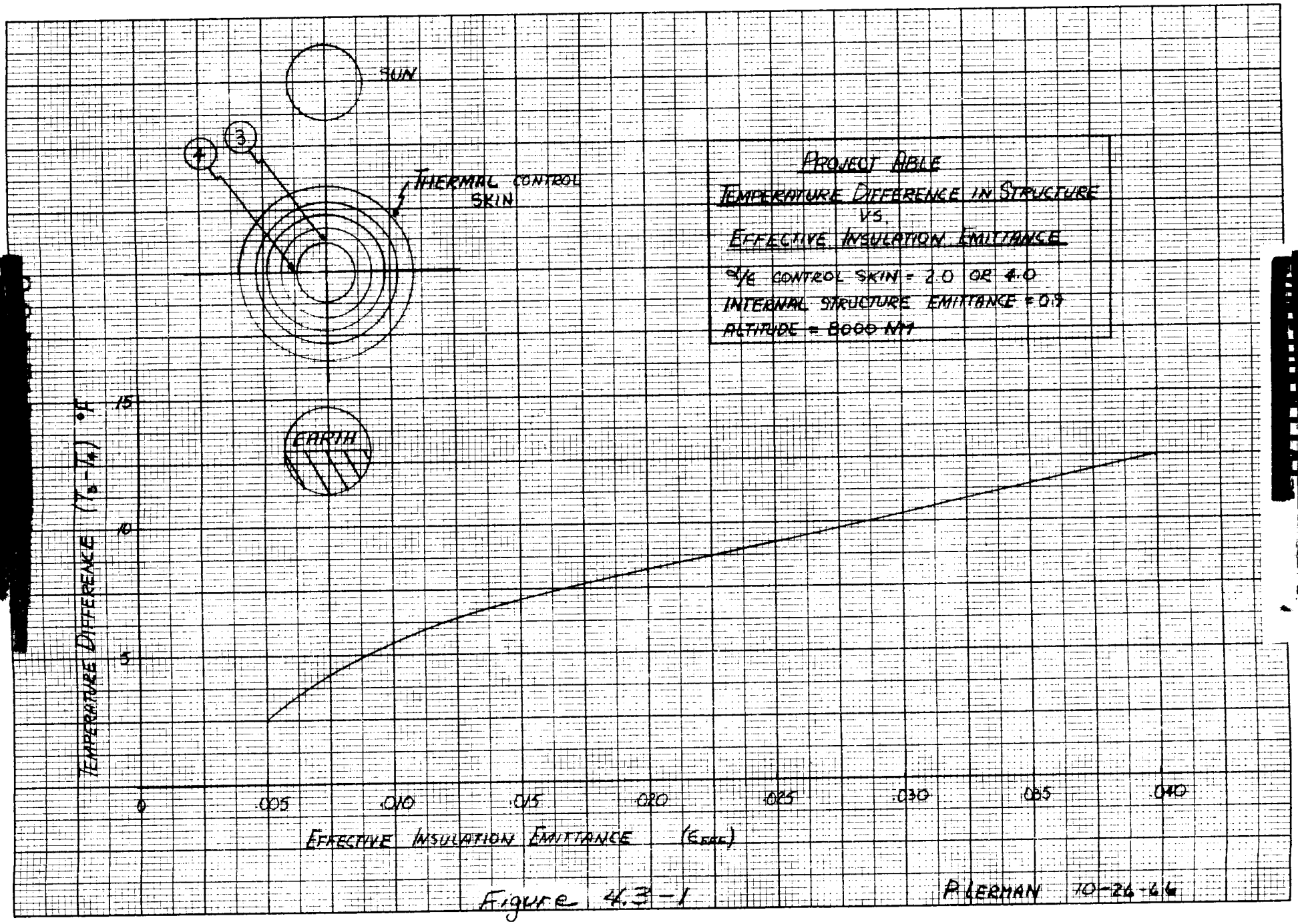
PROJECT ABLE
TEMPERATURE DIFFERENCE IN STRUCTURE
VS.
EFFECTIVE INSULATION EMITTANCE
α/ε CONTROL SKIN = 2.0 OR 4.0
INTERNAL STRUCTURE EMITTANCE = 0.7
ALTITUDE = 8000 NM
SUN
EARTH
THERMAL CONTROL SKIN
3
4
TEMPERATURE DIFFERENCE ($T_B - T_A$) °F
0
5
10
15
.005
.010
.015
.020
.025
.030
.035
.040
EFFECTIVE INSULATION EMITTANCE (ε_{EFF})
R LERMAN 70-26-66

Figure 4.3-1

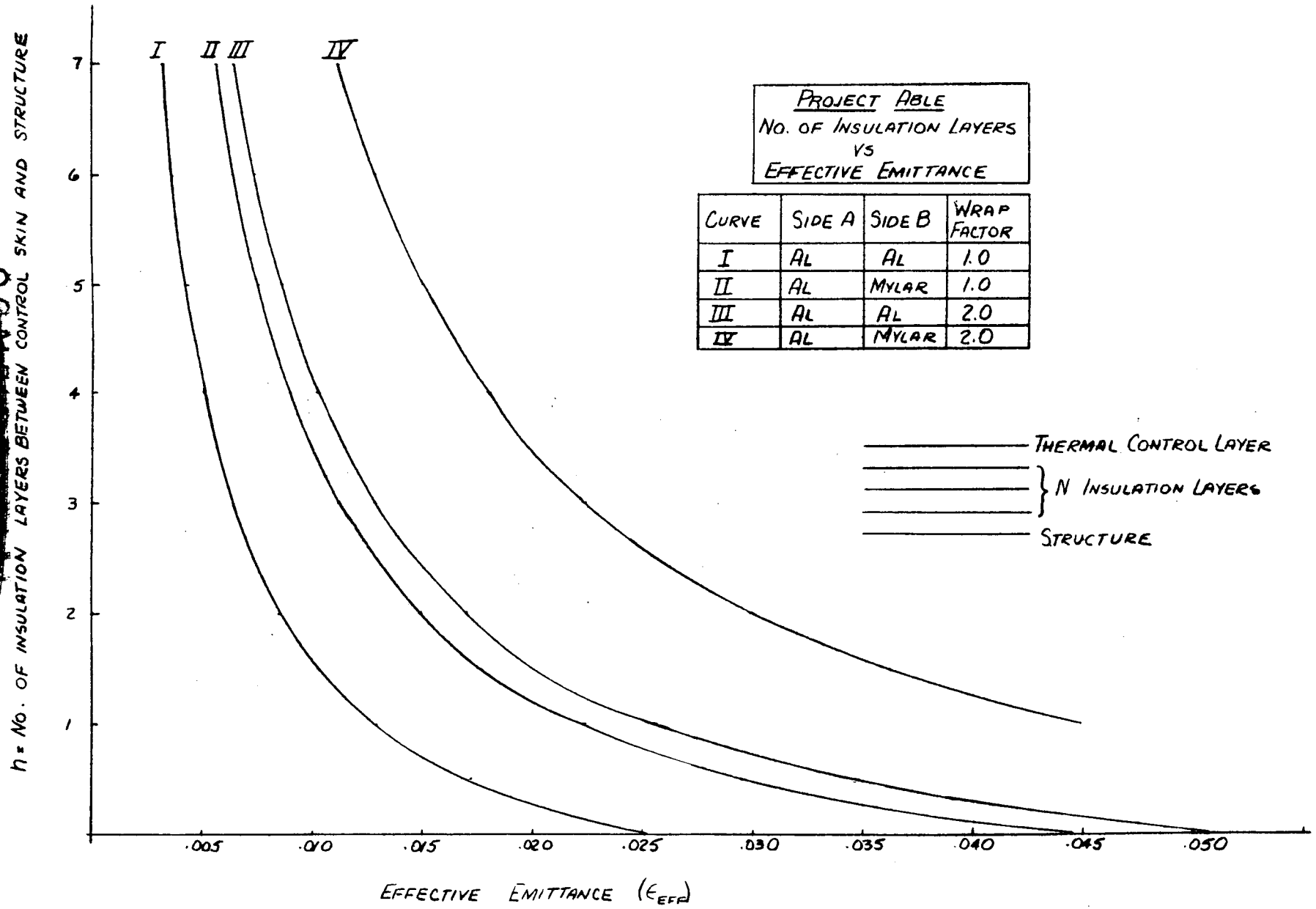

Figure 4.3-2

P. LERMAN 10-24-66

[redacted]

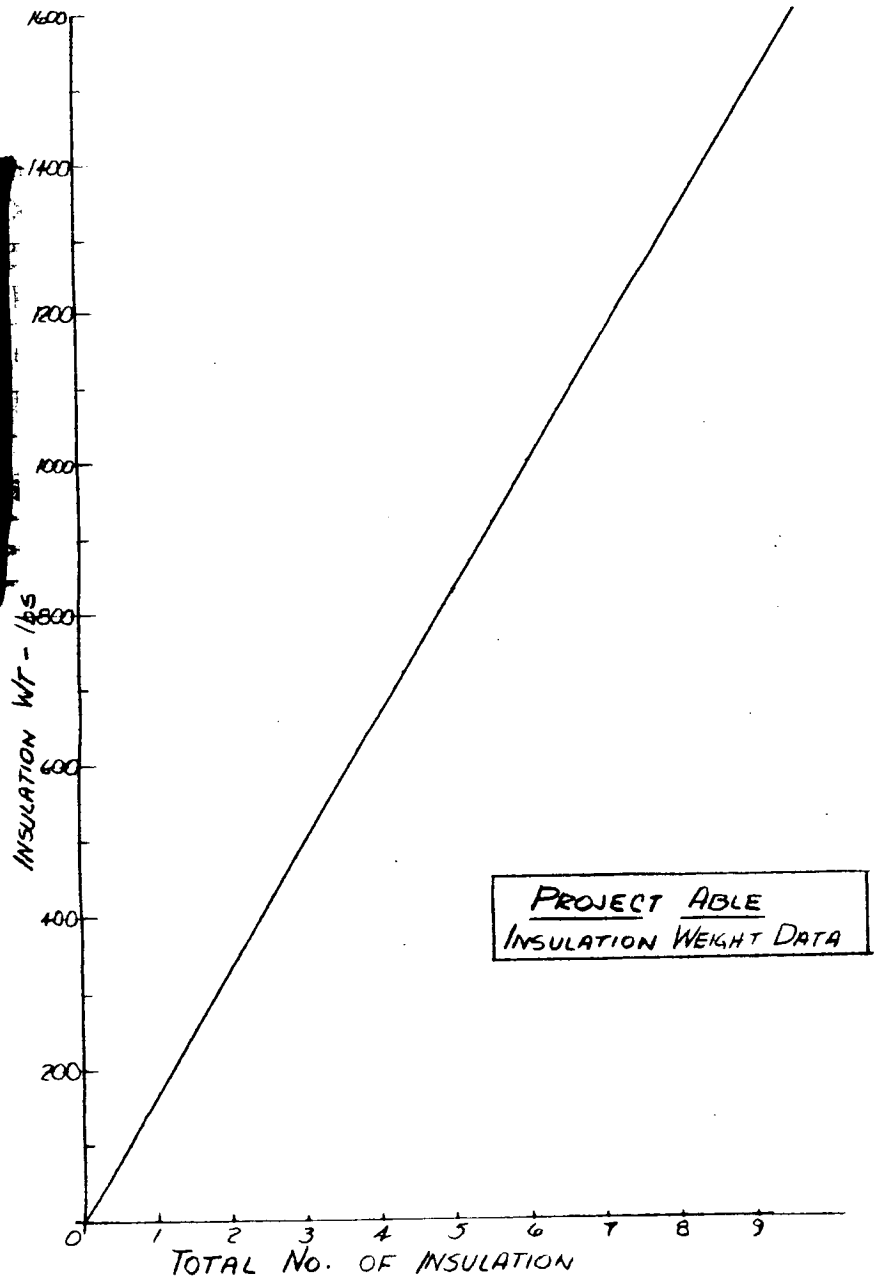

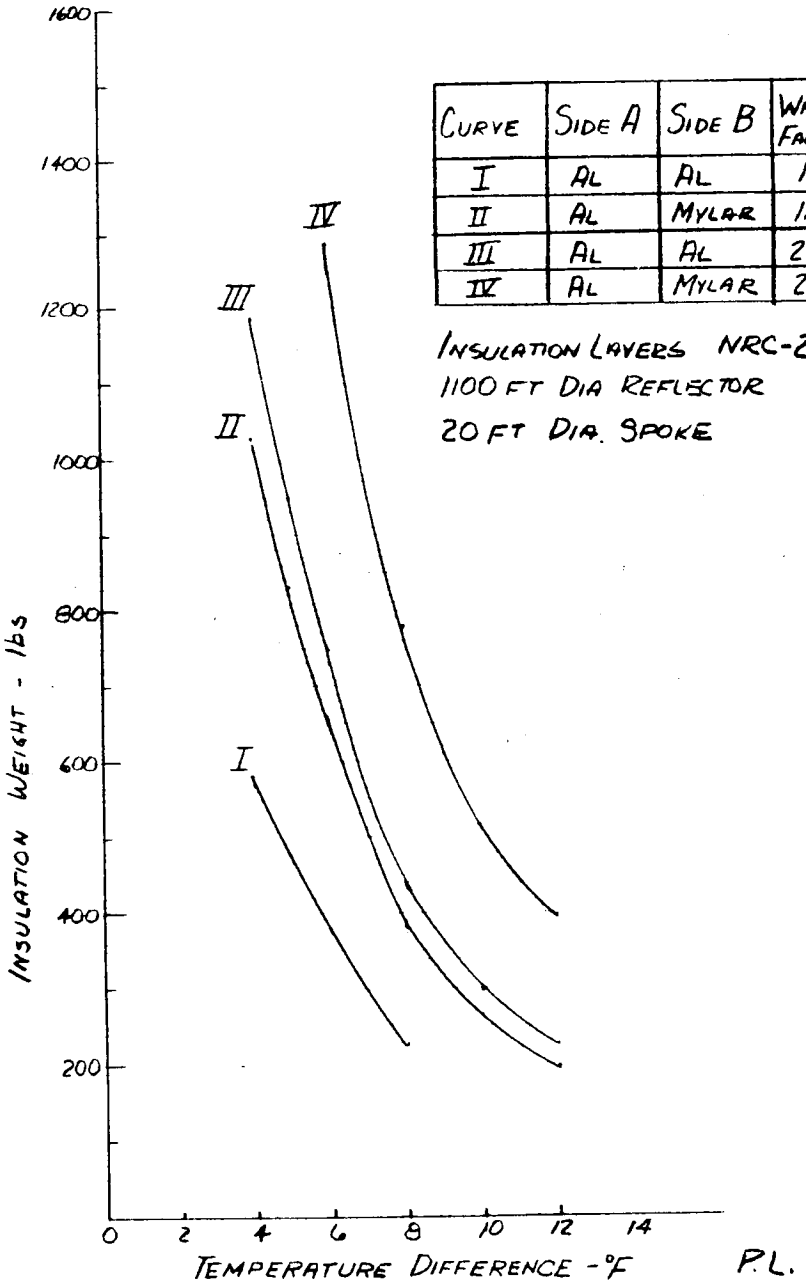

CURVE	SIDE A	SIDE B	WRAP FACTOR
I	AL	AL	1.0
II	AL	MYLAR	1.0
III	AL	AL	2.0
IV	AL	MYLAR	2.0

P.L.

Figure 4.3-3

[redacted]

[redacted]

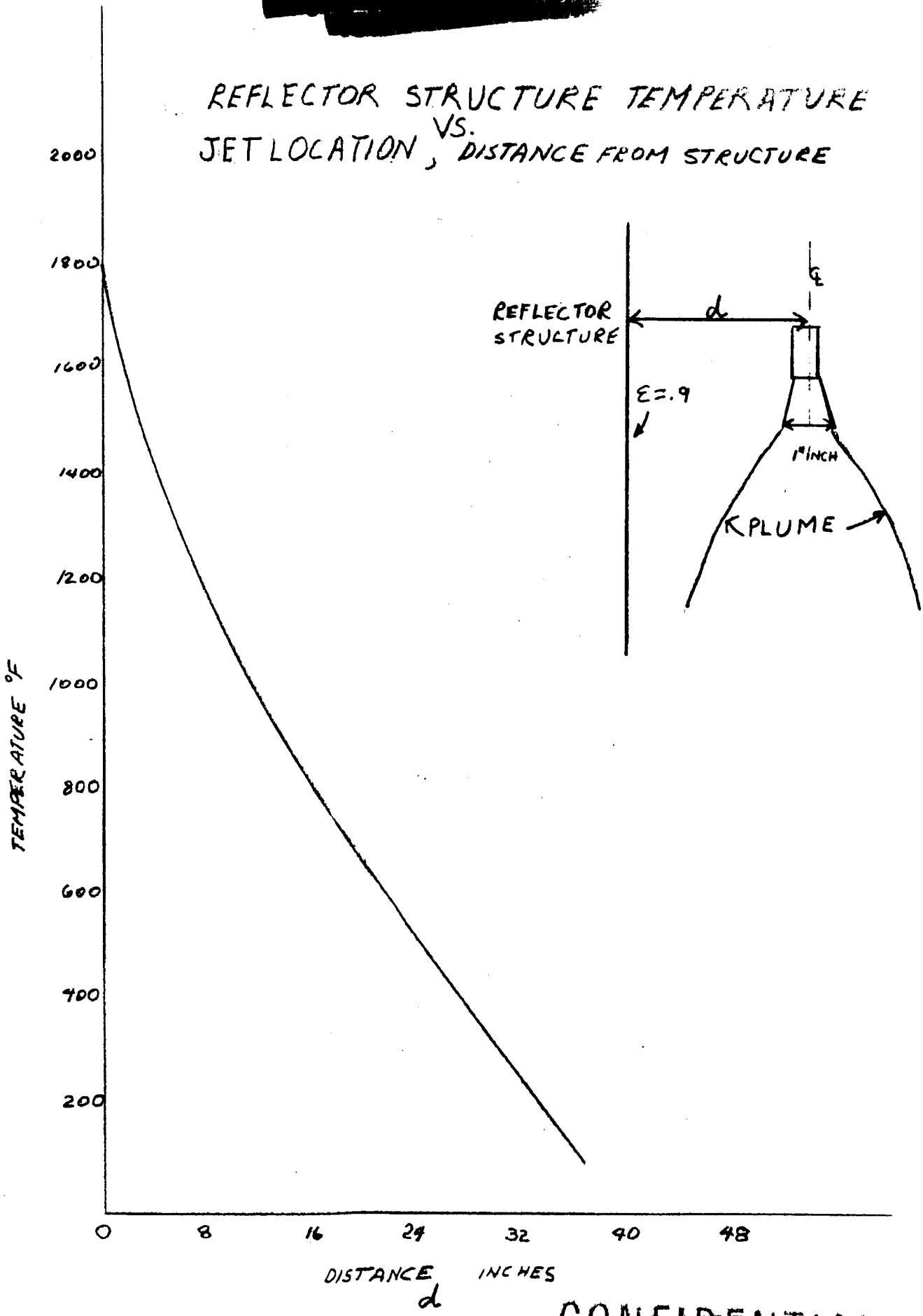

Figure 4.3-4 [redacted]

[redacted]

4.4 MATERIALS

Organic films were considered for the reflector material and for use in expandable support structure design. The principle properties of interest for this application are low and high temperature serviceability, tensile strength, elongation, creep, specific gravity, tear strength and radiation resistance. In addition, other factors such as fabrication, width and thickness availability and cost must be considered. Of the plastic films presently available, Mylar (polyester) and Kapton (polyimide) offer the best combination of these properties. Comparative properties of Mylar and Kapton are shown in Table 4.4-1.

4.4.1 Reflector

Since it is recommended that the film be reflective on both sides (Section 3.2), it should be coated with vacuum deposited aluminum on both surfaces. The aluminum provides the added function of protecting the plastic film from the damaging effects of ultra-violet (U.V.) radiation.

When this reflector is in sunlight, however, the temperature of the aluminized film can rise to about 400°F. This temperature would have to be lowered by passive thermal control coatings or else mylar is unsuitable for the reflector material. It should be noted that if the mission requirements are such that only one side of the film need be reflective, there seems to be no problem with the use of mylar for this application, with respect to its thermal limitations. These passive thermal control coatings must also be trasparent to visible light so that reflectivity is not appreciably affected. These transparent coatings can be obtained in some cases by conversion coatings, paints, or vacuum deposition.

Aluminum surfaces naturally form a very thin oxide film in air. The oxide film would make a good thermal control coating if it could be made thicker through the use of conversion coatings. However, because the vacuum deposited aluminum is so thin (approx. 2200°A), conversion coatings appear unsuitable for this application. For example, nitric acid which forms a thin passive film was tried. Samples of aluminized Kapton were immersed for various times in nitric acid.

[redacted]

In all cases, the porosity in the thin aluminum coating allowed the acid to attack the aluminum--Kapton interface and destroy the bond.

The major disadvantage of paint is that relatively heavy buildups (greater than one mil) would probably be required to obtain desired properties. These paints would also lose some transparency under prolonged exposure to U.V. radiation.

Vacuum deposited silicon monoxide provides a stable transparent thermal control coating. This coating presently offers the most feasible approach for reducing the maximum temperature of the reflector but also represents a costly and time consuming process. The deposition involves a complex reaction which limits deposition to slow rates, and from a time standpoint could prove impractical for use on large surface areas.

For the above reasons, it is recommended that the reflector be designed with no thermal control coatings. This constraint necessitates the use of Kapton as the reflector material since 400°F is outside the useful temperature range of Mylar.

Data on Kapton is tabulated in Table 4.4-1. Presently, the minimum gauge available is 0.5 mil but Dupont representatives indicate that experimental work on thinner gauges will be undertaken in 1967. It is anticipated that 0.35 mil will therefore be available for use on this program. Adhesives are presently being tested and developed by Schjeldah for bonding of the Kapton and there are indications that satisfactory adhesives will shortly be available.

Creep of the Kapton could cause dimensional changes beyond those compensated for in the reflector design. Although this magnitude of creep would be undesirable, a small amount of creep was found to be suprisingly beneficial, since it eliminates wrinkles in the reflector caused by fabrication and packaging. These wrinkles represent stress concentrations, and when the material creeps these areas are the first to be relieved. The applied stress should be the minimum value which eliminates these wrinkles in a short time (about 1 day at 400°F) and yet not cause excessive creep in 6 months. Visual observations of 0.5 mil aluminized Kapton specimens under load at 400°F indicate that stresses of 50-200 psi relieve a majority of the wrinkles in one day.

One specimen was exposed at 500°F and 200 psi for one day and all wrinkles were removed. (Scatter in the thermal characteristics of the vacuum deposited aluminum could result in temperatures above 400°F). Figure 4.4-1 is a photograph of unexposed and exposed samples showing the elimination of wrinkles. Three additional samples of 0.5 mil Kapton were exposed to 50, 100 and 200 psi at 400°F to measure the amount of creep. The change in length over a 6 inch gauge length was measured under load and temperature using optical equipment. The test was run for one week with readings taken daily. Readings after one day indicated a small residual shrinkage in the specimens (0.3%). After 5 days, there was no net change in length within the accuracy of the measurements (about 0.1%). Apparently, the small residual shrinkage was balanced by the creep. From the fifth to the seventh day additional creep was too small to measure.

The conclusion, from this preliminary data, is that loads of 50-200 psi will not present a creep problem. This conclusion should be verified by additional testing.

4.4.2 Support Structure

A typical support structure consists of a composite of 0.5 mil aluminum - 0.35 mil plastic - 0.5 mil aluminum. Since (a) thermal control coatings on the support structure keep the maximum temperature within the useful range of Mylar (b) manufacturing techniques for fabricating an aluminum-Mylar laminate have been developed and successfully used on the Echo II program and (c) Mylar is available in wider widths than Kapton, Mylar is preferred for use as the plastic in the laminate.

The proposed coatings on the torus are those used on the Echo II balloon (i.e. exterior alodine, interior-carbon black) as processing equipment and procedures have already been developed for the Echo program. The thickness of the aluminum makes alodine processing practical for the support structure, but not for the reflector.

The recommended approach to minimize the structural deflections caused by the temperature gradient is to wrap the spokes with layers of "superinsulation".

These layers are 0.125 mil Mylar aluminized on both sides. The layers would be made about 2-5% oversize to account for residual shrinkage in the mylar. For thermal control reasons, the Echo II black coating is proposed for the interior of the aluminum laminate and the exterior of the outer insulation sheet. As stated above, this coating has been successfully utilized on large surface areas.

The photolyzable film-wire concept is another rigidization technique which could reduce temperature gradients in the support structure. This technique was not extensively studied since the temperature gradient profile could not be accurately predicted. Other rigidization techniques such as gas cured resin systems are not recommended for the total structure because of their relative complexity while offering no major advantages over the yielded aluminum concept. They may have advantages, however, for selected small areas of the structure.

[redacted]

Table 4.4-1

Comparative Properties of Mylar and Kapton Films

Properties	Mylar	Kapton
Specific gravity (gr/cc)	1.39	1.42
Service Temp. Range °F Min/Max	-320/+250	-450/+600
Tensile Strength (KSI)		
-320°F	-	35
+ 77°F	25	25
+400°F	9	17
Tensile Modulus (PSI)		
-320°F	-	510,000
+ 77°F	550,000	430,000
+400°F	20,000	260,000
% Elongation		
-320		2
+ 77	120	70
+400		90
Coef. of Exp/in/in/°F x 10^{-6}	9.5	11
Tear Strength, initial lb/in	1300	1000
Radiation dosage for threshold damage Ergs/gm-(C) x 10^{8}	4.4	5000
Min. thickness/max. width (inches)	0.00015/60	(1) 0.0005/36
(1) See Section 4.4.1		

[redacted]

[redacted]

YIELD TEST OF

$\frac{1}{2}$ MIL ALUMINIZED KAPTON

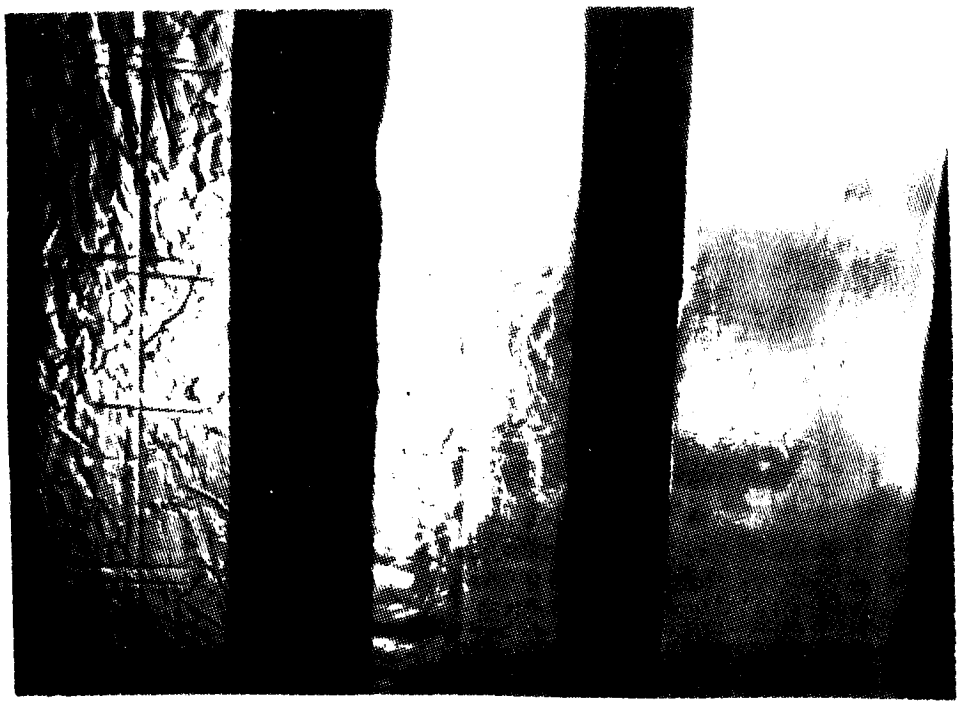

A B C

A - UNEXPOSED

B - EXPOSED AT 200 PSI, 400°F, 1 DAY

C - EXPOSED AT 200 PSI, 500°F, 1 DAY

FIGURE 4.4-1

[redacted]

[redacted]

5.1 ABLE LM THERMAL ANALYSIS

5.1.1 ECS Performance

The recommended ECS configuration is the LM system with the following modifications:

- Addition of two 30 ft^2 radiator panels located 180° apart on the sides of the Descent Stage
- Addition of two radiator control valves
- Addition of an intermodular control valve
- Addition of a regenerative heat exchanger and control valve
- Change coolant from 35% glycol, 65% water to 62½% glycol, 37½% water

The ABLE LM Ascent Stage passive thermal design is almost identical with that of the current LM. The single exception is to provide insulated shades for the ABLE LM windows.

The Heat Transport System is designed to handle the six month operational phase loads with a radiator heat sink exclusively. For the phases of the mission preceding the six month operational phase, a combined radiator water sublimator heat sink is employed. Since the pre-operational phase is of relatively short duration, the design approach has been to utilize the least complicated system at the expense of requiring some additional water rather than optimizing the system with respect to weight.

The system is shown schematically in Fig. 2.2-1 and described in greater detail in Section 6.2. The system performance is presented in Table 5.1-1. Table 5.1-1 shows that no water requirement (zero sublimator load) exists for the 6 month unmanned phase. For all other mission phases, cooling is accomplished by sublimating 130 lbs. of water to supplement radiator heat rejection. For cold environment and low load conditions, the radiator fin effectiveness is reduced by radiator control valves. One radiator panel can become a heater for hot environment conditions. This panel is wiped out by the action of an intermodular valve. The 6 month

[redacted]

5.1.1 (Continued)

unmanned phase cold environment condition was investigated for a 500 watt load. This load is lower than presently anticipated and shows the ability of the system to accommodate a larger load range than required. For the 26.5 hour manned phase, the same system flexibility is exhibited by assuming a structural load variation of 400 watts.

The Heat Transport System can be utilized as a heat source for helium if a cryogenically stored helium system is used for reflector pressurization. The gas heat exchanger, shown in Fig. 2.2-1 can be used to heat the helium with glycol. During the 26.5 hour manned phase, 2000 BTU/Hr. can be extracted from the glycol with the radiators in the cold environment condition.

A Grumman funded radiator test program was conducted to verify the performance of a typical radiator panel under conditions of full capacity, and during bypass operation. A description of the test program and the obtained results have been documented in Ref. 5.1-1.

5.1.2 Reflector Inflation

The reflector inflation system utilizes helium to deploy and rigidize the reflector support structure at a controlled rate. Initial deployment is accomplished using helium stored in two LM RCS helium tanks located on the periphery of the outer torus. After initial deployment, the support structure is inflated to strain rigidization pressure by helium stored in the LM Descent Propulsion System Cryogenic Tanks. The LM Descent Propulsion Fuel/Helium Heat Exchanger can use waste heat from the Environmental Control System to heat the helium from the cryogenic stated to the ambient state.

The number of cryogenic tanks required depends on both the reflector diameter and the diameter of the support structure. The following table shows the required number of cryogenic tanks for different reflector diameters, with a 20 ft. diameter support structure in sunlight, but with no restriction on attitude:

MAXIMUM REFLECTOR DIAMETER (FT)	NO. LM CRYOGENIC HELIUM TANKS REQ'D
620	1
1280	2
1900	3

TABLE 5.1-1

ECS PERFORMANCE

Mission Phase	6 Months (Unmanned)		26.5 Hr. (Manned)		2 Hr. (Manned)		26.5 Hr. (Unmanned)	
Environment	Hot	Cold	Hot	Cold	Hot	Cold	Hot	Cold
Elect. Load on HTS - Watts	670	500*	1155	1155			818	818
Structural Load - Watts	0	0	+200	-200			0	0
Metabolic & LiOH Load - Watts	0	0	370	370			0	0
Total Glycol Load - Watts	670	500	1725	1325	ESSENTIALLY SAME AS 26.5 HR. MANNED		818	818
Radiator Absorbed Radiation $\frac{BTU}{Hr\text{-}FT^2}$	15	0	15	0			15	0
Radiator Area - Ft^2	30	60	30	60			30	60
Radiator Glycol Flow - lbs/hr	222	50**	222	80			80	50**
Radiator Inlet Temp - °F	52	49	65	57			46	46
Sublimator Load - $\frac{BTU}{Hr}$	0	0	3300	1870			1250	1200
Radiator Fin Effectiveness	.96	.35	.96	.52			.72	.32

* Arbitrarily Assumed Minimum Load

** Minimum Radiator Flow Rate

5.1.2 (Continued)

The energy required to heat cryogenic helium during the inflation phase can be supplied by the Heat Transport Section of the Environmental Control System (ECS). During inflation, between 2,000 and 4,000 BTU/Hr. of available ECS waste heat can be transferred from the glycol loop to the cryogenic helium using the LM Descent Propulsion Fuel Helium Heat Exchanger, without the danger of freezing the ECS radiator. The maximum amount of heat required by the helium is 622 BTU/lb. Therefore, the helium delivery rate to the support structure is between 3.2 lbs/hr and 6.4 lbs/hr and the cryogenic tank emptying time varies between 15.3 and 7.7 hours per tank.

5.1.3 Solar Paddle Temperatures

The temperature of the solar paddle is dependent on the orientation and surface properties of the paddle. The maximum paddle temperature occurs when the paddle is aligned perpendicular to the rays of the sun. The minimum temperature occurs when the spacecraft is in earth shadow and the paddle is blocked from any view of the Earth by the reflector. The minimum temperature requirement for the solar cells is -168°C (-270°F). Table 5.2-2 provides solar paddle temperature and heater power data for two values of emittance on the side of the paddle containing no solar cells. These required heater powers places no restriction on paddle orientation when the spacecraft is in the Earth's shadow. If the paddle were oriented such that it has its best view of the inner torus the heater power requirements could be reduced by 10 per cent.

It is apparent from the Table that by utilizing a low emittance coating on the paddle a reduction in heat power to maintain T_c is realized, however a severe power output penalty arises due to a higher T_h. The preferred coating is the high emittance coating.

The selected high emittance coating utilized on the non-cell side of the paddle results in a maximum paddle temperature of 60°C.

[redacted]

TABLE 5.1-2

SOLAR PADDLE DATA

PADDLE EMITTANCE - NON CELL SIDE	0.9	0.1
MAXIMUM PADDLE TEMPERATURE °F	140	239
MINIMUM PADDLE TEMPERATURE °F	-270	-270
REQUIRED HEATER POWER TO MAINTAIN T_{min} W/Ft2 Cell Area	1.1	0.55
POWER OUTPUT AT T_{max} W/Ft^2 Cell Area	8.600	6.156
NET POWER OUTPUT W/Ft^2 Cell Area	7.50	5.60

[redacted]

5.1.4 Canister Temperatures

The allowable canister temperature is limited by the allowable limits of the components and materials within the canister. The desirable temperature range for the interior of the canister is 40°F to 100°F. A maximum canister temperature below 100°F can be assured by utilizing an external thermal control coating having an absorptance to emittance ratio no higher than 0.4.

The minimum temperature can be maintained by utilizing aluminized mylar super insulation or heaters or a combination of both. The time period prior to reflector deployment would be approximately two days (Section 3.5). By enclosing the canister in a one inch blanket of super-insulation (100 layers/inch) it is possible to take advantage of the thermal lag of the system and keep the minimum acceptable temperature of the canister above 40°F for the specified two day time period. The weight of insulation for this application is approximately 90 lbs. A minimum weight system consisting of a combination of super-insulation and battery powered heaters would weigh approximately 70 lbs. However, the weight saving of 20 lbs in utilizing this system over the insulation only system is not sufficient to render it preferrable in view of the additional complexity of adding heaters.

If the pre-deployment time period exceededtwo days, a dual system of insulation and heaters becomes more attractive and is preferrable.

5.1.5 LM Equipment

All electronic equipment located aboard the ABLE LM vehicle will be temperature controlled in the same manner as in the present LM. The majority of equipments are mounted on a cold rail or cold plate through which glycol flows, absorbing the dissipated heat. Some of the low dissipating display and control equipment located in the cabin is controlled by passive means, free convection and radiation to the cabin area.

Temperature control of externally located equipment such as the LM RCS jets and the LM S-band steerable antenna is achieved by existing thermostatically controlled heaters.

5.1.5 (Continued)

The LM ABLE vehicle requires the addition of an optical auto star tracker. The tracker is located outside the vehicle. One configuration considered is to attach the tracker to the IMU in the location of the present AOT, using the present LM navigation base mounted in the docking structure. When the tracker is operating, cooling is required. This is accomplished by extending the coolant loop to the tracker heat-dissipating areas. During the stand-by mode, the tracker will be turned off (no internal heat generated). In this mode, heat will be lost from the IMU to the colder tracker, and in turn radiated to space (approximately 3.5 sq ft of tracker area is exposed to space). This heat drain would increase the output of the IMU proportional heater. If it is desirable to conserve heater power, a glycol by-pass of the IMU, when it is not operating, can be easily incorporated into the design. The two main modes of heat loss from the IMU are as follows:

- Heat lost through the navigation base to the vehicle structure
- Heat lost to the auto tracker, and out to space.

The above heat losses can be minimized if the following is incorporated into the design:

- Minimization of the conductive path between the IMU and star tracker by use of low-conductive supports, such as titanium tubing.
- Minimization of the conductive path between IMU and outer structure (also considering titanium tubing).
- Insulation of the tracker assembly below the thermal shield and provision of a protective cover over the outer tracker telescope to minimize heat leakage to space.
- Insulation between IMU and vehicle skin.

5.1.6 LM RCS Plume Heating

Although the LM RCS thruster firing time history during a typical mission has not been determined, it appears that the worst thermal loading will occur when the thrusters are used to slew the LM. The cyclic firing that occurs during an attitude hold condition does not appear to be critical, since the firing time of

5.1.6 (Continued)

the jet is of the order of milliseconds, and the off time is of the order of minutes. The longest possible firing time for the downward jet would be about 10 seconds. Therefore, the performance of the protective systems was evaluated for a 10 second duration firing.

The maximum heating rate occurring directly under the plume axis is 30 BTU/sec ft^2. As the distance from the plume axis increases the heating rate decreases rapidly. Three possible protective systems were found feasible. Evaluation of each approach was based upon the maximum heating rate. The different approaches have different weight penalties associated with them, and the various design factor will have to be traded off before an optimum design can be selected.

5.1.6.1 High Heat Capacity Shield

The use of high heat capacity shield a few inches above the shround area exposed to the plume heating, represents the simplest but heaviest approach. Three shield materials were considered, titanium, steel, and nickel; with the back surface of the shield polished so that the emittance of the surface is 0.15 or less. When the shields are exposed to the maximum heating rate for the 10 seconds, the nickel and steel shields prevent the shroud from reaching 100°F while the titanium shield prevents the shroud from reaching 130°F. The temperature rise as a function time for the shields and shroud are shown in Figure 5.1-1. The solid lines represent the temperature rise of the shields, the dashed line are the temperature rise of the shroud they protect.

5.1.6.2 Multiple Layer Heat Shields

The use of multiple-layer, reflective, high temperature insulation blankets placed over the shroud in the area of plume impingement was investigated. A 1/3 mil nickel inconel mesh foil was considered. The temperature rise of the back face of the last foil is shown in Figure 5.1-2 for a ten foil blanket and a five foil blanket. The data was obtained by a finite difference one dimensional method that calculated the radiation heat transfer from foil to foil. It is estimated that a 10 layer blanket would be sufficient to prevent the shroud from reaching a temperature of 90°F. The weight of such a system will be .25 lb/sq. ft.

5.1.6.3 Ablative Protective Coating

The ablative approach utilizes the high heat of ablation and the blocking effect of the ablative vapor to absorb the plume heat flux. The ablative paint considered was Thermo Lag-500 (actually it sublimates). The paint will be applied directly to the shroud. The thickness of ablative coating as a function of thruster firing time is shown in Figure 5.1-3. Curves for turbulent flow and for laminar flow are presented, the difference being in the blockage factor which is the amount of heat carried away by the sublimated gases, this being greater for laminar flow. It is estimated that the flow for a flat plate impingement is in the laminar region (Reynolds 100,000) and .032 inch of paint will be required.

5.1.7 References

5.1-1 Grumman Report No. 378C-6, dated 10 August 1966.

Figure 5.1-1

TEMPERATURE RISE DUE TO FLUXE HEATING

[redacted]

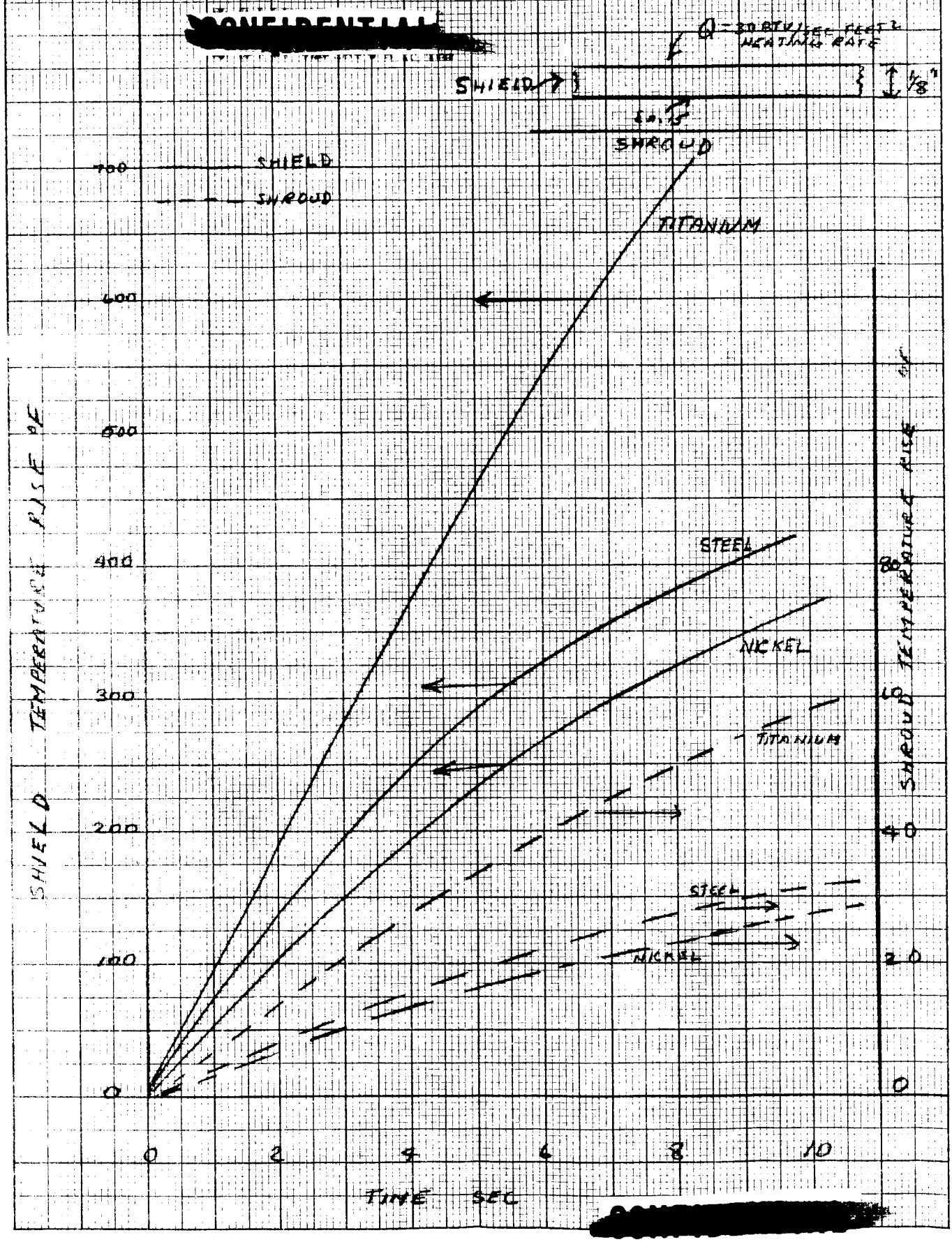

[redacted]

Figure 5.1-2

MULTIPLE-LAYER INSULATION

TEMPERATURE OF LAST FOIL VS TIME

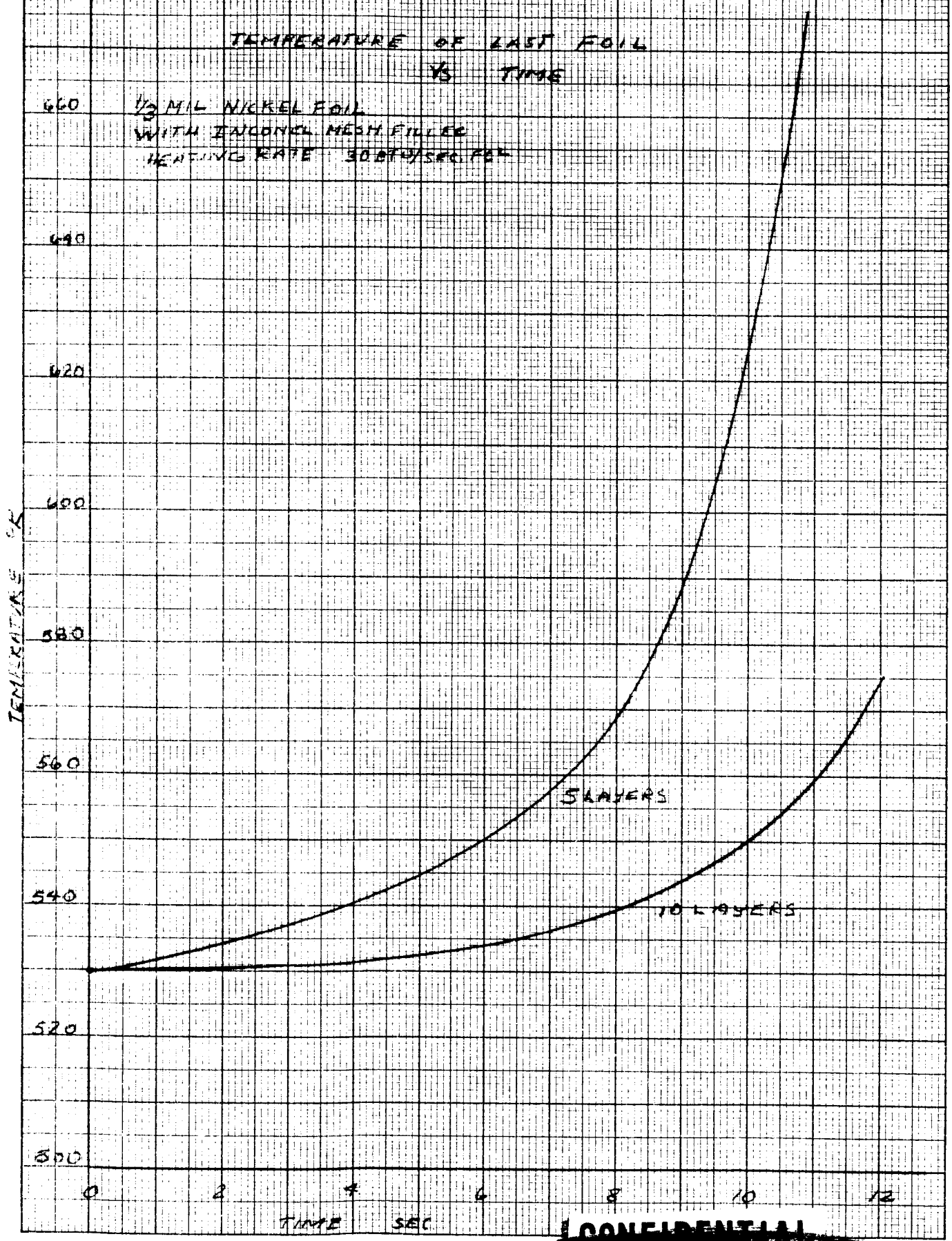

[redacted]

Figure 5.1-3

REQUIRED THICKNESS VS JET FIRING TIME

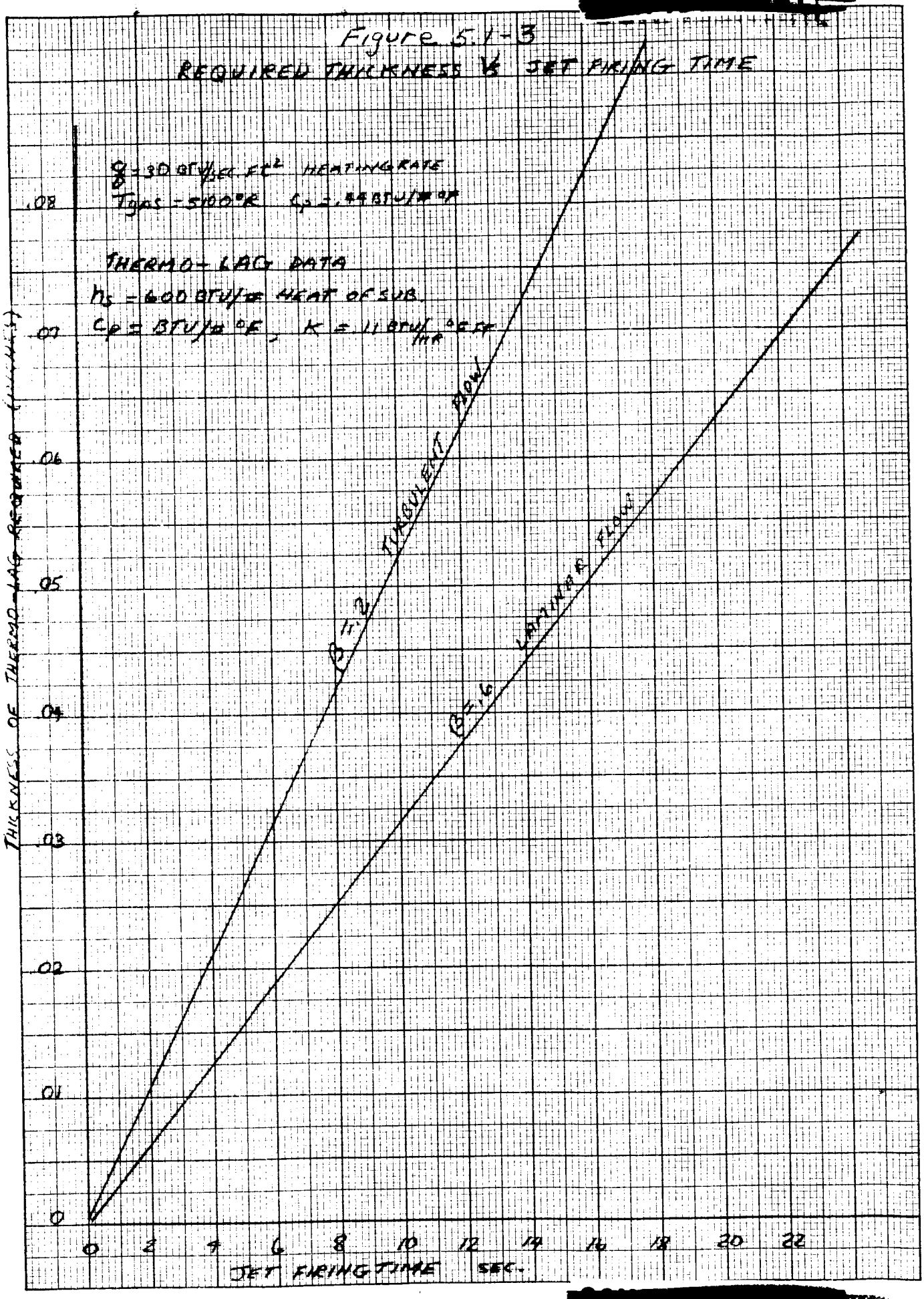

[redacted]

5.2 GUIDANCE AND CONTROL ANALYSIS

5.2.1 System Requirements

The Guidance, Navigation and Control System (GNCS) requirements were derived from the mission described in Section 3.5. An analysis of this mission identified functions which the GNCS must provide. They are:

- Stabilization function - to be used if the LM is to separate from the CSM
- Attitude Hold function - during the deployment of the reflector
- Manual Control function - for use by the crew to perform translation and rotation of the vehicle
- Alignment function - to establish an inertial reference
- Target Acquisition function - to compute the target position or acquire it from ground command
- Pointing function - to point the reflector to the acquired target
- Orbit Keeping function - generate maneuver commands to compensate for orbital changes
- Reacquisition function - to acquire an inertial reference that was lost
- Remote Control function - to redesignate the aim point of the reflector.

In order to provide the functions specified above the following modes of operation can be identified for the GNCS.

- Manual Mode - for use by the crew for translation and rotation commands
- Alignment Mode - for establishing and updating an inertial triad in space
- Attitude Hold Mode - to be used during the deployment of the reflector

5.2.1 cont'd

- Reacquisition Mode - used to reacquire the inertial reference after it has been lost due to some contingency
- Remote Control Mode - Used to reposition the aim point of the reflector
- Orbit Maintenance Mode - used to compensate for orbital changes
- Targeting Mode - Target position computation and pointing of the reflected light beam to the target.

5.2.2 Alternate GN&C System Concepts

In order to provide the functions defined above, particularly with respect to providing the capability of directing the reflector beam to illuminate the target, referred to as targeting, several alternate system concepts were considered. These ranged from the utilization of LM equipment, to the synthesis of a completely new system. The alternate systems considered were:

- Existing LM PGNCS (IMU, AOT, LGC, ATCA) with MSFN
  This system requires alignment via the AOT and the astronaut; consequently, the alignment and realignment of the inertial platform can only be accomplished when an astronaut is in the LM. Since the IMU drift rate is at least 0.72°/day (1σ) and the pointing accuracy required is within 0.5° (the angle subtended by the beam of the reflector), extended operation with the existing LM PGNCS without an astronaut is not feasible.
- Modified LM PGNCS (IMU, LGC, ATCA, LM Optical Tracking Systems (LOTS)) with MSFN
  Replacement of the AOT with the LOTS provides the capability for automatic realignment of the IMU thereby allowing operation of this system in an unmanned mode. The normal operation of the PGNCS when coupled with the LOTS requires an initial coarse alignment of the IMU to within the field of view of the LOTS star tracker. This coarse alignment could be accomplished prior to launch, or through a transfer alignment when the LM is attached to the CSM. Fine alignment of the IMU is accomplished by using the LGC to designate the star tracker gimbal angles so

5.2.2 cont'd

that a star appears in the star tracker field of view. The star tracker is then allowed to lock onto the star and the gimbal angles are entered into the LGC, establishing the star line of sight. This procedures is repeated for anther star. The LGC then uses the star line of sight information to compute the IMU gimbal angles required to align the stable member to the specified inertial reference. Appropriate commands are then issued to the gimbal torquers to align the stable member to the inertial reference. Loss of attitude information for short time periods can be compensated for by using the last values of attitude rate together with the elapsed time, to compute a new coarse alignment of the IMU. Fine alignment then follows in the normal manner. The contingency duration which can be tolerated with this technique is dependent on the vehicle limit cycle rates.

- Star Tracker Systems

In these systems Star Trackers would be used to establish an inertial reference for data processing in the guidance computer or alternatively, error signals generated from the star tracker gimbal angles could be fed directly into the control system. A cursory investigation of the latter approach indicated that the complexity of the rror signal generation for pointing to a fixed point on earth would be excessive. Studies were therefore concentrated on investigating the capabilities of star tracker systems to establish an inertial reference for processing by a computer such as the LGC or AEA. The computer would use the inertial orientation data and navigation data (assumed supplied by MSFN) to compute attitude error and error rate signals for the control system to use to generate pointing commands. The control system could utilize either an analog or digital autopilot. The computer would

5.2.2 cont'd

also generate commands, based on guidance requirements, for thrusting maneuvers.

The number of star trackers required for implementing this system would be a minimum of two. Assuming that two star trackers were used, the stars sighted to determine the inertial reference must be sufficiently far apart to generate conclusive information about all three axes, implying that one star must be of a very high positive or negative declination, while the other must have a low declination without being occulted by the earth at any time in the orbit. It is considered that it would be desirable to have the star trackers located on the dark side of the reflector so that the maximum field of view is avialable to the trackers, without interference from the sun or reflector surface. With this configuration attitude constraints would be imposed during the earth-sunlit phase of the orbit, and problems associated with occultation of the stars by the reflector also exist. The reflector must also always be oriented so that the same side points to the sun. In order to overcome these problems, more star trackers can be added to the system. A preliminary investigation indicated that a maximum of six star trackers mounted on both the upper and lower surfaces of the LM would give satisfactory coverage. However, accuracy problems may be encountered where trackers are mounted to the LM lower surface. Major problems associated with this system are the initial establishment of the inertial reference, and the reacquisition of the inertial reference after loss of inertial orientation caused by a temporary power loss or similar contingency.

- Gimballed Star Trackers, Sun Sensor, MSFN, Computer Systems
  In order to overcome the difficulties of acquisition associated with the previously discussed system, the effects of inclusion of a sun sensor into the system for acquisition and re-acquisition of the inertial reference were investigated. Two different types

5.2.2 cont'd

of sun sensor were considered, null seeking and aspect type sun sensors.

Null Seeking Sun Sensor - In addition to the star trackers used for establishing the inertial reference a null seeking sun sensor is used for acquisition and reacquistion of the inertial reference. The acquisition/reacquisition mode for this system would consist first of a search mode to allow the sensor to coarsely align to the sun, followed by a mode in which the vehicle x axis is aligned to the sun line of sight. The star tracker gimbal angles are then set at a value, determined by the computer, which will give acquisition of known stars by the trackers when the vehicle x axis rotates about the sun line. Acquisition is completed by a x axis rotational maneuver of the vehicle which is terminated when the appropriate stars are acquired by the trackers. Although this system eliminates problems associated with the acquisition mode, the problems of occultation associated with the star tracker system described above still remain. Again, a possible solution lies in increasing the number of star trackers.

Aspect type Sun Sensor - The aspect type sun sensor would be used to generate information for the acquisition (reacquisition) mode and for aiding in the establishment of an inertial reference. In the acquisition mode the sun sensor would operate in the same manner as the null seeking sun sensor described above. The inertial reference, however, would be established jointly by the sun sensor and a star tracker. Because of occultation problems more than one star tracker would probably be required. In addition, if the reflector is surfaced on both sides to reduce slewing requirements, two sun sensors would be required. Again, accuracy problems associated with mounting sensors on the descent stage may be encountered. An attitude constraint would also be imposed on the vehicle because of the limited dynamic range of the sun sensor (typical vaues of this dynamic range are ±64° from the axis). Switch-

5.2.2 cont'd

ing to an inertial reference generated by the star trackers alone could be used to alleviate this constraint in periods when targeting is not required, implying the use of more star trackers than the basic system may require.

- Sun Sensor/Target Sensor Systems-Sun Sensor, ground beacon (at target), on board beacon sensor, Computer, MSFN
  This guidance and control system concept uses sensor information directly, to generate the attitude error signals required by the control system. The sun sensor would be used to establish the line of sight to the sun and would be of the aspect variety. The ground beacon with the associated on board beacon sensor would be used to establish the line of sight to the target. Using the line of sight information the reflector normal would be commanded to lie in the plane established by the lines of sight, and bisect the angle between them. The control system associated with this concept could use either an analog or digital autopilot. Guidance commands for performing orbital maintenace thrusting maneuvers could be generated by using MSFN navigation data, relative to the state of the vehicle, in conjunction with the vehicle orientation established by the lines of sight, the position of the sun, and the position of the target. The maneuvers would have to be performed so that the thrust vector can be oriented in the appropriate direction without loss of acquisition by the sensors. For periods when the target is out of line of sight of the vehicle, a coarse attitude orientation could be maintained by using a rate command mode. This mode would use a rate gyro assembly to establish the rate error signal.

  Two different types of on-board sensor system were considered, one of which used interferometer techniques, the other utilizing difference in time between sensing a pulse at discrete points on the surface.

5.2.2 cont'd

Interferometer system - This system utilizes two antennas which are situated a known distance apart, typically between 10 and 100 ft. The accuracy with which the line of sight can be established with two antennas spaced 10 ft apart is approximately 15 arc min. when the incoming signal is normal to the antenna planes. The accuracy improves as the distance between the antennas is increased, (although a precise value has not been identified) and varies inversely as a function of the cosine of the angle between the signal carrier beam and the antenna plane. The accuracy figures quoted are for an ideal antenna location, and the effects of the neighboring reflector structure on the system have not been evaluated. This system is presently only in a breadboard stage and it is questionable whether developed hardware could be fabricated in the available time period.

Pulse Timing Difference Systems - A number (probably 4) omnidirectional antennas would be mounted on the periphery of the reflector. The antennas would receive a pulsed signal and an electronic processor would sense the difference between the times when the leading edge of a pulse is received at the antenna locations. Using this information the angle between the vehicle/target line of sight and the reflector can be determined. This system gives a direct measure of the orientation of the antenna planes to the incoming signal, but the correct orientation of the reflector is dependent on lack of distortion of the reflector plane. Alternatively, a compensation technique for establishing the relative reflector/antenna orientation must be devised.

5.2.3 Selected GNCS Configuration Functional Description

Based on the characteristics of the systems described above, the LM PGNCS configuration with the addition of the LM Optical Tracking System (LOTS) is generally

5.2.3 cont'd

recommended. The fundamental reasons for this decision are:

- The PGNCS - LOTS configuration can perform the ABLE mission
- All other systems require either design and development of new hardware, utilize unproven systems concepts, or would present serious interface problems if incorporated into existing LM subsystems.

The LM PGNCS is an integrated, aided, inertial Guidance, Navigation and Control System. The basic components of the system, which would be used for the ABLE GNCS function, consist of a stable platform (IMU) to provide an inertial reference, a star tracker system (LOTS) to realign the stable platform, a digital computer (LGC) which provides the guidance and navigation function and contains the digital autopilot (DAP), astronaut hand controllers for rotational and translational maneuvers (ACA and T/TCA), a data entry device (DSKY), and an interface with reaction jet thrusters through the jet driver preamplifiers in ATCA. (See Section 6.3 for a hardware description of the GNC subsystem).

Several modes of operation are available with this system ranging from fully automatic modes to manual modes in which the astronaut can directly control the vehicle. In the automatic modes guidance commands originate in the guidance computer and are supplied to the digital autopilot (DAP) in the form of attitude and attitude rate error signals and translational thruster commands. The DAP processes this information and, through a jet select logic, issues jet - on commands which are routed through the ATCA to the RCS, firing the appropriate jets (commands are also issued directly to the descent and ascent engines where required). In the manual modes except the direct modes, the astronaut commands pass through the ATCA to the DAP from where the automatic control path is followed. Assist from the autopilot in maintaining vehicle stability and control is dependent on the mode selected. In order to define the applicability of the LM-PGNCS to the ABLE GNCS requirements, and to identify the modifications which would be required to the PGNCS, a brief description of the LM system functions in the areas of guidance, control and control torquers will be presented, with a discussion of the ABLE GNCS implications associated with each area.

5.2.3.1 Guidance Functions

A detailed description of the guidance functions in the LM mission would be lengthy and is considered to be outside the scope of this discussion. However, the broad classifications of the LM guidance functions would be:

- Transfer orbit insertion maneuver - The guidance system generates the attitude and thruster commands for the insertion of the LM into the transfer orbit. A similar guidance law could probably be used on the ABLE vehicle for the orbit maintenance maneuvers in which transfer orbits would be used for orbit corrections.
- Powered descent - During this phase of the LM mission the guidance computer uses an explicit guidance law to guide the vehicle to the desired lunar landing site. This guidance function is not applicable to the ABLE GNCS.
- Powered Ascent - The guidance computer uses an explicit guidance law to guide the vehicle to ascent burn out conditions such that a rendezvous can be made with the CSM within midcourse correction capabilities.
- Midcourse Guidance - the Guidance computer uses information relative to the CSM state, using estimates in the inertial system and rendezvous radar information in an optimal recursive filter, to determine the attitude and thrust commands for the midcourse correction. The thrust commands are executed by the RCS. This function, with modification of the midcourse guidance equations, may also be considered applicable to the ABLE GNCS requirements.

From this brief description it can be seen that the LM PGNCS has an extensive guidance capability that will enable it to satisfy orbital maintenance and station-keeping requirements. However, the LM system does not presently possess the capability for generating the attitude information required by the control system, to enable it to issue commands to direct the reflector beam at a specified point on the earth. To accomplish this function in the ABLE GNCS a new guidance subroutine will be written for the LGC. This guidance subroutine will utilize navigation information from MSFN to establish the position of the earth, the target, the sun and the ABLE LM in an inertial

[redacted]

5.2.3.1 cont'd

reference frame. Using this data the line of sight unit vectors from the LM to the sun ($\underline{U}_{SUN}$) and from the LM to the target ($\underline{U}_{TARGET}$) can be established. The desired orientation of the LM vehicle relative to the inertial reference frame is such that the vector normal to the reflector plane ($\underline{U}_{NORMAL}$) is coplanar with $\underline{U}_{SUN}$ and $\underline{U}_{TARGET}$ and bisects the angle between these two vectors (see Fig. 5.2-1). (This orientation of $\underline{U}_{NORMAL}$ will be referred to as $\underline{U}_{NORMAL\ DESIRED}$).

In the computation of $\underline{U}_{NORMAL\ DESIRED}$ three inertial coordinate systems are required, a sun-centered system, an earth-centered system and the LM-centered stable member (SM) system. It is assumed that the orientation of one system with respect to any other is known, in particular for this discussion, that they are parallel. From the equations of motion and initial conditions, the state of the Earth ($\underline{R}_{EARTH}$, $\underline{V}_{EARTH}$) and the LM ($\underline{R}_{LM}V_{LM}$) can be determined at any instant. The two required vectors are:

$$\underline{U}_{SUN} = \text{UNIT}\ (\underline{R}_{EARTH} + \underline{R}_{LM})$$

$$\underline{U}_{TARGET} = \text{UNIT}\ (\underline{R}_{TARGET} - \underline{R}_{LM})$$

where $\underline{R}_{TARGET}$ is the position vector of the target and assumed known.

The desired direction to point the unit normal vector can be determined from the expression:

$$\underline{U}_{NORMAL\ DESIRED} = (\text{Matrix})^T\ \underline{U}_N$$

where: $$(\text{Matrix}) = \begin{bmatrix} \text{UNIT}\ (\underline{U}_{SUN} \times \underline{U}_{TARGET})^T \\ \underline{U}^T_{SUN} \\ \text{UNIT}\ (\underline{U}_{SUN} \times \underline{U}_{TARGET} \times \underline{U}_{SUN})^T \end{bmatrix}$$

the angle θ = $\cos^{-1}\ (\underline{U}_{SUN} \cdot \underline{U}_{TARGET})/2$,

and the vector $$\underline{U}_N = \begin{bmatrix} 0 \\ \cos\theta \\ \sin\theta \end{bmatrix}$$

[redacted]

5.2.3.1 cont'd

Having determined the desired direction of $\underline{U}_{NORMAL}$, it is necessary to know the actual direction of the unit vector normal to the reflector surface with respect to the SM system. This is obtained by measuring the PGNCS gimbal angles. The gimbal angle matrix, created from the measured angles, relates $\underline{U}_{NORMAL}$ in the Nav Base system (ALM fixed axis system to which the orientation of the reflector is known) to the $\underline{U}_{NORMAL}$ in the SM system.

$$\underline{U}_{NORMAL} = \begin{bmatrix} \text{Gimbal} \\ \text{Angle} \\ \text{Matrix} \end{bmatrix} \underline{U}_{NORMAL\ NAV\ BASE}$$

The control system attitude error signals are computed from the values of $\underline{U}_{NORMAL}$ and $\underline{U}_{NORMAL\ DESIRED}$.

Using the above approach, the theoretical reflector normal can be oriented to the desired direction within the accuracy of the MSFN navigation data and the knowledge of the inertial orientation of the stable member. The accuracy of the latter information is dependant on the time from the last alignment of the stable member by the LOTS.

The orientation of the mean reflector plane relative to the LM will probably not be accurately known and it is therefore considered desirable to have some means available for correcting the guidance system to compensate for errors in alignment of the reflector. The remote command capability of the LMP for commanding vehicle rotational maneuvers by earth command will be used to slew the vehicle until the reflector beam is directed to the target. The incremental attitude changes resulting from these slewing maneuvers will be stored in the guidance computer, and used to correct the knowledge of $\underline{U}_{NORMAL\ NAV\ BASE}$.

During the deployment phase, the ABLE - LM will be required to maintain some specified orientation either to an inertial orientation or to the earth local vertical. Control to an inertial orientation already exists in the LM-PGNCS, and control to a local vertical orientation can be accomplished in a manner similar to that described above for the target pointing function.

5.2.3.2 Control System Functions

The control system function is to operate on the attitude error signals generated by the guidance computer, or by the astronaut through the hand controllers, to command control torquer operations to reorient the vehicle. In the case of the LM, the control torquers are reaction control jets and the required torquer commands are generated by a Digital Autopilot (DAP) contained in the PGNCS. The DAP has the following major modes of operation:

- Automatic Mode - In the automatic mode orientation requirements are generated in the guidance computer and implemented by the DAP and control torquers.
- Rate Command/Attitude Hold Mode - This is a normal astronaut control mode. It is semi-automatic in nature since the DAP uses sensor information to control vehicle commands. In this mode the vehicle is commanded to rotate at a rate proportional to the attitude controller displacement. When the ACA controller is returned to neutral (detent) the vehicle rate is nulled as rapidly as possible and the attitude existing at a rate of approximately 1°/sec is commanded by the guidance computer.
- Minimum Impulse Mode - In this manual mode a minimum impulse RCS jet firing is commanded each time the controller is moved out of detent. It is an open loop mode (not closed by the guidance or control systems) and is used for maneuvering at low rates.

The LM PGNCS DAP accepts attitude error signals from the guidance computer and computes rate by means of a digital filter to enable rate error signals to be generated. In order to understand the functioning of the DAP recourse will be made to a phase plane description. The error and error rate functions describe the vehicle phase plane trajectories. The DAP switching logic is arranged so that the jets are commanded on when the vehicle phase plane trajectories cross predetermined jet-on switch lines. In order to determine jet on times knowledge of the errors and error rates is used in conjunction with an optimal control law. The switch lines are shaped so that optimum

5.2.3.2 cont'd

performance, with respect to propellant consumption, of the system will be obtained for a non-disturbed limit cycle and for a torque disturbed limit cycle where the disturbance torque is large (e.g. those torques generated by descent or ascent engine thrust vector offsets). In summary, the LM digital autopilot was designed to have the following capabilities:

- Generate a minimum propellant non-disturbed limit cycle
- Generate a minimum propellant limit cycle when large disturbance torques act on the vehicle
- Provide adequate transient response and good propellant economy for automatic maneuvers.

In addition the DAP provides flexibility to simply change switching logic, gains, etc. which offset autopilot performance.

An analysis of the ABLE GNCS requirements indicates that the above described DAP will provide all the functions required during manned phases of the ABLE mission and during reflector deployment. When the reflector is deployed, however, the inertias of the vehicle become very high and the torque environment relative to the vehicle inertia is very low. In this environment the LM DAP would tend to operate inefficiently but, because the DAP has considerable flexibility for changing the control laws (by reprogramming the LGC) without hardware modifications, an efficient system can be provided for all the phases of the ABLE mission.

The modification which have been identified for the ABLE GNCS DAP are:

- Provide a variable computation rate to accommodate different phases of the mission. During separation, deployment, or maneuvering phases when the rates are relatively high a small computation time step is required. During the normal target pointing phase very low slewing and limit cycle rates will exist in one or more axes, and efficient operation of the DAP will require a long computation period. As an example, the

5.2.3.2 cont'd

x axis limit cycle rate for a 1000 ft reflector is approximately 3.6×10^{-5} deg/sec assuming a 10 sec firing of thrusters which develop a torque of 10 ft lb. The rate and acceleration information for DAP is predicted from CDU information via the digital filter. Hence, the accuracy of the rate information is dependent on the CDU quantization, 37 arc sec., and the LGC sampling rate. With the attitude rate of the 1000 ft reflector, a CDU bit would be obtained every 280 sec. If the sampling rate were 0.1 sec, as it is on the LM, satisfactory rate derivation would not be achieved, since 2800 new rates would be computed in a 280 sec period with no change in attitude information. Therefore, in order to predict rate accurately, it will be necessary to open up the sampling period to at least 280 sec during limit cycle phases for the 1000 ft reflector (when vehicle rates are extremely small).

- Modify the control logic so that propellant consumption can be minimized in the presence of very low disturbance torques. This requires modification of the switching logic and possibly a means for identifying the approximate magnitude of the disturbance torque so that the appropriate switching logic can be determined.

- Incorporate a control logic which will estimate where the solar pressure is acting (c.p.) relative to the vehicle c.g., and command rotations about the vehicle X axis such that the solar torque is of the opposite sense to the gravity gradient torque. This technique may require appreciable study before it can be incorporated into the control system, but should provide a propellant saving.

By incorporating the above modifications, which only require software changes in the LGC, into the LM PGNCS, the ABLE - GNCS DAP would be an efficient control system for the ABLE mission.

In the normal mode of operation, in association with a rigid body, it is not anticipated that the DAP configuration outlined above would encounter any stability problems. The DAP is also designed

5.2.3.2 cont'd

to operate in a stable manner with a vehicle whose fundamental bending frequency is as low as 1 c.p.s. With the reflector deployed, a preliminary structural analysis has shown that the fundamental bending mode frequency will vary between 0.1 c.p.s. for a reflector of approximately 500 ft in diameter, to 0.001 c.p.s. or less for a reflector of 3000 ft diameter. A detailed analysis of the vehicle stability under these circumstances has not been performed because of the lack of adequate structural data. A qualitative investigation indicated that for frequencies of the order of 0.1 c.p.s. the problem should not be severe because the sampling period in the DAP will be an order of magnitude bigger than the structural period. As the frequency approaches 0.01 c.p.s. the problem becomes more difficult to solve because the structural period approaches the sampling period. In this case it may be possible to devise a logic system and/or a digital filter in the DAP which prevents pulsing frequencies of the jets exciting the structural modes, by delaying firing for a short time period. For structural frequencies below 0.01 c.p.s. it is difficult to make any assessment of the vehicle stability characteristics without a detailed analysis. In conclusion it should be stated that the design of an analog autopilot which can operate in the presence of very low structural frequencies appears to present problems of far greater magnitude than those associated with the digital autopilot.

5.2.3.3 Control Torquers and Thrusters

The LM PGNCS is interfaced with a reaction control system (RCS) which is used to provide translational motion in response to guidance system thrusting commands and rotational motion in response to control system commands. The RCS utilizes 100 lb thrusters at a nominal moment arm of 5.5 ft, giving a control torque of 1100 ft lb when jets are fired to give a pure couple. The minimum translational thrust is 100 lb, but this results in a rotational motion because of the unbalanced torque generated.

5.2.3.3 cont'd

Analysis of the applicability of this system to the ABLE vehicle indicates that during mission phases when the reflector is not deployed, or is in the process of deployment, the RCS can be used to provide control torques and translational motion.

When the reflector is deployed, however, the capability of the reflector to absorb the relatively high thrusts and torques associated with the RCS must be considered. Preliminary structural estimates indicate that firing of short duration from pairs of RCS jets can be tolerated providing long time periods elapse between firings. The influence of this on stationkeeping requirements has not been assessed. The capability of the structure to withstand torques is limited to a maximum of 100 ft lb, and compared to the RCS torque of 1100 ft lb it is indicated that another torquer system must be considered. Also, an analysis of the propellant requirements for the RCS indicates that a more efficient method of control must be found.

Various types of control torquers were considered including control moment gyros, inertia wheels, fluid fly wheels, and moveable reflector panels (in connection with solar sailing techniques) in addition to thrusters (mass expulsion devices). Both control moment gyros and inertia wheels were eliminated as possible torquers for attitude control because of the large total impulse requirements in one cycle, leading to excessive torquer size, or alternatively, leading to an excessive number of unloadings.

In the investigation of fluid flywheels it was assumed that mercury would be used as the fluid. For the largest size reflector considered, it was found that 12,200 lb of mercury would be necessary for control about the Y and Z axes. Two equally sized wheels are needed, one centered about each axis, and in order to keep the fluid requirements to a minimum the diameter of the wheels should equal the diameter of the reflector. Fluid flywheels were not pursued further because of the large weight and awkward physical configuration required.

A solar sail control technique, consisting of varying the shape of the reflector to induce a solar pressure torque about its c.g., was also investigated. For example, a 3,000 ft reflector in synchronous orbit tilted at an angle of 45° with respect to the earths surface has a gravity gradient torque of about 2.7

5.2.3.3 cont'd

ft lb. If the reflector's shape is altered by rolling up sections of the reflector near its edge, an area of 1.92×10^4 sq ft (a section of reflector 139 ft square) would have to be furled.

Mass expulsion devices such as ion engines were considered for the ABLE mission. Two factors made ion engines unattractive, the problem of hardware availability for the ABLE launch date, and the high inherent dead weight of the system, 700 lb.

Based on these preliminary results it was decided that reaction control thrusters are probably best for attitude control. The selection of the reaction control thruster configuration was predicated on obtaining small propellant requirements. The propellant required for a pair of thrusters to generate a given rate change ($\Delta\dot{\theta}$) is given by the expression:

$$W = \frac{2F_{t\ on}}{I_{sp}} = \frac{2T_{t\ on}}{I_{sp}L} = \frac{2\,(\Delta\dot{\theta})\ I}{I_{sp}L}$$

where	W	=	propellant weight	lb
	F	=	thrust level per thruster	lb
	T	=	torque generated	ft lb
	L	=	thruster lever arm	ft
	t_{on}	=	jet on time	sec
	$\Delta\dot{\theta}$	=	rate change	rad/sec
	I	=	vehicle inertia	slug ft^2

This expression shows that for a given vehicle and rate change, W will be minimized if the quantity $I_{sp}L$ is maximized. Clearly, this happens when I_{sp} is increased or L is increased. The maximum value of L is obtained when the thrusters are situated on the periphery of the reflector. The value of I_{sp} is dependent on the type of system used (monopropellant, cold gas, etc) and the decision as to which system to use is governed by hardware complexity and reliability considerations. In general the choice of system is based on the total impulse requirements (and resultant propellant weights and system volumes).

5.2.3.3 cont'd

The maximum ratio in I_{sp} between cold gas and bipropellant systems is of the order of 10 to 1, whereas the ratio of the moment arms between thrusters mounted in the LM RCS clusters and thrusters mounted on the periphery is of the order of 100 to 1. Therefore, it is always more efficient to mount the thrusters on the periphery irrespective of the propellant used, peripheral thrusters are recommended for the ABLE vehicle.

The propellant requirements for the peripheral thruster system is obtained by dividing the total angular impulse required by the thrust moment arm to yield total impulse, from which the propellant weight is obtained by dividing by the propellant I_{sp}. Curves for computing propellant weight are given in Fig. 5.2-2.

The maximum thrust level required of the peripheral thrusters is determined by dividing the peak torque by the thruster moment arm. The minimum thrust per jet (assuming pure couples are used) is shown in Fig. 5.2-3 as a function of reflector diameter.

FIGURE 5.2-1

NAVIGATION FUNCTION

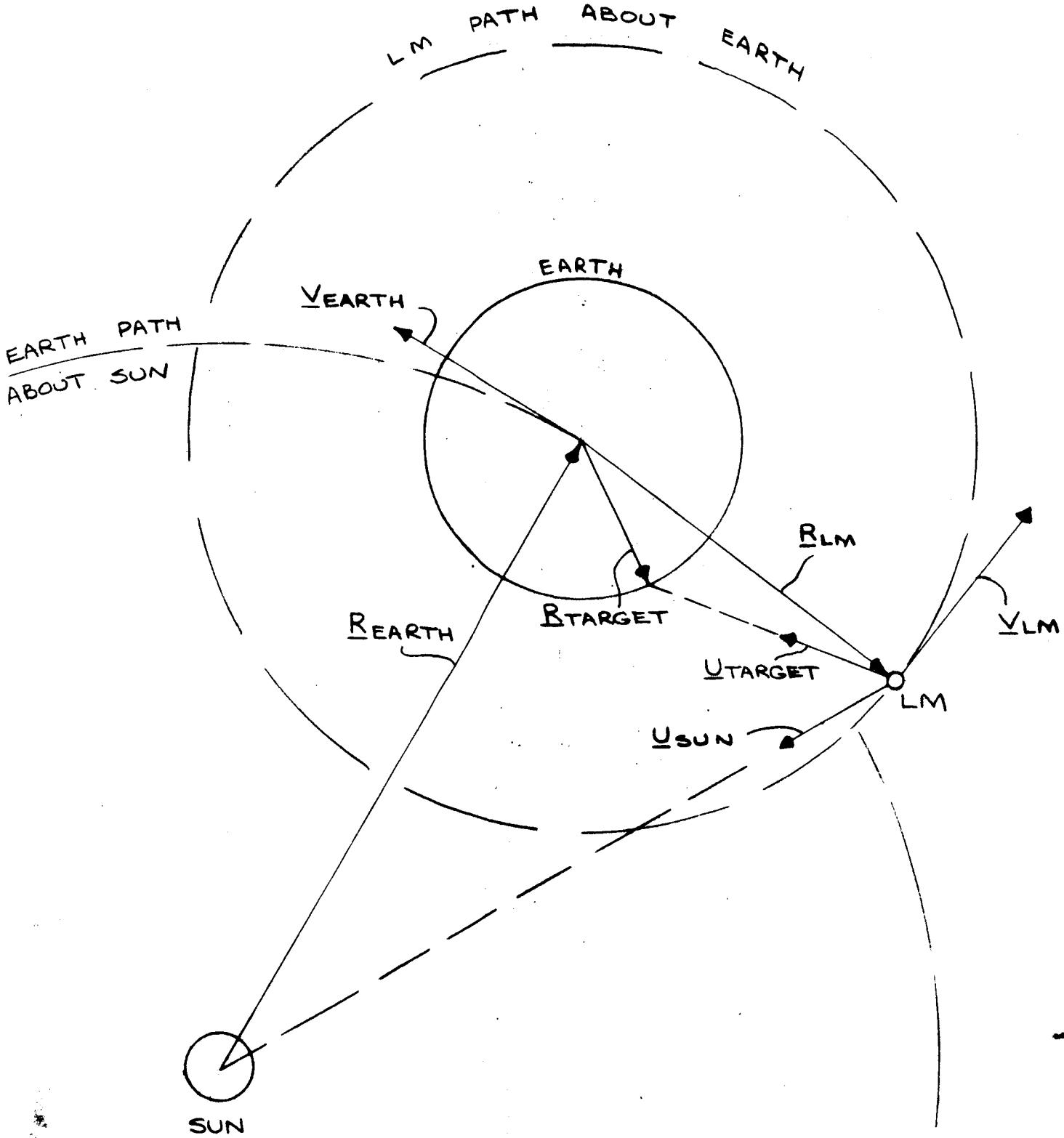

TOTAL IMPULSE & PROPELLANT REQUIREMENTS
AS A FUNCTION OF TOTAL ANGULAR IMPULSE

FIGURE 5.2-2

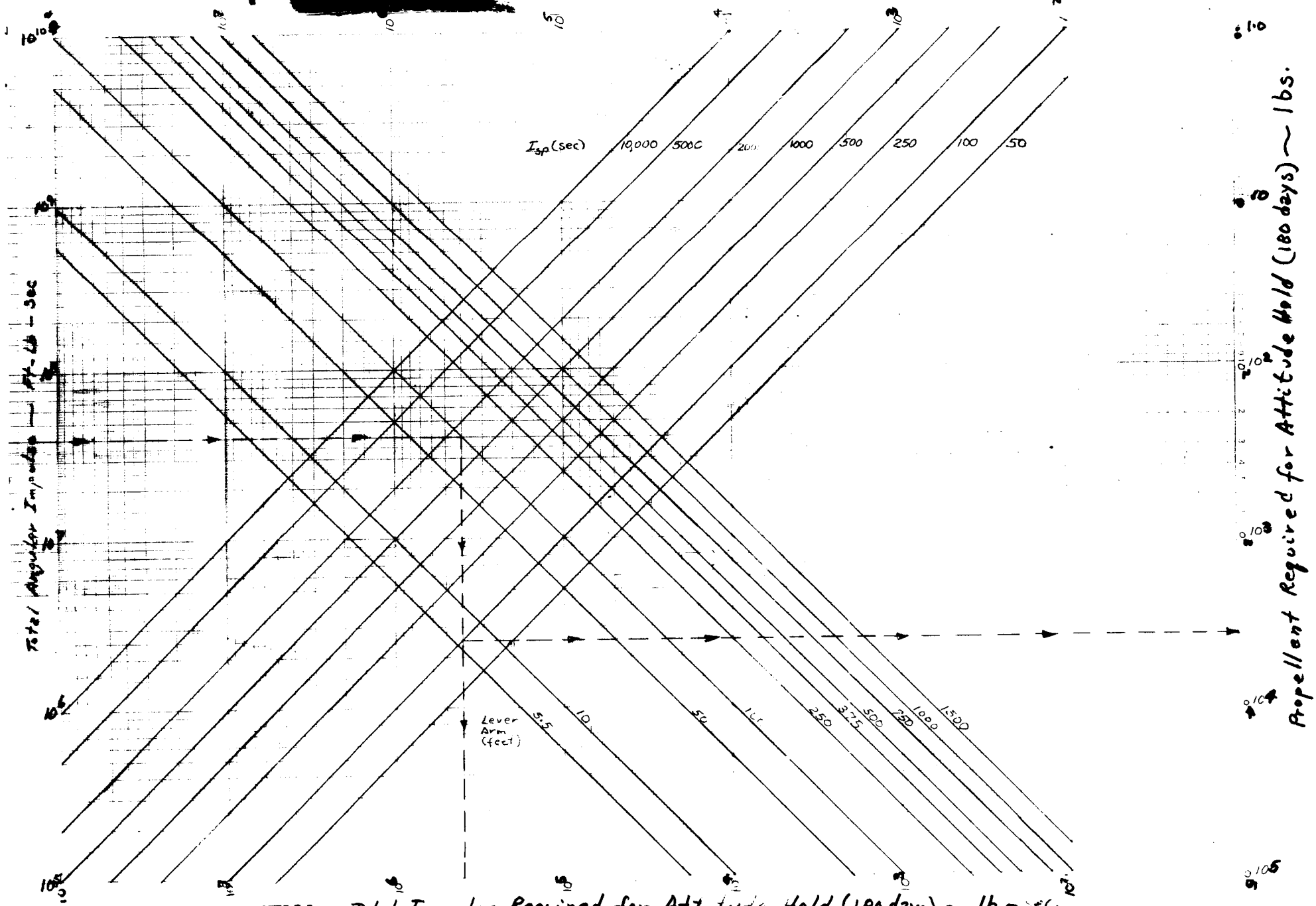

FIGURE 5.2-3

THRUSTER LEVEL REQUIREMENTS
FOR EQUATORIAL ORBITS

[redacted]

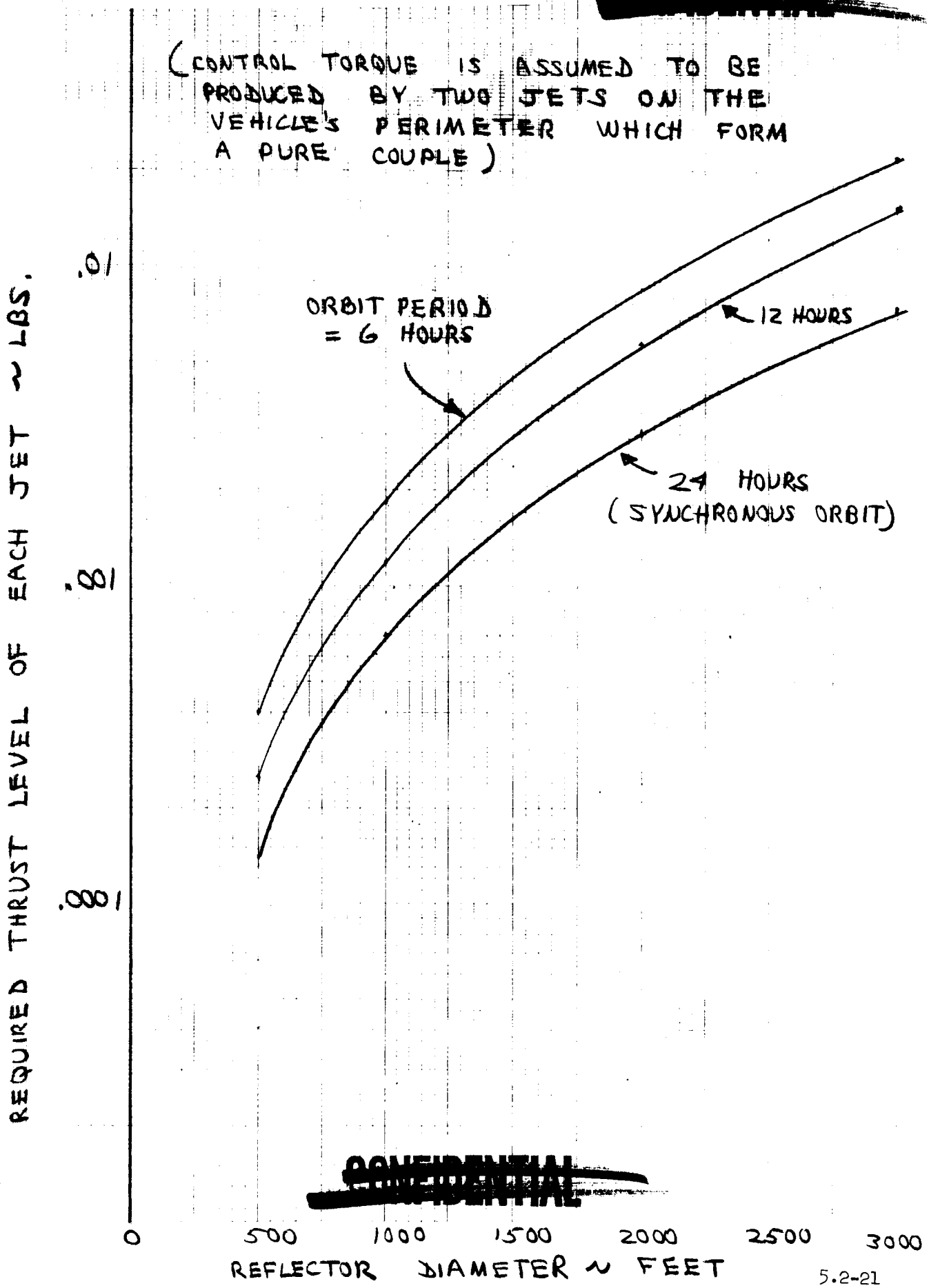

[redacted]

5.3 REACTION CONTROL ANALYSIS

The type of propulsion system to be selected for reaction control of the ABLE spacecraft is dependent upon a number of considerations. Such parameters as weight, volume, thrust level, system complexity, availability and compatibility must all be considered. Table 5.3-1 summarizes these selection factors for various types of systems as they apply to the ABLE spacecraft.

System weight (less plumbing and engines) vs total impulse over the range of interest is presented in Fig. 5.3-1. It should be noted that for the range of total impulse considered, it is proper to omit plumbing and engine weight since it represents a small percentage of the system weight and is approximately equal for the various systems. As far as possible, common assumptions were made for all systems, i.e., for cold gas, monopropellant and bipropellant systems, all tanks were assumed to be titanium (Ti 6 Al-4V) spheres with a factor of safety of 1.5. Other assumptions are as follows:

- Cold Gas System
  - Gas = Nitrogen
  - Storage Pressure = 3000 psia
  - Isp = 60 sec.
- Monopropellant
  - Propellant = Hydrazine, $N_2 H_4$
  - Pressurant = Helium
  - Pressurant Storage Pressure = 3000 psia
  - Propellant Tank Pressure = 200 psia
  - Isp = 200 sec.
- Bipropellant
  - Propellant = $N_2 O_4$ and UDMH/$N_2 H_4$
  - Pressurant = Helium
  - Pressurant Storage Pressure = 3000 psia
  - Propellant Tank Pressure = 250 psia
  - Isp = 250 sec.
- Subliming Solid
  - Tank Weight = 11.5% of propellant weight
  - Isp = 75 sec.

5.3 cont'd

Propulsion system propellant and/or pressurant volume for the various systems is plotted in Figure 5.3-2 as a function of total impulse. The volume of the cold gas system is large for this application over the entire range of total impulse while the volume of the subliming solid system is large over a large portion of the total impulse range considered.

Fig. 5.3-3 presents the maximum allowable thrust, based upon structural moment limitations, as a function of distance between thrusters. This curve depicts thrust regimes for various propulsion systems and can be used in conjunction with Figure 5.3-4 in order to select an applicable system.

The use of ion engines was dropped from consideration because of its operational complexity in comparison with other systems, without any gross weight savings. In addition, it is felt that ion engine systems are not far enough along in development to keep them in contention with the other systems. It should be mentioned that the ion engine system weight and volume parameters are not included in Figs. 5.3-1 and 5.3-2 because they are not solely a function of total impulse.

In conclusion, the monopropellant and bipropellant systems are the favored choices for large reflectors. When engine thrust level requirements and problems associated with materials compatibility are considered, monopropellant systems appear to be more desirable. If reflector sizes in the range of 400-750 ft are decided upon, subliming solids and cold gas systems again become competitive.

TABLE 5.3-1

ABLE PROPULSION SYSTEM SELECTION FACTORS

System Type	Weight	Volume	Available Range of Thrust Level (LB)	Complexity of Operation	Development Status	Remarks
Subliming Solid	Medium	High	$<10^{-3}$-10^{-1}	Low	Flight	Volume high at larger total impulses
Cold Gas	High	Very High	2×10^{-3} - 1.0	Low	Flight	Volume high at all total impulses
Monopropellant	Low	Low	3×10^{-2}->100	Moderate	Flight	
Bipropellant	Low	Low	1.0 - >100	Moderate	Flight	Thrust level too high. Oxidizer compatibility problems for long durations
ION System	Dependent on duty cycle required	Dependent on power supply	$<10^{-3}$ - 10^{-2}	High	Under Development	Overall system operation too complex and system not developed.

CONFIDENTIAL

[redacted]

FIGURE 5.3-1

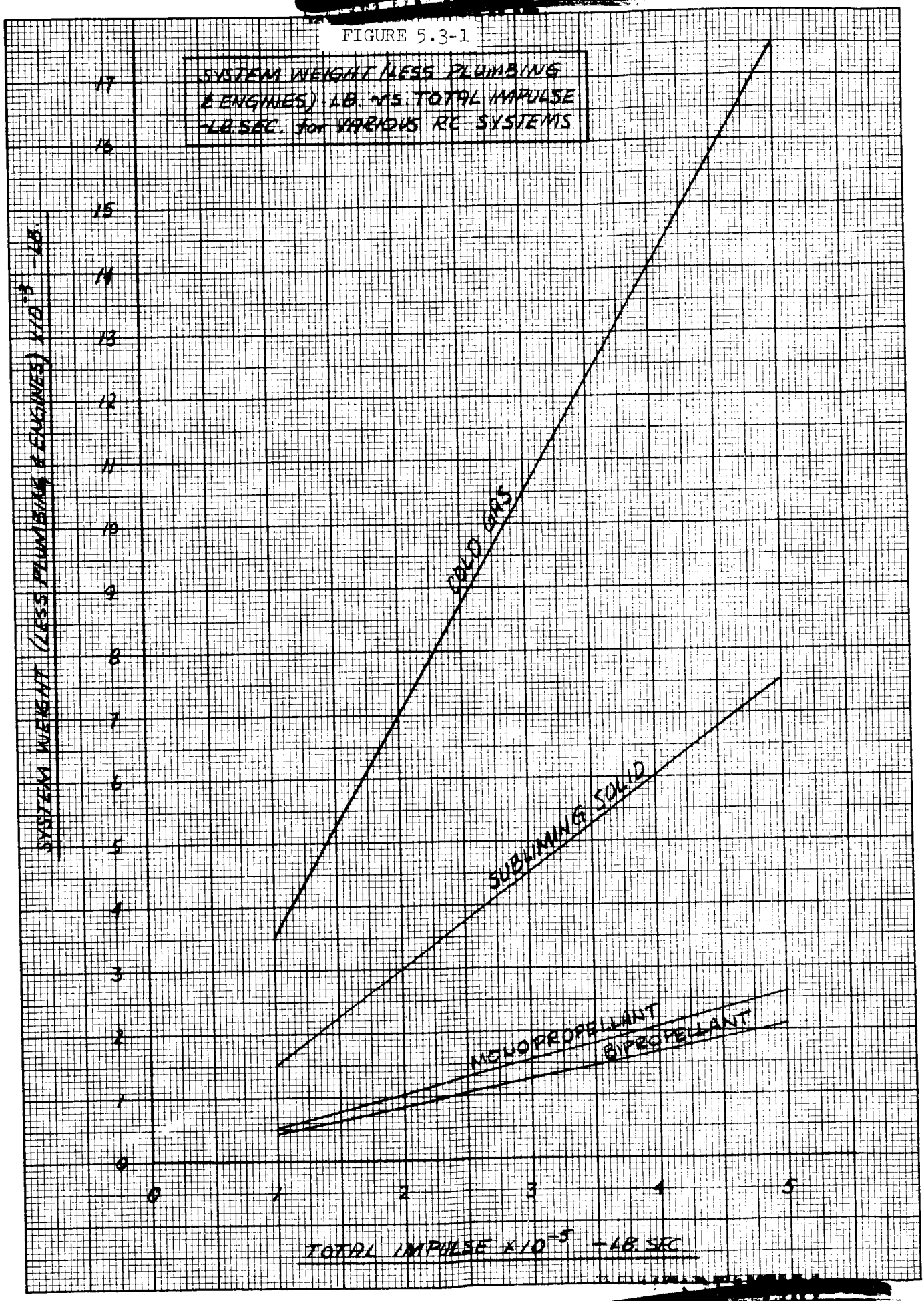

[redacted]

FIGURE 5.3-2

PROPELLANT AND/OR PRESSURANT VOLUME - FT^3 VS. TOTAL IMPULSE - LB. SEC. for VARIOUS RCS SYSTEMS

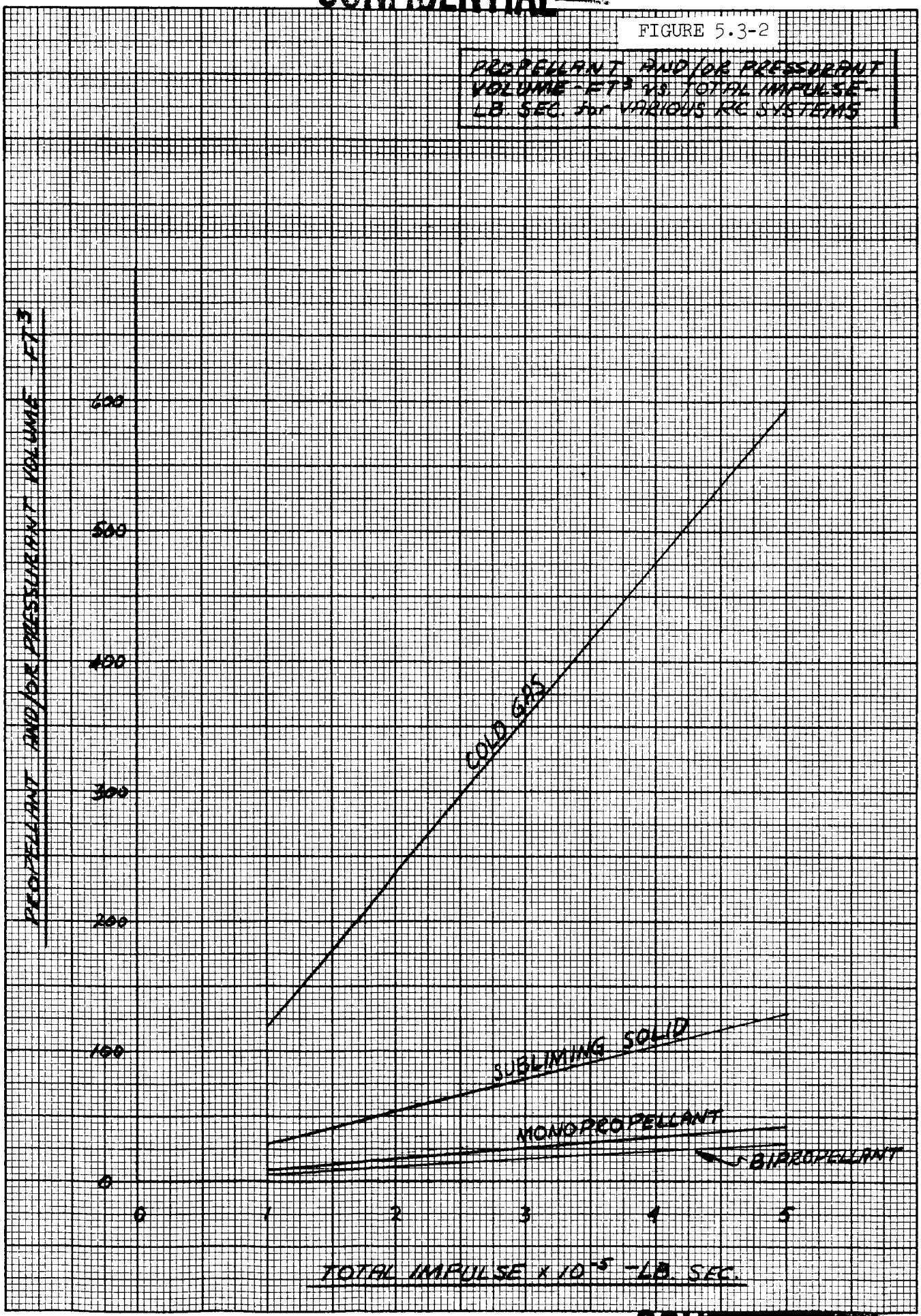

[redacted]

FIGURE 5.3-3

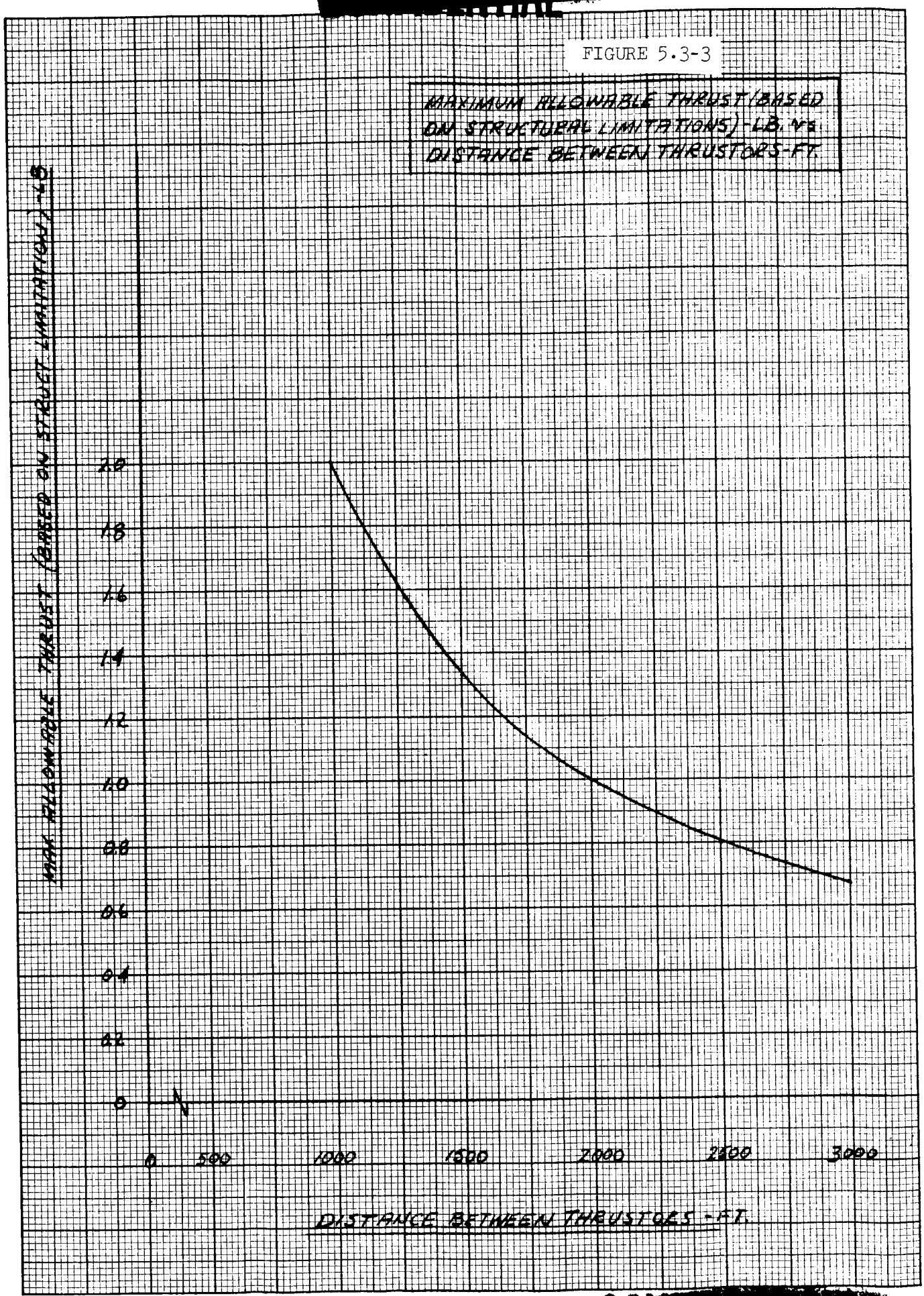

[redacted]

FIGURE 5.3-4

THRUST REGIMES for VARIOUS TYPES of PROPULSION SYSTEMS

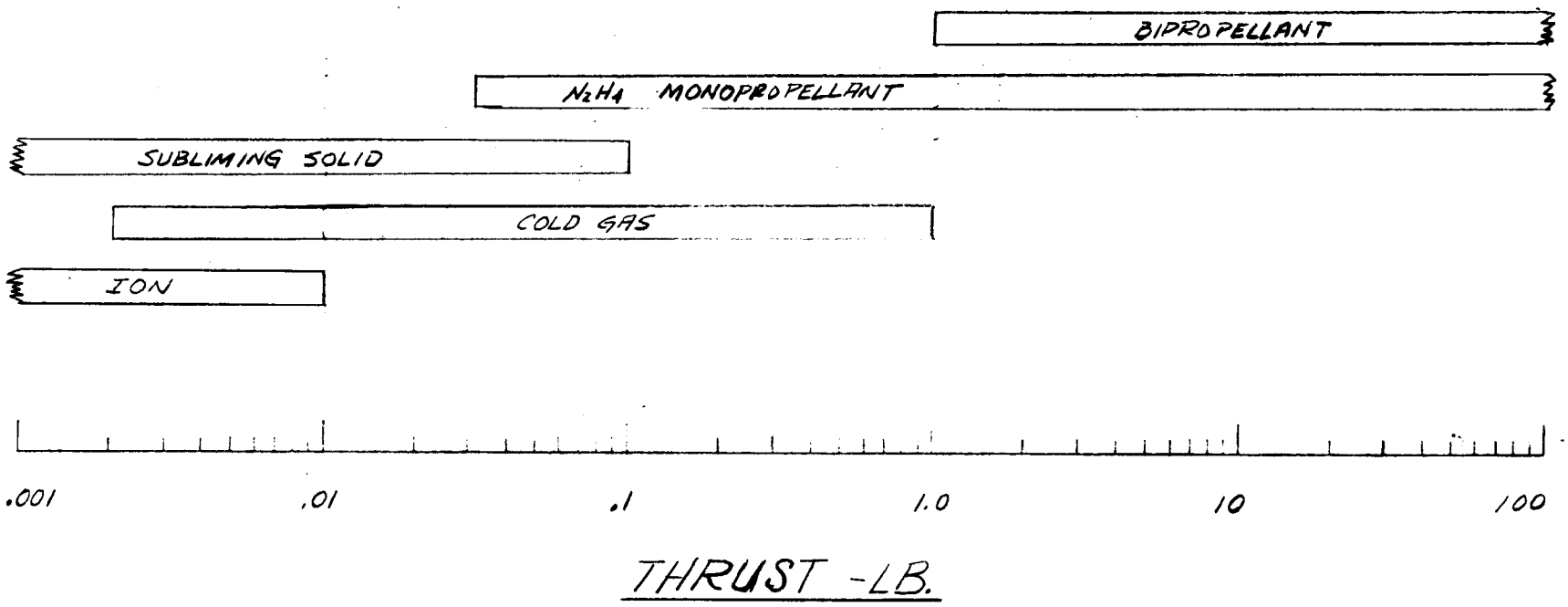

5.4 RELIABILITY

5.4.1 Introduction

In order to properly assess the Reliability and Maintainability aspects of Project ABLE, the following areas were investigated:

- The relative merits of both manned and unmanned mission and flight vehicle configurations
- Reliability estimate for a manned ABLE LM mission
- The identification of LM equipment that would provide the functional redundancy to negate single failures
- The degree of both on-board and downlink status monitoring which would enable the crew or MSFN to take remedial action to permit continuation of the mission
- The identification of those equipments which because of their present design may be categorized as limited life items.

Both mission success, and crew safety, where applicable, were considered in the reliability analysis. Mission success was defined as the achievement of the primary objectives of the mission such as reflector deployment, alignment and check-out, and up to a six month operational phase. The crew safety evaluation was a consideration of the fact that there are combinations of failures which could result in a hazard to the crew.

5.4.2 Comparison of Flight Vehicle Configurations

In evaluating both manned and unmanned missions, the following configurations were considered:

- Case 1 - Single unmanned Saturn V launch
- Case 2 - Dual launch with the LM/Reflector on one vehicle and the manned CSM on the other vehicle
- Case 3 - Single manned Saturn V launch.

5.4.2 (continued)

The single unmanned Saturn V launch (Case 1) would at first, appear to be the most reliable configuration because of the off-loading of those subsystems or portions of subsystems which are considered as life support equipment and those equipments necessary for a man-in-the-loop operation (e.g. controls, switches, displays, etc.) It must be realized however, that the additional equipment and/or possible changes to present equipment design necessary to perform remotely controlled on-board checkout and calibration, and in the event of a failure fault detection, fault isolation and selection of on-board compensation must be considered sufficiently complex to nullify the above-mentioned reliability improvement. Because of the lack of definition of the required equipment additions, there has been no quantitative reliability assessment made for this configuration.

It was assumed in the dual launch configuration (Case 2) that the first launch vehicle with the ABLE LM would have to be put into orbit approximately 14 days prior to the launching of the CSM because of the required launch complex "turn-around" time. During this 14 day orbital phase, the vehicle could be in one of three possible states:

- All equipment, with the exception of the heater control circuitry for the IMU and reflector canister nonfunctional in a power-down configuration for the entire 14 days
- All subsystems nonoperational for a portion of the unmanned orbital phase and then activated for a vehicle checkout prior to the launch of the second vehicle. These functional modes could be continuous or intermittent
- All equipments could be functional for the entire 14 day period.

This means that much of the complexity associated with Case 1 would also apply here. Here again, because of the undefined nature of the requested modifications, no attempt has been made to compute the probability of success for this configuration.

A manned single launch configuration (Case 3) appears to afford the most reliable mode of operation because of the elimination of many automatic startup and checkout requirements. It is recognized that the additional equipments for life-support during the 36 hour manned phase will affect the probability of success, but this affect will be minimal because of the relatively few components involved and the functionally redundant modes of operation available.

5.4.2 (continued)

For the purposes of determining an estimate of the ABLE LM mission success reliability the following assumptions were made:

- From launch through final alignment, there is one LM battery (primary) available for contingency, thereby giving us a 5 out of 6 configuration
- Failure rates for the Ni-Cd batteries are based on TRW estimates
- Because of the lack of definition of the MIT configuration, the reliability estimates of the vehicle are exclusive of this GFE equipment
- The RCS subsystem on the LM vehicle is assumed to be nonoperational after the manned phases
- The instrumentation subsystem and the communication subsystem were assumed to be operating continuously during the manned phases
- The reflector peripheral monopropellant thrust chambers were assumed to have a 3% duty cycle during the mission
- Failure rates for the peripheral thrust chamber were derived from TRW estimates.

A plot of the probability of mission success during the manned and unmanned phases is shown in Fig. 5.4-1. There was no estimate made of the crew safety reliability, however a preliminary failure mode and effects analysis indicated that the likelihood of crew loss, due to malfunction of the ABLE LM, was extremely small.

5.4.3 Functional Redundancies

The configuration proposed for ABLE LM, which is basically the LM as modified for the specific mission objectives, contains inherent redundancies which will enhance the probabilities of mission success and crew safety during the various phases of the mission. These are summarized below by subsystem.

5.4.3.1 RCS

Functional redundancy inherently exists in the LM RCS configuration. The LM

5.4.3.1 (continued)

has RCS thruster failure detection and compensation capability. Furthermore, during manned phases of the ABLE mission, selective initiation of the pressurization system can render "operational" redundancy. The utilization of LM pressurization system "A" until depletion and then employing System "B" leaves System "B" unpressurized for a greater length of time. Hence, even though the total propellant quantity of systems "A" and "B" may be required to fulfill mission objectives, "operational" redundancy may still be achieved (System "B" being kept in reserve for as long as possible). Should the propellant quantity of System "A" be sufficient to satisfy mission requirements, then System "B", used as described above, provides a purely redundant pressurization system. The above operational method are presently dependent on having man in the loop.

As presently configured the reflector, low thrust, monopropellant thrusters do not have any functional redundancies. Capability for incorporation of the LM jet select logic for correction of thruster failures is possible with certain minor additions to the reflector jets functional configuration.

5.4.3.2 ECS

The proposed coolant pump configuration will consist of three parallel pumps, each of which can provide normal flow for the heat transport system. During the manned phases of the mission, the astronaut could switch from one pump to another in the event of a failure. During the unmanned phases this could also be done by means of an uplink command.

During the manned phase the closed loop atmosphere revitalization system is considered back-up to the nominal "helmet off" operational mode. In addition, the switch fans, water evaporator, water separator, and PLSS cartridges are functionally redundant within the ARS.

5.4.3.3 EPS

A redundant NiCd rechargeable battery is provided to increase mission success during the six months unmanned phase. During the launch through alignment phases one LM battery would be available for contingencies and is considered redundant to the required five batteries.

5.4.3.4 Communications

Redundancies in the communications subsystem consist of the following items:

- S-Band Transceivers - Either transceiver may be used during manned or unmanned phases. Selection of either unit can be made manually during the manned phase. Selection during the unmanned phase is telemetered to the uplink Command Receiver and is carried out by the DCA.
- S-Band Power Supply and Amplifier - Same as above.
- VHF A and B Transmitters and Receivers - Either receiver and either transmitter may be used to communicate with the CSM during the manned phase. However, during an EVA the VHF B receiver must be used because of its bio-med data handling capability. Under this condition either transmitter may be used. The LM VHF equipment will not be used during the unmanned phase.
- Audio Centers - The audio centers are both used during the manned phase. However, should one fail both men can plug into the other center. Both centers are required for EVA with no backup mode provided.

5.4.4 On-Board On Ground Monitoring

An integral part of the LM Instrumentation, Controls and Displays and Communications Subsystems, is the capability for both on-board and/or ground detection of malfunctioning equipments for the purpose of isolating the faulty equipment and taking the necessary remedial action.

During the manned phase the data obtained by LM Instrumentation is presented in three ways. First, all of the data is coded and relayed to the MSFN via the S-Band communications subsystem. Second, the Caution and Warning subsystem is designed to evaluate instrumentation data obtained from the various subsystems and to advise the astronauts of the apparent development of minor problems (caution) or of the presence of major problems (warning). Third, being made aware of problems by the Caution and Warning subsystem, there are sufficient Displays and solution capability on the vehicle to aid the astronaut in analyzing the seriousness of a subsystem problem. He can then take corrective action and decide whether to continue with the mission. Also, if time permits, he can consult with the MSFN for concurrance on the data, his analysis of the problem and his decision. Furthermore, the astronauts can periodically observe the

[redacted]

5.4-4 (continued)

various Displays to note existing conditions.

During the unmanned phase, the data obtained by LM Instrumentation is telemetered to and monitored by the MSFN. Such items as vehicle position and temperature gradients on the reflector can be monitored and corrected as necessary by reorientation of the vehicle. Also, other parameters are recorded by the MSFN and analyzed. All corrections, adjustments and decisions will be made by the MSFN via the uplink, during this unmanned phase.

5.4.5 Limited Life Study

A review of the LM equipment proposed for the ABLE LM was conducted to determine the effect of their performance of a six month operational period. The following assumptions were established for this task:

- The duty cycle of the electronic equipments is as detailed in EPS load profiles
- The RCS system is fully pressurized and remains so from the commencement of the manned phase
- The ECS heat transport system is operative and remains so for the entire duration of the mission.

The results of this limited life study are listed in Table 5.4-1. The major purpose in identifying these limited life items is to ensure that appropriate engineering attention be directed to them early in the design effort.

In addition to the potential limited life items noted in Table 5.4-1, the LM program will be continuously monitored for signature trend data that will modify this preliminary listing.

[redacted]

TABLE 5.4.1

LIMITED LIFE EQUIPMENT

~~CONFIDENTIAL~~

Subsystem	Equipment	Part	Potential Problem Areas
ECS	Glycol Accum (LSC-330-210)	(a) Diaphragm	Wearout characteristics function of duration of cyclic operation and exposure to ethylene glycol/water solution. High leakage rates would occur if material fatigues.
		(b) Piston bearing	Potential teflon loss due to vaporization in high vacuum. (teflon coating for shaft lubrication)
	Cabin Temp. Control Valve (LSC-330-203)	(a) Control piston and housing	Continuous modulation for 6 months. Water/glycol solution may cause corrosion of piston and housing assembly.
		(b) O-rings	Exposure to water/glycol solution for long duration could have degrading effect on dynamic seals. Decomposition of seal would cause excessive leakage.
	Recirculation Assembly (LSC-330-290)	(a) Armature bearings	Wear characteristic function of cycles rotation. Loss of lubricant will result if seal fails.
		(b) Glycol filter	Potential blockage due to entrapped particles in glycol solution; pump will be inhibited if build up is excessive.
		(c) Seals	Rubber silicone seals may decompose due to reaction with glycol solution.
RCS	Positive Propellant Tank (LSC-310-405)	Teflon Bladder	Long term "sloshing" of porpellant in bladder may produce three corner fold tears resulting in pinhole leakage. Problem will be more severe in fuel tank because oxidizer (N_2O_4) vapor has the characteristic of softening the teflon bladder. Resultant propellant leakage contact with titanium shell should present no significant corrosion problems (using "green" N_2O_4 as oxidizer and A-50 as fuel).
	Helium Regulator (LSC-310-305) and Quad Check Valve (LSC-310-306)	O-Ring Seals and Ball	Accumulated exposure to mixed propellant vapors may cause deposits of ammonium salts to form on seals, balls and poppets preventing proper seating. This could result in excessive leakage and loss of regulation in regulators and increased reverse flow in check valves.
	~~CONFIDENTIAL~~		NOTE: RCS hardware has been qualified for 44 days compatibility with the propellants. There is no reason to believe that longer times cannot be achieved. However, test data for longer durations is lacking.

RELIABILITY versus MISSION DURATION

[redacted]

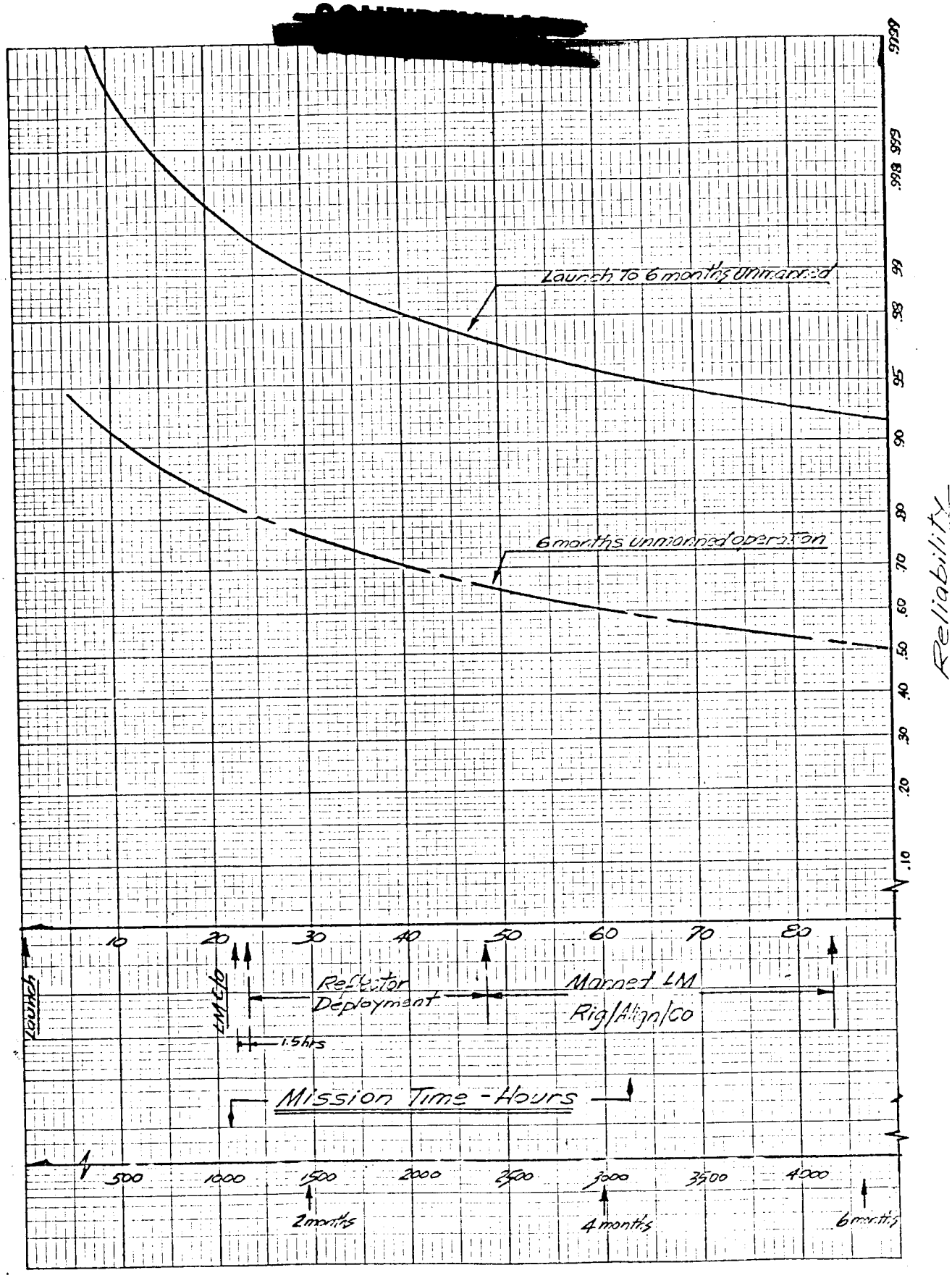

FIGURE 5.4-1

[redacted]

[redacted]

5.5 MASS PROPERTIES

The complete weight statement for the ABLE LM Program Planning Configuration (PPC) is listed in Table 5.5-1. This weight statement was generated by starting with the control weight of the Apollo LM AS-504, at translunar injection, and then adding and deleting hardware as defined in Table 2.2-1. A reference 1100 ft. diameter reflector was chosen for the PPC. The total weight of the PPC ABLE LM was estimated to be about 27,100 lbs. leaving 4900 lbs. (18%) for growth contingency. The following expendables carried onboard the Apollo LM AS-504 were retained in the ABLE LM configuration:

- Water - 288 lbs.
- Gaseous Oxygen - 55 lbs.
- RCS Propellant - 539 lbs. useable.

[redacted]

[redacted]

Table 5.5-1

ABLE LM WEIGHT STATEMENT

LM - AS-504 CONTROL WEIGHT - TLI	32,000
Ascent Structure	
Unchanged	
Descent Structure	
Remove:	
Base Heat Shield	-146
Add:	
ABLE Canister & Supports	1,000
LM/Reflector Attachment Penalty	100
Guidance, Navigation & Control	
Remove:	
DECA	-7
GDA	-6
ASA (AGS)	-32
AEA	-20
RGA	-2
DEDA	-8
AOT	-22
Rendezvous Radar	-75
Landing Radar	-38
Added:	
PCA	60
LOTS	24
Crew Provisions	
Unchanged	
Environmental Control	
Add:	
Fixed radiators (Installed Wt.)	50

[redacted]

[redacted]

Table 5.5-1

- continued -

Landing Gear	
Remove:	
Total Landing Gear	-465
Instrumentation	
Same weight as Apollo/LM mission	
Electrical Power	
Added:	
Deployable Solar Arrays Rechargeable Batteries (2) ECA's (2) Battery Chargers & Voltage Regulators Wiring, Supports, etc.	1200
Propulsion	
Ascent Propellant - Total	-5090
Descent Propellant - Total	-17,749
D/S Propellant Tanks	-440
A/S Propellant Tanks	-172
D/S Engine	-377
A/S Engine	-212
A/S Helium	-13
A/S Helium Tanks	-111
Added:	
D/S Supercritical Helium Tank	100
Helium	55
Plumbing & Supports	15
Reaction Control	
Unchanged from LM	
Communications	
Remove:	
TV	-8
S-Band Erectable & Steerable Antenna	-38
Add:	
VHF Antenna	3
DCA & CMD Rcvr	40

[redacted]

Table 5.5-1

- continued -

Controls & Displays	70
TOTAL LM	9686
1100 ft. diameter reflector	17,400
TOTAL ABLE LM	27,086
GROWTH ALLOWANCE	4914
	32,000 lbs.

6.0 ABLE LM SUBSYSTEM ENGINEERING

6.1 ELECTRICAL POWER

6.1.1 Electrical Load Analysis

6.1.1.1 Assumption for Manned Mission

The electrical load analysis was based upon the reference mission profile and time-line (Section 3.5) and on the following assumptions:

- Vehicle status monitored once per day during the six month unmanned phase.
- Reflector attitude control is provided by four monopropellant thruster modules located at the periphery of the reflector. Each thruster module is packaged with electrical heaters for thermal control.
- LM provides electrical power requirements from Earth launch to CSM transposition and docking.
- CSM provides LM with electrical power requirements, through existing umbilical, from CSM docking until the start of LM activation.
- During initial reflector deployment, the LM remains activated in an unmanned controlled attitude mode.
- Solar arrays are deployed and checked out after reflector deployment is completed. It was assumed that the array starts operating at the 50th hour. The LM primary silver zinc batteries are then used to supplement the array for the higher spacecraft loads encountered during the manned phases.
- An additional 10 hours of manned LM operation are allotted for reflector readjustment and contingencies.

6.1.1.2 Power Profile for Manned Mission

Table 6.1-1 details and summarizes the average power and energy requirements. Solar array heater power of 160 watts is required after array deployment. This occurs because heaters are required to maintain the arrays above -160°C while

[redacted]

6.1.1.2 cont'd

they are in the shadow of the reflector as discussed in Section 5.1 Control power for the array, the voltage regulator, battery charger and controls were included as continuous loads. However, voltage regulation inefficiency, line losses from the array to the LM and battery charging inefficiencies are not included in this table, but have been taken into account in the array and battery sizing (Table 6.1-3).

Figure 6.1-1 is the mission average power profile derived from Table 6.1-1. The profile shows the division of required energy between the LM primary batteries and the solar array. With solar arrays supplying power at the 50th hour, 15 kwh of energy is available from the LM primary batteries for EPS contingency.

6.1.1.3 Requirements for Unmanned Mission

The unmanned mission power requirements would be the same as the unmanned portions of the manned mission except for an increase in the Instrumentation and Communication duty cycles for continuous monitoring and control of the LM from Earth. The major difference in the power profile is that all the LM subsystems would probably be fully activated prior to Earth launch. LM/SIVB separation would be identical to LM-1 separation using the LM RCS. The ABLE LM would be subject to earth control during reflector outgassing, deployment and the final alignment period.

The estimated average power level for the entire 49 hours period from countdown until solar array deployment (see Section 3.5) is 1050 watts. Therefore the total energy that must be supplied by the LM primary batteries is 51 kwh. This leaves 15 kwh of LM battery energy available for support of final deployment, alignment and calibration of the reflector system.

6.1.2 Orbital Mechanics Consideration

6.1.2.1 Orbital Altitudes

The orbital altitude parameters considered for sizing the ABLE LM EPS are shown below. The occultation times shown are the maximum possible per orbit based on a circular equatorial orbit.

[redacted]

6.1.2.1 cont'd

Period Hr.	Altitude N.Mi	Occultation %	Occultation Hr
6	5591	12.0	0.72
12	10931	7.5	0.90
24	19330	5.0	1.20

6.1.2.2 Spacecraft Orientation (See Attitude Time-Line Curves in Section 3.2)

The spacecraft was assumed to rotate around the right ascension axis (parallel to earth polar axis) exposing each side of the reflector in succession to the sun. The spacecraft will also be subject to angular variation around the declination axis.

6.1.3 EPS Configuration

The recommended ABLE LM EPS Configuration is shown in Fig. 2.2-1. In this configuration, the existing LM EPS is retained and supplemented, for the six month unmanned phase, with a solar cell array and rechargeable battery power supply. The existing LM EPS, which does not require vehicle orientation, supplies the ABLE LM power requirements until the solar arrays are deployed. From that time to the end of the manned phase, the solar arrays and the LM batteries are operated in parallel to meet the relatively high power requirements during manned ABLE LM operations. During the six month unmanned phase, power is entirely supplied by the solar array and secondary battery power supply.

For the unmanned mission the EPS configuration remains the same with the exception that the manned control and switching requirements are replaced by remote uplink command.

The supplementary power supply includes two silicon solar cell arrays, one on each side of the reflector, two secondary NiCd batteries (one for redundancy), battery charger assemblies, and a voltage regulator to maintain the power source output voltage within allowable voltage limits.

6.1.3.1 Solar Cell Configuration

The EPS configuration makes use of existing space electrical power technology and equipment. Conventional N/P 10 Ωcm, high radiation resistant silicon solar cells

[redacted]

with 0.006 inch glass cover, consistent with the expected radiation environment are applicable. The radiation environment used for the solar cell configuration studies is summarized in Section 3.4. Solar cell module designs already developed for other space programs appear to be usable as component parts of the array. Examples of these are presented in Table 6.1-2.

Several configurations of solar cell arrays were investigated and their size and weight compared for the three orbits studied. Table 6.1-3 presents the criteria used and a sample calculation of solar array and secondary battery sizing.

6.1.3.1.1 Solar Array with Two Degrees of Freedom. This configuration is one in which each solar array contains an orientation and drive mechanism, whose function it is to maintain the array normal to the sun vector so as to minimize the required solar cell area. This system would be unaffected by vehicle attitude changes. The required angular movement, rates, and masses are such that existing space system hardware can probably be utilized for the orientation and drive mechanism. The orientation control function could be accomplished by a closed loop servo system using intelligence from a sunsensor and or from the LM guidance computer. The ABLE LM has the capability for receiving "uplink" command override signals from Earth.

Fig. 6.1-2 shows the variation of required solar cell array area and weight vs orbital altitude for this type of system. It can be seen that the variation of orbital altitude from 5 to 20 thousand miles results in only a 50 lb variation in solar array weight and 40 sq ft of area.

6.1.3.1.2 Solar Array with Single Degree of Freedom. This configuration differs from the previous configuration only in that the solar arrays have one degree of freedom instead of two. The rotation axis of the arrays are parallel to the right ascension axis. This compensates for the major movement of the vehicle. Additional solar cell area over the two degree of freedom required area would be needed to compensate for the vehicle declination angle as shown in Fig. 6.1-3.

[redacted]

6.1.3.1.3 Fixed Solar Arrays. An alternate solar cell configuration that was considered is a fixed array. This configuration eliminates the need for a sun seeking and positioning system but consequently results in the maximum required solar array area. Each of the two arrays would consist of 2 panels set at a sixty degree included angle in the plane of the 180° vehicle motion to compensate for that movement. For vehicle declination angles less than ±60° in the normal direction, flat panels (which minimize array area) would be utilized. The variation of total panel area with vehicle declination angle for the fixed array and a comparison with other configurations is shown if Fig. 6.1-3.

6.1.3.2 Rechargeable Battery Configuration

It is proposed to use rechargeable NiCd batteries in conjunction with the solar arrays for the six month unmanned portion of the mission. The number of cycles and total duration of the ABLE mission are well within the present capabilities of NiCd space qualified batteries. Fig. 6.1-4 shows the variation of battery weight and capacity with orbital altitude for maximum occultation times per orbit (para. 6.1.2.1). An increase in orbit altitude from 5 to 20 thousand nautical miles results in a battery weight increase of approximately 150 lb.

6.1.3.3 Battery Charger

The battery charger is designed to replenish the secondary batteries at the maximum rate consistent with:

- Maximum allowable battery temperature and pressure
- Solar array capability and vehicle bus loading

After a predetermined charge level has been reached, the battery is maintained on a trickle charge rate. Controls for periodically discharging and reforming the battery that is being cycled is also included.

6.1.3.4 Voltage Regulator

The function of the voltage regulator is to maintain the power source output voltage within allowable limits compensating for the solar array and battery output voltage variations. The voltage variations of the solar array will be

6.1.3.4 cont'd

largely due to the long duration (several hours) of occultation by the reflector structure and the resulting low cell temperature. Variation of cell temperature from -168 to +60°C are expected (even with heaters) causing voltage variations of over 50 per cent above the LM bus limit.

6.1.4 Alternate Configuration

A survey of other types of power supplies capable of performing the ABLE mission was made. The only other power supply which appeared to have the development status, power delivery capability, weight and configuration which could be considered for this mission was the SNAP 10A system.

The utilization of a SNAP 10A power supply appears to be feasible for the ABLE mission. This generator has the nominal power and life required for this mission and has been successfully flown in space for a period of 45 days. The system would be mounted on the LM in a shutdown state prior to launch, and, after reflector deployment and vehicle alignment, the SNAP 10A would be deployed on a boom. In a manned mission, start-up would occur after the astronauts have left the vehicle.

The SNAP 10A is attractive because it does not have any orientation requirements. In addition, the unit is a developed and qualified package and has been started-up and utilized in space. The unit would supply power to the vehicle through a voltage regulator and require the addition of peaking batteries and a recharger to handle short duration high power requirements.

The required reactor/LM separation distance and the resulting deployment procedures for a 1000 lb mass, and prelaunch handling operations require further evaluation.

6.1.5 Comparison of Configurations and Conclusions

A comparison of the different power supplies considered for the LM ABLE is presented in Table 6.1-4. A comparison of total system weight vs orbit altitude for all configurations considered is presented in Fig. 6.1.5. It is concluded that it is feasible to provide a power supply for this mission utilizing either a solar

6.1.5 cont'd

cell or SNAP 10A configuration supplementing the existing LM EPS. The selection of a particular EPS configuration must involve a detailed comparison of cost, schedule, development status, reliability and vehicle integration.

TABLE 6.1-1 LOAD ANALYSIS DATA SHEETS

EQUIPMENT	Watts Steady	Watts Peak	22 Hrs(3) Launch to LM Activation (Unmanned)	1.5 Hrs LM Activation & C/O (Manned)	24 Hrs Initial Reflector Deployment (Unmanned)	36 Hrs Final Deploy., Align & Calib. (Manned)		4320 Hrs 6 Month Unmanned Operation (Unmanned)
010 - Communications								
Audio Center (Voice & Analog Data)	12.	--	--	12.	--	12.		--
VHF (CSM & EVA Voice) RCVR	2.		--	2.	--	2.		--
VHF X Mitter	30.		--	15.	--	15.		--
Premod. Proc. (Downlink Data)	15.		--	3.	7.5	3.		3.
S-Band (Up/Downlink Voice,Data) RCVR	25.		--	25.	25.	25.		25.
S-Band X Mitter	170.		--	34.	85.	34.		1.7
SUBTOTAL				91.	117.5	91.		29.7
020 - Crew Provisions								
EL Lighting (AC)	6.2		--	6.2	--	6.2		--
Flood Lights	75.		--	37.5	--	37.5		--
SUBTOTAL				43.7		43.7		
030 - Displays & Controls								
Meters & Indicators	29.4		--	29.4	--	29.4		--
AC Indicators (AC)	5.3		--	5.3	--	5.3		--
SUBTOTAL				34.7		34.7		
					SEE NOTES (1) (2)			
040 - EPS								
Solar Array Heater (2)	160. ea		30.*	30.*	30.*	160.	160.	160.
Solar Cell/Batty-Control Power	10.		--	--	--	--	10	10.
Batty Chgr & Volt Reg Cont Pwr	10.		--	--	--	--	10	10.
Descent Batty Control (ECA)	20.		10.	20.	20.	20.	20	--
Ascent Batty Control (ECA)	10.		--	Neg.	--	Neg.	Neg.	--
Gen'l Purpose Inverter	65% Eff.		--	6.4	--	6.4	6.4	--
Lighting Control Assembly	15.6		--	14.	--	14.	14	--
Solar Array Position Cont Assy	10. ea	40.	--	--	20.	--	20	20.
SUBTOTAL			40.	70.4	70.	200.4	240.4	200.

TABLE 6.1-1 - cont'd

EQUIPMENT	Watts Steady	Watts Peak	22 Hrs(3) Launch to LM Activation (Unmanned)	1.5 Hrs LM Activation & C/O (Manned)	24 Hrs Initial Reflector Deployment (Unmanned)	36 Hrs Final Deploy., Align. & Calib. (Manned)	4320 Hrs 6 Month Unmanned Operation (Unmanned)
050 - ECS							
CO_2 Sensor	1.	1.	--	1.	--	1.	--
Cabin Fan (2)	78.	430.	--	39.	--	39.	--
Suit Fan	156.	875.	--	156.	--	156.	--
Glycol Pump	28.9	122.	--	28.9	28.9	28.9	28.9
ECS Relay Box	3.5	28.	--	3.5	3.5	3.5	3.5
Misc. Control Valves	Neg.	176.	--	Neg.	--	Neg.	--
SUBTOTAL				228.4	32.4	228.4	32.4
060 - Instrumentation							
Transducers	12.		--	12.	12.	12.	.5
Sig Cond Electrical Assembly	37.		--	37.	37.	37.	2.
Caution & Warning	22.		--	22.	--	22.	--
PCMTEA	12.9		--	12.9	12.9	12.9	1.
Voice Storage Receiver (AC)	2.3		--	.3	--	.3	--
SUBTOTAL				84.2	61.9	84.2	3.5
070 - GN&C							
LGC (+DSKY) LM Guide Computer	110.		--	110.	110.	110.	110.
IMU (+PTA+PSA+CDU)	300.		60.	300.	300.	300.	300.
ATCA (Attitude Thrust Cont Assy)	56.5		--	56.5	56.5	56.5	56.5
ACA / TTCA Manual Controls	3.		--	3.0	--	3.0	--
LOTS (Star-Tracker)	40.		--	40.	40.	40.	40.
PCA (Iron Astronaut)	14.		--	14.	14.	14.	14.
SUBTOTAL			60.	523.5	520.5	523.5	520.5
080 - Propulsion	TBD		--	--	--	--	--
090 - RCS							
Thruster - Heaters	96.		--	30.	30.	30.	--
SUBTOTALS				30.	30.	30.	

TABLE 6.1-1 cont'd

EQUIPMENT	Watts Steady	Watts Peak	22 Hrs(3) Launch to LM Activation (Unmanned)	1.5 Hrs LM Activation & C/O (Manned)	24 Hrs Initial Reflector Deployment (Unmanned)	36 Hrs Final Deploy.,Align. & Calib. (Manned)		4320 Hrs 6 Month Unmanned Operation (Unmanned)
100- Experiment								
Reflector Canister Heater	15.		15.	--	--	--		--
Reflector RCS Thruster Heater(4)	10. ea	--	--	--	20.	20.		20.
SUBTOTAL			15.	--	20.	20.		20.
				SEE	NOTES	(1)	(2)	
Average Watts Total			115.	1105.9	852.3	1255.9	1295.9	806.1
+ 7½% Dist. Losses			8.6	83.	64.0	94.2	97.2	60.5
Design Av. Power Watts			123.6	1188.9	916.3	1350.1	1393.1	866.6
Energy in Kw-Hrs			2.8	1.78	22.0	4.05	46.0	3744.

NOTES:

(1) Before solar array deployment - Duration 3 hrs - Power from batteries.

(2) After solar array deployment - Duration 33 hrs - Power from batteries plus solar array.

(3) LM supplies power from launch to CSM docking (4 hours). CSM supplies power from docking to LM activation (18.5 hrs)

* Folded and Insulated.

[redacted]

TABLE 6.1-2

DATA ON STATE OF THE ART LARGE SOLAR ARRAYS			
MANUFACTURER	GAEC	TRW	LOCKHEED
Spacecraft Series	OAO	OGO	Agena
Number of panels per spacecraft	4 Main plus 4 Outboard	2	2
Array Type	Deployable	Deployable	Deployable
Movement	Fixed	Single Axis	Fixed
Panel Dimensions, Ft.	4.4 x 5.5 (largest Main Panel)	7.6 x 6.1	20 x 5
Panel Area, sq ft	24.1	43.2	94
Panel Power *	230 W, 29°C	370W, 65°C	750W, 55°C
W/sq ft at above Temp	7.12	8.6	8
Temp Range, °C	-57 to 110	-160 to 80	-130 to 94
Panel Weight, Lb	42 (with solar cells on one side only)	69 (Panel - 57 Drive - 12)	99.5
Lb/sq ft	1.74	1.32	1.06
Basic Blk Dim. in.	65" Length 2" to 4" Width	Not applicable	18" x 4"
No. of Modules per Block	81 in series	Not applicable	4
No. of cells per Module	5,6,7,8,9 or 10	112	Not applicable
Module Dimensions	2 cm high (one cell) and 5,6,7,8,9 or 10 cm in Length	3" x 13"	4.5" x 14"
Cell type	1 x 2 cm, N/P	N/P	N/P
Glass Cover	.006"	.006"	.004"
Module Wiring	Parallel	7 Parallel 16 in series	Not Available
Drive	None	TRW hermetically sealed electric motor with conical nutation output gear	None

*At airmass zero, normal to solar vector.

[redacted]

TABLE 6.1-4

COMPARISON OF ABLE POWER SUPPLY CONFIGURATIONS

	2 Axis Movable Array	1 Axis Movable Array	Fixed Array	SNAP 10 A
Orbital Dependency	Dependent	More dependent	Max dependency	Not dependent
Radiation Sensitivity	Yes	Yes	Yes	No
Radiation Emmitance	No	No	No	Yes
Aiming System	Most complex	Complex	None	None
Deployment	2 Booms (Low Mass)	2 Booms (Low Mass)	2 Booms (Low Mass)	1 Boom (Large Mass)
System Weight, Lb	960-1040	980-1060	1725-1745	1350
Vehicle Orientation Requirements	No	Yes	Yes	No
Solar Array Area	Least	Mid	Most	Not Applicable

TABLE 6.1-3

ARRAY AND BATTERY SIZING CRITERIA

Power Required at LM busses: 867 W (Table 6.1-1)		
Voltage regulator efficiency = 0.95		
Line losses from array to voltage regulator:	7	per cent
Battery charge/discharge cycle efficiency:	0.65	per cent
Solar cell operating temperature (normal to sun)	60°C	
Initial solar cell ouput at 60°C (normal to sun)	8.6	w/sq ft
Solar cell degradation due to space radiation	11	per cent
Solar cell output used 8.6 x .89 (normal to sun)	7.65	w/sq ft

Occultation data for equatorial orbit

Altitude N. Mi	Period Hr	Occultation %	Occultation Hr
5591	6	12.	0.72
10931	12	7.5	0.90
19330	24	5.	1.20

Sample of System sizing for 12 hr orbit (PPC configuration)

° Battery

Energy for one occultation of 0.90 hour with 0.95 voltage regulator efficiency

$$\frac{867 \times 0.90}{0.95} = 820 \text{ wh}$$

Battery discharge at 28 volts

$$\frac{820}{28} = 29.2 \text{ amp. hrs}$$

Assuming a depth of discharge of 55 percent which is very conservative considering the small number of cycles (360) during the six month unmanned phase, the required initial capacity for one battery is

$$\frac{29.2}{0.55} = 53.0 \text{ amp. hrs.}$$

The voltage per cell of NiCd battery varies from 1.35 to 1.22 from full charge to 55 percent discharge; hence 23 cells are required to produce the required voltage range.

[redacted]

TABLE 6.1-3

cont'd

° Battery cont'd

For 23 cells in series the specific weight is 2.4 lb per amp. hour allowing 20 percent for the battery casing.

The weight of one 53 amp. hr. battery is:

$$2.4 \times 53 = 130 \text{ lb}$$

Using two batteries for redundancy therefore requires 260 lb.

° Array

$$\text{Array gross power} = \text{Net Power} \left[1 + \left(\frac{1}{\frac{1}{\%} - 1} \right) \frac{1}{Nb} \times \frac{1}{N_{vr}} \right]$$

% = Percent of occultation

N_{vr} = Voltage regulator efficiency = .95

Nb = Battery charge/discharge cycle efficiency = .65

$$\text{Array Gross Power} = \frac{867}{0.88*} \left[1 + \left(\frac{1}{\frac{1}{.075} - 1} \right) \frac{1}{.65} \times \frac{1}{.95} \right]$$

$$= 985 \times 1.131 = 1115 \text{ watts}$$

$$\text{Array Area} = 1115/7.65 = 146 \text{ sq ft}$$

* 0.88: Loss coefficient allowing for line losses and voltage regulator inefficiency

Battery average recharge power

$$1115 - \frac{867}{0.88} = 113 \text{ W}$$

[redacted]

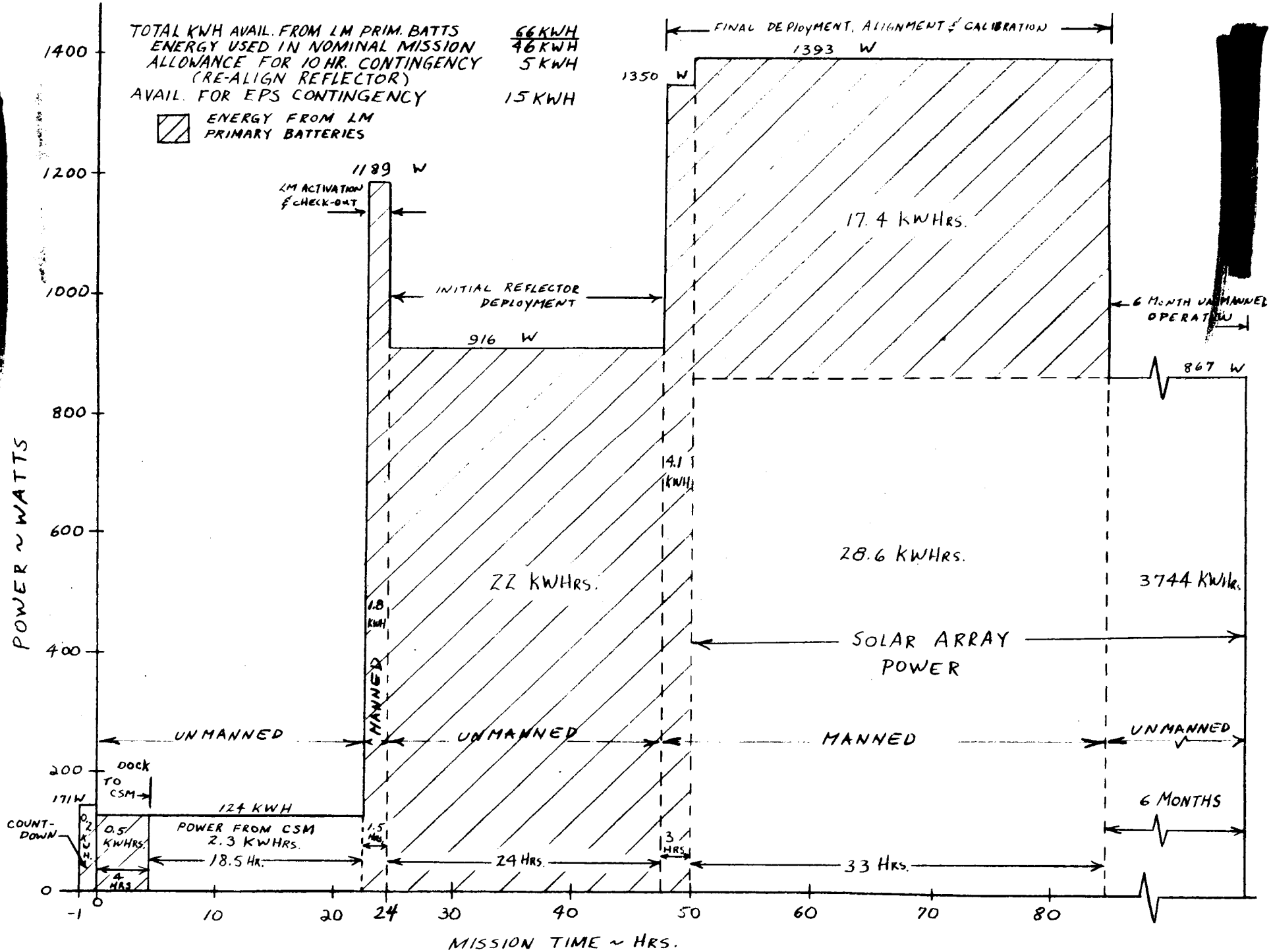

FIGURE 6.1.1 ELECTRICAL POWER PROFILE

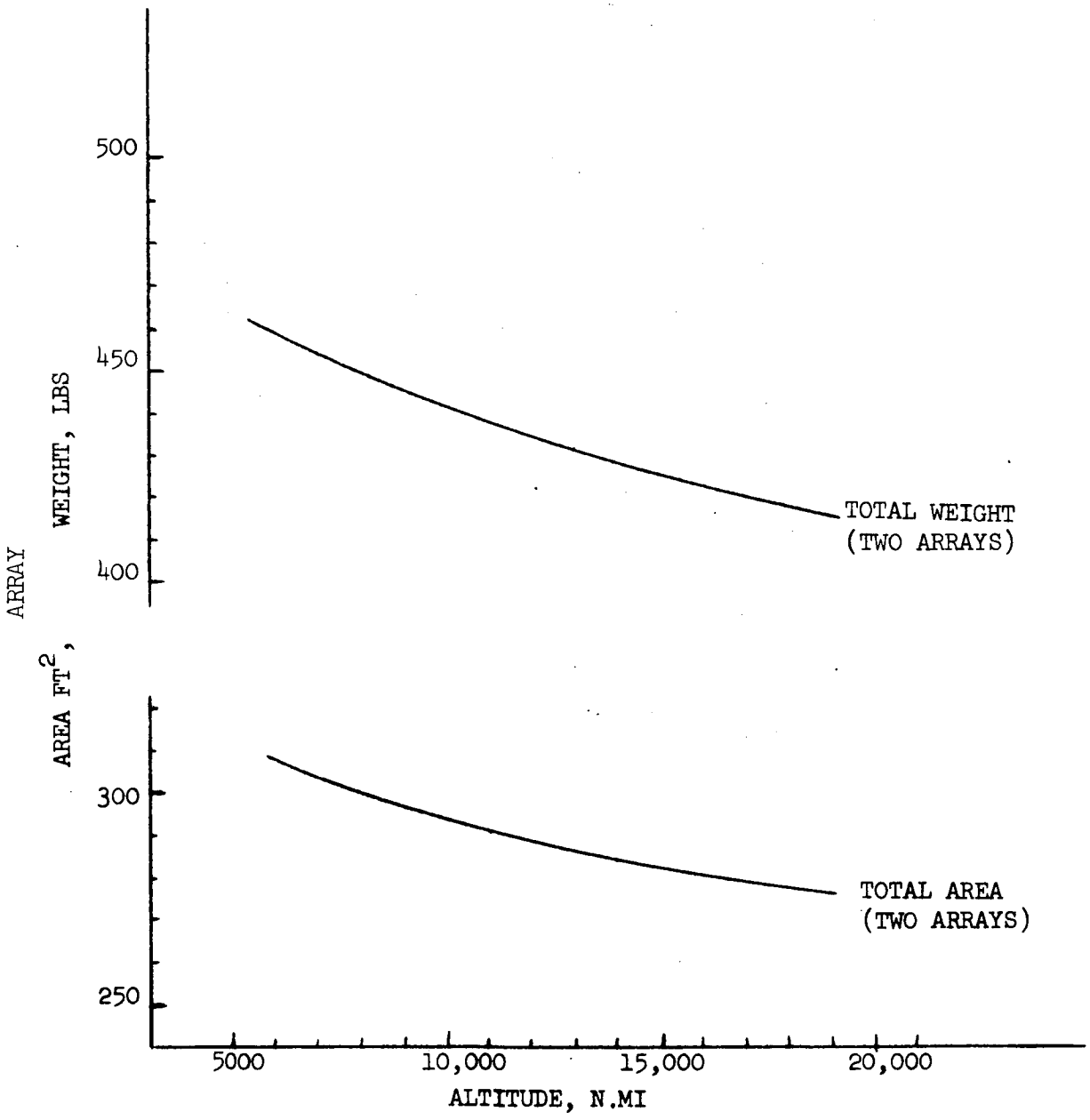

FIG. 6.1-2

VARIATION OF TWO DEGREE OF FREEDOM ARRAY AREA AND WEIGHT WITH ALTITUDE

[redacted]

[redacted]

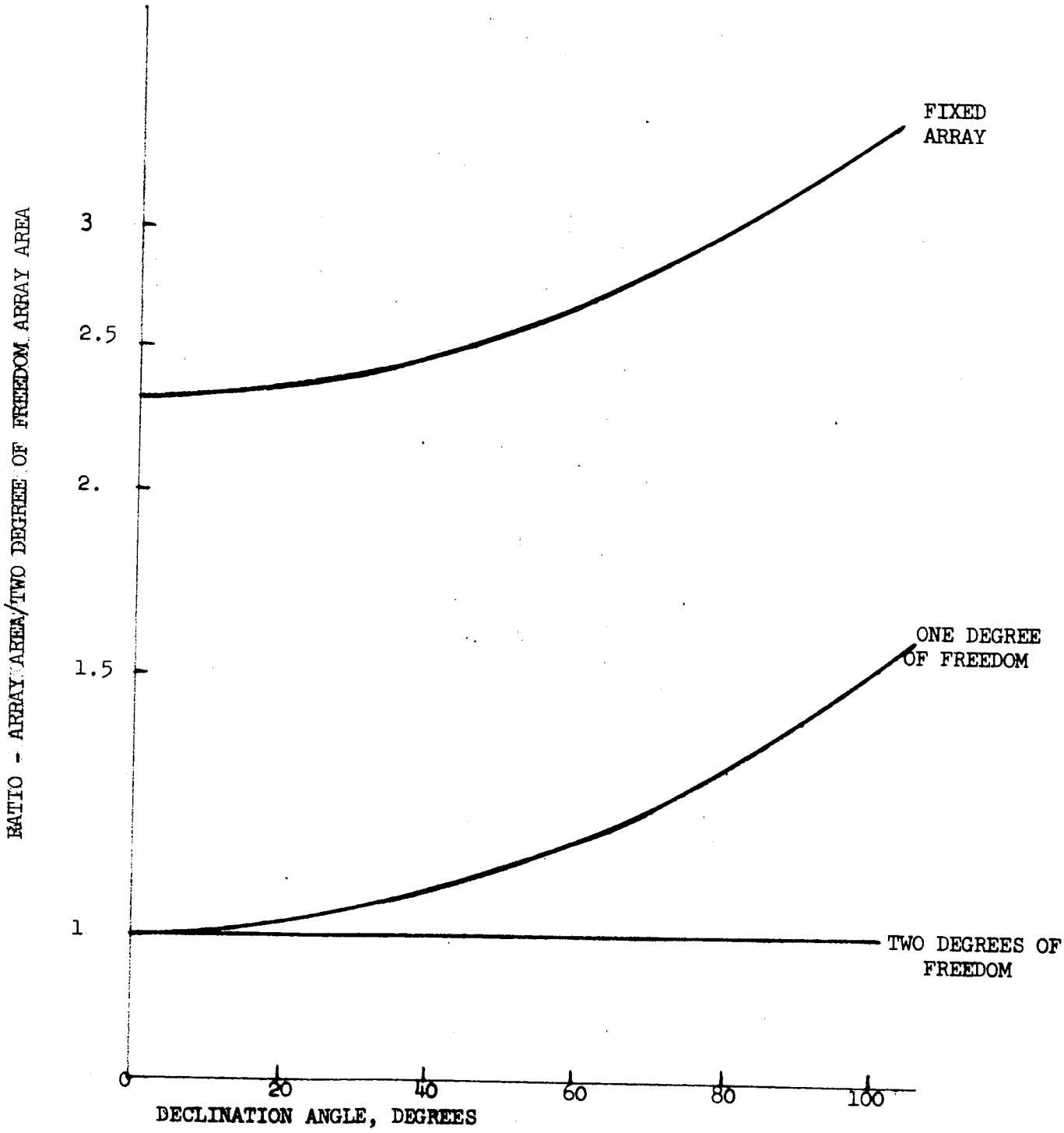

FIG. 6.1-3

RELATIVE EFFECT OF VEHICLE DECLINATION ANGLE ON SOLAR ARRAY AREA

NOTE: BATTERIES ARE SIZED FOR 55 PERCENT DEPTH OF DISCHARGE AND ARE REDUNDANT.

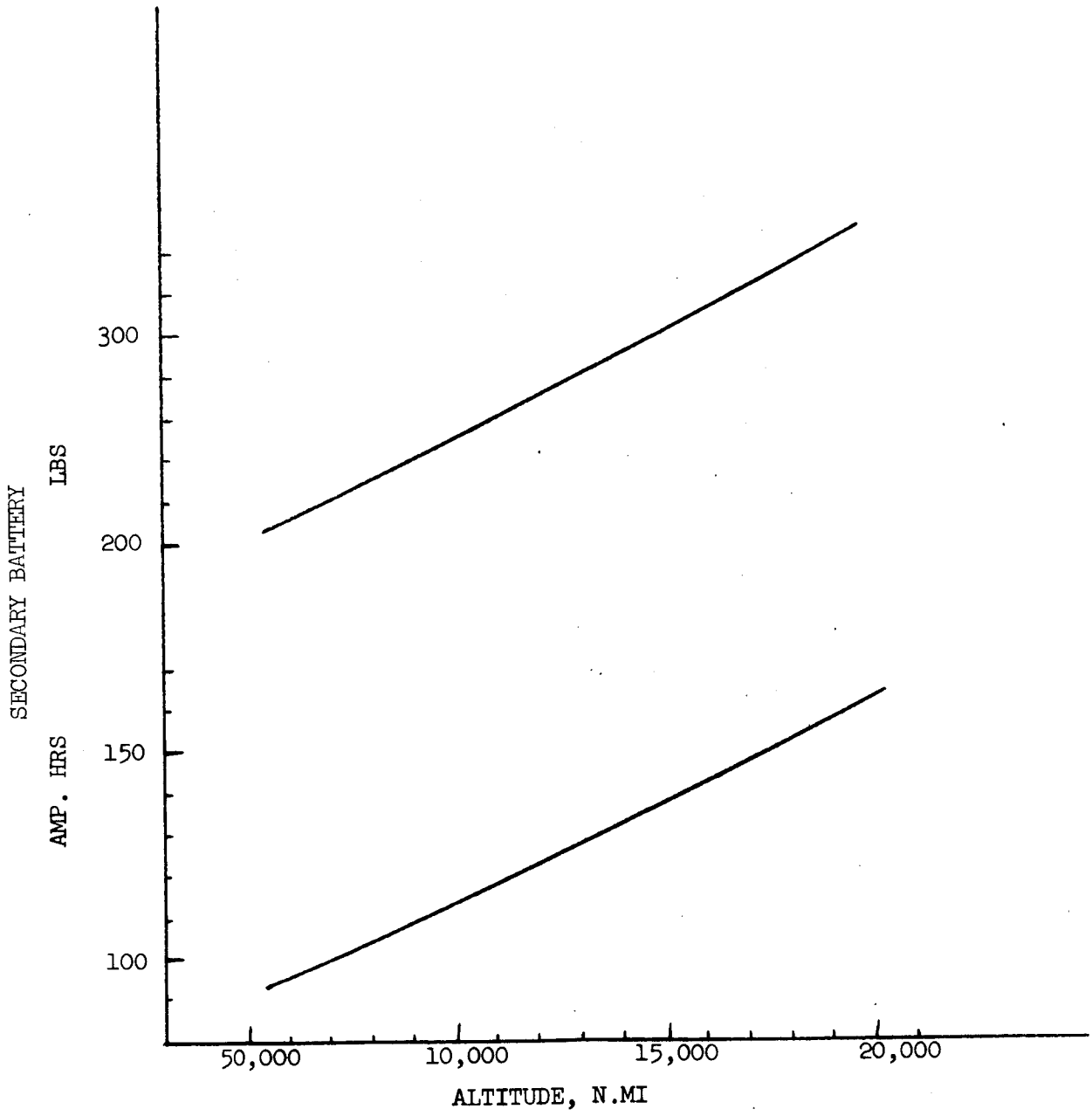

FIG. 6.1-4

VARIATIONS OF SECONDARY BATTERY CAPACITY AND WEIGHT WITH ALTITUDE

[redacted]

[redacted]

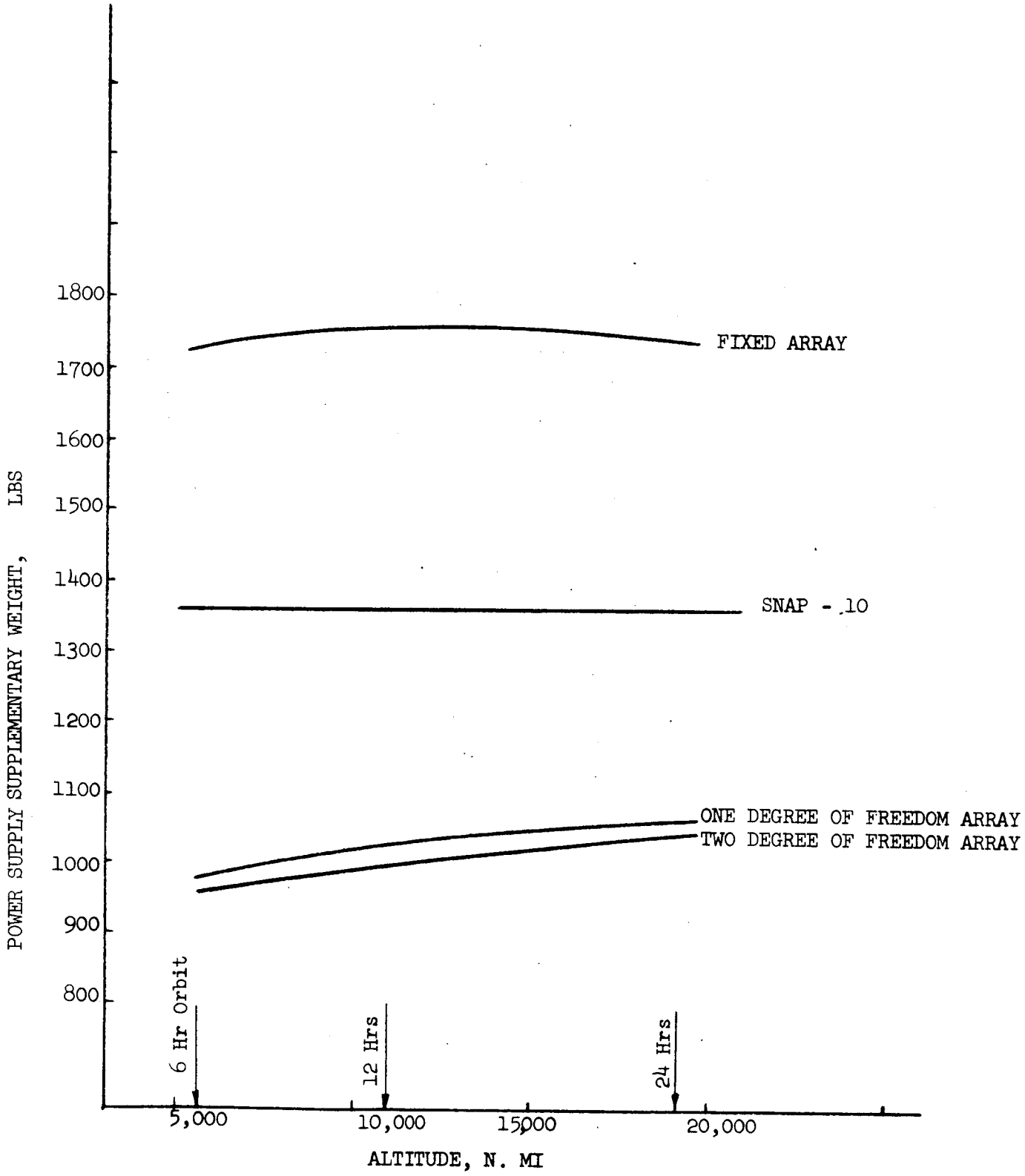

FIG 6.1-5

VARIATIONS OF SUPPLEMENTARY POWER SUPPLY WEIGHT (OVER LM) WITH ALTITUDE

[redacted]

6.2.2.2 Continued

ECS functions:

- Supplies oxygen for metabolic consumption
- Pressurizes the LM cabin and/or spacesuits
- Permits cabin decompression
- Prevents overpressurization of the cabin
- Provides emergency pressurization in the event of a cabin puncture.
- Provides for PLSS recharge

The OSPCS stores, in gaseous form, all oxygen required by the ECS. Oxygen from a descent stage GOX tank is fed to a high pressure oxygen control module which provides first stage regulation and a relief capability for this tank. Descent stage oxygen is then directed to an oxygen control module in the LM cabin as is oxygen stored in the ascent stage.

Oxygen is filtered and delivered to the suit circuit assembly by one of two demand regulators in response to signals from pressure sensors. Each of these valves is equipped with a manual override. A cabin repressurization and emergency oxygen valve delivers oxygen to the LM cabin for repressurization or to delay cabin pressure decay if the cabin pressure shell is punctured, in response to signals from the cabin pressure switch. The valve has a manual override.

Over pressurization of the cabin is prevented by cabin pressure relief and dump valves. These valves automatically relieve excess pressure by venting oxygen overboard. The valves can be manually operated from inside or outside the cabin to dump cabin pressure overboard.

The maximum useable oxygen storage capability of the LM OSPCS is 49.6 lbs, 45.2 lbs of which is stored in one descent stage tank (at 2850 psia) and 4.4 lbs in two identical ascent stage tanks (at 850 psia).

During routine flight, ECS oxygen is consumed at an average rate of 0.37 lbs per hour (two man crew, leakage included), while 6.9 and 0.91 lbs are required to repressurize the LM cabin subsequent to EVAS and refill the PLSS backpack respectively.

6.2.2.2 (continued)

A mission profile with no requirements for EVA would thereby permit 134 hours of manned routine flight. Each EVA would decrease this capability by approximately 21 hours.

A Block II CSM is capable of providing sufficient oxygen to support currently projected manned LM operations in a docked configuration (see paragraph 6.2.3). Separated flight would, of course, require self sufficiency on the part of the LM ECS.

6.2.2.3 Heat Transport Section

The Heat Transport Section developed for the Able mission is shown schematically in Figure 2.2-1 and has the following functional capabilities:

- Provide active thermal control of electronic equipment in the Able/LM
- Provide latent and sensible heating or cooling of the O_2 flow in the suit circuit assembly
- Provide sensible heating or cooling as required to control cabin temperature
- Provide for the rejection of waste heat by water sublimitation and/or the utilization of space radiator panels.

Coolant (62½% ethylene glycol, 37½% water) is circulated by one of three coolant pumps in the coolant recirculation assembly. Since each pump can provide normal flow, only one pump is operated at a time, the remaining 2 pumps serving as backups. After leaving the pump, a portion of the coolant flows through a suit circuit heat exchanger and, during the manned phase, heat from the oxygen is transferred to the coolant. The remainder of the coolant flows through part of a coldplate section, where it absorbs heat from electronic equipment. The flow then divides between a regenerative heat exchanger and its bypass, providing the required heat for the cabin heat exchanger. The flow is divided by a cabin temperature control valve which is controlled by the cabin heat exchanger coolant discharge temperature. The control valve in turn maintains the heat exchanger discharge temperature and the resulting cabin temperature within the range required during manned operation.

6.2.2.3 (continued)

The coolant passes through another coldplate section where it removes heat from additional electronic equipment and then flows to the suit circuit regenerative heat exchanger for suit circuit heating. The amount of heating is manually controlled by the suit temperature control valve. The coolant then flows through the heat rejection portion of the loop and then back to the pump to repeat the cycle.

The heat rejection portion of the network consits of space radiators to reject heat during both manned and unmanned phases and a water sublimator to supplement the radiators during the period of time from LM activation thru final deployment. In addition, 5 modulating valves and a regenerative heat exchanger are provided to control the coolant temperature and the performance of the radiators.

The radiators are located on the descent stage of the vehicle in vertical positions at 2 locations 180° apart as shown in Section 7. The two radiator locations comprise a total radiator area of 60 sq ft and are integrated into the system to form 2 parallel radiator circuits.

The control characteristics of the heat rejection portions of the coolant loop are best discussed by continuing the description of the coolant path.

The coolant first flows through the hot side of a regenerative heat exchanger. From this point it bypasses and/or is diverted to the radiator circuits by the radiator bypass valve. This valve senses the coolant temperature of the combined flow downstream of both radiator circuits and attempts to control this temperature by bypassing coolant around the radiators. This requirement exists because downstream of the radiator the coolant enters the water sublimator which, while operating, requires a minimum inlet coolant temperature to prevent it from freezing.

Before entering the radiator circuits the coolant passes through an intermodular control valve which controls the relative flow to each circuit. This valve compensates for two conditions: (1) the effects of manufacturing tolerances and different passage lengths on the pressure drop and resulting flow and outlet temperature of each radiator circuit and (2) since the radiators are on opposite sides of the vehicle, the effects caused by each citcuit being simultaneously subjected to different external environments. The desired flow split is accomplished by the valve control sensing the outlet temperature of each circuit and commanding the valve to divert greater portions of the coolant flow to the

6.2.2.3 (Continued)

radiator having the lower outlet temperature. The valve and controller recommended for this use are existing space qualified components currently being used on the Apollo CSM, consequently no development schedule or cost penalties are anticipated.

Downstream of the intermodular control valve, the fluid flows directly into the two radiator panels. Each radiator consists of a series of evenly spaced tube passages arranged on the surface of the panel in a parallel configuration. Also on the panel is a single passage in parallel with the main parallel circuit except that this passage has a separate outlet from the panel. Downstream of the panel, the outlet from the main circuit and that of the single passage are joined by a radiator temperature control valve which senses the mixed fluid temperature downstream of itself. At temperatures above 30°F the flow is evenly distributed through all the tubes in the panel allowing the maximum heat rejection capability of the panel to be utilized. As the sensed temperature drops below 30°F the valve will direct more fluid to the single passage. At temperatures of 0°F or below, the valve diverts full flow through the single passage retaining approximately 30% of the radiator's maximum capacity. After leaving the radiator control valves, the two radiator circuits combine and pass through the radiator bypass valve which is discussed above. The fluid then enters the water sublimator which rejects 1200 BTU/hr, during minimum load and cold environment conditions and rejects 3300 BTU/hr during maximum load conditions (See Section 5.1). As a result of these loads, the sublimator will consume approximately 1300 lb of water. While operating, its coolant outlet temperature under all load conditions will be 29°F. This temperature is below the minimum allowable inlet temperature for certain equipment; consequently a regenerative heat exchanger and a coolant temperature control valve are provided to elevate the sublimator outlet temperature to an acceptable level.

As discussed above, the intermodular control valve is an existing Apollo CSM component. The remaining 4 valves; namely, the radiator bypass valve, the 2 radiator control valves and the coolant temperature control valve, are all an existing LM componenet (cabin temperature control valve), requiring only that its sensor setting be adjusted for each application. Being a mechanical device, this can be accomplished by either a minor shim adjustment or a modification to the sensor itself. The regenerative heat exchanger mentioned above is also a LM component and will be used without modification.

6.2.2.3 (continued)

Since the controls provide compensation for malflow distribution, the radiators can be of a simple design having nominal dimensional tolerances and fabricated using state of the art techniques.

6.2.2.4 Water Management Section

The LM Water Management Section (WMS), retained without modification for the Able LM, has the following functional capabilities:

- Separates metabolic water from the suit circuit and delivers it to the water sublimator
- Stores water required for sublimator cooling and/or metabolic consumption and PLSS refills
- Refills the PLSS water tanks
- Regulates water pressure and delivers it to the water sublimator

A block diagram of the WMS is shown as part of the ECS in Fig. 2.2-1. Water is supplied to the water control module from the ARS water separators and/or the water storage tanks. The tanks are of the bladder type and are initially pressurized from launch with nitrogen to approximately 50 psia. Water from the tanks is regulated for compatability with the water separator pressure by regulators within the water control module. Water is then distributed to both the water sublimator and PLSS recharge station. A manual shutoff valve is provided upstream of the water sublimator. This valve alone controls the operating status of the sublimator.

The maximum usable water storage capability of an unmodified LM WMS is 406.4 lbs, 328 lbs of which is stored in one descent stage tank and 78.4 lbs in two identical ascent stage tanks. Table 6.2-1 presents the water requirements for the Able/LM mission time line described in Section 3.5.

6.2.2.3 (continued)

Table 6.2-1
Able Water Requirements

Water Sublimation	(2.3 lb/hr avg.)	130 lb
Metabolic Consumption	(8 lb/man-day)	17 lb
PLSS Refills	(6.8 lb/3 hr EVA, 6 EVAs)	41 lb
	TOTAL	188 lb

As shown, water storage capacity of the LM provides considerable growth in manned operating times and/or EVA activity.

6.2.3 Alternate Configuration - LM/CSM ECS Interfaces

In the event that the Able mission requires an extension of the capability of the LM to support manned operations, LM/CSM ECS interfaces may be implemented to fully exploit the combined spacecraft ECS capability.

In a docked configuration, with open hatches and the forced exchange of LM and CSM cabin atmospheres, most the functions of the LM suit circuit assembly and of LM oxygen storage and delivery equipment can be performed by the CSM ECS alone, regardless of crew location. However, the oxygen supply and atmosphere revitalization equipment is required to support EVA and/or separated LM flight and should be retained unless these modes of operation are definitely not required for performance of the Able mission.

The implementation of LM/CSM ECS interfaces have been thoroughly explored and defined in previous AAP definition study efforts.

6.2.4 Radiator Meteoroid Protection

A study was conducted to evaluate the effects of the meteoroid environment on the Able/LM radiators and to determine techniques to protect the radiators against such environments. It should be pointed out, however, that large degrees of uncertainty still exist in the characteristics of the meteoroids and the resulting damage phenomena. Protection techniques considered included redundant tubes and/or panels,

6.2.4 (continued)

selfsealing tubes, preferred orientation, and meteoroid bumper configurations. Based on the Able/LM mission requirements and constraints, it was concluded that the meteoroid bumper approach is the preferrable configuration from an overall consideration of design development and simplicity, fabrication, weight, and reliability. A bumper configuration, which for the Able/LM radiator panels would yield a probability of no puncture of 0.9999 results in a weight increase of less than 20 lb for the Able LM radiator system.

[redacted]

6.3 GUIDANCE, NAVIGATION AND CONTROL

6.3.1 Groundrules and Assumptions

- An On-Board Inertial Sensor Reference System will be employed as the primary means for maintaining pointing (attitude hold).
- The requirement for remote control of the ABLE LM/Reflector during the unmanned portion of the mission (up to 6 months) necessitates the inclusion of an uplink capability and corresponding modifications to the GN&C Subsystem.
- Abort guidance (for back-up modes) is not a requirement, nor is a rendezvous radar.
- The Apollo LM Reaction Control Subsystem (RCS) will be employed for attitude control prior to reflector deployment and for orbit maintenance (stationkeeping). A monopropellant low thrust engine system will be used for attitude control after the reflector is deployed.
- The LM Optical Tracker System (LOTS) and the Program Coupler Assembly (PCA) are LM developed hardware.

6.3.2 GN&C Subsystem Configuration #1 (Modified LM PGNCS)

A typical GN&C subsystem configuration investigated during the study is shown in Fig. 6.3-1. This system is essentially an Apollo LM Primary Guidance, Navigation and Control System (PGNCS) which is modified to enable it to perform the ABLE mission. The hardware modifications required are:

- Incorporate the LM Optical Tracker System LOTS (to provide the automatic inertial reference alignment capability).
- Incorporate a modified Program Coupler Assembly (PCA) (to provide a capability to remotely control, via ground stations MSFN) the LM/Reflector equipment and performance.
- Provide an interface and command signals to a low level peripheral thruster system.

[redacted]

- Provide an interface and command signals to an EPS Solar Array and to the S-band antenna (as required).

The DSKY, ACA, and TTCA have also been included as part of the ABLE GN&C Subsystem, since this equipment will be required and employed during the manned deployment and manned initial operation phases of the Project ABLE mission. In addition to the hardware modifications, the LGC Programs will have to be modified to satisfy the ABLE Guadance and Control requirements. The implications of these modifications are discussed below.

6.3.2.1 Incorporation of LOTS

Because of the requirement for automatic alignment of the stable platform, the applicability of the LM Optical Tracker System to the Project ABLE mission was investigated. References 6.3-1 and 6.3-2 were employed in determining performance and operational characteristics of the LOTS:

Reference 6.3-1 defines the following Optical Tracker characteristics:

a) Sensitivity - can track to 3rd magnitude star in presence of 5th magnitude star

b) Can track to within: 30 degrees of sun
5 degrees of sun - illuminated Earth
6 degrees of tracker Zenith (Gimbal lock position)

c) Angular Freedom - Azimuth ±360° (0° parallel - Y Axis) Elevation 20° below +Z axis to 20° above -Z axis

e) Acquisition Characteristics - Tracker locks on to designated target within 30 seconds after tracker axis is positioned to within 1° of target position.

f) Instantaneous Field of View - ±7 mrad.

The LOTS, which is mounted on the LM Navigation Base, is gimballed to allow two axis movement - Azimuth and Elevation.

According to Reference 6.3-2, the LOTS performs the primary function of providing IMU alignment data, as follows: "The LOTS in association with the LGC and CDU,

[redacted]

automatically acquires and tracks a star. The star position data is then entered into the LGC via the CDU for use in IMU alignment. The LGC then computes the proper IMU gimbal orientation and proceeds to accomplish alignment by initially generating the coarse alignment commands and then fine aligning by torquing the IMU gyros."

Since the Apollo LM vehicle (LM-4) configuration does not include a LOTS as part of the GN&C Subsystem, the addition of a LOTS and its corresponding interfaces are considered as a modification to the reference PGNCS. The definition of the modifications required (wiring diagrams, schematics, interface c control documents, etc.) in order to incorporate a LOTS into the GN&C Subsystem has already been performed in a preliminary manner within the Apollo LM Program, when consideration was being given to utilizing a LOTS in place of the Rendezvous Radar. When NASA/MSC made the decision to retain the Rendezvous Radar on LM, it was simultaneously indicated that NASA intended to complete development of the LOTS for future use in the LM Program. As a result of the above discussed engineering effort (Design and Development), the LOTS has been included in the Project ABLE GN&C Subsystem Program Planning Configuration to provide automatic IMU alignment data.

6.3.2.2 Incorporate a Modified LM Program Coupler Assembly

As outlined in the overall groundrules and assumptions, a requirement exists for remote control of the LM/Reflector during the unmanned portion of the Project ABLE Mission. This requirement will necessitate the inclusion of a communications uplink capability and corresponding additions and modifications to the Project ABLE GN&C Subsystem.

[redacted]

Among the mission functions that must be performed remotely (during Operation Phase) are the following:

- Systems/Subsystems Status Monitoring
- Redesignation of LM/Reflector attitude
- MSFN navigational update information to LGC
- LM/Reflector equipment functions (e.g. Antenna switching)

Note: The final definition of the required switching functions to be performed during the unmanned phase will be a follow-on study task.

It is proposed to employ portions of the LM Mission Programmer, namely the Program Coupler Assembly (PCA) to provide the functional relay switching for the execution of ground commands and/or primary sequence commands originating from the LGC. The PCA will interface with the LGC, Communications Uplink System, and all other LM/Reflector equipment requiring remote activation and/or deactivation capability.

The PCA contains two relay matrices:

(1) A 16 x 16 matrix, containing 127 discrete on-off commands driven from the LGC through relay drivers, and

(2) A 16 x 16 matrix containing 48 discrete on-off commands driven by relay drivers contained in the Digital Command Decoder Assembly.

6.3.2.3 Interface With Peripheral Thruster System

As presently proposed, a monopropellant low-thrust engine system mounted on the periphery of the reflector will be employed for attitude control of the LM/Reflector vehicle. The existing Apollo LM Reaction Control System (RCS) will be used prior to Reflector deployment and for Orbit Maintenance (Stationkeeping) after Reflector deployment. The firing commands (maneuver signals) to the monopropellant low-thrust engine system will originate in the LM Guidance Computer. An initial approach could be to mount these engines in a manner geometrically similar to the LM RCS cluster configuration. In order to define the final configuration and the resulting LGC engine select logic, further studies concerning structural limitations, and cluster locations will be required.

It has been initially proposed in the Project ABLE feasibility studies to employ the primary pre-amplifiers and jet drivers in the Attitude and Translation Control Assembly (ATCA) for control of both the RCS and Monopropellant low-thrust engines. The PCA could provide the switching functions to enable transfer from one system to another. The feasibility and applicability of this entire approach will have to be evaluated during the preliminary vehicle definition studies. Alternate methods and approaches will also be studied. The obvious advantage of employing the same Jet Drivers to control the Monopropellant engines, as well as the RCS jets, is the possible reduction in hardware modifications to the Apollo LM System.

A possible major problem area may result in terms of transmitting the monopropellant engine firing commands from the LM vehicle to the engines on the periphery of the reflector. The separation distance between the LM vehicle and the monopropellant engine clusters will be between 500 and 1500 feet depending on the radius of the selected reflector.

In addition, the question of signal characteristics and conditioning to fire the monopropellant engines will have to be considered.

6.3.2.4 Interface With EPS Solar Array and S-Band Antenna

A requirement may exist on Project ABLE for the GN&C Subsystem to supply sun reference line information to the Electrical Power Subsystem (EPS) two-degree of freedom solar panel arrays. Information generated for pointing commands can be used to define the relation between the LM/reflector vehicle and the sun line of sight vector.

Assuming that the solar array has at least one axis in common with the LM/Reflector vehicle coordinate frame, then the state vector information will be the digital representation of the two remaining coordinates. This digital data transfer will require a hardline interface between the LM Guidance Computer (LGC) and the two degree of freedom solar panel assembly. To minimize the number of lines a serial, rather than parallel, transfer of data is suggested. The two-degree of freedom solar panel assembly will include the required interface circuitry for accepting the LGC digital outputs.

An additional requirement exists on Project ABLE for the GN&C Subsystem to perform the necessary computations and then based on these computations to provide the required switching signals so as to insure continuous S-Band Antenna coverage. The LGC will perform the computations and then generate via the PCA the required switching signals to the S-Band Antenna Assembly.

6.3.2.5 Ability to Change LGC Software

The present LM procedure requires a minimum of 3 months to be allowed for the vendor to wire the LGC fixed memory in accordance with mission requirements. To provide for a checkout of the completed memory at GAEC prior to shipment to KSC, the release date for the final wiring configuration should be approximately eight months before the launch date.

In addition, the final draft of the mission program should be available approximately fourteen months before the launch date. This will allow six months for program checkout and modification at GAEC test facilities.

Based on the present LM Program complement for an unmanned earth orbital mission, the Basic Program requirements are approximately 13,500 words of fixed memory. With an estimated 8,000 words required for mission programming, there is still approximately 15,000 words of fixed memory available for ABLE functions.

6.3.2.6 Limitations of Modified LM PGNCS

In the above discussion of the modified LM PGNCS incorporating a LOTS, it has been assumed that during the manned initial operation phase of the Project ABLE Mission IMU inertial alignment has been achieved with the aid of the LOTS. During the unmanned phase, the IMU inertial alignment will be automatically updated by employing the LOTS. However, in the event of loss of IMU inertial alignment (e.g., due to power interrupt) for long periods of time, the above discussed system could not automatically re-establish an inertial reference. This is an obvious limitation of the modified LM PGNCS. It should be noted, however, that further studies may provide a method for re-establishing an inertial reference.

An additional problem with this modified LM PGNCS configuration results from the elimination of the Rate Gyro Assembly (RGA). A minor and secondary function of the RGA is to provide weight information to the Controls and Displays Subsystem for a

[redacted]

rate display. As a result, with the elimination of the RGA from the Project ABLE GN&C Subsystem, the required rate information to the Controls and Displays Subsystem will now have to originate from the LGC. This will require new LGC interface requirements and Controls and Displays Signal conditioning. (Digital to Analog Conversion).

6.3.3 GN&C Subsystem Configuration #2

The first alternate GN&C Subsystem configuration investigated is shown in Fig 6.3-2. The only difference between this configuration and the modified LM PGNCS is replacement of the IMU/PTA with an additional LOTS and Sun Sensor System.

The Sun Sensor System is included in order to provide the capability for fine aligning the LM/reflector roll axis to the sun vector reference line. This initial sun line acquisition is the first phase in the establishment and/or re-establishment of an inertially referenced attitude (during unmanned phase of Project ABLE Mission). Once sun line acquisition has occurred, the LGC, in association with the two LOTS, will initiate a star search acquisition, and verification mode in order to establish an inertial reference alignment. Further detailed studies regarding star tracker (LOTS) operational capability, system and mode definition, star map and field analyses, and LGC software modifications will be required before final feasibility and design can be established.

The additional LOTS will be interfaced with the LGC, CDU, and PSA in exactly the same manner as described in the discussion of GN&C Subsystem Configuration #1. Remote control capability and firing commands to the monopropellant low thrust engine system are also the same as described for configuration #1 (PPC).

The implementation of a sun sensor system to this configuration will require additional interfaces. The OAO Sun Sensor System was employed as a model type system in this preliminary feasibility study for Project Able. The present OAO Sun Sensor System employing coarse and fine Solar Sensors is capable of aligning the vehicle optical axis to within ±0.25° of the sun line. It is therefore assumed that the LM/Reflector vehicle can be aligned to within approximately the same accuracy for sun acquisition.

[redacted]

[redacted]

OAO Sun Sensor output signals are proportional D.C. signals. The present LM CDU channels require an 800 cps signal for analog to digital conversion for the LGC. Therefore, additional D.C. to 800 cps conversion equipment is required. These D.C. signals are spacecraft yaw and pitch attitude error signals relative to the sun line. Therefore, two CDU A/D converters would be required for interfacing the pitch and yaw error signals to the LGC.

For this configuration a total of six CDU A/D converters may be required if all sensor channels (2 LOTS + Sun Sensor) are being utilized simultaneously. Since the present Apollo LM CDU configuration consists of only 5 CDU A/D converters, a modification to the present system may be required.

Sun Sensor mountings and location will be determined after the vehicle structural configuration selection has been made.

6.3.4 GN&C Subsystem Configuration #3

A target (Earth tracking) sensor type system employing R.F. Tracking Sensors may be considered as a possible feasible alternate scheme. In this approach, the R.F. Sensors will provide two axis tracking angles - aximuth and elevation to the LGC in order to provide data for the computation of the Earth target vector. The tracking angle signals will be obtained by tracking ground (Earth) based beacons. A digital signal interface must be provided (possibly via coupling data unit) between the R.F. Tracker Sensor Signals and the LGC. In addition to the inclusion of a coarse and fine sun sensor package for initial sun acquisition, a gimballed Sun Sensor or star tracker (LOTS) may be required as part of the GN&C configuration in order to establish an additional inertial (stellar) vector.

6.3.5 References

Reference 6.3-1 - LM Optical Tracker System
Student Study Guide
Subsystem Course 100
Hughes Aircraft Company, Culver City, California

Reference 6.3-2 - Study Guide - LM PGNCS Course, PGNCS Hardware
AC Electronics Division, General Motors Corporation

[redacted]

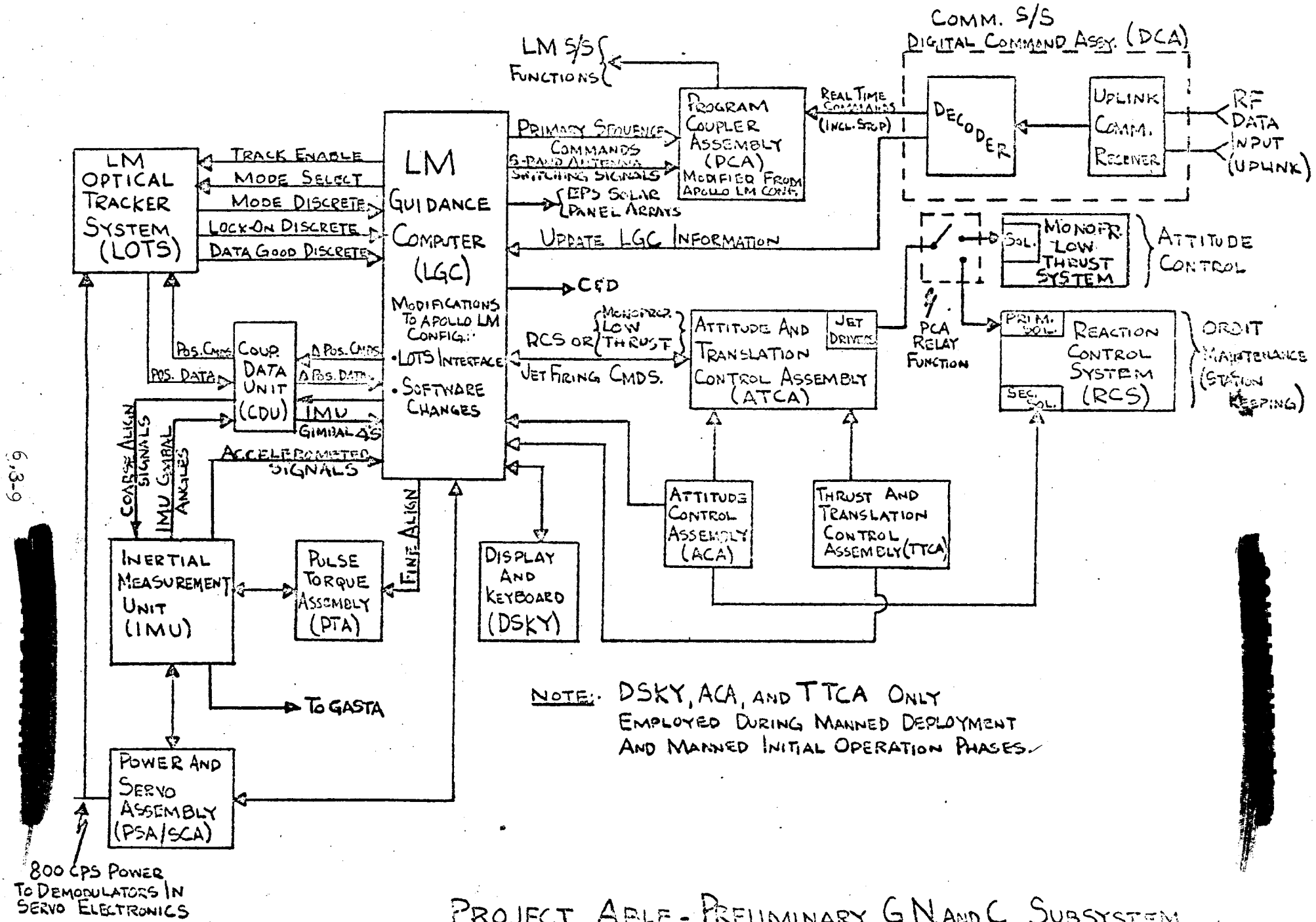

PROJECT ABLE - PRELIMINARY G,N, AND C SUBSYSTEM CONFIGURATION (MODIFIED LM PGNCS) #1

FIGURE 6.3-1

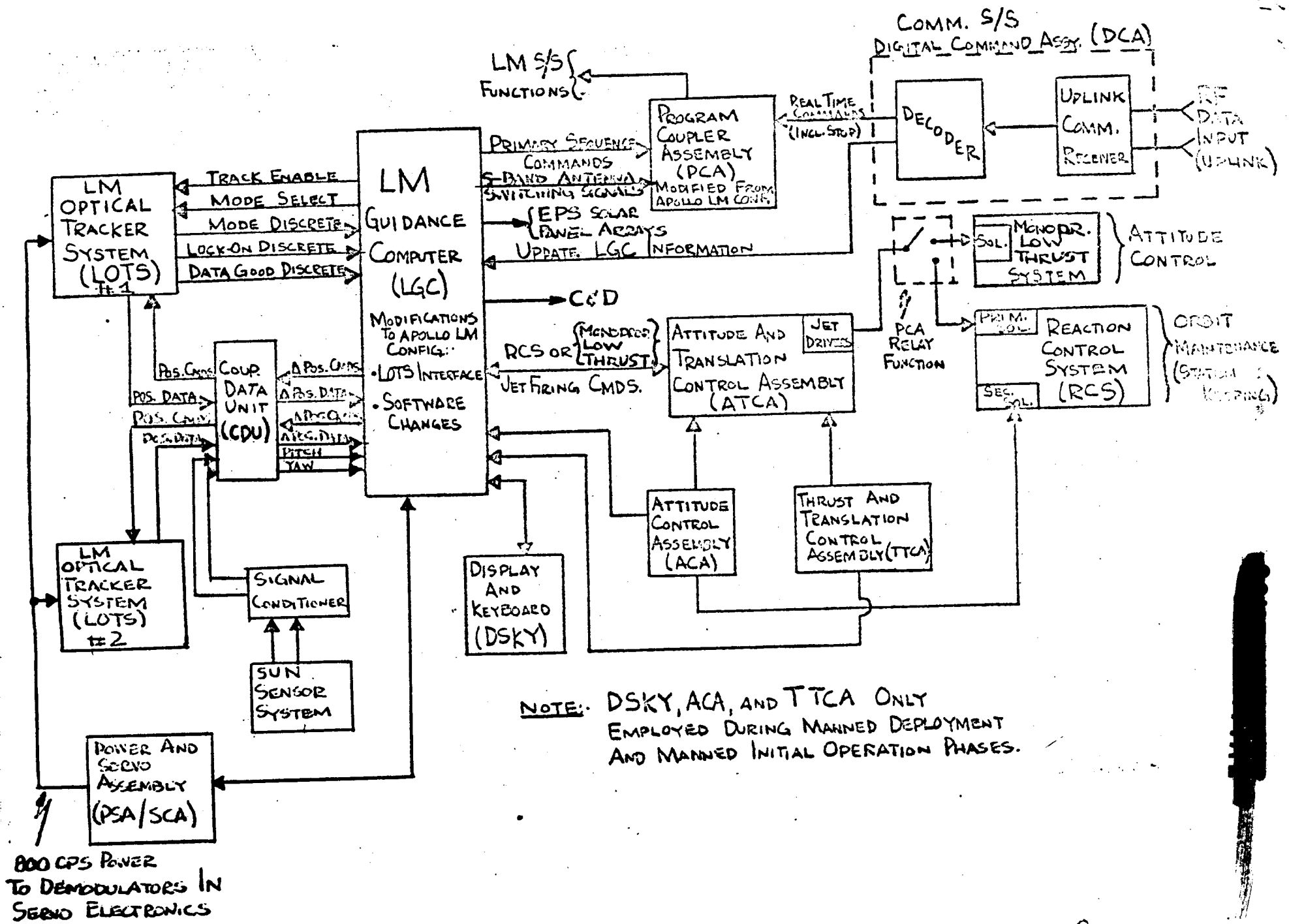

PROJECT ABLE - G, N, AND C SUBSYSTEM CONFIGURATION #2
FIGURE 6.3-2

6.3-10

6.4 REACTION CONTROL

6.4.1 ABLE LM RCS

During deployment and checkout of the reflector, attitude and translational control will be required by the ABLE LM RCS. The basic sixteen thruster LM RCS will be retained except that ascent propellant interconnect valves and filters will not be included, as ascent propulsion is not required for the ABLE LM mission. After completion of the deployment and checkout phase, the RCS would remain activated to support any stationkeeping requirements during the 6 month operational phase.

Further definition of mission requirements could show the need for additional propellant in the RCS. Earlier design studies have indicated the LM thrusters could burn about twice the present LM propellant without exceeding qualification life. Additional propellant and pressurant modules could be added in the temperature controlled volume vacated by the ascent propellant tanks or possibly in the aft equipment bay. A previous design study (Ref. 6.4-1) showed that as many as four sets of LM tanks can be accommodated in this space.

6.4.2 Peripheral Thruster Module

Attitude control of the reflector would be achieved by means of small reaction control jets located at the periphery of the reflector. Consideration was given to using the LM RCS for attitude control of the reflector, but propellant requirements would be on the order of 100 times greater than for thrusters on the periphery and the number of pulses required would far exceed the estimated LM endurance life of 10,000 cycles.

For the peripheral thruster system, with total impulse requirements between 100,000 lb-sec and 500,000 lb-sec, the choice of system is between monopropellant and bipropellant (ref. section 5.3). Since the system weight difference is not large, the simplicity, materials compatibility and reliability of the hydrazine monopropellant system indicate it to be the most likely final selection. On the other hand, if additional mission analysis were to indicate that small reflectors were desirable, with total impulse requirements below 100,000 lb-sec, subliming rockets may be considered.

A preliminary design of a typical monopropellant hydrazine module is shown in Fig. 6.4-1. This module can supply approximately 27,500 lb-sec impulse and utilizes

6.4.2 (continued)

the LM RCS oxidizer tank, with teflon bladder, for storing N_2H_4. LM RCS pressurization components are also shown although some change may be required in the regulator and relief valve pressure settings. A great deal of development work has been done on pulsed thrusters using Shell 405 catalyst from .02 to 5 lb thrust which is the thrust range of interest. One vendor reports tests on a 0.05 lb thrust engine of 100,000 cycles and 50,000 sec burn time with very little degradation (Ref. 6.4-2). It is believed that the required life and duty cycle for the Project ABLE application can be achieved with normal development.

Further study will be required to define the reliability requirements for the peripheral thruster system, but redundant thrusters could be added with a small weight penalty. The total weight of the monopropellant module is approximately 175 lbs, including 138 lbs. of N_2H_4. Four modules are required for the four spoke reflector design.

Each module would be individually insulated and supplied with electrical heaters to maintain the propellant at 40°F to 100°F.

6.4.3 References

6.4-1 "Phase II Laboratory Design Analysis Summary" (U) Vol. IV, AES-LEM Phase B Final Report, dated 8 December 1965 (Confidential)

6.4-2 "Microthrust Monopropellant Rocket Motor Cyclic and Low Temperature Test Data Engineering Study," Rocket Research Corp., Report No. 65-R-46, dated 8 October 1965

[redacted]

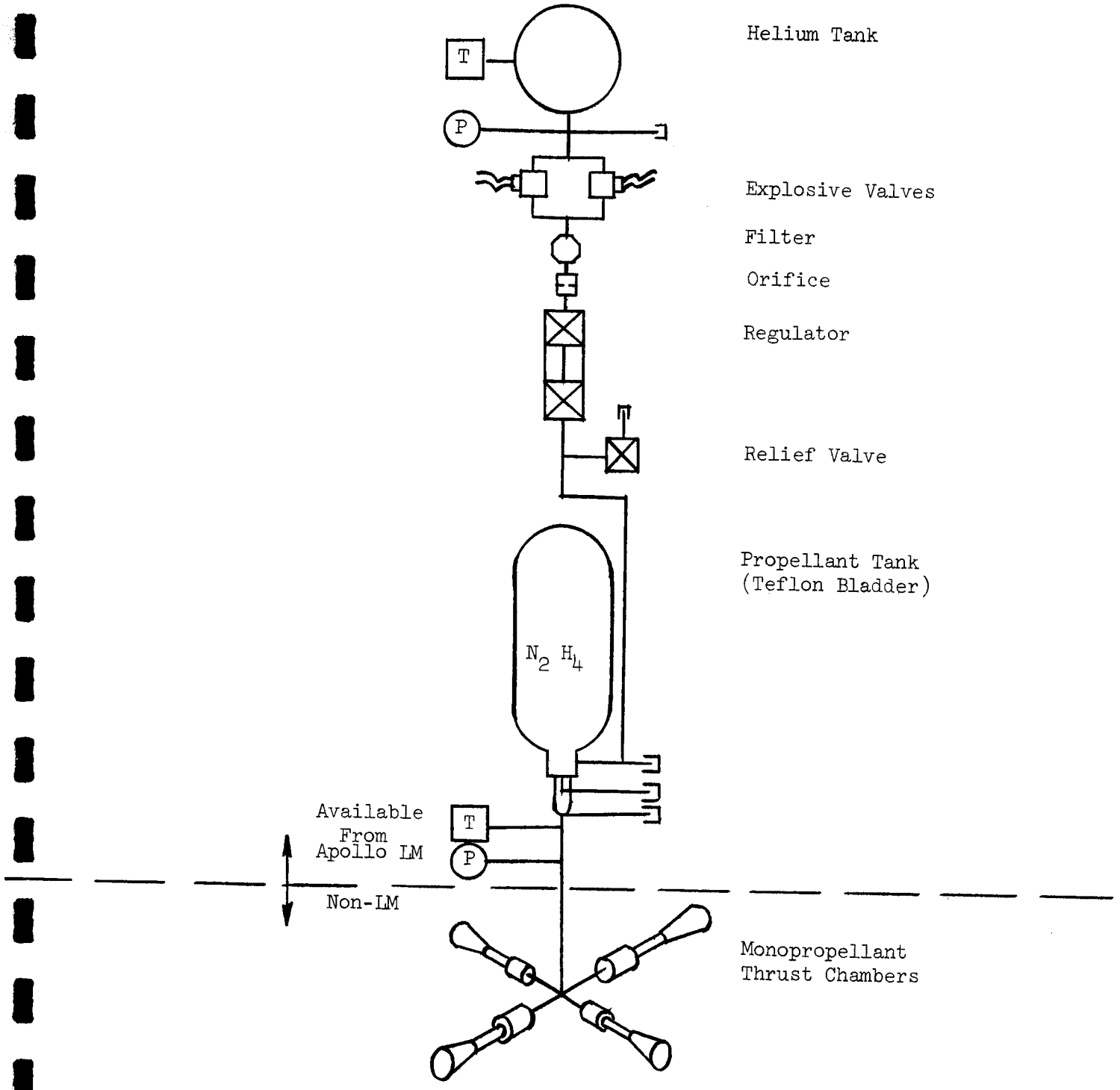

Fig. 6.4-1

Reflector Reaction Control Module

[redacted]

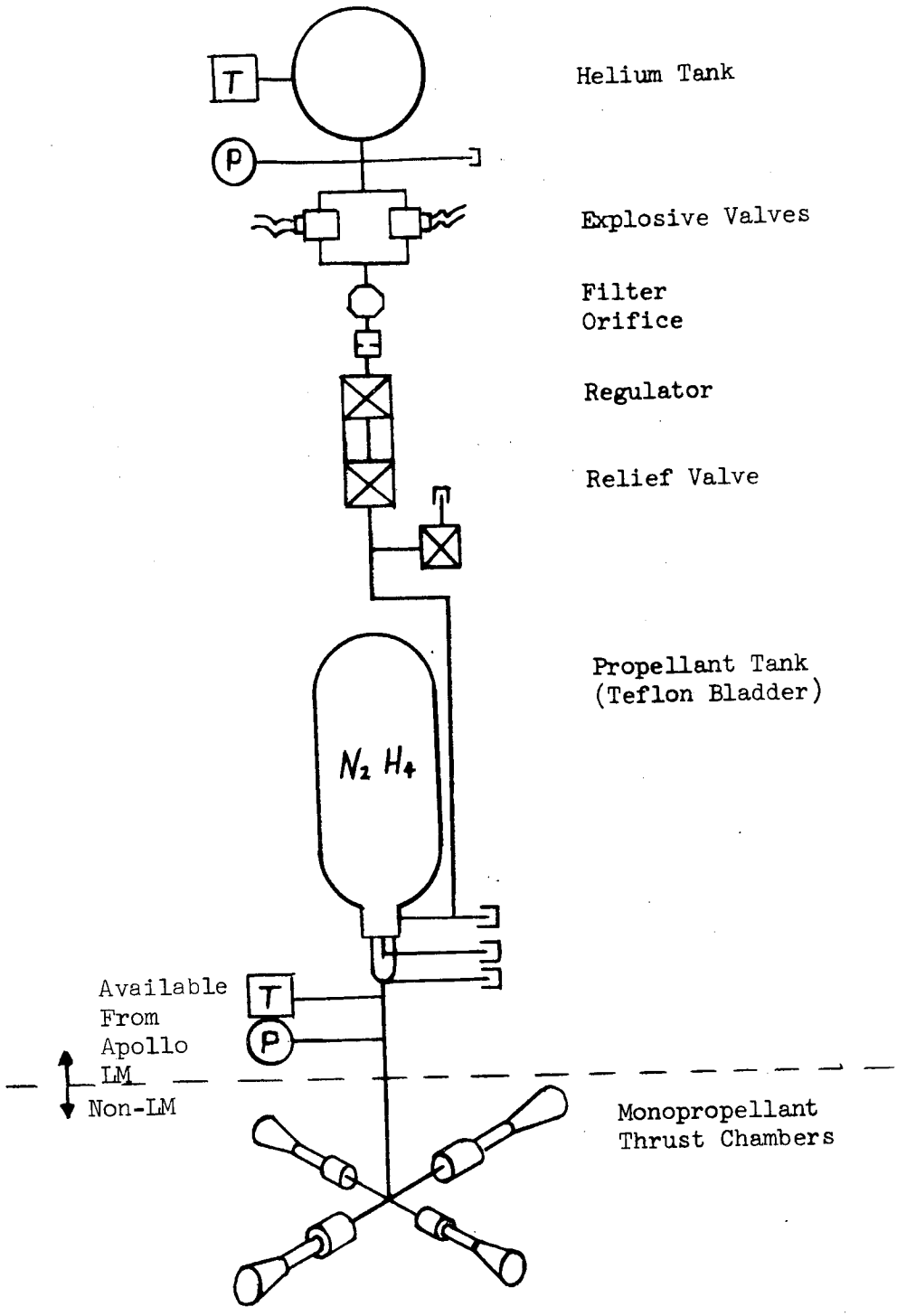

REFLECTOR REACTION CONTROL MODULE

FIG. 6.4-1

6.5 COMMUNICATIONS

6.5.1 Functional Requirements

The general functional requirements of the ABLE LM Communications subsystem are:

- Provide intercommunications between the Able LM and the CSM, Earth, and EVA
- Provide intercommunications for two ABLE LM crewmen
- Provide for processing and transmission of ABLE LM operational status, voice and biomed data to earth
- Provide an aid to tracking and ranging by earth
- Provide a command uplink capability to implement remote system activation and ground controlled operation.

6.5.2 Study Guidelines

The following guidelines were established for this study:

- ABLE LM Communication Link will be with NASA MSFN or DSIF stations only (i.e. LM frequencies)
- Only one EVA will communicate with the ABLE LM at one time (i.e. two or more EVA's cannot be supported simultaneously)
- Command Control of the ABLE LM systems will be by earth ground stations.

6.5.3 Ground Station Parameters

Ground station parameters affecting line-of-sight (LOS) and circuit margines involve the following:

- Station coverage as a function of orbital parameters
- Station equipment capability
- Station location and relation to ABLE mission target area.

6.5.3 cont'd

Of the fourteen MSFN stations utilizing the unified S-bandconcept only three posses 85 foot diameter antennas (Madrid, Canberra, Goldstone). The remaining stations have antennas of 30 foot diameter. Ten of the above fourteen stations also possess the UHF uplink - VHF downlink capability (KSC, Grand Bahama Island, Ascension Island, Guam, Antigua, Bermuda, Canary Island, Carnarvon, Hawaii, and Texas). One of the fourteen possesses only the VHF downlinke capability (Guaymas). An additional station possessing only the UHF/VHF capability (i.e. no S-Band) is Grand Turk Island.

The "prime-concern" target zone limited the study to an inclination range of 0° to 28.5°. Within this inclination range, the following is observed:

- For altitudes between 6000 and 10,000 n.mi. almost 100% continuous coverage can be provided by the entire MSFN network (includes overlapping of individual ground station coverage)
- For altitudes greater than 10,000 n.mi., the three MSFN stations with 85 ft diameter antennas can provide communication coverage approaching 100%.

6.5.4 LM/Reflector Configuration and Mission Attitude

The ABLE LM antenna system is the most sensitive section of the communication equipment relative to the overall vehicle/reflector configuration. The ABLE LM antenna gain is a critical item in maintaining adequate downlink circuit margins. An ideal antenna system performance would be omni directional about the center of the reflector plane, thereby removing any constraints on the LM/Reflector attitude during the mission.

Due to the inherent requirement for large diameter reflectors the antennas will be working effectively with an infinite ground plane at S-band. Antenna locations will have to be constrained within the near vicinity of the LM vehicle because of the high cable losses encountered when an ideal antenna location on the reflector periphery is considered (i.e. 90-100 db cable loss for a 1500 foot diameter reflector using LM space qualified coaxial cable characteristics, cable weight would be approximately 225 lbs for four antennas). In order

[redacted]

6.5.4 cont'd

to minimize antenna radiation pattern distortion resulting from diffraction and scattering by the LM non-uniform conducting boundaries and the reflector ground plane, circular polarization is desireable.

Antenna location and implementation techniques are dependent on the symmetry characteristics of the LM/Reflector system relative to the Reflector axis. This is illustrated in Fig. 6.5-1 along with the approximate deployment extent required, which is a function of Reflector attitude variations during the mission operation.

The following nomenclature was used in Fig. 6.5-1:

Angle α : The distorted antenna radiation area due to the diffraction and back scattering of propagated energy. A nominal area of 20° from the reflector surface is used.

Angle β : The undistorted antenna radiation area free of detrimental cancellations due to diffractions and back scattering. A nominal area of 70° included between the unit normal to the reflector surface ($\bar{u}_N$) and the bounds of angle .

Low Angle Transmission/Reception: Vehicle LOS to Earth through the bounds of angle α .

It should be noted that angles α and β are to be taken as solid angle projections about the unit normal ($\bar{u}_N$) except in Fig. 6.5-1 (a) where angle α exists only along the reflector/vehicle common axis.

Figure 6.5-1 (a) (Radial and axial asymmetry) indicates that fixed vehicle mounted antennas on the LM ±X axis can be used. Deployment is not required since it is assumed that the reflector is attached on either the +Y or -Y LM axis and therefore antenna pattern distortion (i.e from diffraction and scattering) would be primarily along this reflector axis leaving the antenna radiation on the other axis free of deep null areas. For this configuration and those of Fig. 6.5-1(b) and (c), the uplink/downlink antennas are automatically switched since the R.F. cable loss and 3db inherent coupling loss would only serve to further reduce

communication circuit margins. It is evident from the figure that this configuration would have the least attitude restraints with respect to communication up and down links. For instance, communications to/from the ABLE LM is possible when the reflector/vehicle configuration has the LOS to Earth parallel to the reflector surfaces and the vehicle is between the reflector and Earth).

Figure 6.5-1(b) (Radial symmetry, axial assymmetry) indicates that one vehicle mounted antenna fixed on the LM +X axis and one antenna deployed on the -X axis is required to maintain the uplink/downlink capability when either side of the reflector is facing the Earth.

General antenna deployment must be accomplished from the descent stage through the center of the inner torus to a length such that this antenna can provide radiation distribution approaching that of the fixed vehicle antenna; i.e. equal to or greater than ±70° about the unit normal to the reflector surface, $\measuredangle 2\beta$. A deployment length of 40 ft appears to be adequate for this accomplishment. This configuration increases the restraint on the "Vehicle attitude vs Communications timeline" as is evident from the figure (i.e. low angle transmission/reception is through the distorted radiation region). The configuration precludes a communications link when the LOS to Earth is parallel to the reflector surface.

Figure 6.5-1(c) (Radial and Axial Symmetry) indicates that antennas deployed on both ±X axis of the ABLE LM vehicle are required. Deployment lengths of from 5' to 10' appear to be adequate to duplicate the radiation characteristics of the configuration of Fig. 6.5-1(b). Vehicle attitude constraints would also be similar in that the expected distortion in the pattern would limit the uplink/downlink capability to time periods within a reflector variation of ±70° (through $\measuredangle$ of 2β) about the unit normal to the reflector surface. This angular coverage (in the undistorted region, $\measuredangle\beta$) appears to be adequate to provide the communications capability throughout a full nightime operation.

[redacted]

[redacted]

6.5.5 Additional Discrete Mission Requirements

There are particular additional subsystem functional requirements associated with manned and unmanned launches. These requirements were considered to assure that at least one of the basic subsystem configurations derived and discussed later would provide the needed capabilities.

6.5.5.1 Single Launch - Unmanned ABLE LM

The unmanned single launch mission requires ground command control, operational status data monitoring, and tracking and ranging during launch, orbital insertion, vehicle removal from the SIVB stage and SLA (Saturn LM Adapater) and initiation of reflector deployment. These functional capabilities can essentially be provided with the Apollo LM 1 subsystem equipment described in Section 6.5.6.2. Altitude restrictions are discussed in Section 6.5.4 and 6.5.6.3.

6.5.5.2 Split Launch - Unmanned LM and Manned CSM

The unmanned LM launch requirements are as indicated in the previous section. The time interval between vehicle launches may cause an orbital storage period for the ABLE LM at a low altitude. This may require a more intricate operational time line for status data monitoring with the possible necessity for additional interfaces and associated relays for checkout (systems activation/deactivation).

6.5.6 LM Hardware Applicability

6.5.6.1 Antennas

The Apollo Lunar Landing LM has the following antennas:

- VHF "in-flight" Antennas - These are multifiliar helical antennas on a simulated ground plane (4 conducting arms at base). The antennas are right hand circularly polarized and have a spec requirement for an antenna gain (two anntennas) greater than -6db. There are two antennas, only one being used at a time (the operational antenna being selected by the astronaut. Spherical coverage and the associated gain requirement is defined when the radiation patterns of each antenna are superimposed over the sphere (i.e. defined about the LM). These Antennas are used with the LM VHF voice/Bio-med subsystem for CSM/LM, and LM/EVA links.

[redacted]

6.5.6.1 cont'd

- VHF "manually erected" EVA antenna - this single antenna is used on the lunar surface for the LM/EVA voice/bio-med link. It is a discone type antenna, predominantly linearly polarized in the vertical plane. The radiation pattern provides coverage with a minimum gain of -3db within a ±15 degree elevation angle of the LM Y-Z plane.

- S-Band "in-flight" antennas - These two antennas are used as a back up antenna system to the S-Band steerable high gain antenna. One antenna is used at a time, the astronaut selecting the antenna for operation. They are log conical spirals, each theoretically providing hemispherical coverage with right hand circular polarization. Gain is -3db, over no less that 85% of the radiation spere about the LM, (i.e. superimposed patterns as with the VHF in flights). Figure 6.5-2 and 6.5-3 illustrate the antenna and free space patterns at the transmitting and receiving S-band frequencies. It is noted that these patterns are similar to those required and discussed in Section 6.5.4.

- S-band steerable high gain antenna - this is a 26 inch diameter dish antenna gimbal mounted to the LM. Antenna gain is nominally 20 db with right hand circular polarization. Utilization of this antenna on the ABLE LM is dependent on altitude and subsystem transmitting losses for the downlink.

The following antennas are those used on the LM-1 R&D subsystem configurations:

- UHF/VHF Scimitars - The UHF/VHF scimitar antenna is designed to operate at 450 mc (UHF uplink) and over the frequency range of 230-260 mc (VHF operational status data telemetry at 237.8 mc, 51.2 kb/s). There are two sets of coupled antennas on the LM 1. Two coupled antennas are located diametrically opposite on the SLA outer surface (VHF downlink telemetry prior to LM separation from SLA for unmanned single ABLE LM launch). Two coupled antennas are also located in the same manner on the LM 1 vehicle. The gain of

6.5.6.1 cont'd

either coupled antenna assembly on the spacecraft is designed to be greater than -9db over 85% of the radiation sphere. This gain includes the 3 db power split which occurs with the associated power divider.

- C-Band Transponder Antennas - these are cavity backed helix types used to support the C-Band transponder tracking/ranging system aboard the LM 1. For each antenna polarization is right hand circular and gain is 8 db boresight.

6.5.6.2 Communications Subsystem

The LM subsystem can be divided into the following fundamental divisions:

- VHF, Voice/Bio-med
- Unified S-Band, Voice/Bio-med/Telemetry/Ranging
- UHF Command Uplink/VHF Telemetry Downlink (LM 1)

The VHF section is used primarily for the LM/EVA and LM/CSM communication links. The operational modes are Duplex voice with the CSM or EVA, and receive voice/bio-med from EVA. There is an additional capability of transmitting 1600 b/s (i.e. split phase modulation of the PCM 51.2 kb/s operation status data) to the CSM. However, the VHF section cannot receive CM data.

The VHF section contains two transmitters and receivers. The designated VHF "B" transmitter (259.7 mc) is the only one capable of transmitting PCM data, and only voice or data can be transmitted at one time (not simultaneously). The VHF "B" receiver (259.7 mc) is the only one capable of receiving EVA voice/bio-med. These are received simultaneously. The LM/EVA operational modes can be summarized as following:

- Primary mode
  - VHF B = 259.7 mc Duplex, EVA voice/bio-med to LM
  - VHF A = 296.8 mc Duplex, Voice only, LM to EVA
- Back Up Mode
  - VHF A = 296.8 mc Duplex voice only, EVA to LM
  - VHF B = 259.7 mc Duplex voice only, LM to EVA

6.5.6.2 cont'd

The LM/CSM VHF link is via the antenna system. During an EVA only one LM astronaut can be accommodated with a voice link since one of the two audio control centers is used for the EVA communications to the LM. EVA voice/bio-med and/or the LM occupant's can be transmitted to Earth from the LM over the S-band link.

The S-Band section is a replica of the unified S-band concept (i.e. voice, TV, telemetry multiplexed on a common S-band carrier). An uplink capability exists for voice communications and PRN ranging.

Some of the available operation modes are illustrated in Fig. 6.5-4. Transmission of both the FM and PM modes is precluded. There are two power amplifiers at the output stage before the antennas. Only one of these amplifiers is used a time.

The PM mode has been selected as the primary operational mode for an ABLE LM mission. Actually as yet there is no requirement to use the FM mode which would cause a time sharing type operation between modes during a mission (i.e. a function of ranging requirements).

Apollo equipment most readily available and applicable for the required ABLE LM data uplink and command function is that additional UHF section used on the LM 1, 2 and 3 R&D flights. The uplink is UHF (450 mc) and possesses the capability to receive, process, and route command messages to the LM Guidance Computer (LGC), LM Program Reader Assembly (PRA), and effecting real time commands via the relays within the Program Coupler Ass'y (PCA). The following are brief descriptions of the R&D uplink associated equipment for use on the ABLE LM mission:

- C-Band transponder system to provide ranging/tracking independent of the communications system
- Digital Command Assembly - this unit houses the UHF receiver and Decoder Assembly. The DCA can accommodate 128 commands or control 64 relays.
- VHF telemetry transmitter - this is used for the downlink and has a data handling capability of 51.2 Kb/s (similar to the S-Band PCM bit rate)
- RF Switch - This allows selection of the SLA or LM UHF/VHF scimitar antennas.

6.5.6.3 LM Communications Circuit Margins

Apollo LM data has been extrapolated (Ref 6.5-1,-2 and -3) for the more critical ABLE LM communication links and is presented in Figures 6.5-5 through 6.5-7 as circuit margins vs LOS slant range. It is simple to account for variations in design parameters such as transmitter power output, antenna gain, cable loss, etc. This is done by shifting the vertical 0 db circuit margin line as required. This data includes the required system S/N ratio and is for the LM vehicle communications system. Additional cable losses and decrease in antenna gain were not considered. For an ABLE LM configuration that maintained present LM Antenna gains and no additional cable loss, the following is observed:

- Fig. 6.5-5 - The VHF telemetry downlink circuit margin reaches 0 db at approximately 1500 n.mi.
- Fig. 6.5-6 - The UHF uplink circuit margin on the carrier frequency reaches 0 db at 21,000 n.mi.
- Fig. 6.5-7 - For the S-Band downlink full PM mode the limit is the voice signal reaching 0 db at approximately 24,000 n.mi. Since this slant range and that indicated in the figure for the uplink limit is greater than the highest considered ABLE LM mission altitude (synchronous circular), an S-Band uplink/downlink appears to be the most favorable type of configuration.

6.5.7 Basic Configurations

Two basic configurations have been derived within the subsystem functional requirements and LM equipment capabilities discussed in the previous sections. These are the following:

- S-band uplink/downlink
- UHF uplink, VHF/S-band downlink

The predominance of one configuration over another due to circuit margins vs altitude is difficult to assess at the present time because of the potential variations in antenna gain and cable losses for an ABLE LM configuration.

[redacted]

6.5.7 cont'd

Figure 6.5-8 illustrates the S-band uplink/downlink configuration. This is compatible for altitudes up to a synchronous circular orbit and the manned-unmanned mission phases of a single launch (CSM and LM).

This configuration is discussed further in Section 8.0 since it was chosen for the Program Planning Configuration (PPC).

Figure 6.5-9 illustrates the UHF uplink, VHF/S-band downlink configuration. It is compatible for altitudes up to synchronous, the unmanned single launch (LM only), and the split launch missions.

Fundamentally the LM 1 UHF command uplink is retained along with the VHF downlink (for low altitude mission phases). If necessary, backup operational modes would utilize the S-band downlink. If desired the C-band transponder system provides a ranging/tracking aid independent of the S-band system. In actuality, the C-band system cannot be used until the LM is separated from the SLA. Ranging/tracking is provided via the SIVB stage (6 to 8 hour capability after launch) until the altitude of 1500 n.mi. is reached (VHF limit, Section 6.5.6.3) at which time the S-band mode would be required. If the LM is not withdrawn from the SLA prior to achieving the 1500 n.mi. altitude then an S-band antenna would probably have to be mounted on the SLA.

6.5.8 Alternative Approaches Considered

A brief evaluation was made of the following alternative approaches:

- L-band/S-band system
- Utilization of the AAP derived Shelter uplink system and the LM high gain S-band steerable antenna.

This L-band/S-band system concept was introduced to examine the feasibility and technical aspects of utilizing more than one ground station network for the ABLE LM control. The investigation was confined to the ABLE LM communications receiving section requirements only.

[redacted]

TABLE 6.5-1

CONFIGURATION	ADVANTAGES	DISADVANTAGES	NEW OR MODIFIED EQUIPMENT
I a) Dual phase lock Receiver	°Normal ranging and tracking for S and L-Band uplink °Minimum number of components	°Transponder is an all new design	°Transponder - (new)
b) Single phase lock Transceiver	°Uses near minimum of components	°Tracking rate accuracy comprised °Completely new design	°Converters - (new) °Phase Lock Transceiver (new)
II L-Band converter	°Minimum number of new components °Maximum use of LM components	°L-Band tracking rate accuracy is comprised °Possible junction degradation for S-Band use °Modified LM transponder	°Converter (new) °Transponder (LM modified)
III L-band/S-band Transponder	°Normal ranging and tracking for S and L-Band stations °High degree of independence (few common components)	°New L-Band transponder °Modified LM transponder (as in 2) °Maximum number of components	°L-Band Transponder - (new) °S-Band Transponder - (LM modified)

6.5.8 cont'd

The following are the alternatives identified to enable reception of L and S-band signals:

- Two front ends to a common i.f., detector, and transmitter (Config. I)
- Use of a converter for the L-band signal and a S-band transponder (Config II)
- Separate transponders for L and S-band (Configuration III)

Table 6.5-1 itemizes these approaches along with the related advantages/disadvantages of each, and the number of pieces of new of modified equipment.

The Shelter uplink/downlink system concept was considered in the event the following ABLE LM requirements should occur:

- high gain S-band antenna
- contingency mode capability
- automatic fail safe switching between two command receivers
- more complex command control functions

Figure 6.5-10 illustrates this configuration. The subsystem consists mainly of Apollo hardware with only a few modifications and additional new equipment. The configuration was derived around the LM 1 R&D command control system in order to maintain as much as possible existing LM 1 system/subsystem interfaces. Flexibility of the configuration lies in the two basic distinct routes for commands as follows:

- S-band omni antennas → command receiver → PCA
- S-band steerable antenna → S-band transceiver → DCA → PCA

The former routing is primarily intended for initial activation of equipment. In addition to providing for the main "on/off" functional requirement the command receivers have a limited capability of implementing switching and back up operational modes for contingencies. The latter routing utilizing the S-band transceiver makes control commands available for performance of discrete functions after the required initial equipment has been activated.

6.5.8 cont'd

The configuration is applicable as a basic ABLE LM communication subsystem configuration should the requirements mentioned previously become necessary. An actual ABLE LM mission implementation would require some modifications to the configuration. A more detailed discussion of this configuration appears in Ref. 6.5-4.

6.5.9 Program Planning Configuration (PPC)

During the feasibility study the S-band uplink/downlink basic subsystem configuration was chosen for the PPC. The following guidelines were used in association with the mission definition (i.e., 11,000 n.mi. altitude-circular orbit):

- There will be no downlink required during launch
- Uplink control will not be required until after the manned phase
- No local R.F. remote control devices are required (ie., CSM-ABLE, ABLE-Reflector, etc).
- The PM (Phase modulation) mode of information transmission will be used exclusively (i.e., no TV or wideband data via the FM mode).
- There are no "Orbital Storage" requirements (i.e., single launch) prior to manned deployment.
- When the ABLE vehicle is manned, the CSM will be in the near vicinity of the ascent stage for direct CM/LM-ABLE Communications.
- If ground control of the ABLE configuration is desirable during the early stages of reflector deployment (i.e., for command to blow squibs for deployment mechanisms or other vehicle commands), the ABLE LM +X axis must be approximately normal to the earth's surface.
- Low grazing angle data transmission/command reception will not be required (i.e., ABLE will not transmit/receive when the LOS to earth is parallel to the reflector surface or directed greater than ±70° away from the unit normal to the reflector surface).
- Reflector edge mounted antenna cannot be used due to high cable losses and additional cable weight.

6.5.9 cont'd

The following are listed according to mission phase:

- ABLE launch and Orbital achievement
  - ABLE Communications equipment inactive
- CSM Rendezvous, Docking, and LM SIVB separation
  - ABLE Communications equipment inactive
- ABLE Checkout and Reflector Deployment
  - The ABLE checkout will follow a procedure similar to LM. No unique or new requirements are placed on the Communications Subsystem.
  - The deployment phase will utilize normal LM links (voice, biomed, and spacecraft data).
  - There is no data interface (other than voice) between the CM and ABLE.
  - Intercommunications between vehicles (CM and ABLE) will be via the LM VHF technique.
  - Only one EVA will be supported by ABLE. The general LM technique (EVA voice and biomed relay to earth) will be used. Communications to the Command Module is constrained by EVA (i.e. CM will not use VHF equipment to communicate with ABLE during an EVA) to using the S-band CM-Earth-LM link.
  - PRN ranging (only R.F. form of ranging and tracking on ABLE) is supplied by the CSM during this phase.
- Initial Use and Calibration
  - The ABLE Communications Subsystem (see Fig. 6.5-8) will be fully checked out. The modes will be PM with spacecraft data to ground, PRN ranging to/from earth, and digital command data from earth.
  - No special interfaces (other than those mentioned above) will be required for ABLE calibration (i.e. TV, recorded PCM data, voice, biomed, etc., are not required).
  - The ABLE/Reflector vehicle is unmanned and separated from the Command Module.

6.5.9 cont'd

- Continued Operation
  - The communications equipment will be cycled for the 6 month mission. This will provide updata and ranging capabilities.
  - Spacecraft data transmission will be once a day.
- Resupply
  - The Communications equipment is not designed to be removed, replaced, or repaired on a resupply operation.
  - No R.F. equipment is added to aid in this portion of the ABLE mission. The previously described equipment and operational modes are available.
- ABLE Antenna Configuration

  Two antenna systems are provided on the ABLE configuration
  - S-band antenna system to implement the Uplink Command Control/ Downlink Status Data functions
  - VHF antenna system to implement the voice to CSM/EVA function
- S-Band Antenna System

  The proposed S-Band Antenna System is composed of the following hardware items:
  - One (1) Apollo LM, S-band Conical Log Spiral located aft of the ABLE LM/CSM docking hatch (Fixed Antenna)
  - One (1) Apollo, LM, S-band Conical Log Spiral located approximately 40 ft below the ABLE LM descent stage. This antenna is deployed via Uplink Command after the "Reflector Deployment and Inflation" mission phase.
  - One (1) Coaxial switch capable of automatically switching to the communication s/s switch of the Spiral antennas (Fixed or deployed). The switching command is supplied by the LGC through the PCA.
- VHF Antenna System

  The proposed VHF Antenna System consists of the following hardware items:
  - Two (2) Apollo LM VHF multifilar antennas in Apollo locations
  - One (1) Apollo LM VHF EVA antenna relocated on the ABLE LM descent stage. The Antenna is deployed during the manned mission phase if an EVA is required below the descent stage
  - One (1) manual Apollo LM VHF antenna switch. Switching will be provided manually by the astronaut.

6.5.9 cont'd

- ABLE Communications Subsystem Capability
  The Communications system provides support during the manned and then the unmanned portion of the mission.

During the manned portion of the mission the communications subsystem provides the voice links between the ABLE occupant(s) and EVA, the CM, and Earth. Biomed data of one occupant and/or an EVA can be transmitted to earth. Spacecraft data (PCM at 51.2 Kb/s) is also sent to earth. PRN ranging capability exists, but is not used during the manned phase as the CSM provides this function. In general, the subsystem operates as on LM.

During the unmanned portion of the mission, the Communications System is the ground control link. Updating information and commands are received, decoded and routed to the various vehicle equipments. In addition, PRN ranging data is obtained to aid in orbital parameter, and spacecraft data is sent to ground.

The following equipment is added to the basic LM Communications subsystem to obtain the ABLE configuration:

- Command Receiver - The Command Receiver will interface the DCA (LM 1 Modified) to turn on power and provide the uplink data chain. In addition, other (as yet unidentified) on-off functions may be required of the Command Receiver.
- Modified Digital Command Assembly - The DCA is modified to accept the Command receiver data chain output. The function of the DCA remains the same as on LM 1, and the output interfaces remain unmodified (PCA and LGC).

The updata link is designed to operate independently from the LM type equipment. For example, an uplink message can be received, decoded, and executed without the downlink being turned on. For verification of commands, the downlink must first be commanded on.

The PPC configuration is selected because of the independence of the two phases (manned or unmanned). The unmanned portion of the system (the uplink) could operate in a degraded mode if the manned system (LM equipment) should fail. The lack of ranging information and spacecraft data would definitely constrain opera-

6.5.9 cont'd

tion, however, the uplink and ABLE vehicle might still be operable (pointing could possibly be achieved via a trial and error technique).

6.5.10 Preliminary Conclusions

A final configuration for a particular ABLE LM mission would be composed almost entirely of LM developed hardware. Further study is required on the following:

- Reflector/LM configuration and mission attitude variations
- Extent of required antenna deployment and associated cable losses
- Realistic and practical (achievable) antenna gain is found to be necessarily lower than those of the LM

In particular the overall ABLE LM requirements can be satisfied using the LM communication subsystem. Anyfinal configuration and associated modifications will be a function of the more specific mission requirements.

6.5.11 References

6.5-1 LM ICD No. LIS-380-15006 (S-Band)
6.5-2 LM ICD No. LIS-380-15002 (LM-1 VHF)
6.5-3 LM ICD No. LIS-380-15004 (LM-1 UHF)
6.5-4 AAP Addendum II Final Report, Grumman Report No. 378C-5, Vol I, dated 29 July 1966.

[redacted]

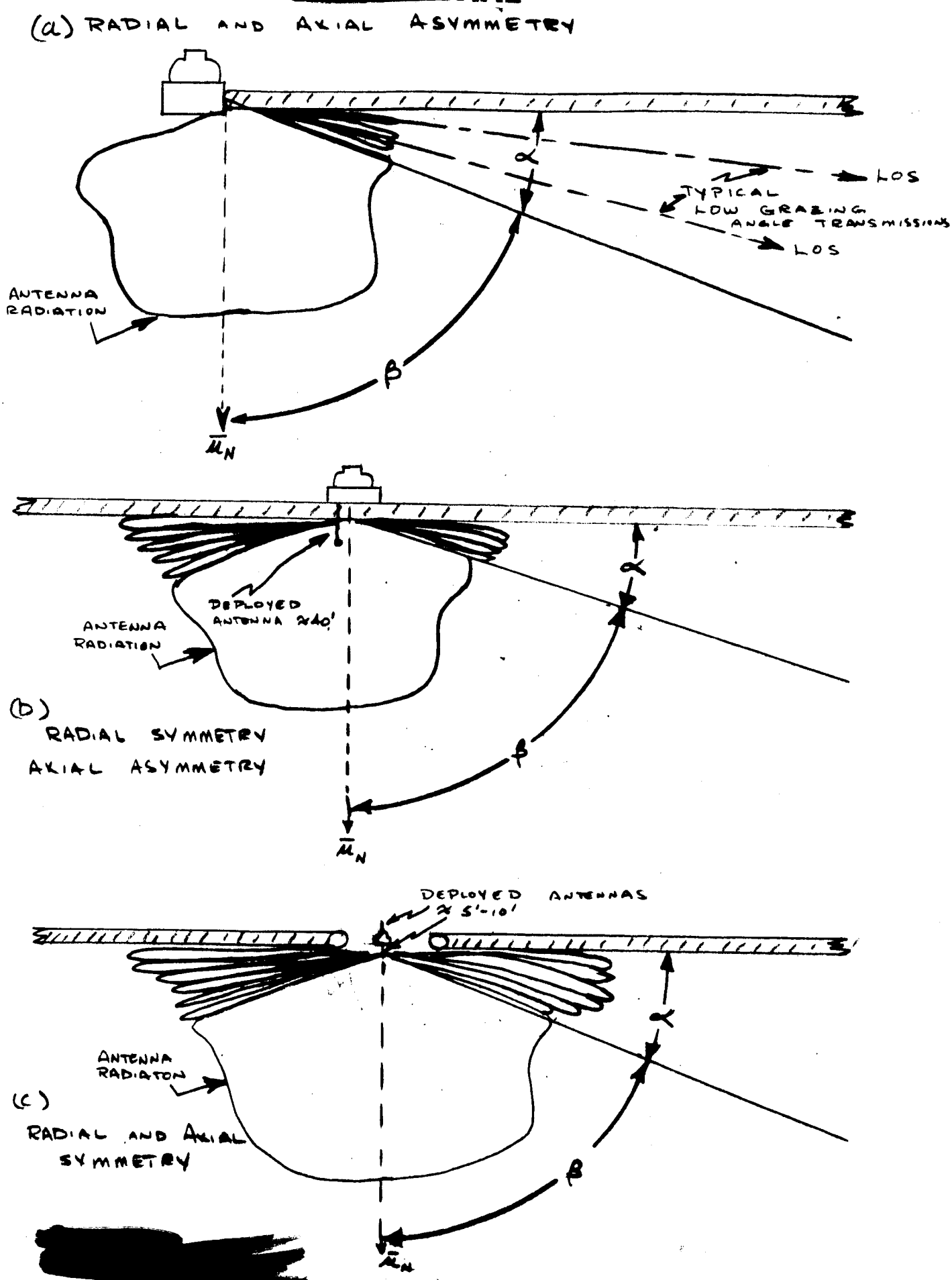

[redacted]

FIGURE 6.5-1

[redacted]

CONICAL LOG SPIRAL ANTENNA

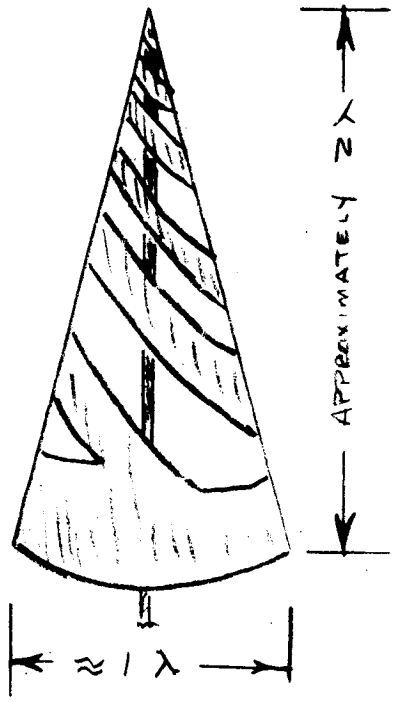

COORDINATE SYSTEM

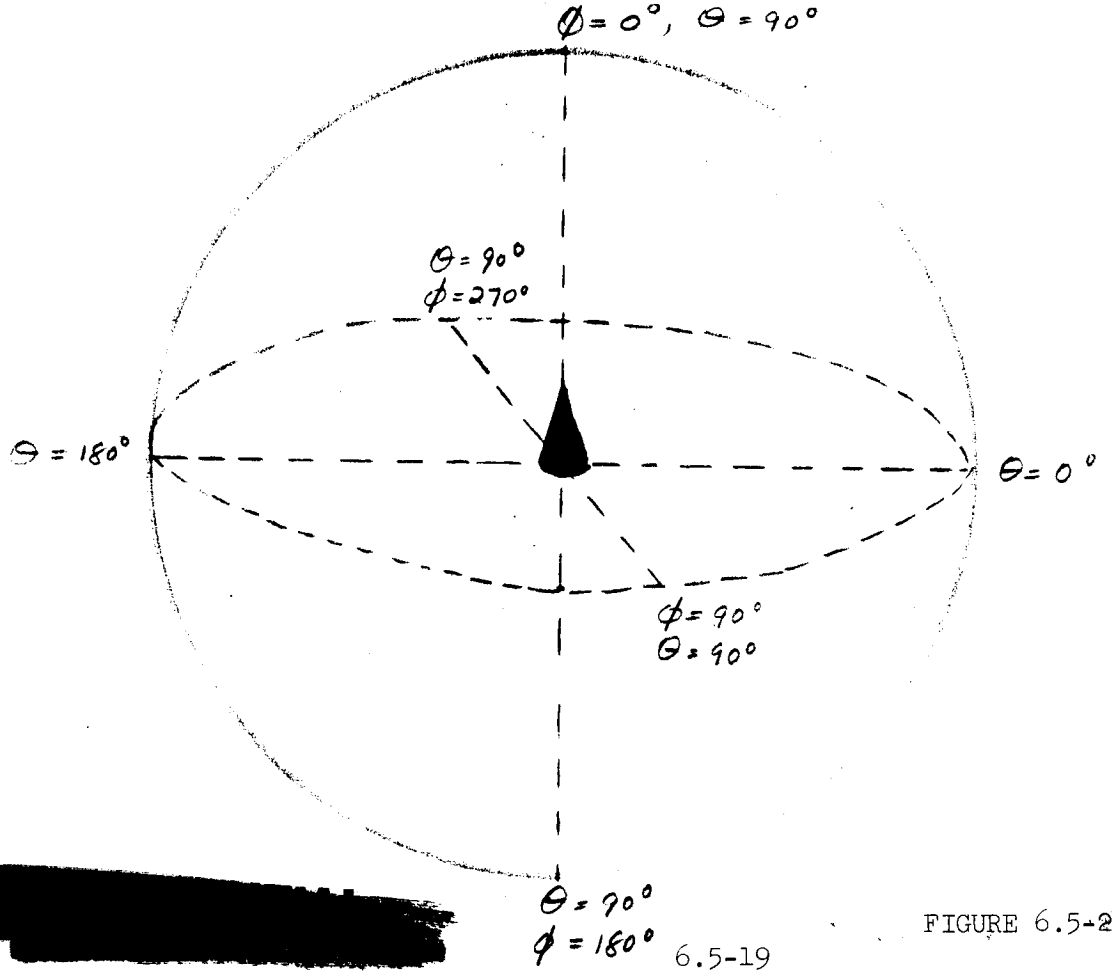

[redacted]

FIGURE 6.5-2

TYPICAL CONICAL LOG SPIRAL ANTENNA PATTERNS

[redacted]

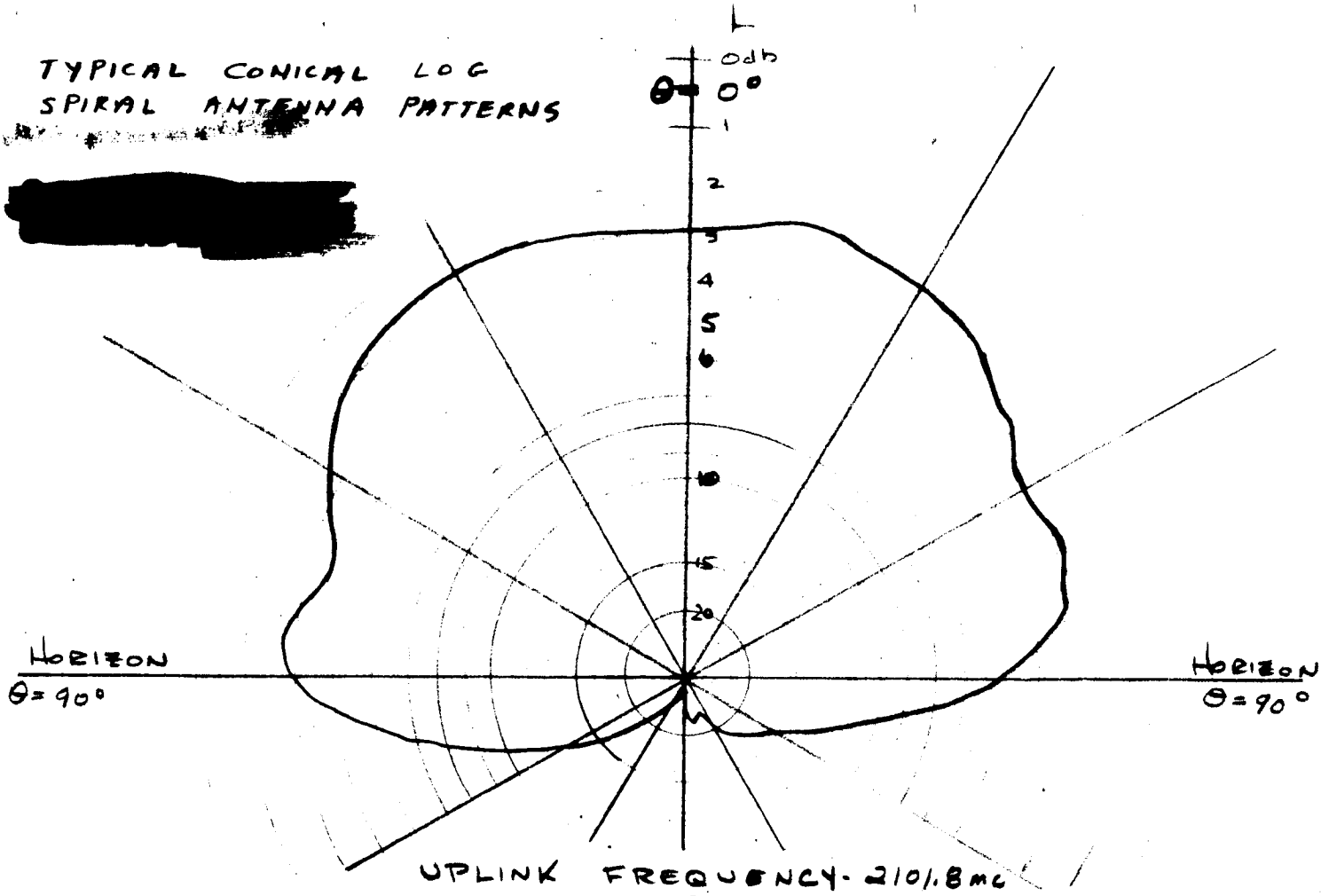

UPLINK FREQUENCY - 2101.8 mc

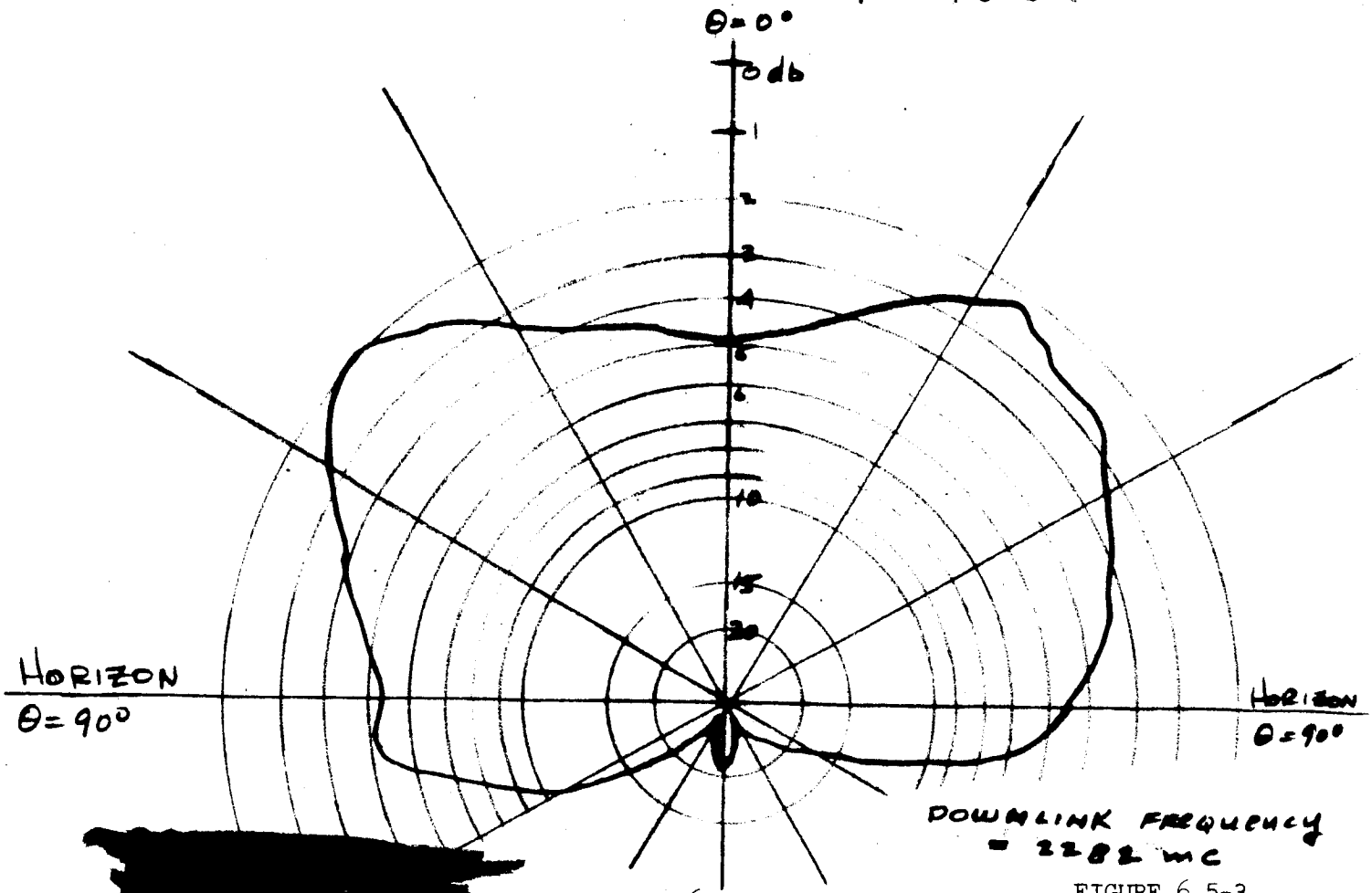

DOWNLINK FREQUENCY = 2282 mc

[redacted]

FIGURE 6.5-3

S-band SECTION OPERATIONAL MODES

[redacted]

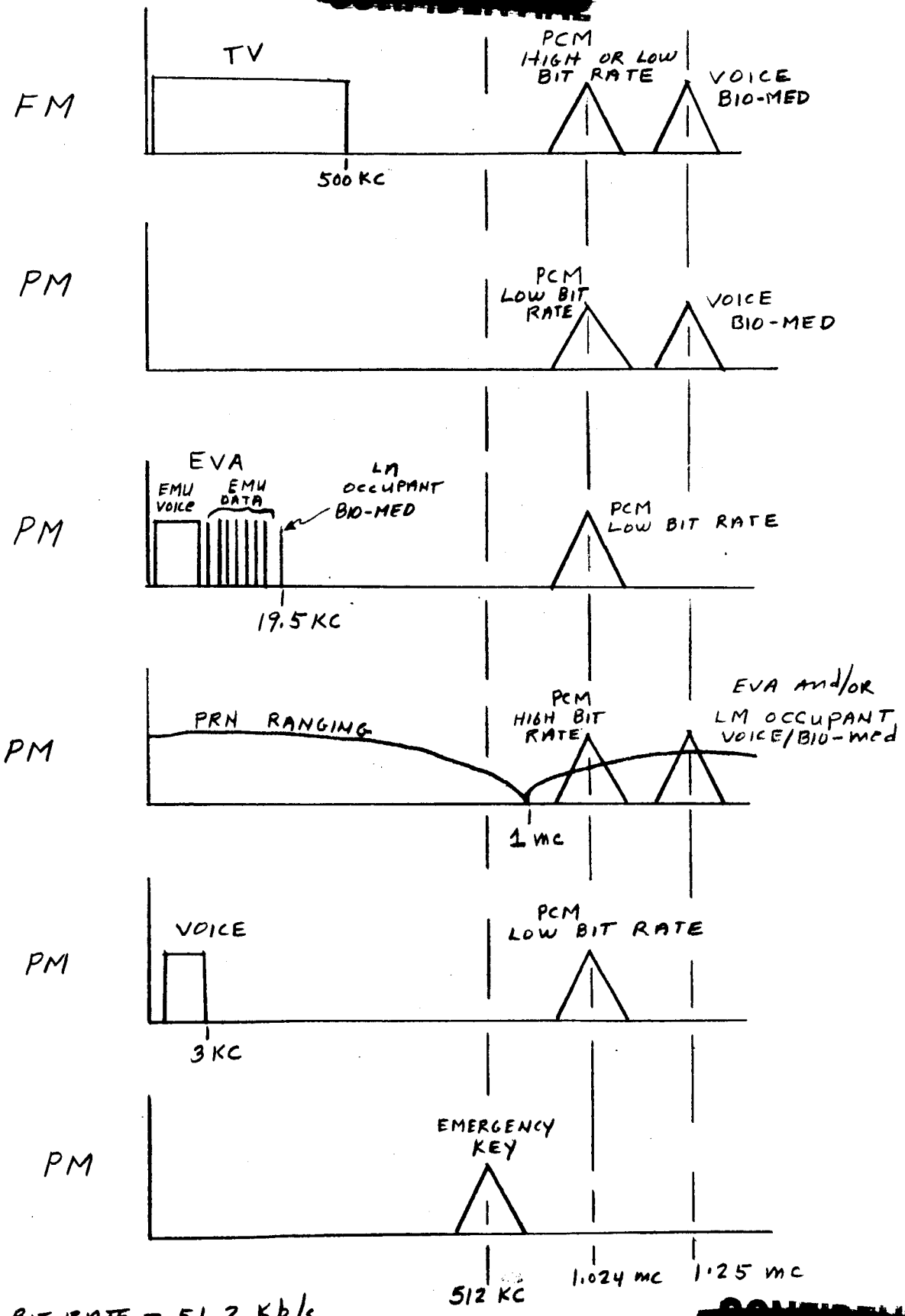

HIGH BIT RATE = 51.2 Kb/s

LOW BIT RATE = 1.6 Kb/s

~~CONFIDENTIAL~~

FIGURE 6.5-4

[redacted]

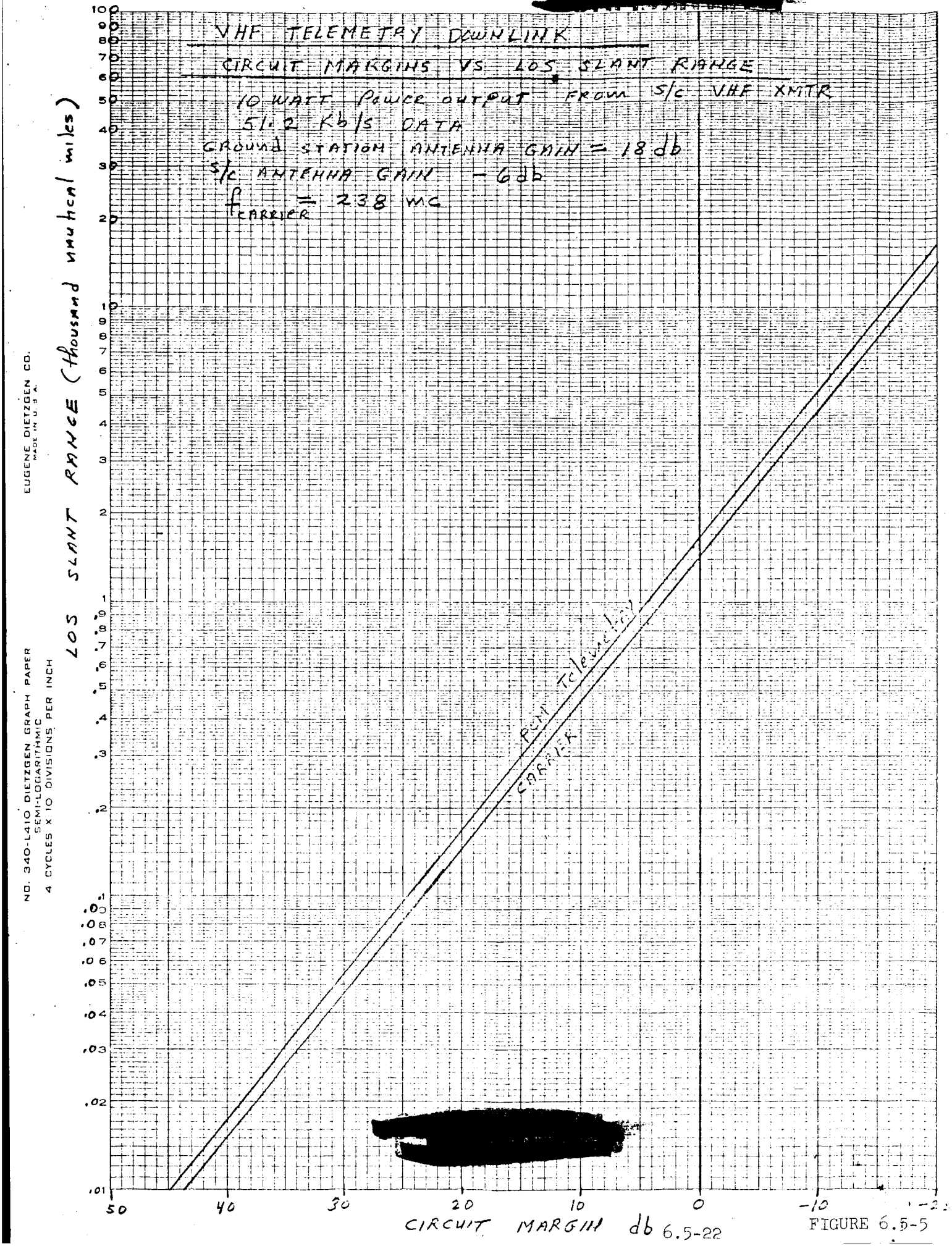

[redacted]

FIGURE 6.5-5

[redacted]

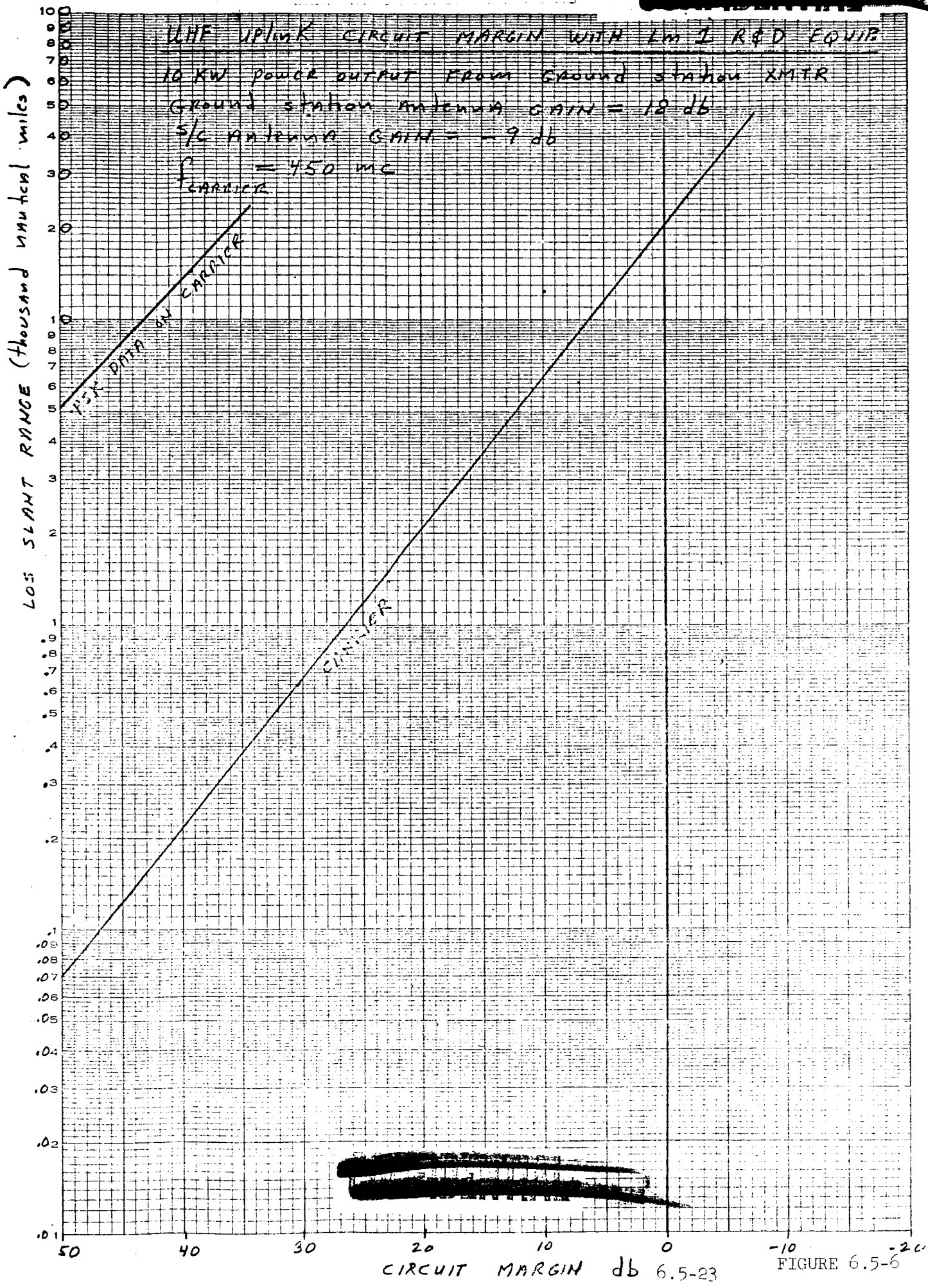

[redacted]

FIGURE 6.5-6

[redacted]

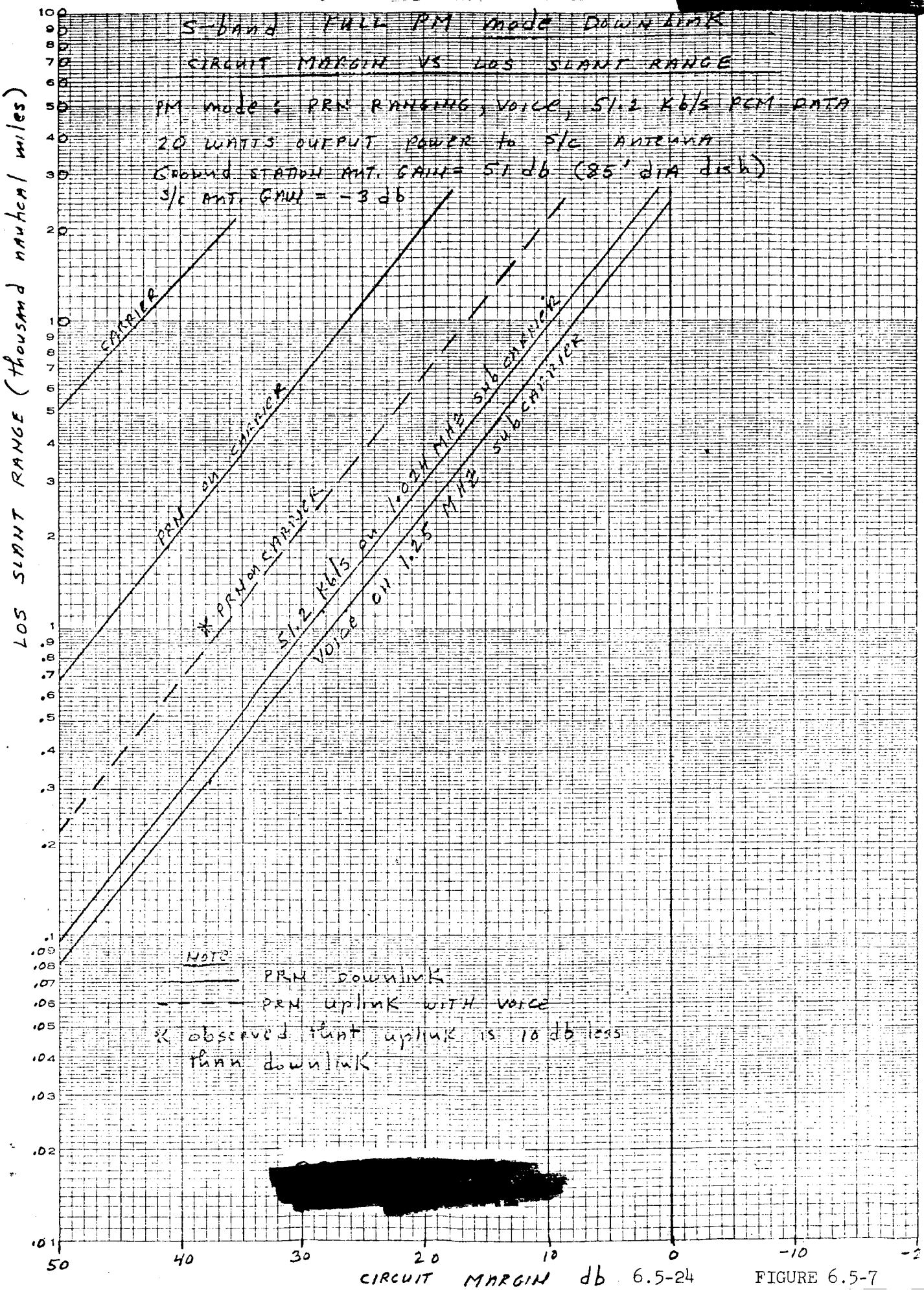

[redacted]

FIGURE 6.5-7

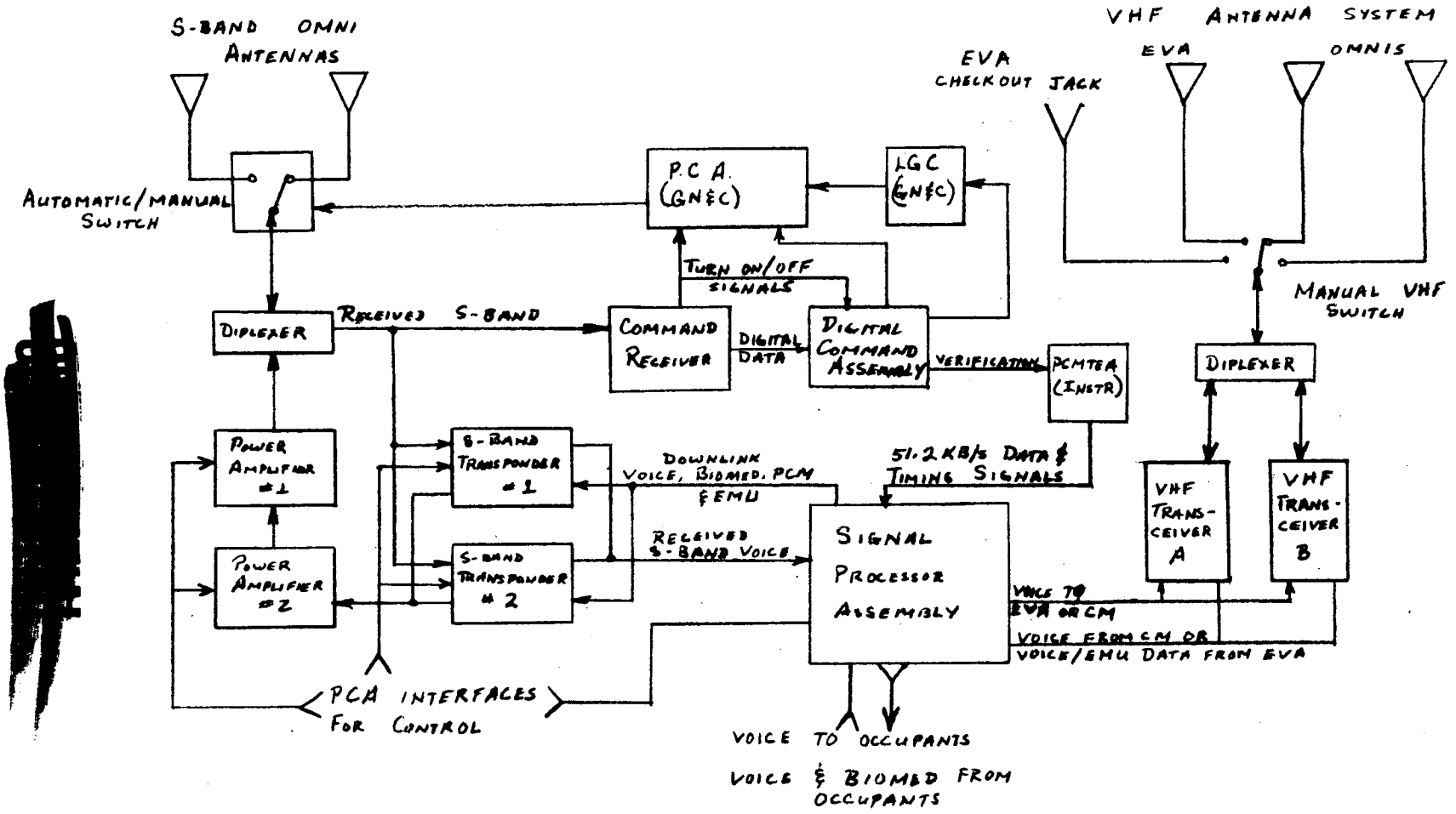

S-band UPLINK/DOWNLINK

FIGURE 6.5-8

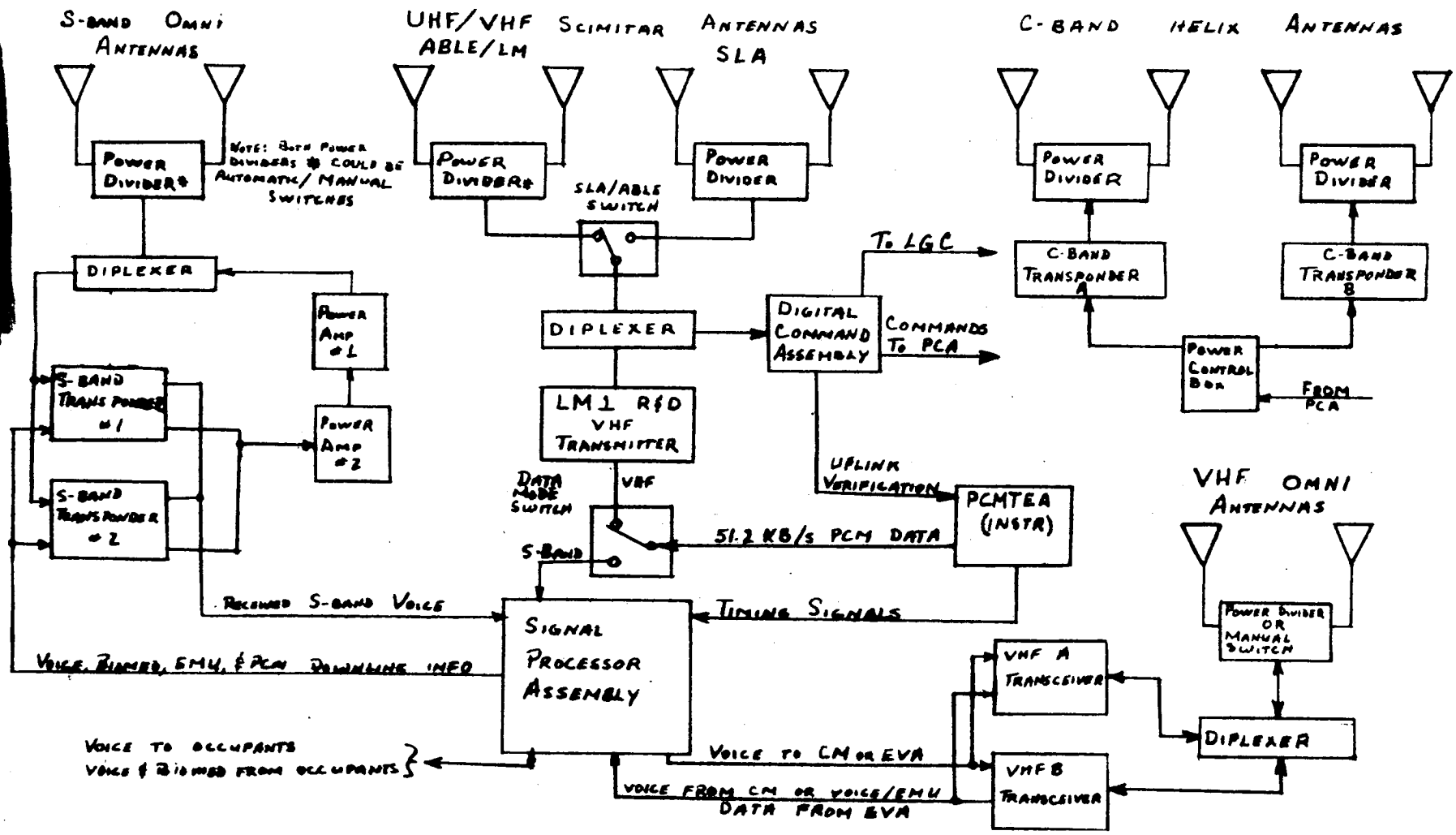

UHF UPLINK, VHF/S-band DOWNLINK

FIGURE 6.5-9

LM SHELTER uplink / downlink system FOR ABLE

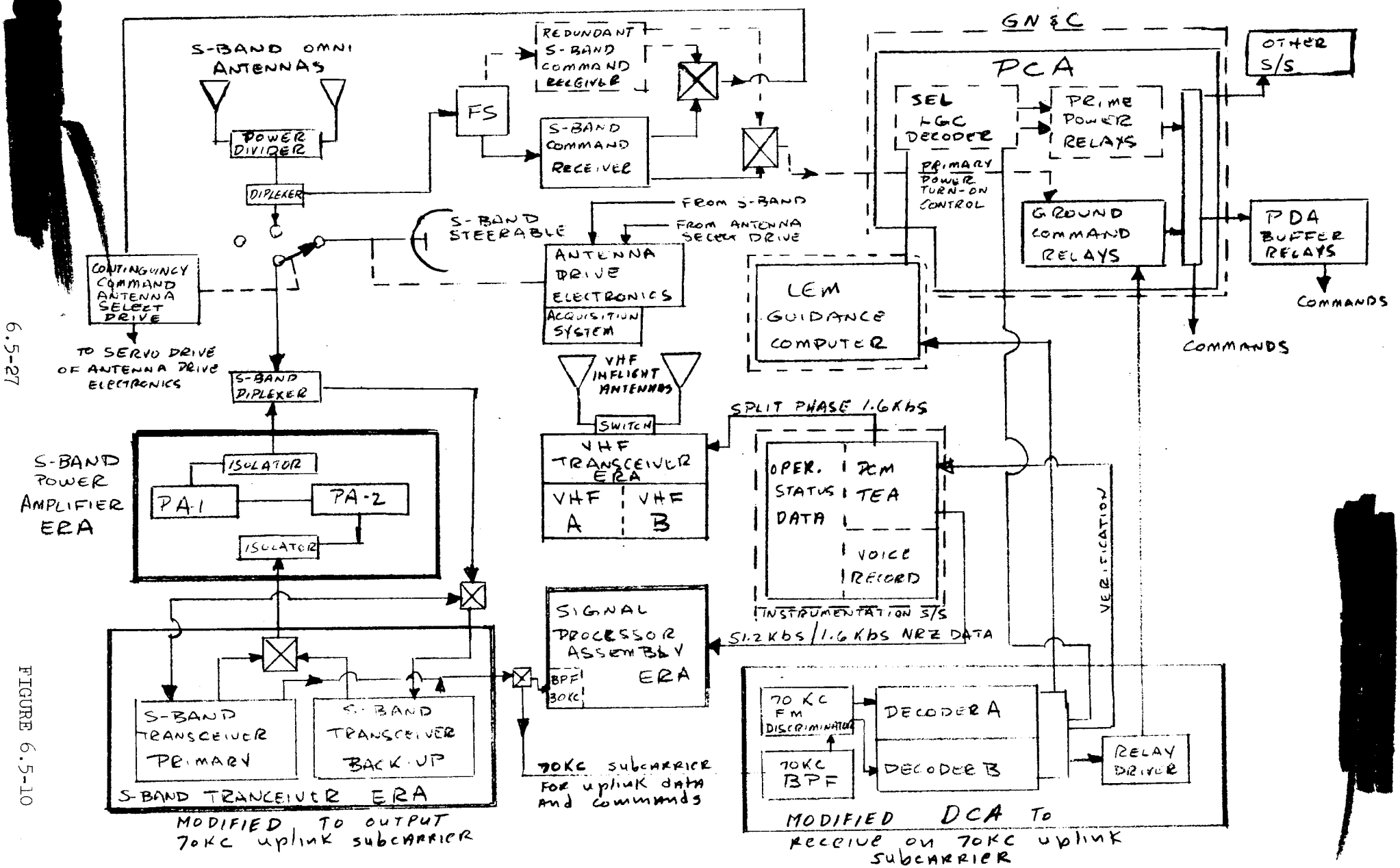

FIGURE 6.5-10

6.6 INSTRUMENTATION

6.6.1 Guidelines and Background Data

The following list of guidelines and assumptions were used:

- All operational data will be presented to the ground during line-of-sight mission phases only. (Real time)
- There will be no on-board recording capability for operational data.
- Vehicle Altitude data will be provided via existing interfaces with Guidance system.

The primary function of the Operational Instrumentation Section is to acquire and present spacecraft housekeeping data to the astronauts and ground monitoring personnel (Fig. 6.6-1). In reviewing the measurement requirements of the ABLE LM it was concluded that the existing LM equipment would be adequate.

6.6.2 Recommended Configuration

The recommended Operational Instrumentation Section for the Able LM is comprised of existing LM assemblies having a certain built-in flexibility which allows for some minor configuration changes. A measurements list prepared for the standard LM vehicle was reviewed and analyzed to assure that the changes to support the requirements of ABLE LM would still be adequately covered using the existing LM system.

6.6.2.1 Transducers

The sensors convert the physical and electrical phenomena of interest into a usable form for presentation to the astronauts or ground station personnel. These measurements from the various subsystems provide the majority of the input sources to the Operational Acquisition System.

New spacecraft subsystem measurement requirements demand additional transducers, and consideration will be given to LM proven units. For any measurement unique to ABLE which requires a transducer not previously used on LM, new transducers will be selected having LM characteristics. Preference shall be given to

transducers which have been developed for other space missions and have a high level output, therefore requiring no additional signal conditioning.

6.6.2.2 Signal Conditioning Electronic Assembly (SCEA)

The LM SCEA is a unit which conditions the signals from transducers and numerous signal monitoring points throughout the spacecraft and properly routes them to the Operational PCMTEA, Caution and Warning Electronics Assembly (C&WEA) or on-board displays. The SCEA assemblies fulfills these basic functions:

- Acts as a junction and routing assembly for all analog measurements and signals being monitored.
- Mechanically support the signal conditioning sub-assemblies which condition the measurement input signals.

The SCEA is comprised of two separate chassis assemblies. Each assembly can accommodate up to twenty-two (22) separate sub-assembly modules. Once the measurements are determined for the ABLE mission, an analysis will be performed on each measurement in order to assign a signal conditioning circuit to that measurement. The total number of signal conditioning sub-assemblies for the mission are than packaged into the two assemblies. A review of the LM listing indicates that the changing requirements for ABLE can still be accommodated within the existing SCEA using adaptation techniques presently employed. No modification to either the assembly or its sub-assemblies, as now used by LM is anticipated. In the SCEA:

- Sub-assembly circuits are bench calibrated and adjusted for each measurement.
- Input signals are grouped in sub-assemblies by types of conditioning required, not by subsystem, therefore, the elimination of a vehicle subsystem does not preclude the deletion of any modules.

6.6.2.3 Caution and Warning Electronic Assembly (C&WEA)

This assembly advises the astronauts of the spacecraft subsystem status by continual monitoring of critical parameters. During the mission the C&WEA performs two basic functions:

- The caution function advises the astronaut of a malfunction which requires his action to correct
- The warning function advises the astronaut of crew safety items requiring immediate action.

The C&WEA accepts inputs from the SCEA or pre-conditioned signal sources from the subsystems. These inputs are compared to preset reference signals within the C&WEA to detect out-of-tolerance conditions. When an out-of-tolerance condition exists, an appropriate indication is initiated. The C&WEA as now used for the Lunar LM operates on discrete voltage changes or switch closures. The deletion of some LM equipment from the ABLE LM make monitoring channels available for additional requirements.

6.6.2.4 Pulse Code Modulation and Timing Electronic Assembly (PCMTEA)

The PCMTEA in the recommended configuration consists of an unmodified Lunar LM assembly. The data acquisition capability of this unit include the multiplexing, encoding, and timing of high-level analog, parallel digital, and serial digital data. The number of channels, sampling rates and word lengths for each of the three data forms are presented in Table 6.6-1. The unit operates at a normal data rate of 51,200 bits per second and a reduced data rate (commanded remotely) of 1,600 bits per second. The PCMTEA will operate as it does in the Lunar LM including accepting a time reference from the LM Guidance Computer and providing various timing signals to interfacing subsystems. The NRZ(C) data output is routed to the Communications Subsystem for real time transmission. Operation of the PCMTEA in the reduced data rate mode is not anticipated for the ABLE mission, due to Guidance system downlink requirements.

6.6.2.5 Voice Storage Recorder

This magnetic tape recorder, originally referred to as the "Data Storage Electronics Assembly", provides a time correlated voice recording of comments and conversation between the astronauts during EVA's. This assembly employs automatic sequential record head switching with four tracks to provide up to a total of 10 hrs. of recording time. The compact recorder is generally used with voice actuation circuits to run only for a required recording time. The

recorder is used:

- To support EVA's
- To record comments of vehicle status when off station coverage
- To record proprietary information

6.6.3 Changes to LM Vehicle

The deletion of some equipments, such as Ascent & Descent Propulsion Systems, allows use of that telemetry for new measurement requirements.

Approximately 10% (5000 bits/sec) of the PCM would be made available due to deletion of equipment from LM. This capability for new measurements is in addition to the 20-25% excess capability which exist in the original vehicle yielding 30% of the LM PCMTEA (15000 bits/sec) available for use by ABLE payload measurements and/or new equipment requirements.

6.6.4 Alternates

Since Instrumentation's design is dictated by other subsystem's designs and requirements, any alternate configuration will affect this subsystem. However, due to the inherent flexibility designed into the SCEA, the excess capability of the PCMTEA, and the nominal effort usually required in selecting and installing transducers, this effect is probably minimal.

[redacted]

Table 6.6-1

PCMTEA Input Data Capability

Data Format: 51,200 bits/sec Output Rate				
Data Form	No. Channels	Samples/sec	bits/word	words/sec
Analog - High Level	5 17 6 35 137	200 100 50 10 1	8 8 8 8 8	1000 1700 300 350 137
Digital - Parallel	1 3 4 1 37	200 100 50 10 1	16 8 8 8 8	400 300 200 10 37
Digital Serial	1 1	50 50	40 24	250 150
TOTAL	248			4834

Note: Internally wired redundancy exists within this format.

* Normalized to 8 bit words.

[redacted]

7.0 ABLE LM DESIGN AND INTEGRATION

7.1 STRUCTURAL DESIGN

After a study of ABLE mission requirements, it appears that the ABLE LM, regardless of reflector size or configuration, would remain basically an Apollo Lunar Module with equipment additions and removals requiring no major redesign.

With approximately 2000 ft^3 of unused space and numerous hardpoints, the LM has room for both growth and possibly additional experiments. The major LM equipment not required for the mission include landing gear, ascent and descent propulsion (except supercritical helium tank), landing and rendezvous radars, and abort guidance. The following equipment would be added as required by the mission (see Figure 7.1-1).

7.1.1 Reflector Canister

Two locations for the reflector canister are possible, each has its limitations and advantages. In the first location (see Fig. 7.1-2a), the canister would be located in the area between the LM Descent Stage and the top of the SIVB hydrogen tank. The canister would be fastened to the eight existing drag strut fittings on the lower surface of the Descent Stage. A maximum volume of 570 ft^3 can be accommodated in this location. Since the majority of the vertical load at the drag strut fittings during launch and boost goes directly into the LM outrigger truss (which can be easily redesigned) and then into the Spacecraft LM Adapter (SLA), the maximum canister weight which can be tolerated is limited only by the structural capability of the SLA. The location below the Descent Stage can be utilized on either a single manned or unmanned launch or on a dual manned launch.

The second location (see Fig. 7.1-2b), places the canister above the LM Ascent Stage, in the area normally occupied by the Service Module. A volume of 2,500 ft^3 or greater is available, which is more than sufficient for the 3000 ft reflector. The canister would be attached to the SLA in a similar manner as is the Service Module and would be limited in weight to the structural capability of the SLA. This location can be used for a single unmanned launch or a dual manned launch.

7.1.2 Solar Arrays

Power for an ABLE Mission would be continuously required from solar arrays. When light is reflected from one side of the reflector only, one solar array would be required. If both reflector sides are to be used, two arrays would be required, one on each side of the reflector. In both cases, the solar arrays could be packaged on the sides of the Ascent Stage and would be deployed by extendable arm mechanisms.

7.1.3 Radiators

Cooling requirements for a mission would dictate the use of two radiators spaced 180° apart on the LM vehicle so that, at all times, one would face away from the sun. To meet this requirement, two radiators were placed, one each on Quads II and IV of the Descent Stage. These locations were compatible with existing structure and are in the same area as the glycol coolant loops.

7.1.4 Antennas

Since one S-band antenna must always "face" the earth, the two S-band antennas would be relocated to points on each side of the reflector when both sides of the reflector are used. One would be placed on the top of the Ascent Stage and the other would be attached to the solar array arm which deploys to the other side of the LM. Only one antenna would be required if one side of the reflector is utilized.

7.1.5 LOTS

The LM Optical Tracking System (LOTS) would be required on the ABLE Mission. It would be attached to the Ascent Stage Navigational Base as it is on the LM-1 flight article. In this location a suitable star field can be viewed.

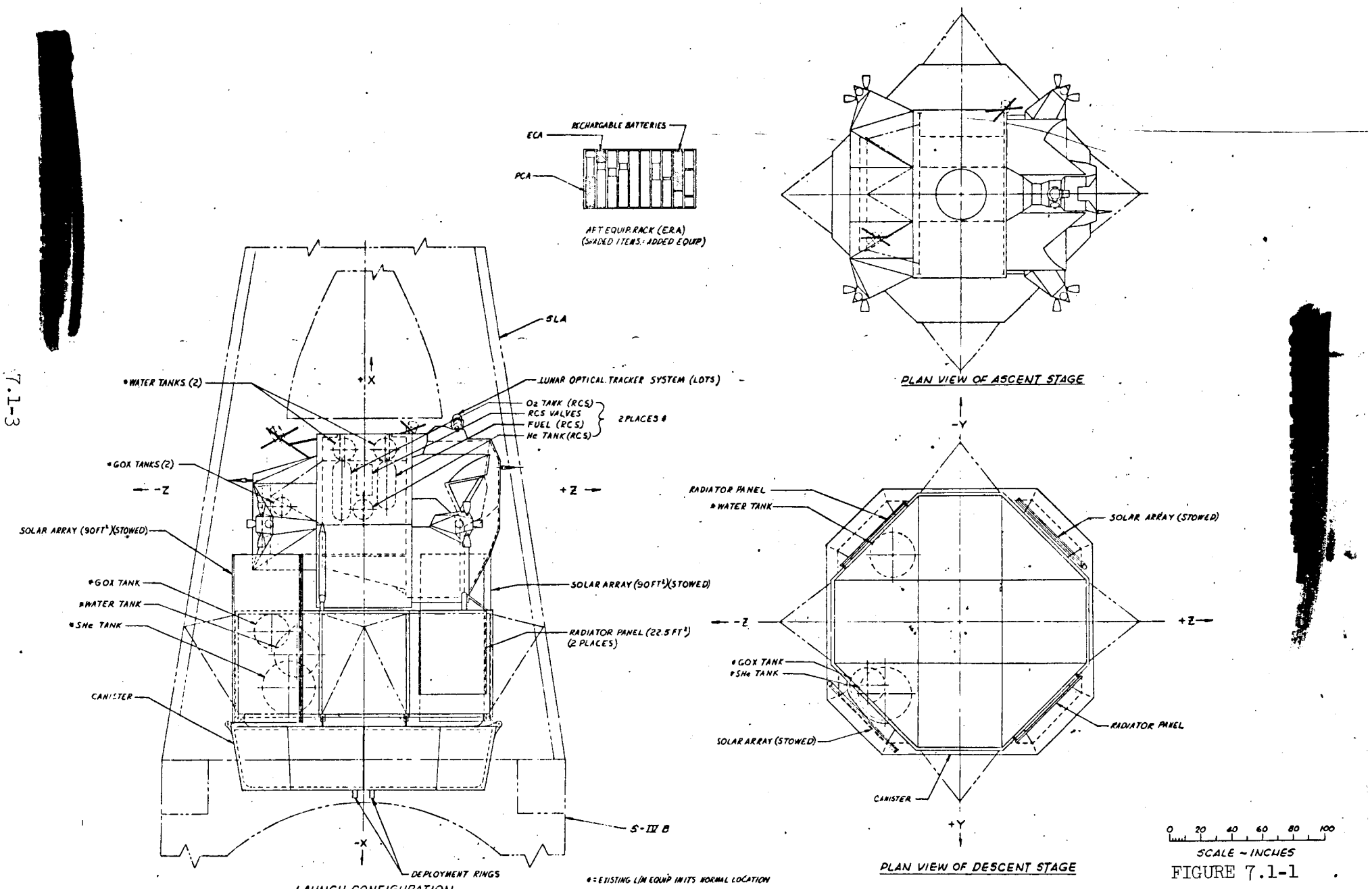

FIGURE 7.1-1

ABLE/LM LAUNCH ARRANGEMENT

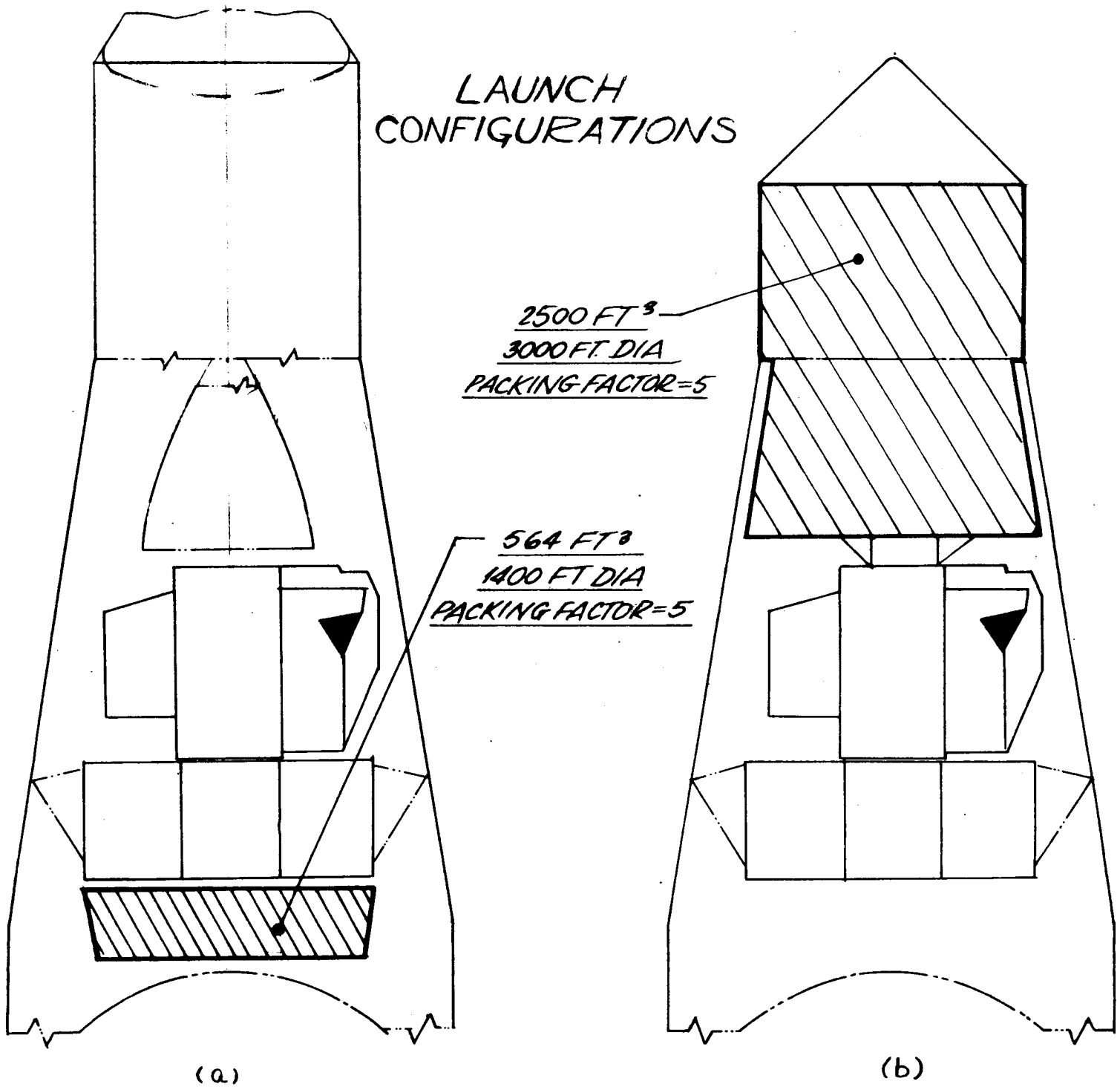
LAUNCH
CONFIGURATIONS
2500 FT³
3000 FT. DIA
PACKING FACTOR=5
564 FT³
1400 FT DIA
PACKING FACTOR=5
(a)
(b)

FIGURE 7.1-2

[redacted]

7.2 MECHANICAL DESIGN

Full advantage will be taken of existing LM systems and technology to perform several new functions required on ABLE LM. LM qualified explosive devices such as the Landing Gear Uplock Cutter will be employed on various deployment devices in conjunction with existing circuitry. It is likely that many mechanical details developed for LM can be successfully integrated into the mechanisms for opening the reflector canister and deploying solar panels. Space-qualified hardware from other programs will also be examined for possible application to ABLE LM.

7.2.1 Reflector Deployment

In one deployment concept (as outlined in the Reference Mission, Section 3.5), the initial steps require that the CSM first engage towing hooks on the packed reflector and then open the canister. The simplest method of engaging the towing hooks would require the CSM to maneuver a few feet from the bottom of the canister and an astronaut, on what might be termed a semi-EVA, would manually engage the hooks with the existing Apollo LM EVA transfer device. This is a STEM device with an engaging hook or ring used to transfer astronauts from LM to the CSM in the event that normal docking is impossible. The astronaut would not be required to leave the CSM, since the entire operation could be conducted while standing tethered in the CM docking hatch.

If it is determined that even a partial EVA is undesirable, it is feasible to automatically engage the towing rings. Parts required to implement such a system would include a flexible extendable probe replacing the normal docking probe on the CM, an automatic catch, a remote release mechanism and a probe guide surrounding the exposed towing rings on the canister. Engaging the probe with the rings would require CSM maneuvers similar to those required for normal docking with a LM though requiring somewhat less precision.

Once the rings have been engaged and the CSM has backed off, the canister is opened to release the reflector. Four formed spring loaded doors attached to a circular backing plate comprise the canister structure. After the reflector is packed, the four sections are folded together and secured with pyrotechnic

[redacted]

fasteners to form the canister structure. Remote actuation of the pyrotechnic fasteners permits the spring loaded doors to deploy and lock open, freeing the reflector.

7.2.2 Solar Array Deployment

Electrical Power Subsystem studies indicate that the ABLE LM may employ two steerable solar arrays. The arrays can be stowed on the descent stage and secured with pyrotechnic fasteners until the reflector has been deployed. Because of their probable size, the solar panels must be folded to fit within the launch envelope. The deployment geometry and mechanism will depend on the distance from the stowed to the deployed array.

For deployment over long distances, the solar array can be extended from the descent stage by means of a multi-section telescoping tube. At full extension of the tube, a release will be tripped permitting the folded solar panels to deploy. An alternate to the telescoping tube could be the STEM developed by Westinghouse. Deployment over short distances can be accomplished by a set of folding spring loaded links. When deployed, the panels automatically unfold.

7.2.3 Solar Array Pointing

A one-or two-axis gimbal drive, powered by independent motors complete with gearing, clutch and position feedback provisions, is probably required if the arrays are steerable. A similar single-axis drive is flying on Nimbus and a two-axis drive has been developed for OGO. Pointing commands can be provided by either the guidance computer or array-mounted sun sensors.

7.2.4 Antenna Deployment

Two antennas, an S-Band on the lower surface and a VHF on the +X axis side of the Descent Stage must be extended after the reflector has been deployed. Both of the antennas would be secured for launch by pyrotechnic or solenoid latches and later deployed by STEM devices. Existing self-powered STEM's with minor modification should be adequate for this task.

7.3 CREW PROVISIONS

The interior of the ALBE LM Ascent Stage will probably be similar to the Apollo LM, with minor modifications associated with the Control & Display consoles.

Equipment required for EVA can be retained as in the existing LM configuration. These items consist of 2 PLSS units, 6 PLSS throwaway batteries (stowed in the Descent Stage), 5 PLSS LiOH canisters plus 1 canister utilized in the ECS/ suit loop package as a backup for cabin LiOH canister replacement, all recharge equipment, 2 thermal meteoroid garments, EV visors, boots, gloves and EV device. When better definition of EVA activity is available, the installation of external crew aids such as hand holds, retention devices and Auxiliary Maneuvering Units may have to be considered.

The existing LM food and waste management system can be retained for possible manned ABLE LM operations while separated from the CSM.

APPENDIX

A. OPTICS ANALYSIS

The effects of bending and deflection on a satellite reflector will significantly influence the choice of orbit and the structural design of the space craft. The following appendix is a description of an optical analysis of plane and spherical reflectors used in the ABLE trade-off studies.

A. 1 Ideal Reflector

The analysis below is valid for flat reflectors in high altitude orbits. Consider a plane reflector, using the incident rays from the sun to illuminate a target on the ground, and so oriented that the reflected rays are approximately normal to the earth's surface. The ground pattern of the resulting illumination is illustrated in Figure A.1. At a point in space at a distance from the sun equal to the mean radius of the earth's orbit, the sun subtends an angle of 32.3 minutes of arc. Thus the sun's beamwidth Θ, in Figure A.1 is assumed to be 32.3 at every point on the reflector. The orbit altitude H_1 is on the order of 6000 n.mi. or greater, and i is the average angle of incidence on the reflector whose diameter, d, does not exceed 0.5 n.mi. The diameter, D, of the ground pattern is given approximately by:

$$D = 2d \cos i + H\Theta \qquad \text{(A-1)}$$

But since $H\Theta \gg 2d \cos i$, this becomes

$$D = H\Theta \qquad \text{(A-2)}$$

Thus the resulting illumination pattern depends chiefly on the sun's angular beam width Θ. The ground pattern, then, is essentially a circle whose perimeter is only slightly modified by the size and shape of the reflector. At nearly synchronous altitude, for example, H = 19350 n.mi. and the illuminated area is 181 n.mi. in diameter.

The average ground illumination $\bar{E}$, is given by:

$$A\bar{E} = \rho \tau E_o A_o \cos i \qquad \text{(A-3)}$$

where: ρ is the reflectivity of the reflector

τ is the transmission of the atmosphere

E_o is the luminous flux/unit area impinging upon the reflector.

A_o and A are the areas of the mirror and ground coverage respectively.

[redacted]

Equation A becomes:

$$\bar{E} = \rho \tau E_o \frac{d^2}{D^2} \cos i \qquad \text{(A-4)}$$

and since $D = H\theta$,

$$\bar{E} = \rho \tau E_o \frac{d^2}{(H\theta)^2} \cos i$$

Using an average value of $\tau = 0.8$, and the value of E_o near the top of the atmosphere (140,000 lumens/m^2),

$$E = 12.7 \times 10^8 \frac{\rho d^2}{H^2} \cos i \qquad \text{(A-5)}$$

Choosing d = 0.5 n.mi., $\rho = 0.8$, i = 45°, and again H = 19,350 n.mi,

$E = 0.48$ lumens/m^2

as compared with the nominal value for full moonlight, $\bar{E} = .15$ lumens/m^2, at ground level.

The central illumination E_n, at point P of Figure A.1 is given by the inverse square law:

$$E_N = \rho \tau \frac{I}{H^2} \cos i \qquad \text{(A-6)}$$

where ρI is the number of lumens/steradian, or candle power, provided by the reflector.

This may also be written as

$$E_N = \frac{\rho \tau \cos i}{H} E_o \frac{\pi d^2/4}{\Omega_\theta}$$

where Ω_θ is the solid angle corresponding to θ, which for small θ is given by:

$$\Omega_\theta = \frac{\pi}{4} \theta^2$$

Thus,

$$E_N = \frac{\rho \tau E_o d^2}{\theta^2 H^2} \cos i \qquad \text{(A-7)}$$

which is identical to equation (A-4). Thus for a plane, regular reflector at high altitude, a good approximation is

$$E_N = \bar{E} \qquad \text{(A-8)}$$

[redacted]

[redacted]

A.2 Bending Effects on Illumination

Considering the above case of the plane regular reflector as ideal, we now proceed to more realistic models. To simulate possible bending out of the plane of the reflector, consider how the ground pattern is affected if a particular plane element on the reflector is rotated through an angle ϕ. This case is illustrated in Figure A-2.

An incident cone of rays from the sun is shown reflected normal to the earth's surface. In addition, the same incident cone is shown being reflected when the reflector has rotated by some small angle ϕ. It is shown in Figure A.2 that the reflected cone has advanced by an angle 2ϕ. If R_1 equals the radius of the ground pattern produced by the reflector in its original orientation, let R_2 be the maximum ground shift of the displaced cone, measured relative to the center of the first cone (point P in Figure A-1).

Since Θ and ϕ are both small we may write:

$$R_1 = \frac{\Theta}{2} H,$$

$$R_2 = \left[\frac{\Theta}{2} + 2\phi\right] H \qquad \text{(A-9)}$$

And we may define the ratio R_2/R_1:

$$R_2/R_1 = \frac{4\phi}{\Theta} + 1, \qquad \text{(A-10)}$$

which, if rotations ϕ are considered in all directions, gives a measure of the increase in the region of ground illumination due to small angle bending in the mirror. Figure A-2 also contains a plot of equation (A-10). The following two points about the ratio R_2/R_1 are pertinent:

- It is independent of H (When H is assumed large)
- It is extremely sensitive to the degree of bending.

The sensitivity of R_2/R_1 to bending is illustrated for $\phi = 8.1$. Equation (A-9) yields $R_2 = 2R_1$, i.e. in the synchronous orbit case discussed above, $R_1 = 91$ n.mi, $R_2 = 182$ n.mi. Since the total luminous flux reaching the earth remains constant, the energy density, and thus the average illumination must

[redacted]

[redacted]

decrease by a factor of $(R_1/R_2)^2$.

A.3 Spherical Reflectors

The ground patterns and illumination intensities are similar for similar concave and convex mirror parameters. Thus only the concave case will be considered here.

Required first are the definitions of several important parameters relating to spherical mirrors. Figure A-3 depicts the cross-section, ABC, of a spherical mirror of diameter d. BB, henceforth referred to as x, is known as the the sagitta, or maximum deflection of the mirror from a plane. The radius of curvature OA will be designated by R, and ϕ is the angle between the tangents at A and C, and the chord AC. In triangle OAB[1]:

$$R^2 = \frac{d}{2}^2 + (R-x)^2 \qquad \text{(A-11)}$$

which becomes,

$$2R\,x = \frac{d^2}{4} + x^2$$

But since $d^2/4 \gg x$ for a reflector in space,

$$R = \frac{d^2}{8x} \qquad \text{(A-12)}$$

Since for a spherical mirror, the focal length $f = \frac{1}{2}R$, we have also,

$$f = \frac{d^2}{16\,x} \qquad \text{(A-13)}$$

In addition, from Figure A-3,

$$\sin\phi = \frac{d/2}{f} \approx \phi \qquad \text{(A-14)}$$

for small ϕ. But, substituting (A-12),

$$\phi = 4\,x/d \qquad \text{(A-15)}$$

[redacted]

[redacted]

The ground pattern for a concave spherical mirror is illustrated in Figure A.4. To simplify the analysis it has been assumed that:

- the reflector receives the sun's rays from an approximately normal direction.
- the principal axis of the reflector is perpendicular to the ground (note that neither Figure A-4 nor Figure A-1 is drawn to scale).

Further for practical values of deflection x, the focal length f will generally be small compared to H.

The diameter, D, of the ground pattern for the spherical mirror is greater than $H\Theta$, the approximate value found for the plane mirror. The rays belonging to the incident cone 1 are parallel to those in cone 2, and their reflections converge at the focal plane denoted by F'F". The reflected rays denoted 1' and 2' intersect the ground at A' and C', and similarly, points A" and C" are defined. Points B, B', and B" are symmetrically distributed between A and C, A' and C' and A" and C", respectively, with B' and B" being defined by the edge rays of the cone incident at B.

Let $C'A' = C''C'' = dg$. Using $B'B'' = H\Theta$, and $D = C'A''$,

$$D = dg + H\Theta \qquad \text{(A-16)}$$

Since AF'C and A'F'C' are approximately similar triangles

$$\frac{dg}{d} = \frac{(H-f)}{f}$$

and,

$$dg = \frac{(2H-1)d}{R} \qquad \text{(A-17)}$$

Sine $R = d^2/8x$,

$$dg = \frac{16Hx}{d} - d \qquad \text{(A-18)}$$

[redacted]

[redacted]

and thus, (A-16) becomes

$$D = \frac{16Hx}{d} - d + H\Theta$$

$$D = \frac{16Hx}{d} + H\Theta, \qquad \text{(A-19)}$$

since $\frac{16Hx}{d} + H\Theta \gg d.$

Figures A.5a and A.5b show D represented parmetrically as a function of x and d, for altitudes of 10,000 and 19,350 n.mi., respectively. As $x \rightarrow 0$, D approaches its value for the plane case, and the ground diameters are 56.3, 93.8, and 181 n.mi. for the altitudes considered. These numbers are independent of reflector diameter, d. The value of d becomes significant however, when $x > 0$. As x increases, D increases very rapidly for small d, but more slowly as d increases.

Returning to figure A.4, there is a region of constant illumination bounded by A' and C". At every point in this region a reflected ray from every point on the mirror is received. The illumination in this region is equal to that which would be provided by a plane mirror of diameter d. From the geometry,

$$D_c = H\Theta - dg \qquad \text{(A-20)}$$

But from (A-18)

$$D_c = H\Theta - \frac{16\ Hx}{d} + d$$

$$\text{and } D_c = H\Theta - \frac{16\ Hx}{d} \qquad \text{(A-21)}$$

since $H\Theta \gg x$

Of particular interest is the special case in which $D_c \rightarrow 0$ as x increases Designating the limiting value of x as x_o (Figure A-6), we get from (A-21),

$$x_o = \frac{\Theta d}{16} \qquad \text{(A-22)}$$

[redacted]

[redacted]

In Figure A-7, x is plotted versus d. If $x > x_o$, the illumination directly below the mirror will decrease. In general this will be the case, as manufacturing tolerances require considerably larger values of x than are in Figure A-7.

The calculation of $\bar{E}$ and $\bar{E}_N$ for the spherical concave and spherical convex mirror is quite lengthy. The results are:

$$\bar{E} = \frac{E_o \tau}{H^2\left[\frac{\theta}{d} + \frac{16x}{d^2}\right]^2} = \frac{E_o d^4 \tau}{\left[16H(x+x_o)\right]^2} \quad ; \quad x \geq 0 \qquad \text{(A-23)}$$

$$E_N = \begin{cases} \tau \frac{d^2 E_o}{\theta^2 H^2} \; ; & 0 \leq x \leq x_o \\ \tau \frac{E_o d^4}{(16xH)^2} \; ; & x \geq x_o \end{cases} \qquad \text{(A-24)}$$

In Figures A-8 and A-9 values of H_1 d and x yielding minimum acceptable and full moon illumination respectively are shown.

A.4 Additional Considerations

Two more aspects of the geometrical problem must be considered for the case of actual reflectors.

- the case of oblique incidence of the sun's rays on the reflector
- the possibility that the target will not lie directly below the target.

In the first case, for small angles of incidence, i, the results are similar to those derived for the plane mirror which has been rotated through an angle ϕ. The projection of the area of the mirror in a plane perpendicular to the sun's rays becomes $A_1 \cos i$, where A_1 is the cross-section for normal incidence; thus $\bar{E}$ is also decreased by a factor of cosi. The entire ground pattern is shifted in a way similar to the case illustrated in Figure A-2. However, as i increases some degree of distortion appears in the pattern. Further study of the case when i is large is required to determine the correction factor needed in addition to cosi. When the reflector is not directly over

[redacted]

[redacted]

the target, the area of ground illumination becomes $A_2 / \cos \alpha$, where α is the complement of the elevation angle of the reflected rays (measured from the target). Thus, effectively, the value of $\bar{E}$ is reduced by a factor of $\cos \alpha$. This is a good approximation for large H.

Additional problems are raised, however, by oblique illumination, involving shadows and contrast on the ground. But before these can be solved, a firm decision is required on the nature of the illumination desired.

[redacted]

[redacted]

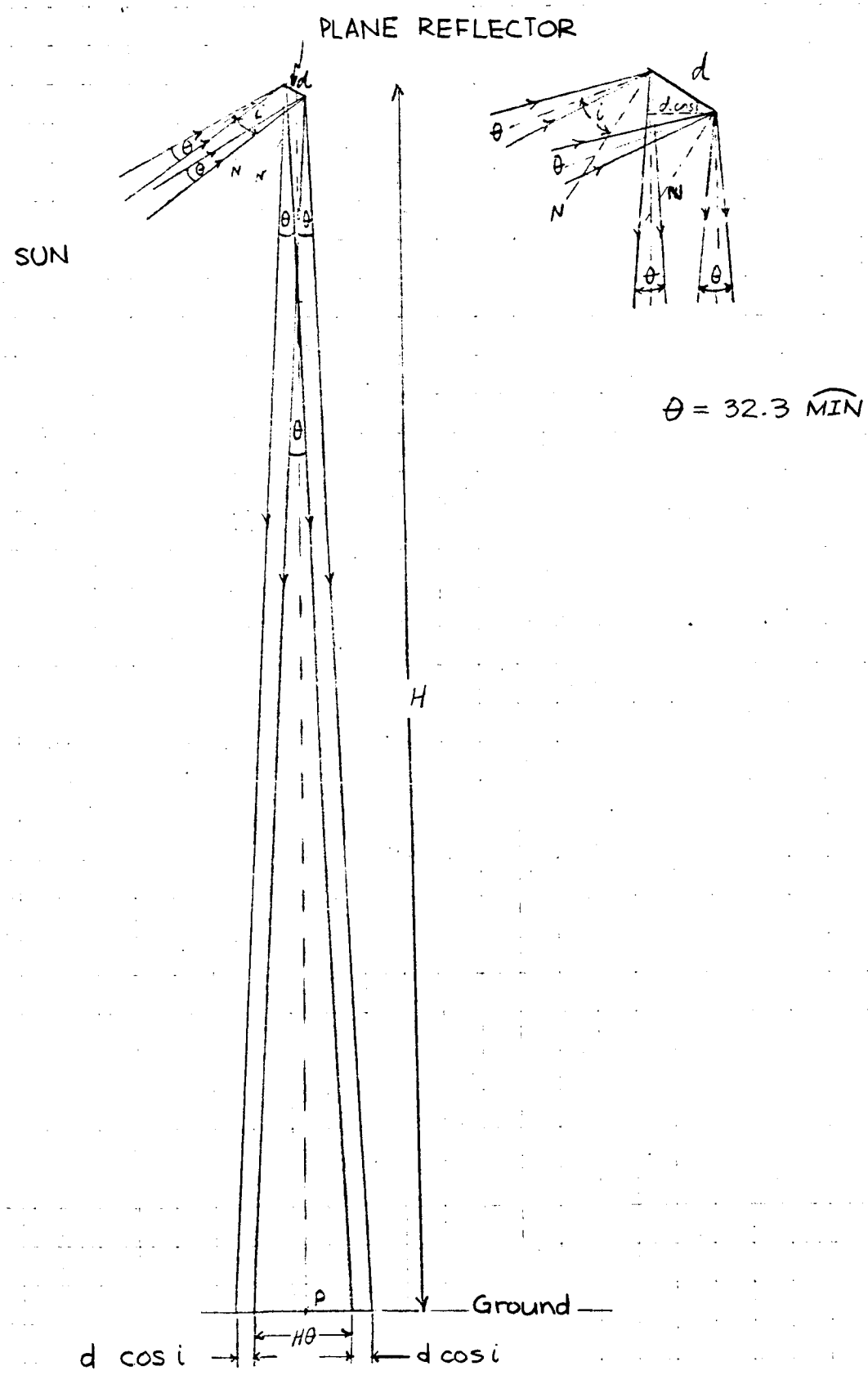

FIGURE A-1 GROUND PATTERN OF A PLANE REFLECTOR

[redacted]

[redacted]

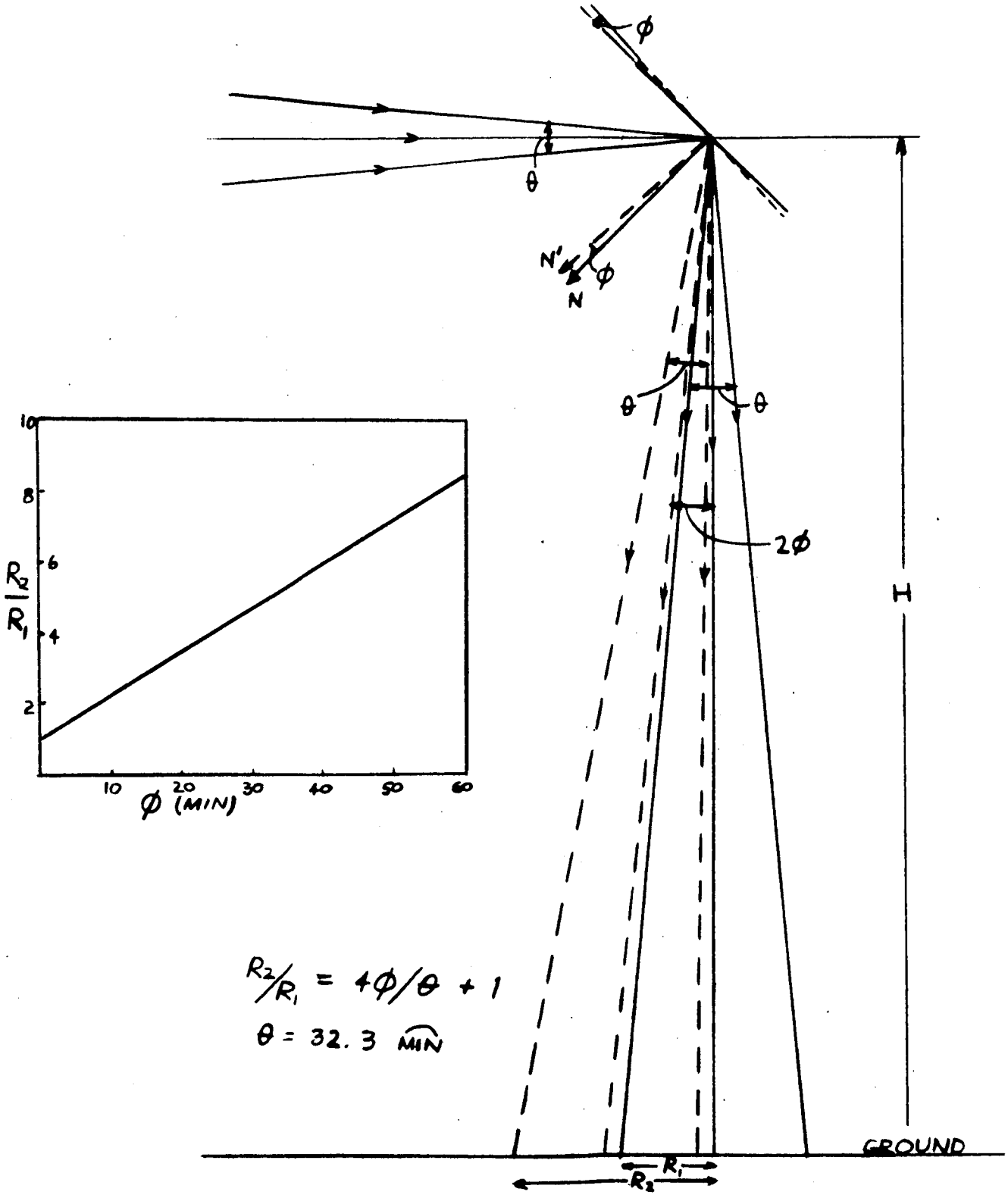

FIGURE A-2 SHIFT OF GROUND PATTERN DUE TO INCLINED MIRROR ELEMENT

[redacted]

[redacted]

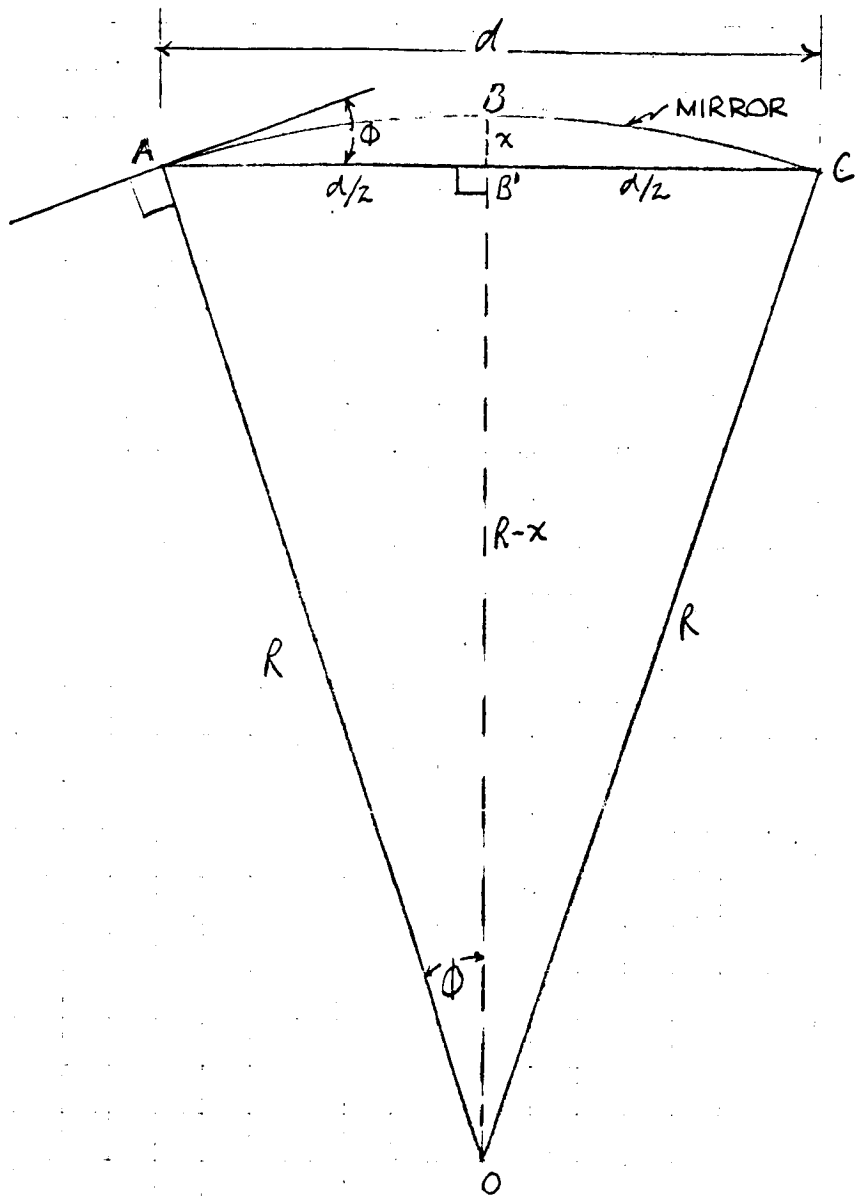

FIGURE A-3 GEOMETRY OF A SPHERICAL MIRROR

[redacted]

[redacted]

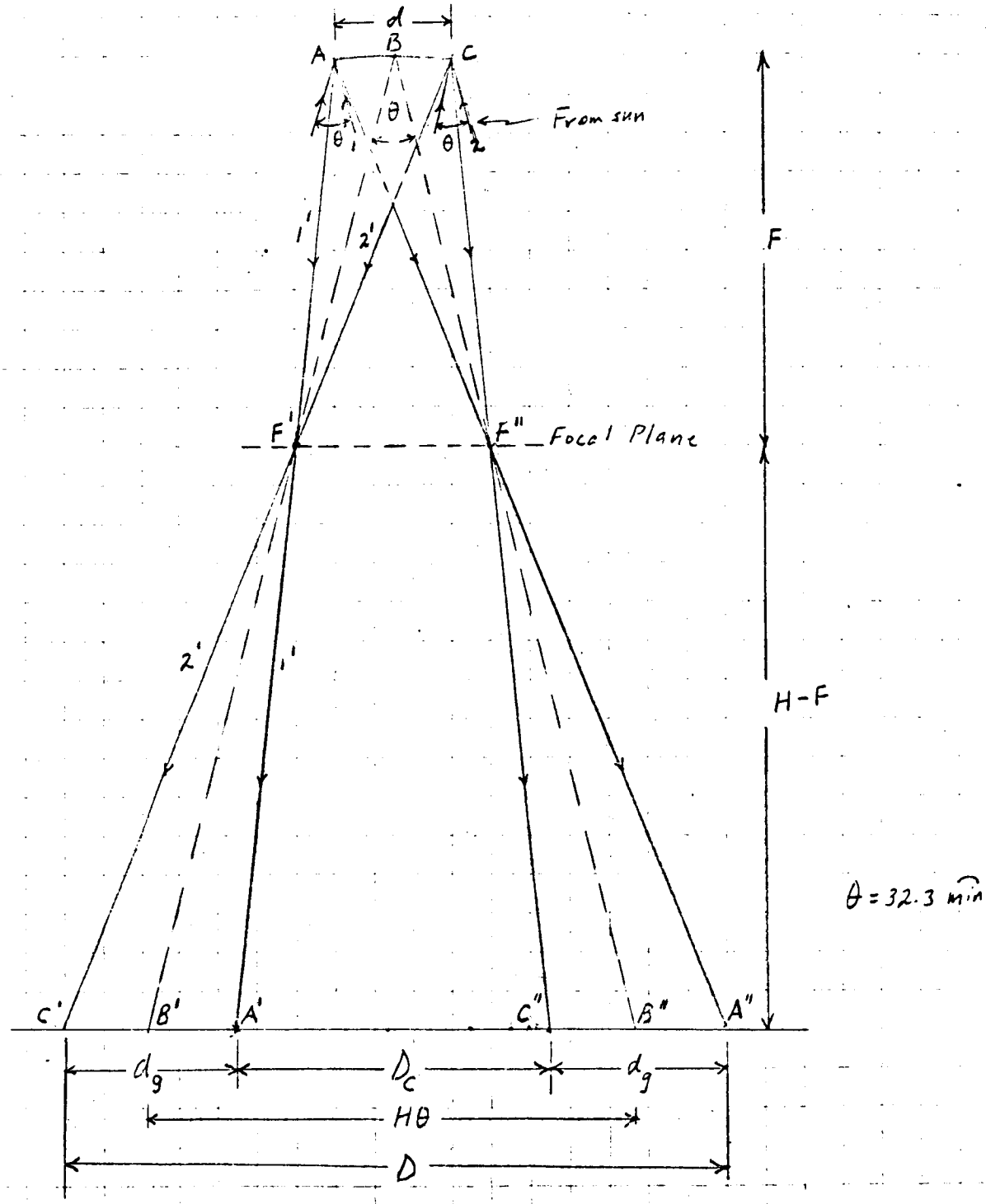

FIGURE A-4 GROUND PATTERN OF A PERFECT CONCAVE REFLECTOR

[redacted]

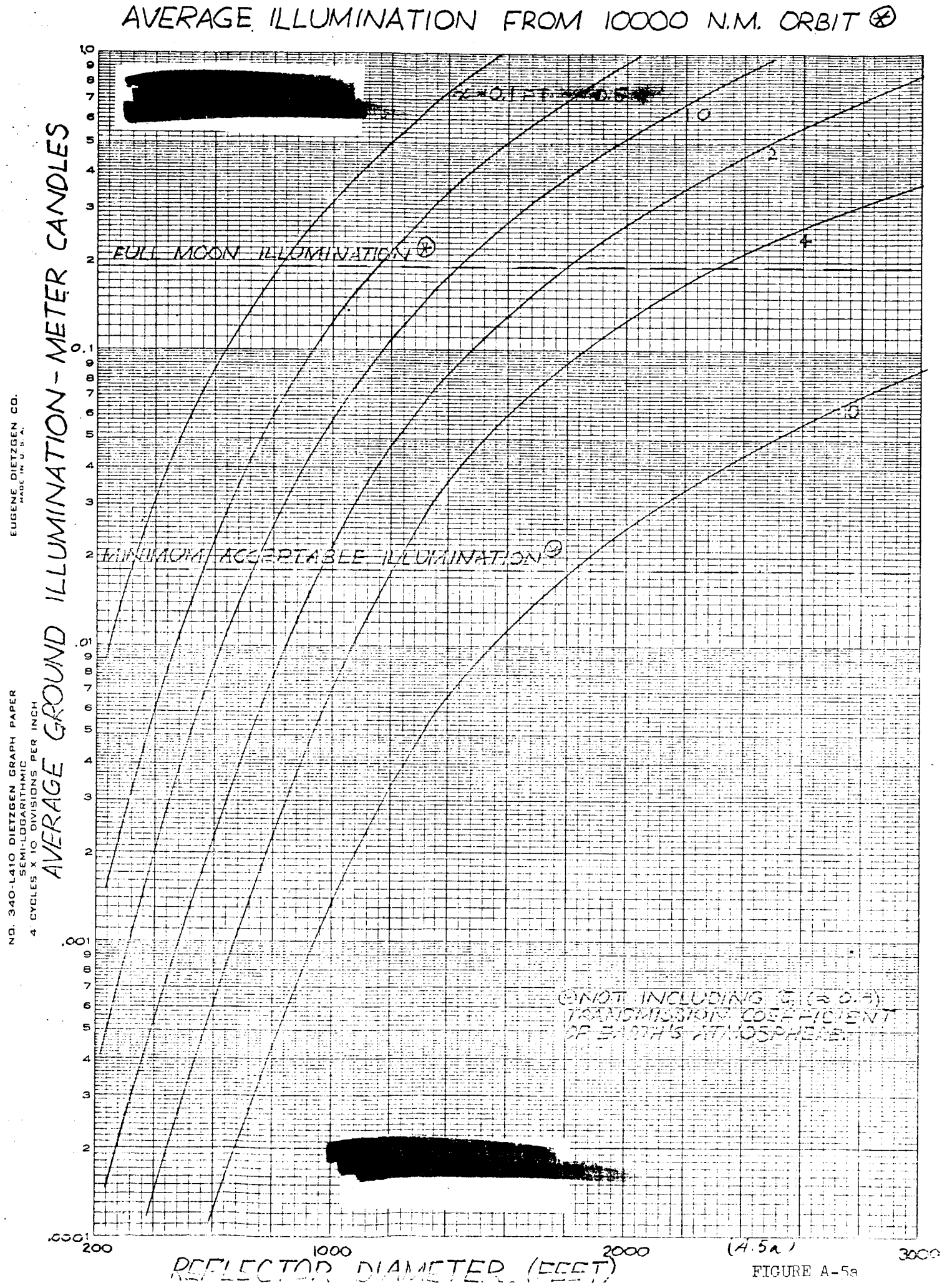
AVERAGE ILLUMINATION FROM 10000 N.M. ORBIT ⊛
[redacted]
FULL MOON ILLUMINATION ⊛
MINIMUM ACCEPTABLE ILLUMINATION ⊛
(NOT INCLUDING G (≈ 0.9) TRANSMISSION COEFFICIENT OF EARTH'S ATMOSPHERE)
[redacted]
AVERAGE GROUND ILLUMINATION - METER CANDLES
REFLECTOR DIAMETER (FEET)
10
1.0
0.1
.01
.001
.0001
200
1000
2000
3000
(4.5a)
EUGENE DIETZGEN CO.
MADE IN U.S.A.
NO. 340-L410 DIETZGEN GRAPH PAPER
SEMI-LOGARITHMIC
4 CYCLES X 10 DIVISIONS PER INCH

FIGURE A-5a

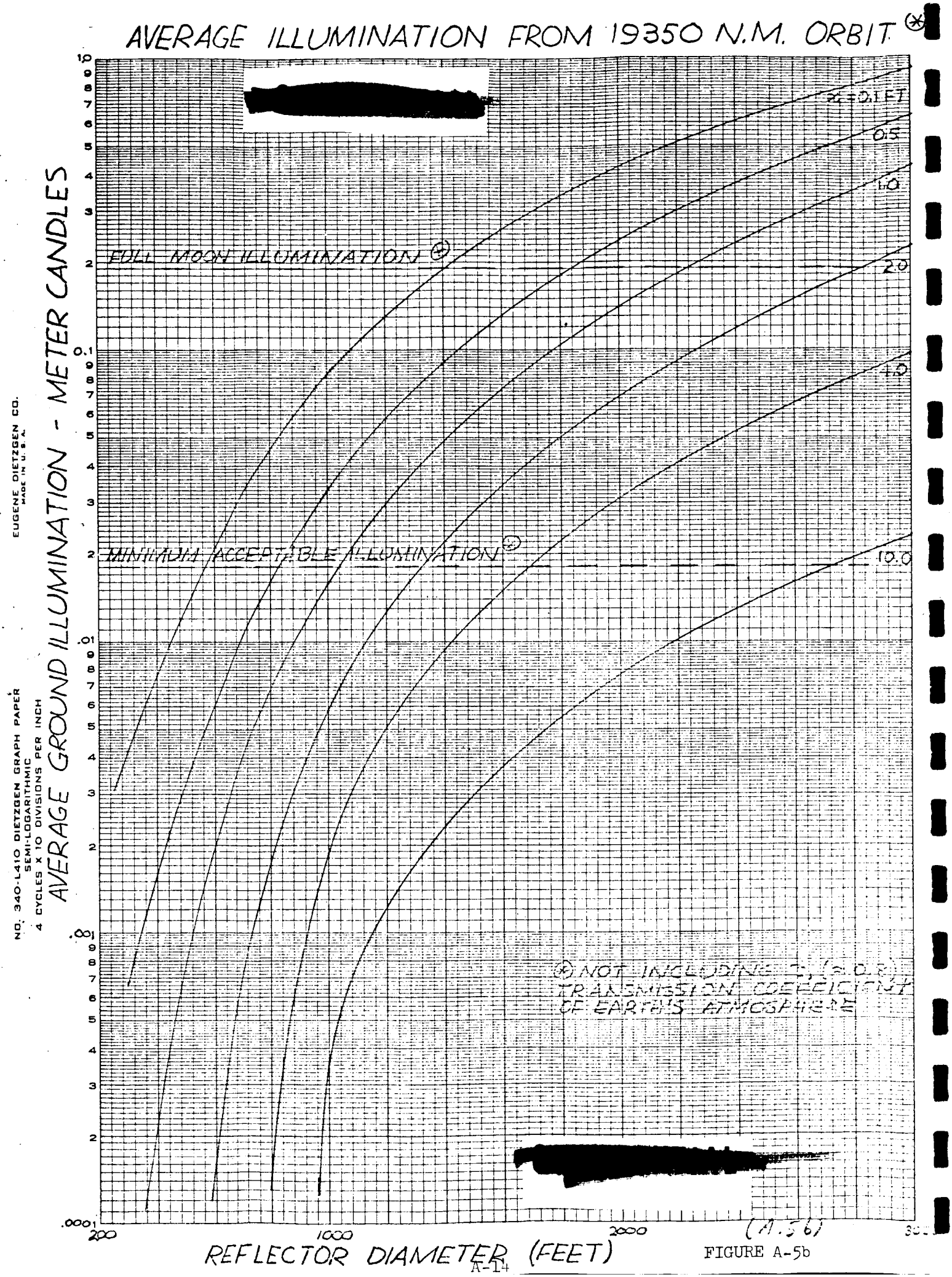
AVERAGE ILLUMINATION FROM 19350 N.M. ORBIT (*)
[redacted]
α_t = 0.1 FT
0.5
1.0
2.0
5.0
10.0
FULL MOON ILLUMINATION (*)
MINIMUM ACCEPTABLE ILLUMINATION (*)
(*) NOT INCLUDING τ_t (≈ 0.8) TRANSMISSION COEFFICIENT OF EARTH'S ATMOSPHERE
[redacted]
AVERAGE GROUND ILLUMINATION - METER CANDLES
REFLECTOR DIAMETER (FEET)
200
1000
2000
(A.5b)
EUGENE DIETZGEN CO.
MADE IN U.S.A.
NO. 340-L410 DIETZGEN GRAPH PAPER
SEMI-LOGARITHMIC
4 CYCLES X 10 DIVISIONS PER INCH

FIGURE A-5b

[redacted]

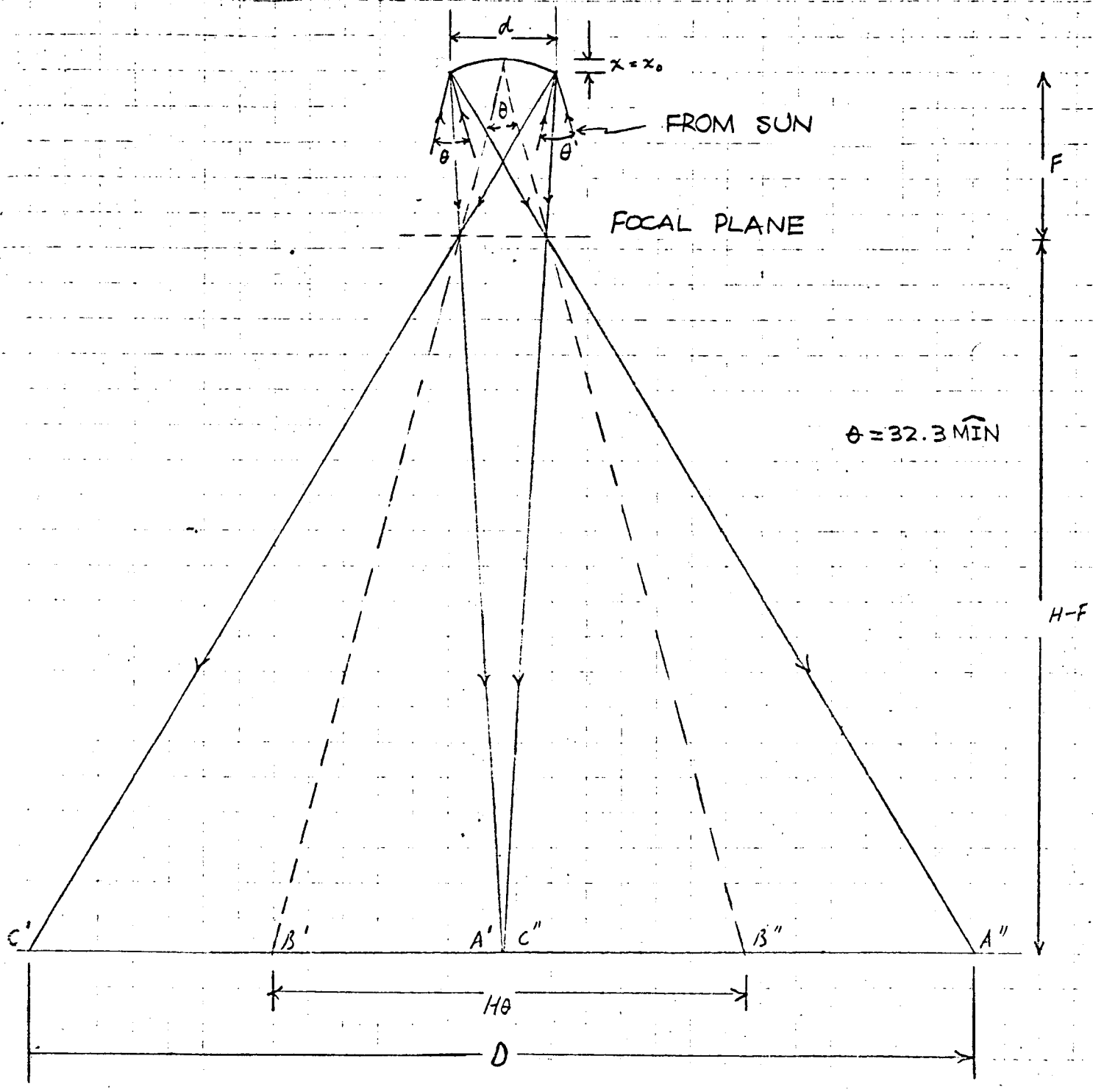

FIGURE A-6

GROUND PATTERN OF A PERFECT CONCAVE REFLECTOR

[redacted]

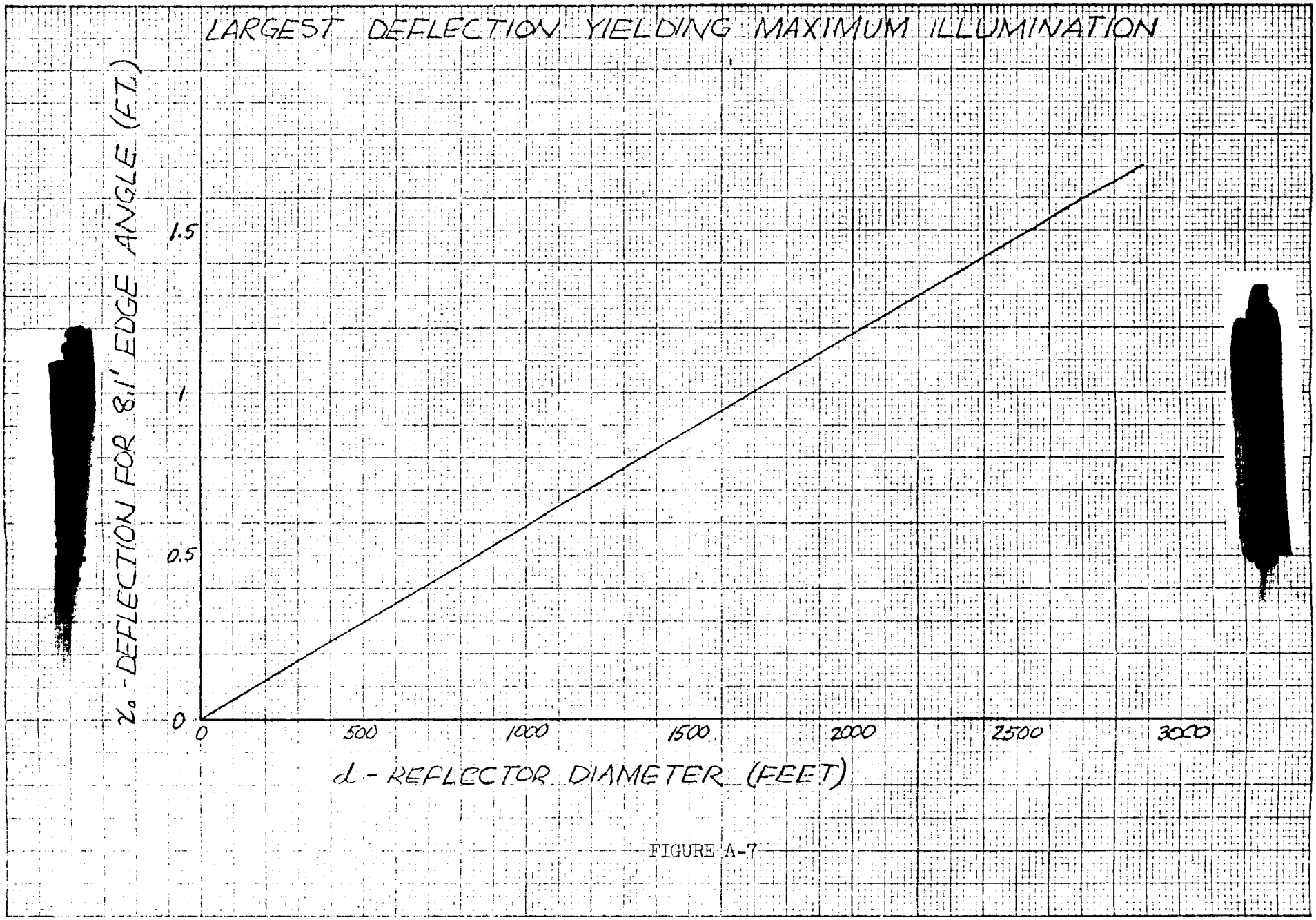
LARGEST DEFLECTION YIELDING MAXIMUM ILLUMINATION
α_0 - DEFLECTION FOR 8.1' EDGE ANGLE (FT.)
1.5
1
0.5
0
0
500
1000
1500
2000
2500
3000
d - REFLECTOR DIAMETER (FEET)

FIGURE A-7

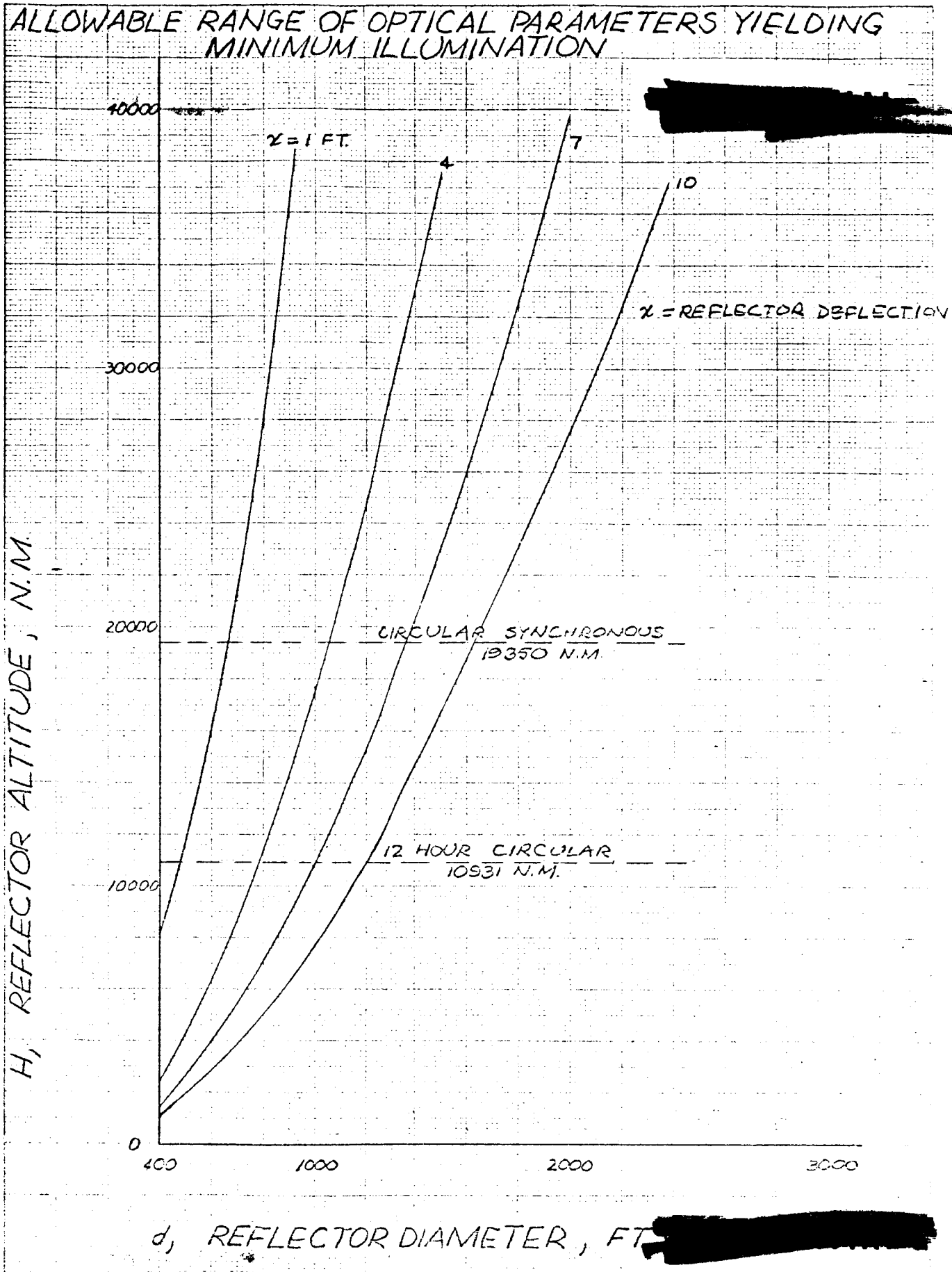
ALLOWABLE RANGE OF OPTICAL PARAMETERS YIELDING MINIMUM ILLUMINATION
[redacted]
40000
30000
20000
10000
0
400
1000
2000
3000
x = 1 FT.
4
7
10
x = REFLECTOR DEFLECTION
CIRCULAR SYNCHRONOUS
19350 N.M.
12 HOUR CIRCULAR
10931 N.M.
H, REFLECTOR ALTITUDE, N.M.
d, REFLECTOR DIAMETER, FT [redacted]

FIGURE A-8

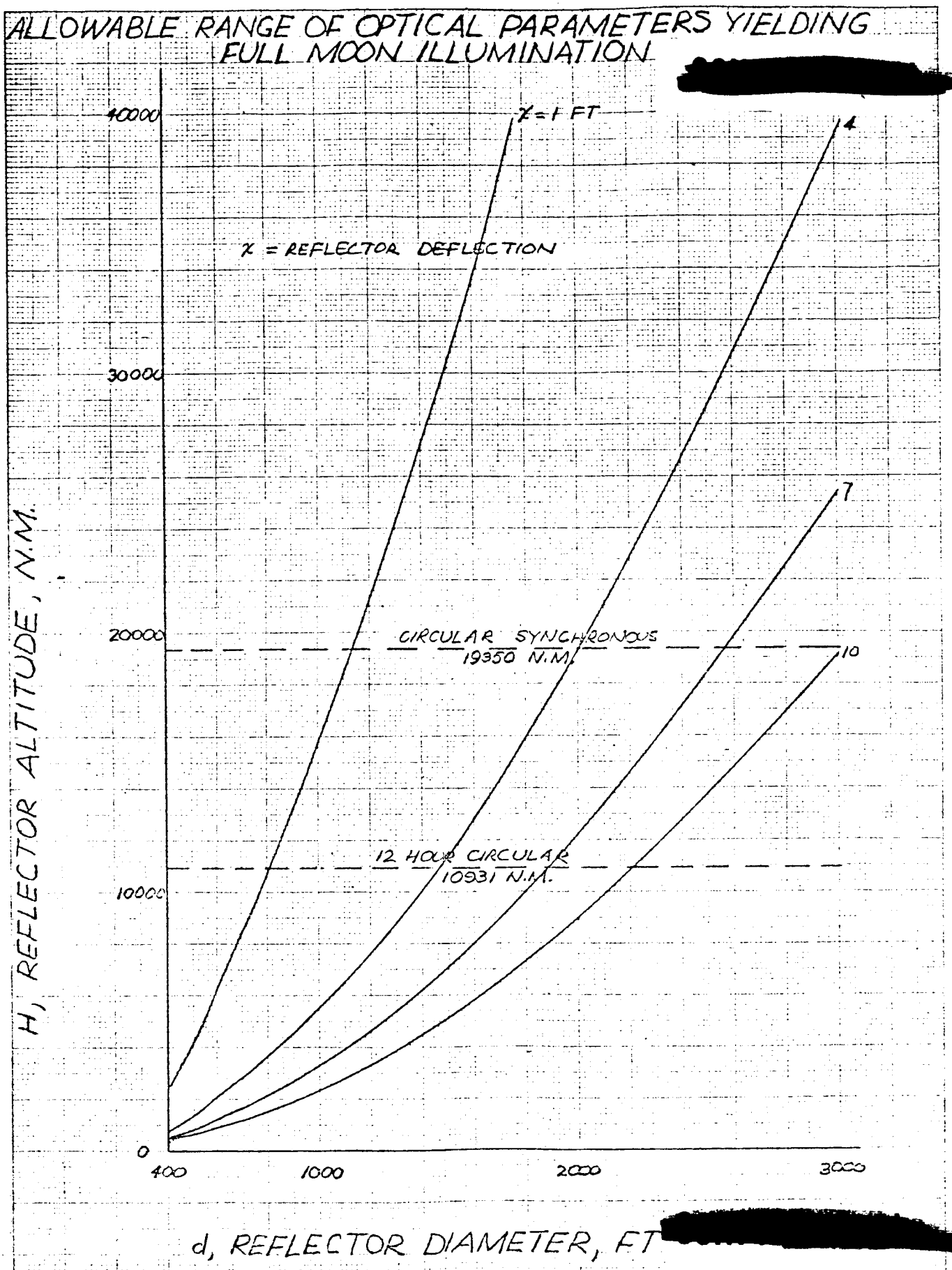
ALLOWABLE RANGE OF OPTICAL PARAMETERS YIELDING FULL MOON ILLUMINATION
[redacted]
χ = 1 FT
4
χ = REFLECTOR DEFLECTION
7
CIRCULAR SYNCHRONOUS
19350 N.M.
10
12 HOUR CIRCULAR
10931 N.M.
40000
30000
20000
10000
0
400
1000
2000
3000
H, REFLECTOR ALTITUDE, N.M.
d, REFLECTOR DIAMETER, FT
[redacted]

FIGURE A-9

[redacted]

APPENDIX B

STRUCTURAL ANALYSIS

B.1 INFLUENCE COEFFICIENTS

A generalized matrix solution for complex structures was utilized to solve for internal member loads and deflections. In particular, the Grumman ASTRAL System in conjunction with the IBM 7094 Digital Computer proved most efficient for rapid solutions. In this analysis, the structure is broken up into basic elements and a mathematical model is defined. The first portion of the program creates a load and stiffness matrix for each element. These matrices thus express the loads as a function of displacements. Thus, $\{f_j\} = [K_G]\{\delta_j\}$, where $\{\delta_j\}$ are the nodal displacements that affect that particular element and $\{f_j\}$ are the nodal forces corresponding to $\{\delta_j\}$. The sub-matrices of the total stiffness matrix $[K_T]$ are created by summing the appropriate member stiffness matrices. Thus, $[K_{Tij}] = \sum^{m} [K_G]$, where the indices i and j indicate the row and column sub-matrix of $[K_T]$ and n are the number of elements that have a node which lie in either zone j or i. The external load matrix is also read into the computer and automatically partitioned into sub-matrices to match the row partitioning of the stiffness matrix. Boundary conditions are applied to both the stiffness and external load sub-matrices to yield the blocks of the final system of equations. Substituting these deflections back into the total stiffness sub-matrices yields: $\{F_{Ji}\} = [K_{Tij}]\,[DEFL_j]\{\mathcal{L}\} = [N_{Fi}]\{\mathcal{L}\}$ which are the nodal forces induced at all the nodes due to the applied loading conditions.

Hence, the $[DEFL]$ deflections express $\{\Delta_j\}$ in terms of $\{\mathcal{L}\}$ and $[N_F]$ nodal forces are obtained as a result of substituting displacements into the stiffness matrix $[K_T]$. Also, realizing that the matrix of stiffness influence coefficients and the matrix of flexibility influence coefficients are reciprocal matrices, one is readily obtained from the other. That is:

$$[K_{ij}] = [BC_{ii}]^T\,[K_{Tij}]\,[BC_{jj}]$$
$$[L_i] = [BC_{ii}]^T\,[L_{Ei}]$$

where $[BC_{ii}]$ refers to the boundary conditions for the ith zone. A table of boundary conditions is maintained in the core of the computer which is used to remove the appropriate rows and columns from the $[K_{Tij}]$ and $[L_{Ei}]$ matrices.

[redacted]

[redacted]

For the solution of nodal displacements, the tri-diagonal stiffness matrix is first split into two matrices $[A]$ and $[B]$, where $[A]$ is a lower triangular matrix and $[B]$ is an upper triangular matrix. The recurrence relations are obtained by multiplying the matrices $[A]$ and $[B]$ and equating the results to the sub-matrices of $[K]$.

The system of equations:

$$[A]\,[B]\,\{\Delta_{JF}\} = [K]\{\Delta_{JF}\} = [L]\{\mathcal{L}\}$$

may be re-written as:

$$[A]\{Z\} = [L]\{\mathcal{L}\}$$

where $\{Z\} = [B]\{\Delta_{JF}\}$

Δ_{JF} = nodal displacement

$\{\mathcal{L}\}$ = column of loading conditions

$[L]$ = loads at free nodes

Since the $[A]$ matrix is a lower triangle, it is easy to solve $[A]\{Z\} = [L]\{\mathcal{L}\}$ to attain values for the intermediate variables $[Z_i]$ as a function of $\{\mathcal{L}\}$. Once the values of $\{Z_i\}$ have been computed, they are used to obtain the nodal displacements $\{\Delta_{JF}\}$ by using the system of equations as given by $\{Z\} = [B]\{\Delta_{JF}\}$. Ultimately, $\{\Delta_{JFi}\} = [D_i]\{\mathcal{L}\}$ is obtained and expanded back into the original order. This is identical to performing the matrix operation

$$\{\Delta_{Ji}\} = [BC_{ii}]^T\,[D_i]\{\mathcal{L}\} = [DEFL_i]\{\mathcal{L}\}$$

B.2 LAUNCH AND BOOST ENVIRONMENT

The canister containing the reflector assembly may be supported under the descent stage structure of the Lunar Excursion Module during the launch and boost phase of the mission. The total package has been designed to withstand the loading conditions resulting from this phase of the mission. Given below

[redacted]

[redacted]

are the loadings experienced by the LM vehicle.

Accelerations

	X		Y		Z	
	g	$\frac{rad}{sec^2}$	g	$\frac{rad}{sec^2}$	g	$\frac{rad}{sec^2}$
Lift-off Condition	+1.60	-	±.65	-	±.65	-
Max q Condition S-IC	+2.07	-	±.30	-	±.30	-
End Boost Condition S-IC	+4.90	-	±.10	-	±.10	-
Engine Hard Over S-IC	-1.70	-	±.10	-	±.10	-
Engine Hard Over S-II	+2.15	-	±.40	-	0	-
Engine Hard Over S-II	+2.15	-	0	-	±.40	-

Acoustics

(Sound pressure levels in db external to LM)

(re. .0002 dynes/cm^2)

Octave Band cps	C5 at Max Level (db)
9 to 18.8	136
18.8 to 37.5	142
37.5 to 75	146
75 to 150	143
150 to 300	139
300 to 600	135
600 to 1200	130
1200 to 2400	125
2400 to 4800	119
4800 to 9600	113
overall	150

Vibration

The mission vibration environment is represented by the following random and sinusoidal envelopes considered separately as inputs to the equipment supports.

[redacted]

1) Input from Exterior Primary Structure

a) Random

10 to 23 cps	12 db/octave rise to
23 to 80 cps	0.0148 g^2/cps
80 to 105 cps	12 db/octave rise to
105 to 950 cps	0.044 g^2/cps
950 to 1250 cps	12 db/octave decrease to
1250 to 2000 cps	0.0148 g^2/cps

b) Sinusoidal

5 to 18.5 cps	0.154 inches D. A.
18.5 to 100 cps	2.69 g peak

2) Input from Interior Primary Structure

a) Random

10 to 23 cps	12 db/octave rise to
23 to 80 cps	0.0148 g^2/cps
80 to 100 cps	12 db/octave rise to
100 to 1000 cps	0.0355 g^2/cps
1000 to 1200 cps	12 db/octave decrease to
1200 to 2000 cps	0.0148 g^2/cps

b) Sinusoidal

5 to 16 cps	0.154 inch double ampl.
16 to 100 cps	1.92 g peak

During the launch and boost phase of flight, the vehicle is exposed to random vibration of varied levels and spectra for 17 minutes. During all but approximately 2.5 minutes of this period, the intensity of random vibration is of such a low level that it is considered to be of negligible design significance. In addition, the launch and boost environment is considered to include peak vibration levels which are represented by the above sinusoidal vibration envelopes. The number of sinusoidal peaks for design can be considered to be one percent of the natural frequency of the equipment being designed times the number of seconds of exposure. For design purposes, the above random spectrum applied for 5 minutes, along each of the three mutually perpendicular axes x, y, z, when applied in addition to the above sinusoidal vibration for 300 seconds exposure time will adequately represent the vibration environment.

[redacted]

B.3 CALCULATION OF NATURAL FREQUENCY

A preliminary analysis was made to determine the natural frequency of vibration of the combined support structure and reflector. For this study, an eight pointed star configuration was used and the results are shown in the curve.

In order to obtain preliminary frequency data, a simplified analysis of an 8 point star configuration was made (see Figure below):

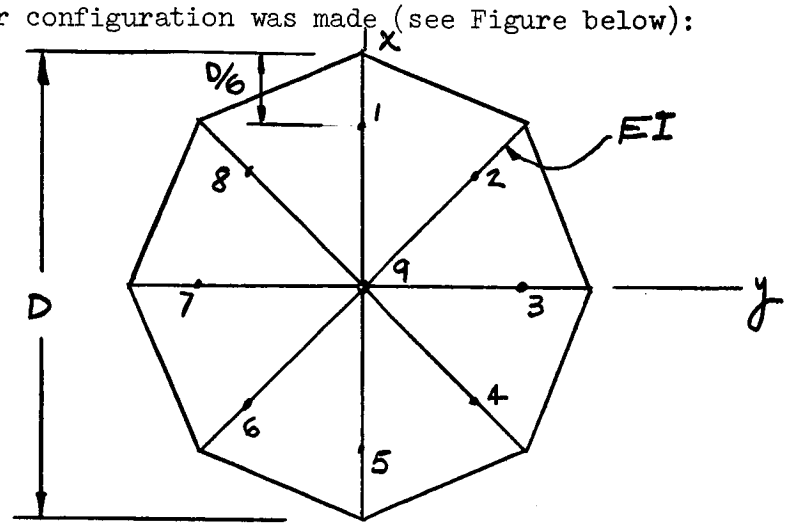

The star was divided into 9 mass points and it was assumed that the first mode was symmetrical bending (i.e., $Z_1 = Z_2 = \ldots = Z_8$). With these assumptions the first natural frequency is given by:

$$f = \frac{1}{2\pi} \sqrt{\frac{24EI}{D^3} \left(\frac{8}{M_9} + \frac{1}{M_1} \right)}$$

Fig. 6.4-6 shows the variation of natural frequency versus diameter (D). It is expected that similar values would be obtained for torus spoke configurations of the same size.

[redacted]

[redacted]

APPENDIX C - THERMAL ANALYSIS

C.1 REFLECTOR THERMAL ANALYSIS

Parameters affecting reflector temperature are (a) orbital parameters such as altitude and attitude, and (b) material thermal properties such as absorptance/emittance ratio (α/ϵ). Figure C.1-1 provides information relating these parameters to reflector temperature.

By far, the most important parameter for a given reflector orientation is the ratio (α/ϵ). The plot shown in Fig. C.1-1(a) is for the case of the reflector normal to the earth-sun line with the reflector in the high noon position (Case A). In this orientation, reflector temperatures ranging from approximately 25°F to 400°F may be obtained by varying (α/ϵ) from 0.4 to 4.0 respectively.

The effect of orbital parameters on reflector temperature is also shown in Fig. C.1-1(a). For the high noon case (Case A) the effect of altitude on temperature is rather insignificant for altitudes above 6,000 miles. However for the case where the reflector is in the shadow of the earth (Case B), the reflector temperature is relatively sensitive to changes in altitude. Since there is no solar energy impinging on the reflector in this condition the ratio (α/ϵ) has no effect on temperature. An additional orbital parameter having a major effect on temperature is orbital attitude. This is shown in Fig. C.1-1(b).

The steady-state temperature range that will be traversed in one orbit, for a particular value of (α/ϵ), orbital altitude, and reflector orientation, is shown in Fig. C.1-2. The same type of information for a synchronous orbit is shown in Fig. C.1-3.

The thermal analysis was based on the heat flux environment as described in Appendix C.3.

C.2 REFLECTOR SUPPORT STRUCTURE THERMAL ANALYSIS

For any given orbital position of the spacecraft the heat flux distribution around a cross section of the support structure will be non-uniform. This leads to temperature differences within the structure and possible thermal distortion problems.

[redacted]

C.2 (continued)

The temperature differences within the support structure as well as the absolute temperatures attained by the various positions on the cylinder cross section, for any given set of orbital parameters, is dependent on internal and external surface thermal properties. Fig. C.2-1 illustrates the effect of internal surface emittance on structure temperatures for two different values of α/ϵ when the structure is in the high-noon position at an altitude of 8,000 n.mi. This plot indicates that the temperature difference across the cylinder cross section decreases with increasing internal emittance. Fig. C.2-2 provides similar information for the orbital condition of the spacecraft in the earth shadow. Fig. C.2-3 is a plot of the temperature distribution around the cylinder cross section for the high-noon position at an altitude of 8,000 n.mi. Note that the entire maximum temperature difference occurs in a 90° section of the structure.

Figs. C.2-4 through -6 provide similar information to Figs. C.2-1 through -3 for the synchronous orbit.

Fig. C.2-7 is a parametric study of the maximum structure temperature difference vs the external absorptance to emittance ratio (α/ϵ) for a series of different solar absorptances (α) and a constant value of internal surface emittance. It can be concluded from this plot that it is possible to maintain relatively low levels of temperature difference if (α/ϵ) is relatively high and (α) is relatively low. However high values of (α/ϵ) are accompanied by relatively high values of absolute temperature as indicated in Fig. C.2-8.

A concept to reduce temperature differences and thereby reduce thermal distortions within the structure consists of effectively isolating the structure from the heat flux environment through use of crinkled aluminized mylar type super insulation. The insulation can be installed in such a manner that it will be free to expand or contract without distorting the structure.

The data presented in Fig. C.2-9 represents the temperature information for a cylindrical structure "isolated" from the space heat flux environment by thermal radiation shields, the outermost shield serving also as a thermal control skin which can be coated to achieve desirable thermal properties. Temperatures at various positions in the structure are plotted as a function of overall effective

C.2 (continued)

emittance of the insulation. All temperatures, are plotted for thermal control skin absorptance to emittance ratios (α/ϵ) of 2.0 and 4.0. In addition Curves 3 and 4 have been replotted in Figure C.2-10 (T_3-T_4) or the temperature difference in the structure as a function of insulation emittance. It should be noted that the use of (α/ϵ) = 2.0 as opposed to (α/ϵ) = 4.0 had an indiscernable effect on temperature difference and thus only one curve is shown in Fig. C.2-10. However, the higher value of (α/ϵ) results in the insulation shields as well as the structure achieving higher absolute temperatures.

The particular value of effective insulation emittance can be obtained by varying either the number of shields or the surface properties of each shield or most likely a combination of both. Fig. C.2-11 provides information that enables selection of a particular combination. Curves I and II provide the effective emittance values for ideal thermal shields having the surface properties associated with the materials described on the Figure. Curves III and IV present a more realistic approach by including a wrap factor of 2.0 to account for additional heat leaks resulting from outgassing orifices, conduction at insulation contact points, etc.

An important factor to consider in establishing insulation requirements is the weight penalty involved. The weight of the thermal control layer utilized in the following analysis was based on the need for a relatively substantial base for a control coating. However as previously noted the external thermal properties of the thermal control layer does not affect the temperature difference in the structure but does affect the absolute temperature. Therefore as long as the temperature of the insulation does not rise above acceptable levels for the material a wide range of thermal coatings could be used therby eliminating the need for a "heavy" control layer. Fig. C.2-12 presents pertinent weight information for a 1,100 ft diameter reflector. Plot (a) indicates the weight of insulation as a function of the number of shields comprising the blanket. Note that for zero layers (i.e., only a thick thermal control layer covering the structure) the weight is 740 lbs. Plot (b) presents a direct tradeoff analysis of insulation weight as a function of temperature difference in the structure. If the thermal control layer is simply an additional layer of super insulation coated with a compatible control coating, a weight saving of 550 lbs may be realized

C.2 (continued)

thereby reducing all weights shown on the scales of Fig. C.2-12 by 550 lbs. This reduction is shown in Fig. 4.4-3 and represents the most likely design concept.

C.3 EXTERNAL THERMAL ENVIRONMENT

The external thermal environment to which the spacecraft is subject consists of direct solar radiation, earth reflected solar radiation (earth albedo), and earth emitted radiation. The thermal radiation intensities depend on the orbit, vehicle orientation and the location of the sun relative to the orbital plane. The angle between the solar vector and the orbital plane Θ_s, varies as a function of the orbit inclination, and the time of launch. The angle Θ_s has been maintained constant at 0° throughout the data presented in this section. In Table C.3-1 the orbital average of incident thermal radiation is presented for a number of differently oriented surfaces. This data is shown as a function of altitude. Table C.3-2 presents instantaneous values of the various heat fluxes during an orbit for an altitude of 8,000 miles.

C.4 ABLE LM ECS PERFORMANCE

C.4.1 Radiator Sizing

Figure C.4-1 shows the radiator area required to handle various loads (without water supplement) when the radiator is subjected to different levels of absorbed radiation. The figure is based on a constant 41°F glycol temperature leaving the radiator. This temperature is suitable for the temperature sensitive electronic components located in the low temperature electronics section.

For the six month operational phase load of 670 watts (2285 BTU/hr) and with the vehicle in the hot orientation, one radiator panel will act as a heater and would be ineffective due to the action of the intermodular control valve. The second radiator panel, located 180° away from the first panel, would be subjected to an absorbed radiation of 15 BTU/hr-ft^2. Figure C.4-1 shows that for this load and absorbed radiation, a 30 ft^2 radiation is required. Thus, the required radiator size will be 60 ft^2 which is split into two sections of 30 ft^2 each and located 180° apart on the Descent Stage of the vehicle.

[redacted]

C.4.2 Selection of Radiator Control Configuration

Figure C.4-2 shows the minimum load that can be accepted by a 93 ft^2 radiator (absorbing a minimum radiation of zero BTU/hr-ft^2) as a function of the radiator system (type of fluid, type of controls, etc.) employed. The minimum loads were adjusted to account for the 60 ft^2 radiator area required to carry the 670 watt load in a hot environment. The results for each of the radiator control configurations shown in Fig. C.4-2 are:

System A - With no radiator controls and no radiator regenerative heat exchanger, the minimum permissible load would be 5,900 BTU/hr (730 W) to prevent the 35% glycol from falling below 35°F at the radiator exit. This temperature would not introduce freezing problems with the glycol and will be compatible with the electronic equipment located in the low temperature section of the loop.

System B - Switching the fluid to 62½% glycol and incorporating a radiator regenerative heat exchanger will allow the minimum load to fall to 3390 BTU/hr (993 W). This load will result in a minimum glycol temperature of -30°F which is still well above the -65°F freezing point. The radiator regenerative heat exchanger will raise the glycol temperature to the value necessary to satisfy the electronic equipment in the low temperature electronic section.

Systems C & D - Utilization of a radiator control valve and a radiator regenerative heat exchanger. Allows minimum loads of 1470 BTU/hr (430 W) for System C with 35% glycol and 826 BTU/hr. (242 W) for System D with 62½% glycol.

Systems E & F - These systems have the radiator in a separate transport fluid loop with a heat exchanger. This loop has its own pump and also has a control on the heat exchanger. The radiator incorporates no control. The transport fluid for System E is coolant 15 with a freezing point of -145°F. The minimum load for this system is 1,740 BTU/hr. (510 W) for a radiator exit temperature of -100°F. The transport fluid for system F is freon 21 with a freezing point of -211°F. The minimum load for this system is 625 BTU/hr. (183 W) for a radiator exit temperature of -175°F.

System D is the recommended configuration.

The radiator system is supplemented with a water sublimating heat sink during the mission phases preceeding the 6 month phase. The combined system is shown in Fig. 2.2-1.

[redacted]

C.4.2 (continued)

The radiator bypass valve acts to hold a 38°F glycol temperature at the inlet to the water sublimator by controlling the flow rate of glycol through the radiator panels. This ensures adequate load on the water sublimator when the water shutoff valve is open. The control valve downstream of the water sublimator acts to hold a 38°F temperature at the coolant recirculation module inlet. This is accomplished by controlling the flow rate of glycol through the regenerative heat exchanger and ensures proper glycol temperature to the temperature sensitive components mounted on the cold plates downstream of the coolant recirculation module. The intermodular valve controls the flow rate to each of the two radiator panels so that equal glycol exit temperatures are obtained from each panel. This valve has the effect of taking a panel off the line when it is in a very hot environment and acting as a heater. The radiator control valves act to divert the glycol flow in a given panel from the main radiator tubes to a bypass tube on the panel. This has the effect of reducing the radiator capacity and preventing the glycol temperature from falling too close to its freezing point.

C.4.3 Alternate Heat Sink

An all water sublimating heat sink to handle the 670 watt load for the six month unmanned mission phase would require approximately 10,000 pounds of water. This weight penalty is obviously prohibitive. However, for a 14 day mission, the water requirement would be 770 pounds which would be within the LM capability.

C.5 REFLECTOR INFLATION SYSTEM

In the selection of a recommended configuration for the Reflector Inflation System the following two types of systems were considered.

The Echo inflation system used a subliming powder to pressurize a 100 ft diameter spherical satellite. This system has the advantage of not requiring any storage tank or gas handling system. The subliming material is distributed in the folds during packaging and after initial deployment in orbit, solar energy vaporizes the powder, resulting in the required pressure. This type of inflation system requires a very careful thermal analysis of the satellite skin temperature in order to select a substance with the proper sublimation temperature/pressure characteristic and to

C.5 (continued)

determine the correct amount of the substance to use. In addition, the use of a subliming solid as the pressurant requires that the mean temperature of the inflated structure be significantly higher than the nominal ambient temperature (75°F). The vapor pressure of the pressurant at ambient temperature must be sufficiently low to prevent any significant loss of material by sublimation prior to deployment and the vapor pressure at the mean reflector skin temperature must be sufficiently high to insure strain rigidization of the skins.

Uncertainties in the skin temperatures on the torus and spoke support structure will exist because of the complex interchange of radiant energy between the reflector, the torus and the spokes. Also, solar blockage effects and variation in thermal control coatings because of manufacturing tolerances will add to the uncertainties. At locations on the torus where the skin temperature falls below the saturation temperature of the pressurant, condensing and freezing will occur with a consequent lowering of internal pressure. Theoretically, a thermal coating could be chosen for the external skins and a vehicle orientation could be selected which would result in high enough skin temperature to eliminate the possibility of condensation. However, the uncertainties in environment and coating could then result in skin temperatures exceeding the allowable high temperature limits for the material. Therefore, despite the simplicity and relatively low weight and volume of the subliming powder inflation system, its sensitivity to the thermal environment, with all the inherent uncertainties, is sufficient to eliminate this system from further consideration.

The second type of inflation system considered uses a gas stored at high pressure. Although weight and volume penalties are incurred as a result of the storage and handling requirements of a pressurized gas system, the ability of this system to adapt itself to various environmental conditions was considered of prime importance.

Therefore, this concept was selected for the Project ABLE Reflector Inflation System. Having selected the high pressure gas concept for the inflation system, the particular gas and its storage and handling system must be chosen. A study of a number of candidate low-molecular weight gases resulted in the selection of helium as the most suitable gas for the inflation system. Helium was selected because its

[redacted]

C.5 (continued)

low molecular weight and its non-toxic, nonflammable properties result in a reasonable compromise between system weight and safety of handling and storage. In addition, the thermodynamic properties of helium are such that there is no possibility of helium condensing (with a resulting pressure loss) at local cold spots on the skin surface The existence of a variety of qualified helium storage tanks both on LM and other Project Apollo spacecraft, makes the selection of helium as the recommended pressurant, the obvious choice.

The range of gas pressures and temperatures anticipated in the deployed satellite permits the use of perfect gas theory to evaluate the parameters influencing the quantity of helium required From perfect gas theory, the required weight of helium in pounds is determined from the following equation:

$$W = \frac{PV}{RT}$$

where

P is internal pressure in lb/sq. ft.

V is the total volume in cu. ft.

R is the gas constant for helium = 386 ft-lb/lb-°R

T is the gas temperature in deg. R

The internal pressure required for strain rigidization depends on the required stress level in the skin, the skin thickness and the geometry of the inflated structure while the total volume depends on the geometry of the satellite. The temperature of the gas is a function of the skin thermal properties and the environmental thermal radiation. These thermal parameters determine the mean radiation temperature of the support structure which is assumed to equal the temperature of the enclosed gas.

Figure C.5-1 shows the weight of helium necessary to provide the required strain rigidization pressure for the support structure as a function of reflector diameter. Helium weight is shown for support structure diameters of 10, 20 and 30 ft and for gas temperatures of +75°F and -85°F. The resulting internal pressure is sufficient to achieve a minimum skin stress of 5000 psi in all inflatable members. The +75°F and -85°F gas temperatures are based on the support structure skins having an α/ϵ ratio of 1.0 and are the extremes of mean skin temperature in a non-occulted orbit.

[redacted]

C.5 (continued)

Figure C.5-1 shows the limits in reflector size determined by the number of cryogenic helium tanks used. The LM Descent Stage cryogenic tank holds a nominal 49 lbs of helium and if no restrictions are placed on vehicle attitude, the -85°F gas temperature must be assumed.

Having selected helium as the inflation system pressurant, the various existing helium storage tanks must be evaluated to determine their suitability for the Project ABLE mission. The following table lists the characteristics of some of the qualified helium tanks used for pressurizing propellant on Project APOLLO:

Apollo Spacecraft/System	TANK SIZE DIA(in)/Vol (Ft^3)	OPERATING CONDITION Temp/Pressure (psia)	WEIGHT (LB) Tank/Helium
Service Module/ Propulsion (Block I)	41 / 21	Ambient / 4400	392 / 47
LM/RCS	12.5 / .60	Ambient / 3050	8.3 / 1.03
LM/Ascent Propulsion	24 / 4.2	Ambient / 3500	53.8 / 6.5
LM/Descent Propulsion	33 / 10.8	Cryogenic / 1550	113.6 / 49.2

The LM RCS helium tanks are recommended for the peripheral tanks used to deploy the reflector. The main tanks used for final inflation and strain rigidizing the structure were selected from among the remaining tanks listed in the table.

Four alternate systems, designated as Configurations A through D, are evaluated in selecting the main helium storage tank. Configurations A and B use LM Descent Stage cryogenic tanks, Configuration C uses LM Ascent Stage Ambient tanks and Configuration D uses Service Module Block I ambient tanks. Figure C.5-2 shows the four configurations schematically.

In the LM Descent Propulsion System, cryogenic helium flows first through an external heat exchanger where it is heated by fuel flowing to the engine. The helium then flows to heat exchanger located within the helium tank where it heats up the helium in the tank. The helium then makes a second pass through the external heat exchanger and goes to the propellant tanks. Since there is no propulsion requirement for the Project ABLE LM, there is no fuel to provide heat for the cryogenic helium. The basic difference between Configurations A and B is the method used to heat the cryogenic helium. Configuration A uses the Descent

C.5 (continued)

Propulsion System Fuel/Helium heat exchanger with glycol from the ECS heat transport loop substituting for the fuel as the heating medium. Using this method, waste heat from the vehicle provides the thermal energy necessary to remove the helium from the tank and heat it to ambient temperature. Configuration B eliminates the Fuel/Helium heat exchanger and uses battery powered electrical heaters to heat the helium. Configurations C and D do not require any heat because the helium is stored at ambient temperatures.

The total inflation system weight as a function of helium weight is shown in Figure C.5-3 for the four configurations. The total system weight includes the helium weight, the tank weight, and an assumed weight of 10 lb for plumbing. Configuration A has an additional fixed weight penalty of 10.5 lbs. for the heat exchanger. Configuration B has an additional variable weight of 2.13 lbs. of battery per lb. of helium. In figure C.5-3 each vertical line segment shown for Configurations A, B and D represents an additional tank. The actual system weight curve for Configuration C consists of numerous small increments because of the small tank capacity, however, the curve shown for Configuration C in Figure C.5-3 is the average system weight. It is seen that for any inflation system requiring more than 10 lbs of helium a cryogenic storage system has a substantial weight advantage over an ambient storage system. Furthermore, for cryogenic storage systems, the weight savings realized by using waste heat from the ECS, instead of electric energy from batteries, is significant.

Another parameter which might be important in selecting the storage and delivery system is the time required for inflating and rigidizing the satellite. In order to illustrate the effects of inflation time for the various configurations, it is necessary to analyze a particular geometry satellite. An 1100 ft. diameter reflector with a 20 ft diameter support structure (having a total inflatable volume of 1,800,000 cu. ft.) was chosen as a representative geometry. Figure C.5-4 shows the inflation time versus the helium flow rate for this configuration for the range of environmental temperatures expected. The configurations with cryogenic storage tanks have a limited rate at which they can deliver helium to the reflector system. Configuration A has a helium delivery rate varying between 3.2 and 6.4 lb/hr depending on the ECS loop heat rejection load. Configuration B is limited to a

[redacted]

C.5 (continued)

helium flow rate of about 11 lbs/hr per battery if the maximum power delivered by a battery is 2 KW. Ambient storage tanks do not require any heat and, therefore, place no constraints on inflation time. Figure C.5-4 shows that the inflation time with a Configuration inflation system varies between 9 and 26 hours.

General conclusions from this study are that cryogenic storage tanks offer substantial weight advantages over ambient storage tanks. However, the cryogenic tanks dictate much longer inflation times.

[redacted]

[redacted]

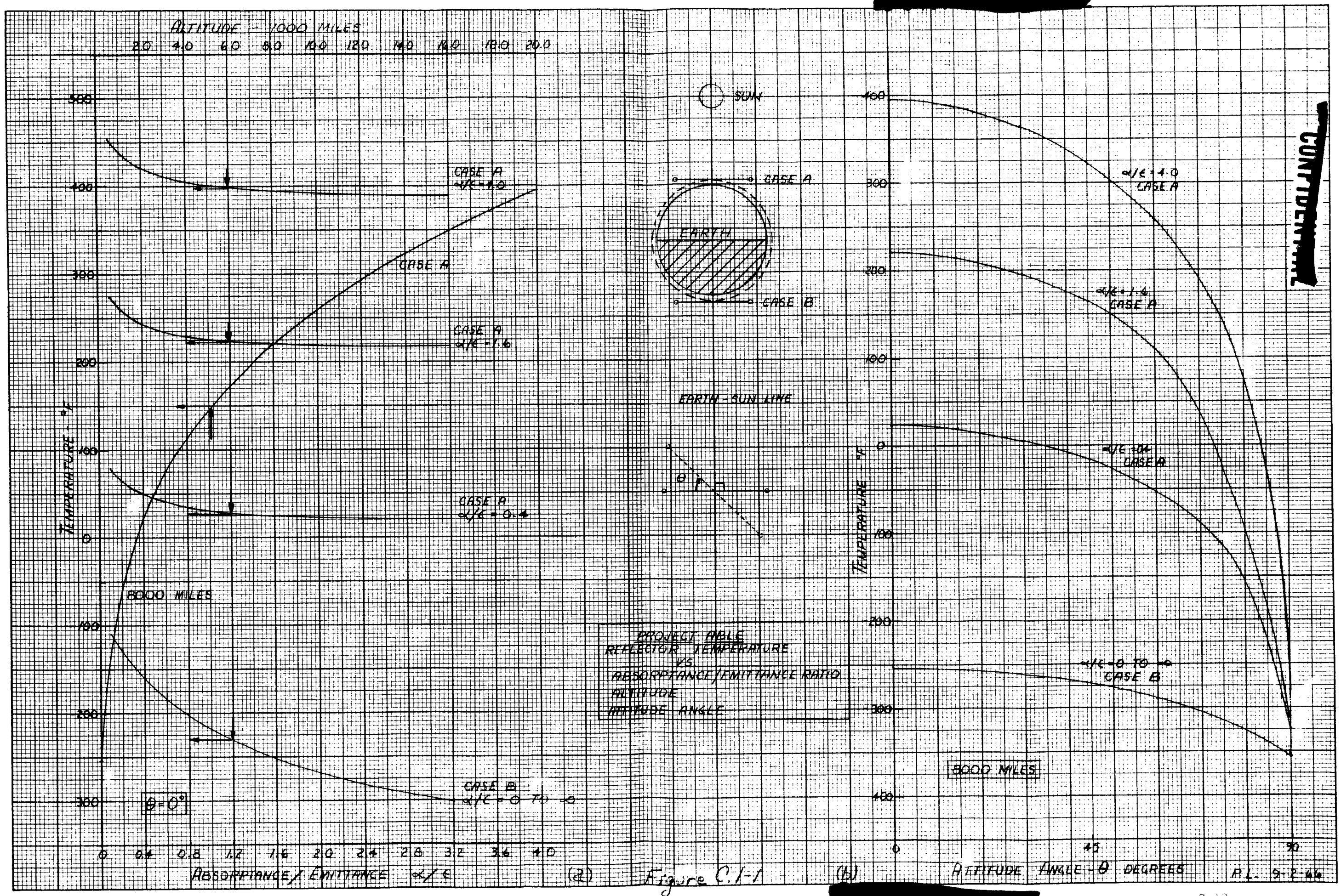

Figure C.1-1

[redacted]

CONFIDENTIAL

KEUFFEL & ESSER CO.

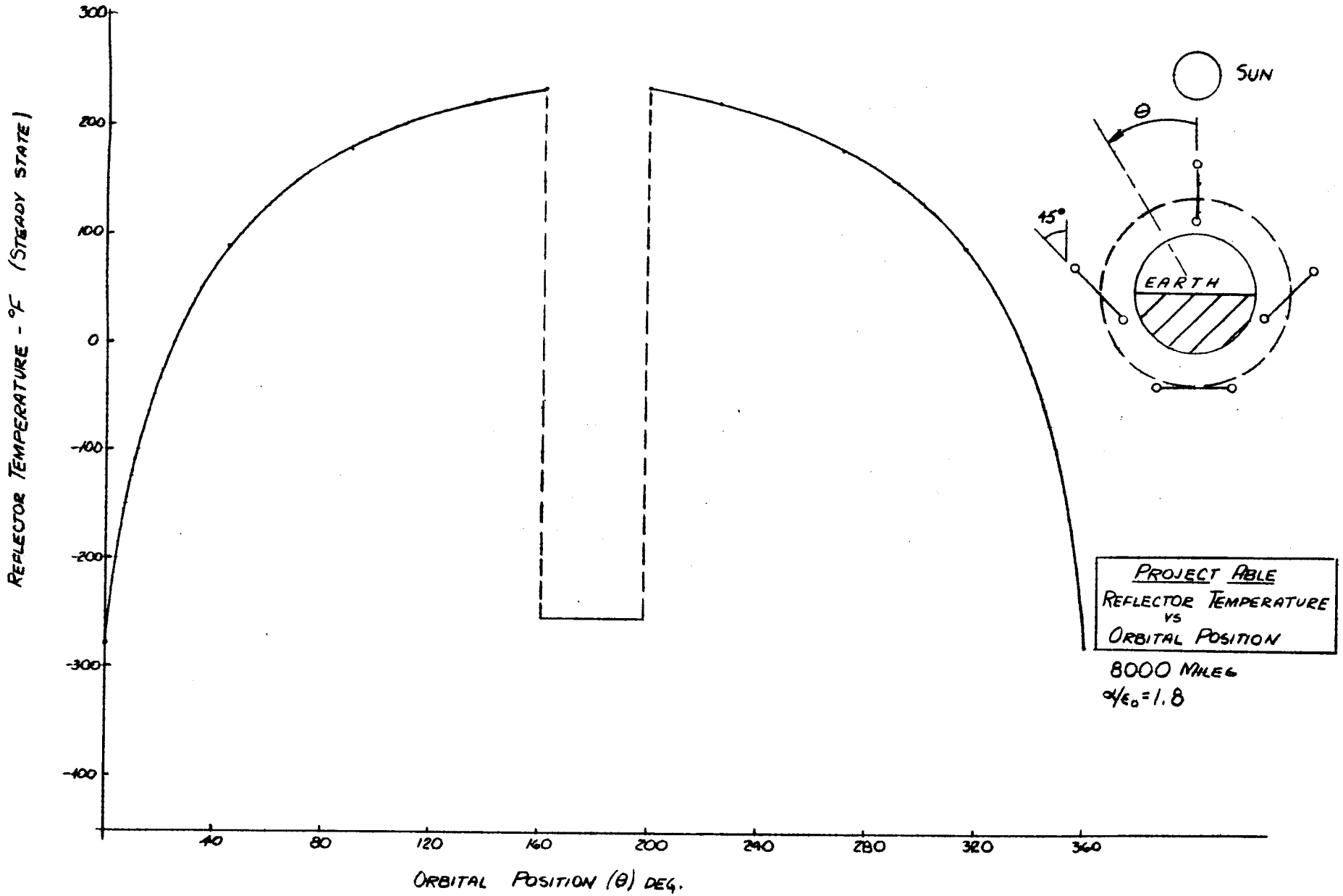

Figure C.1-2

P.L. 9-9-66

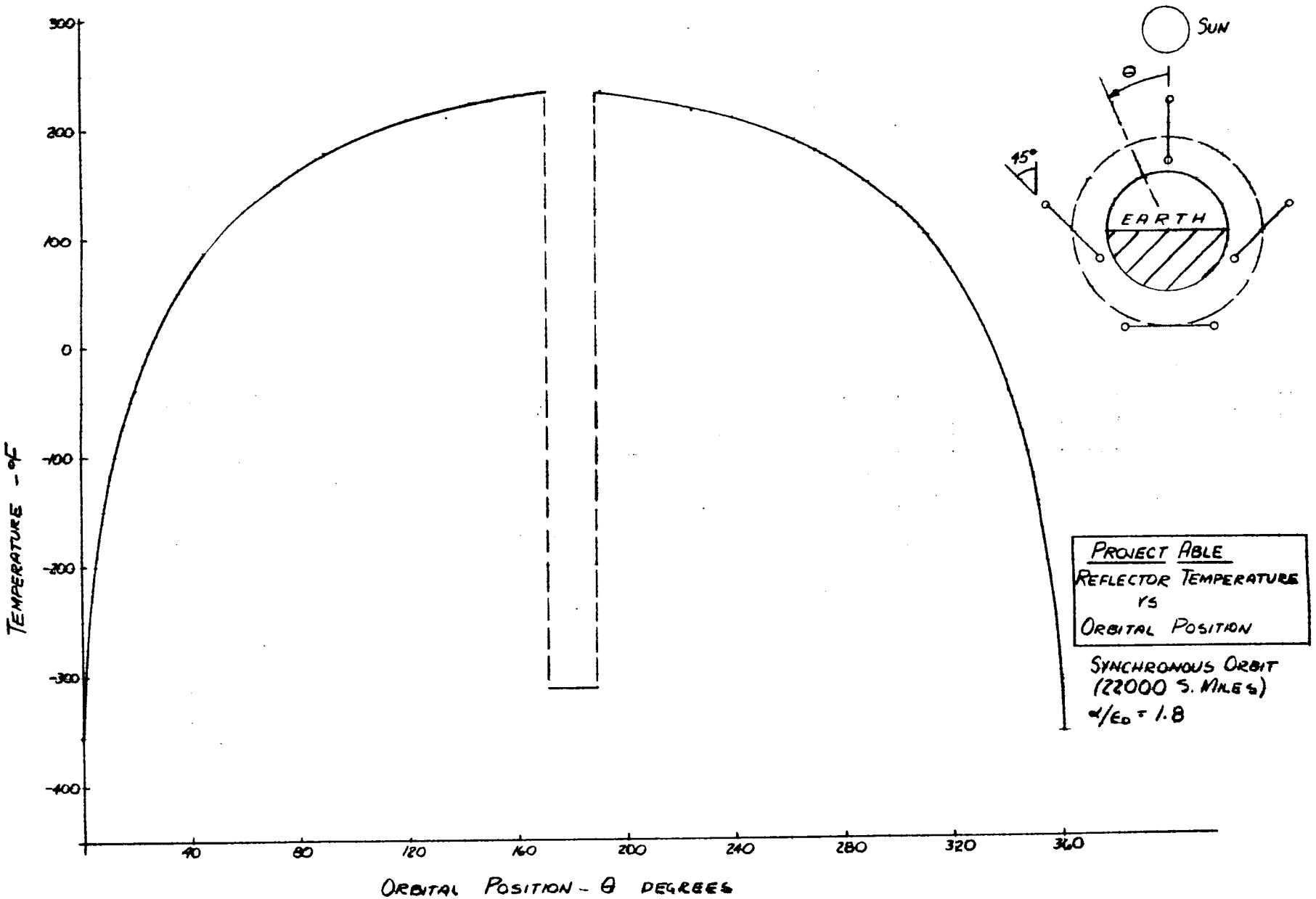

Figure C.1-3

P.L. 9-26-66

[redacted]

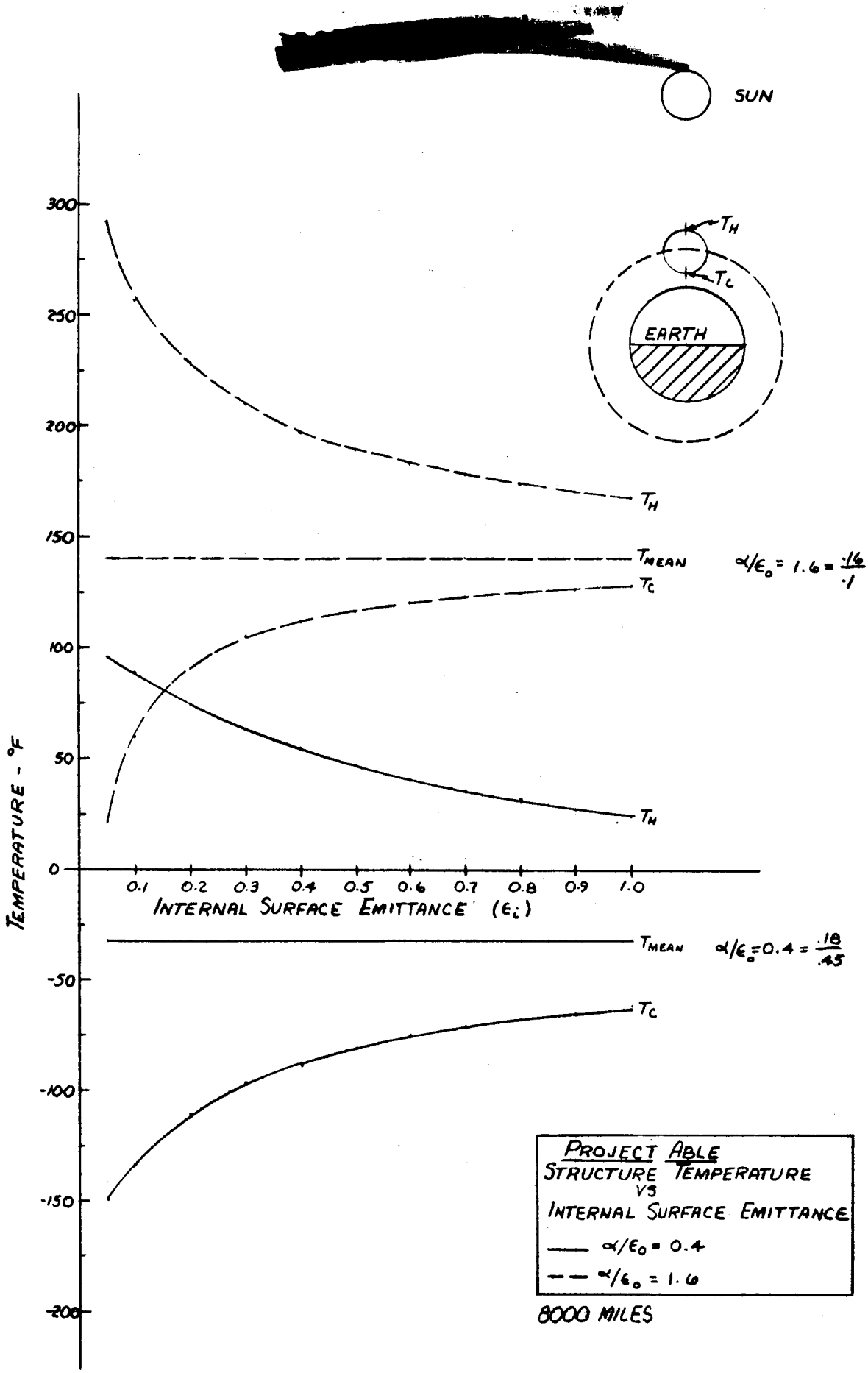

Figure C.2-1

P.L. 9-6-66

[redacted]

[redacted]

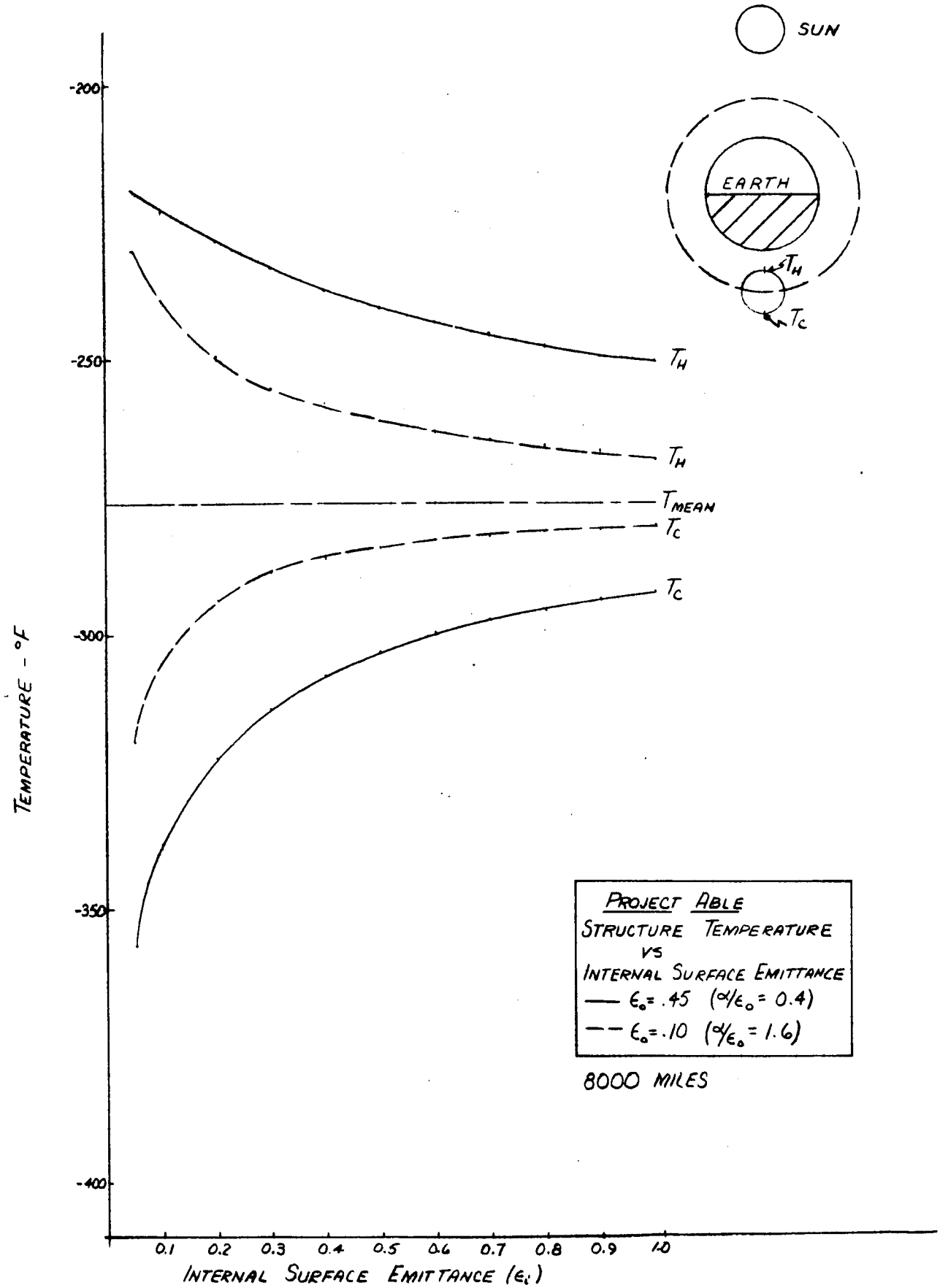

Figure C.2-2

P.L. 9-13-66

[redacted]

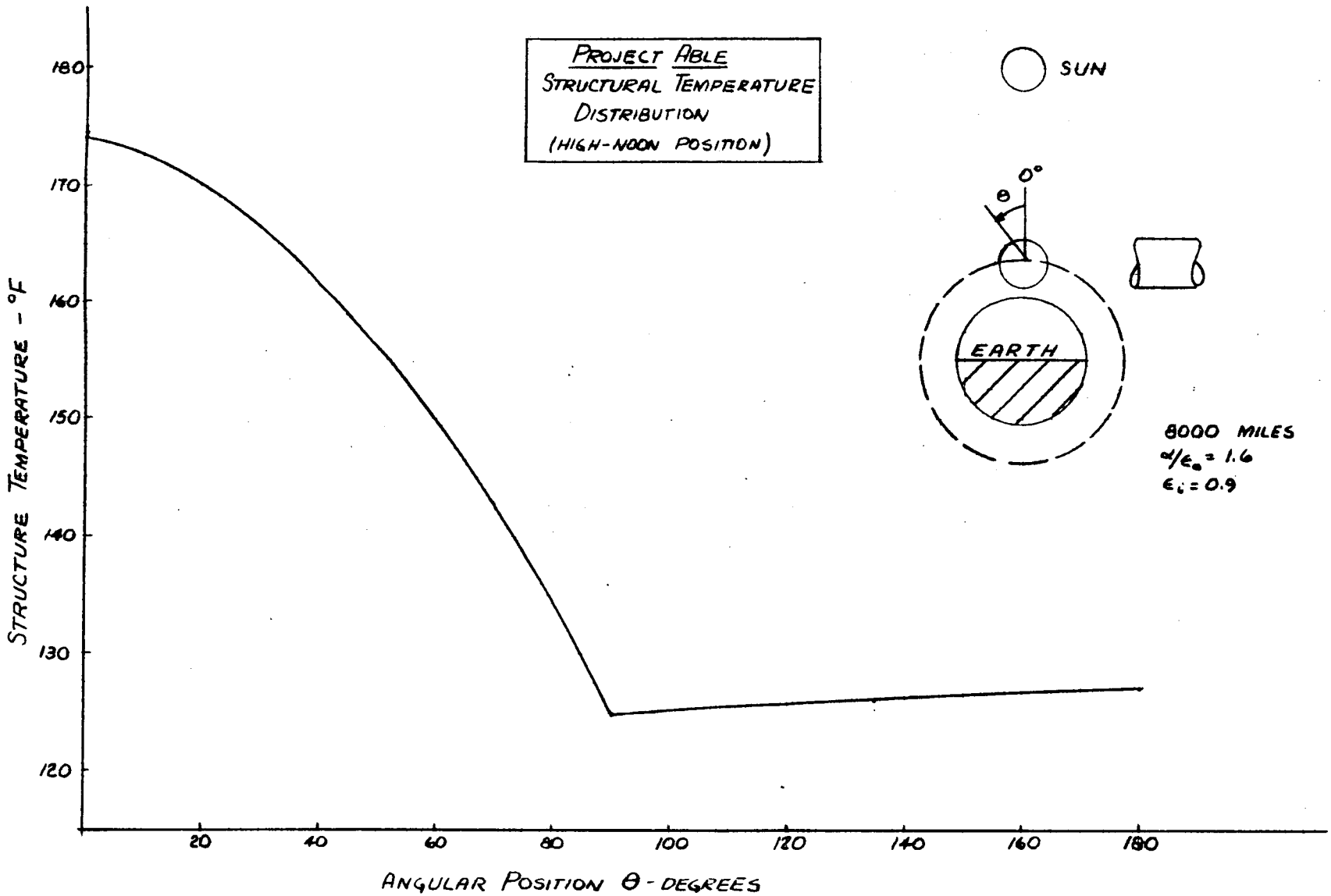

Figure C.2-3

P.L. 9-9-66

[redacted]

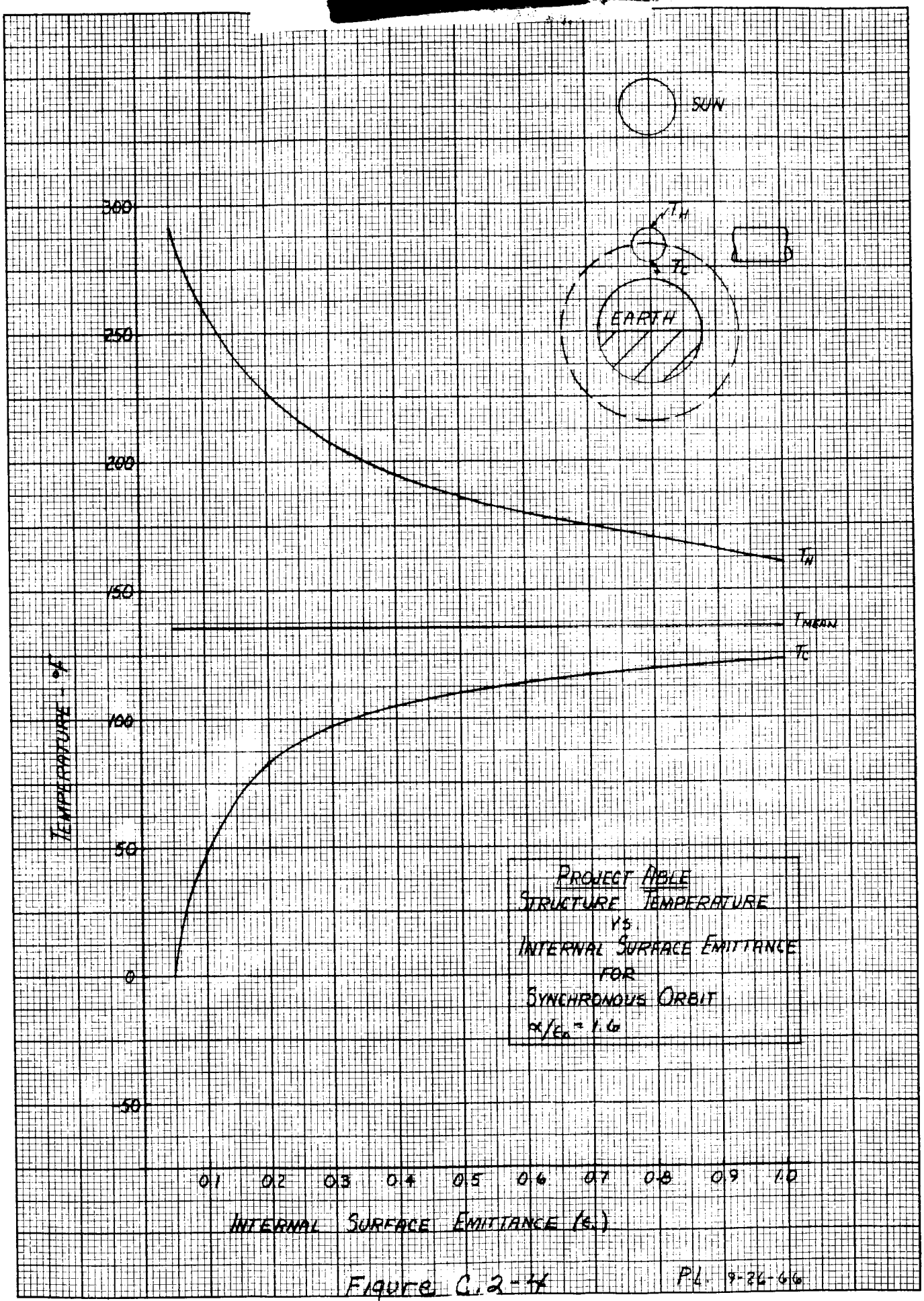

Figure C.2-4 PL 9-26-66

[redacted]

[redacted]

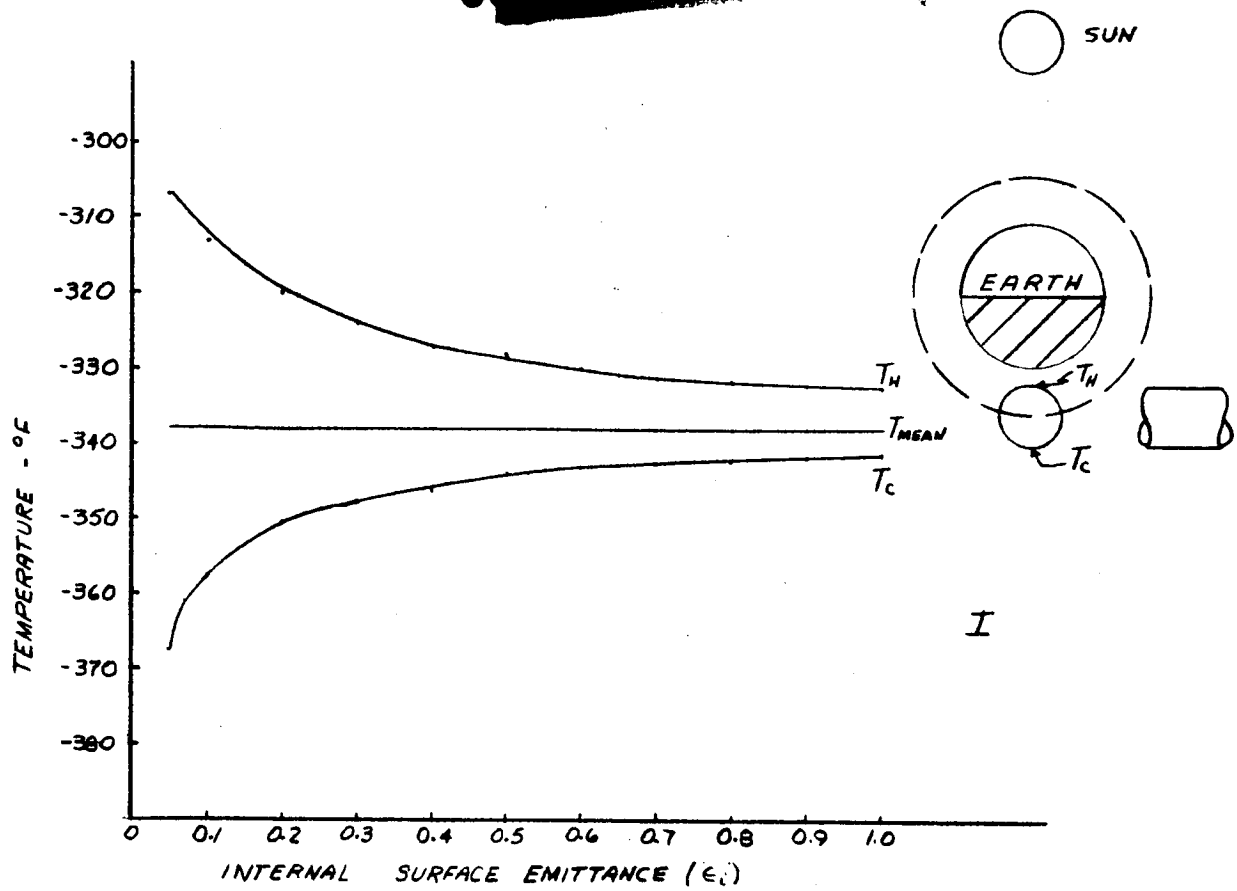

PROJECT ABLE
STRUCTURE TEMPERATURE
VS
I. INTERNAL SURFACE EMITTANCE
II. ANGULAR POSITION ON STRUCTURE
FOR
SYNCHRONOUS ORBIT
(MIDNIGHT POSITION)

$\alpha/\epsilon_o = 1.6 = .16/.1$

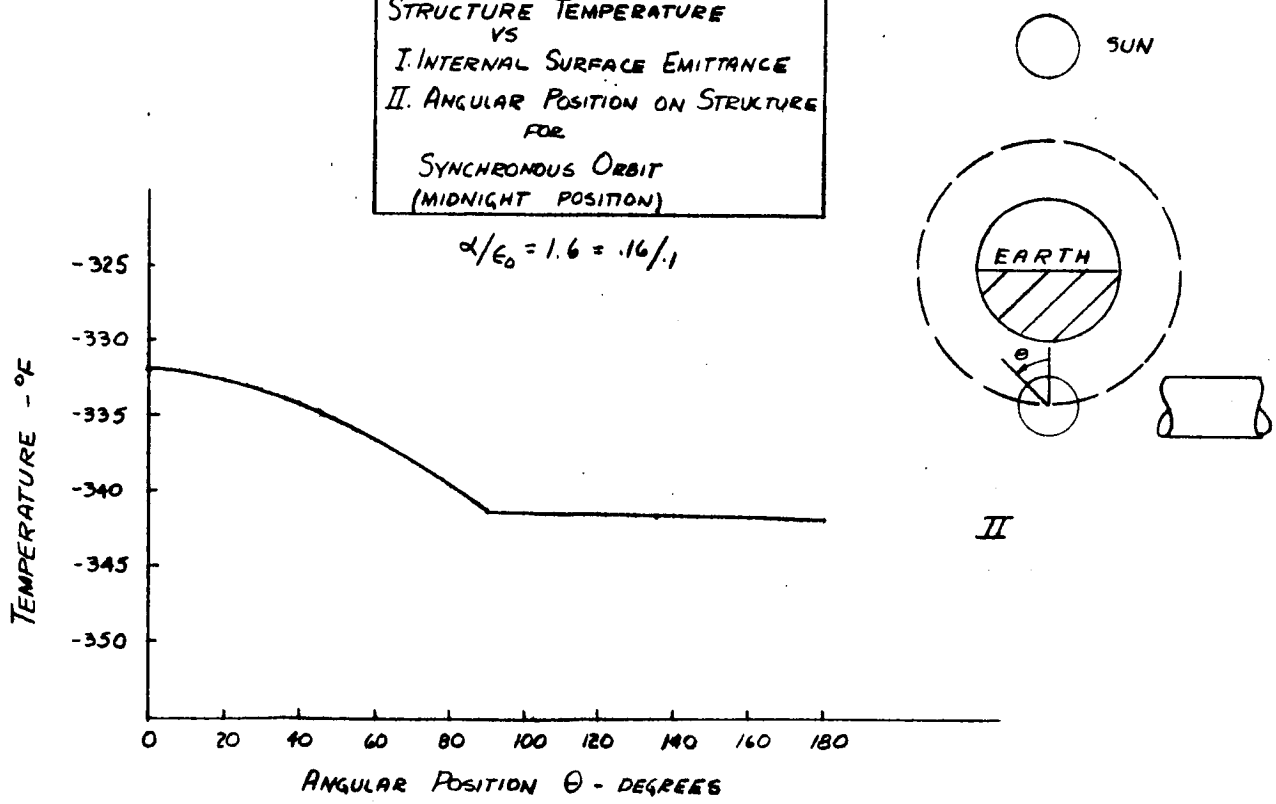

Figure C.2-5 P.L. 9-27-66

[redacted]

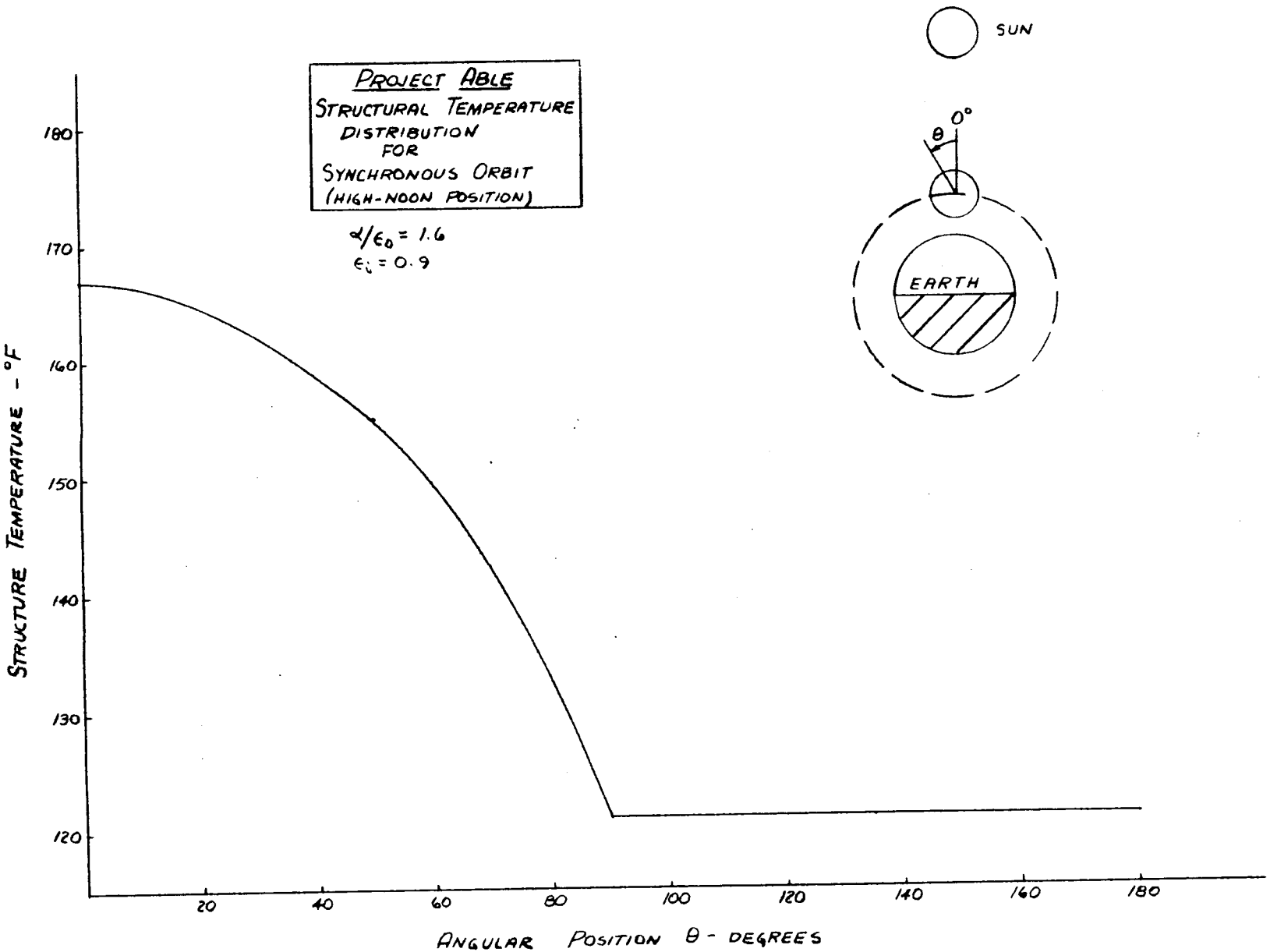

Figure C.2-6

P.L. 9-27-66

[redacted]

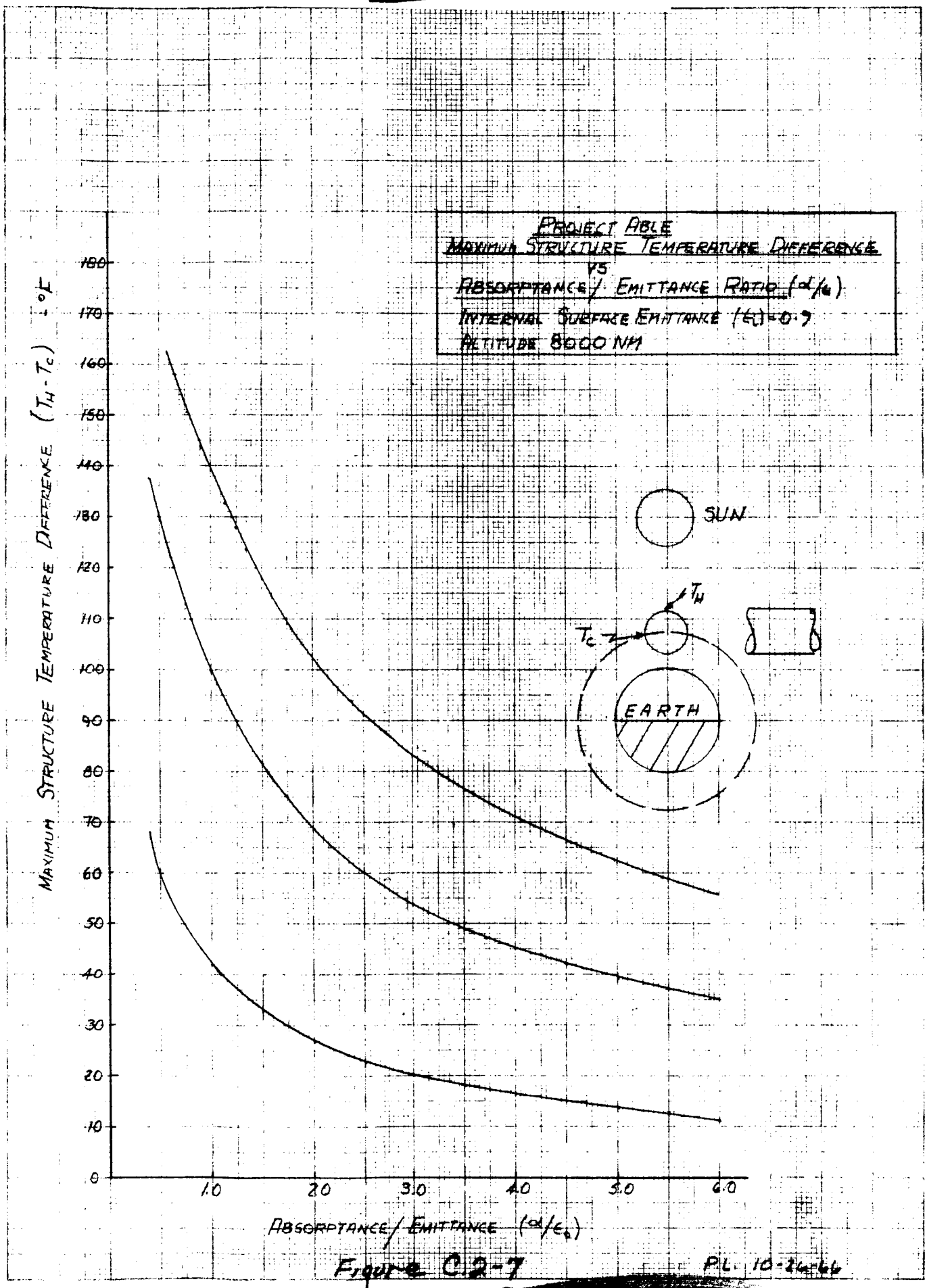

Figure C.2-7

PL. 10-24-66

[redacted]

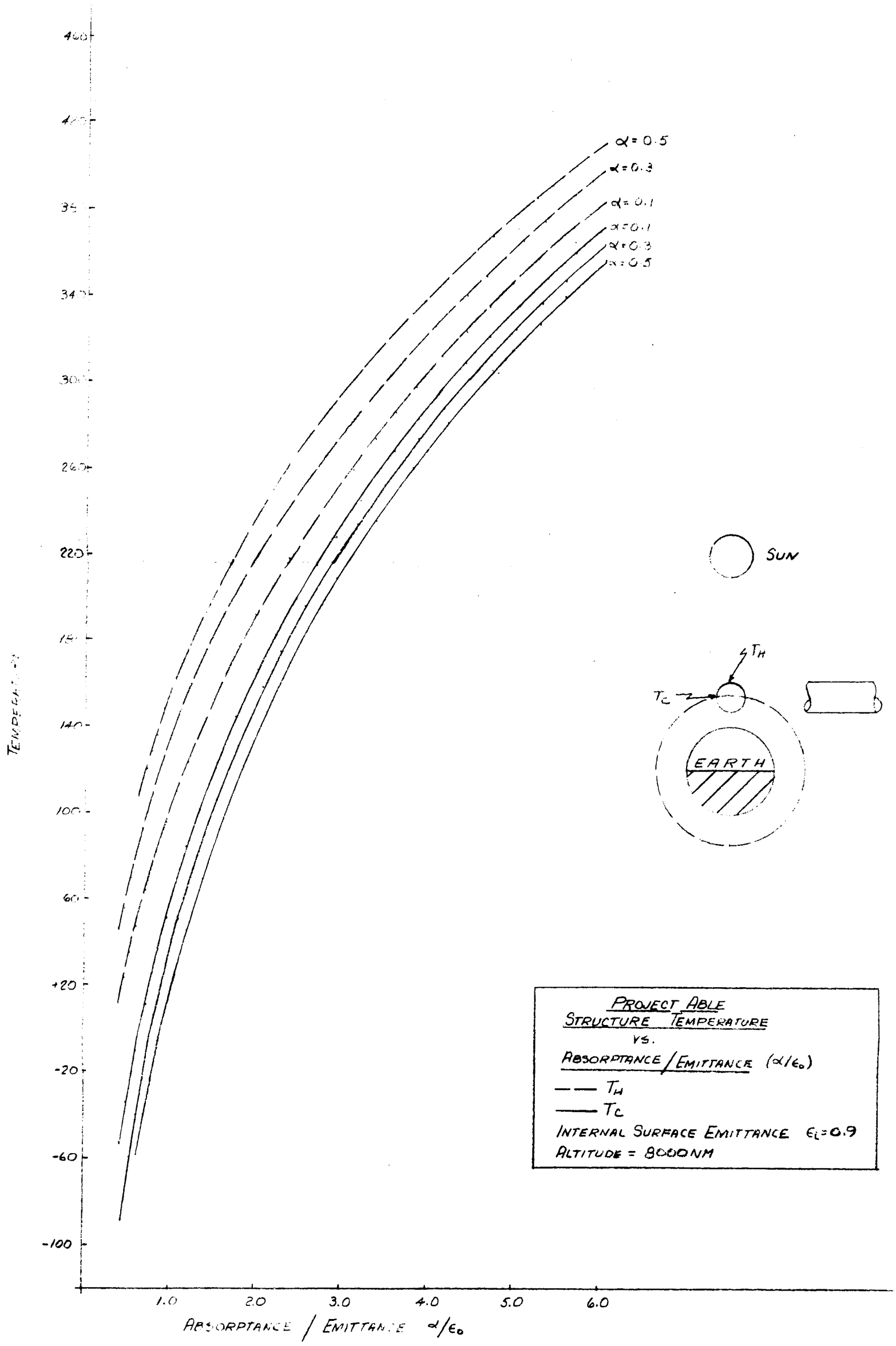

Figure C.2-8

P.L. 10-12-66

[redacted]

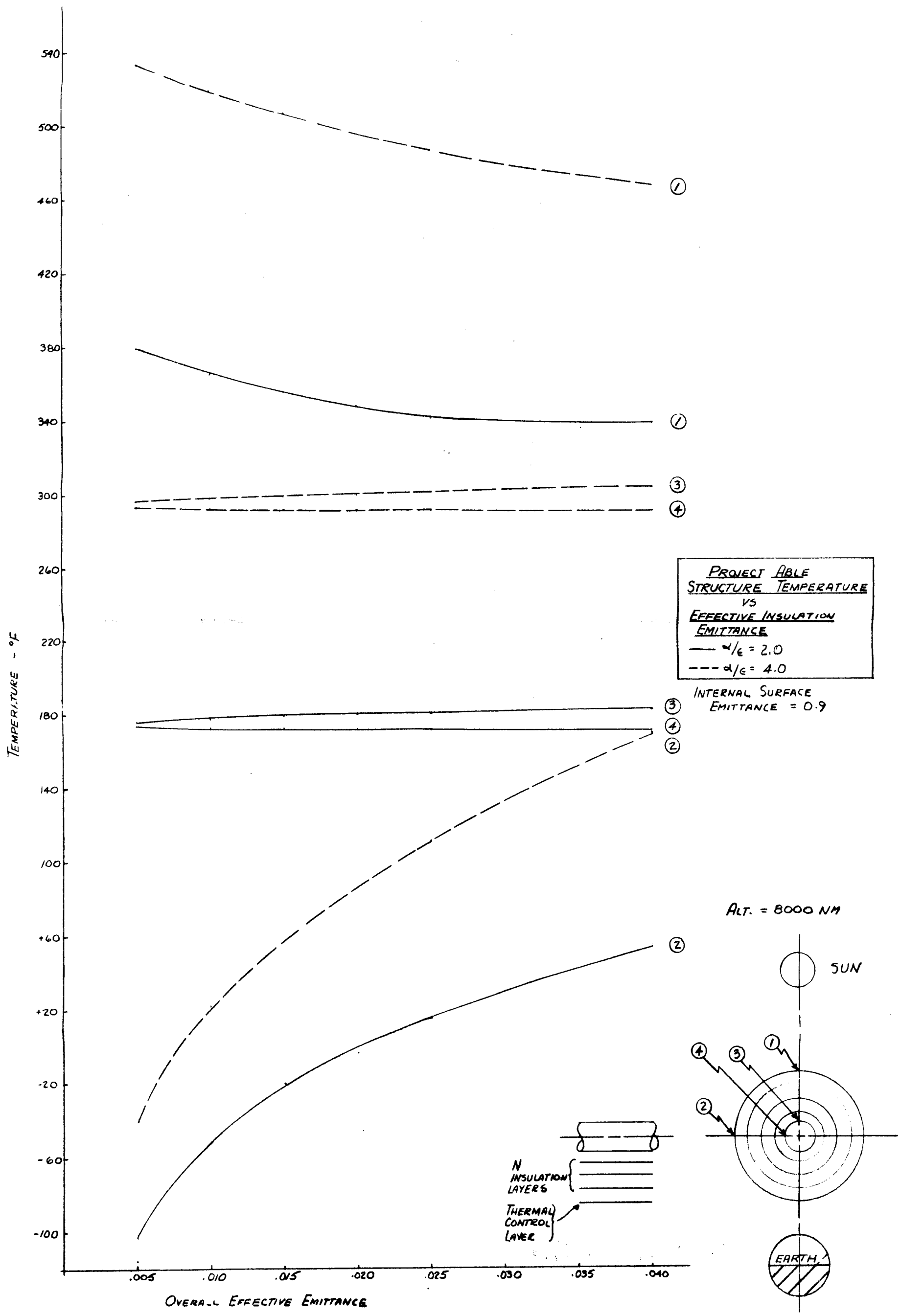

Figure C.2-9

P. LERMAN 10-26-66

[redacted]

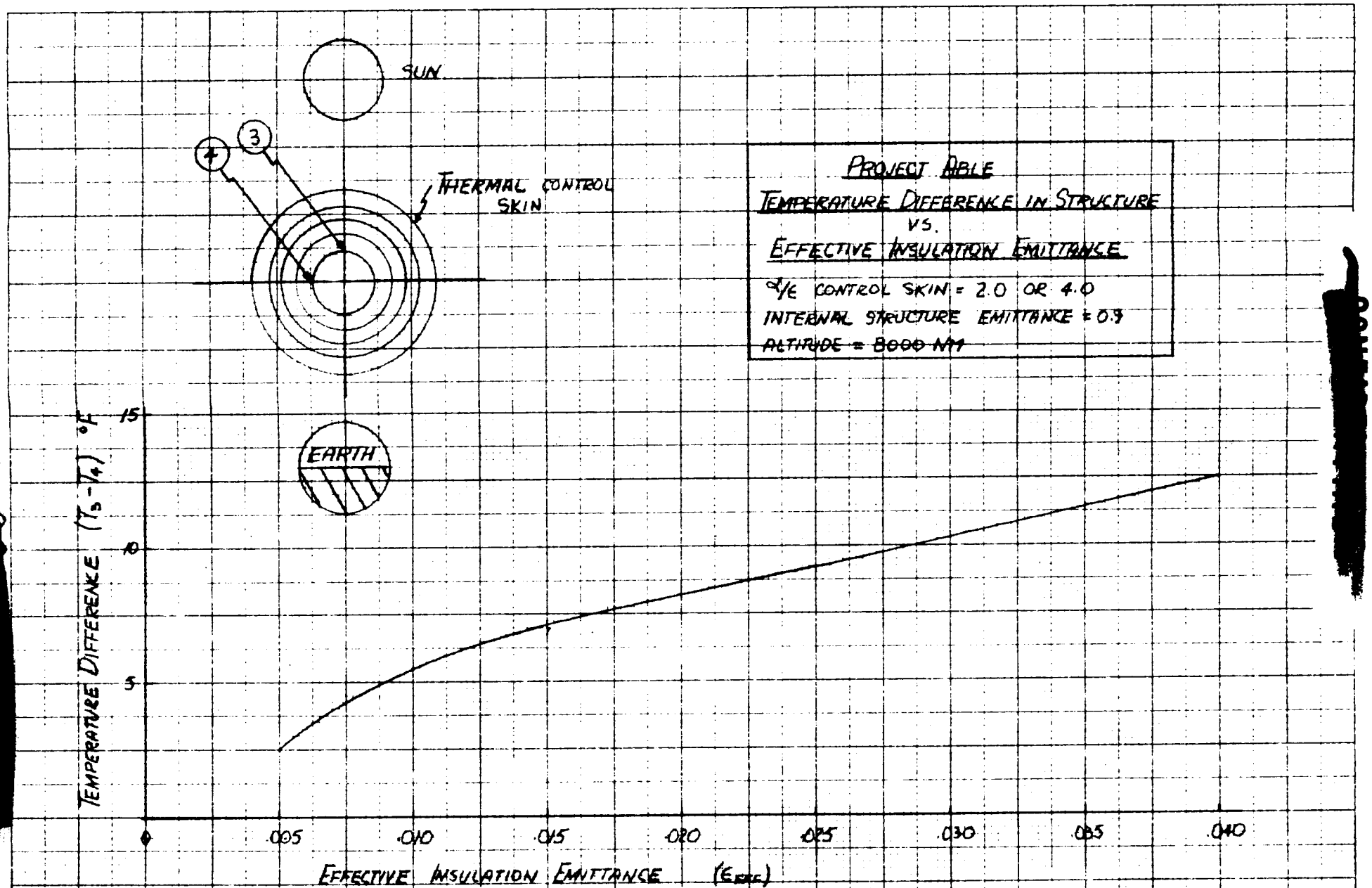

Figure C.2-10

P. LERMAN 10-26-66

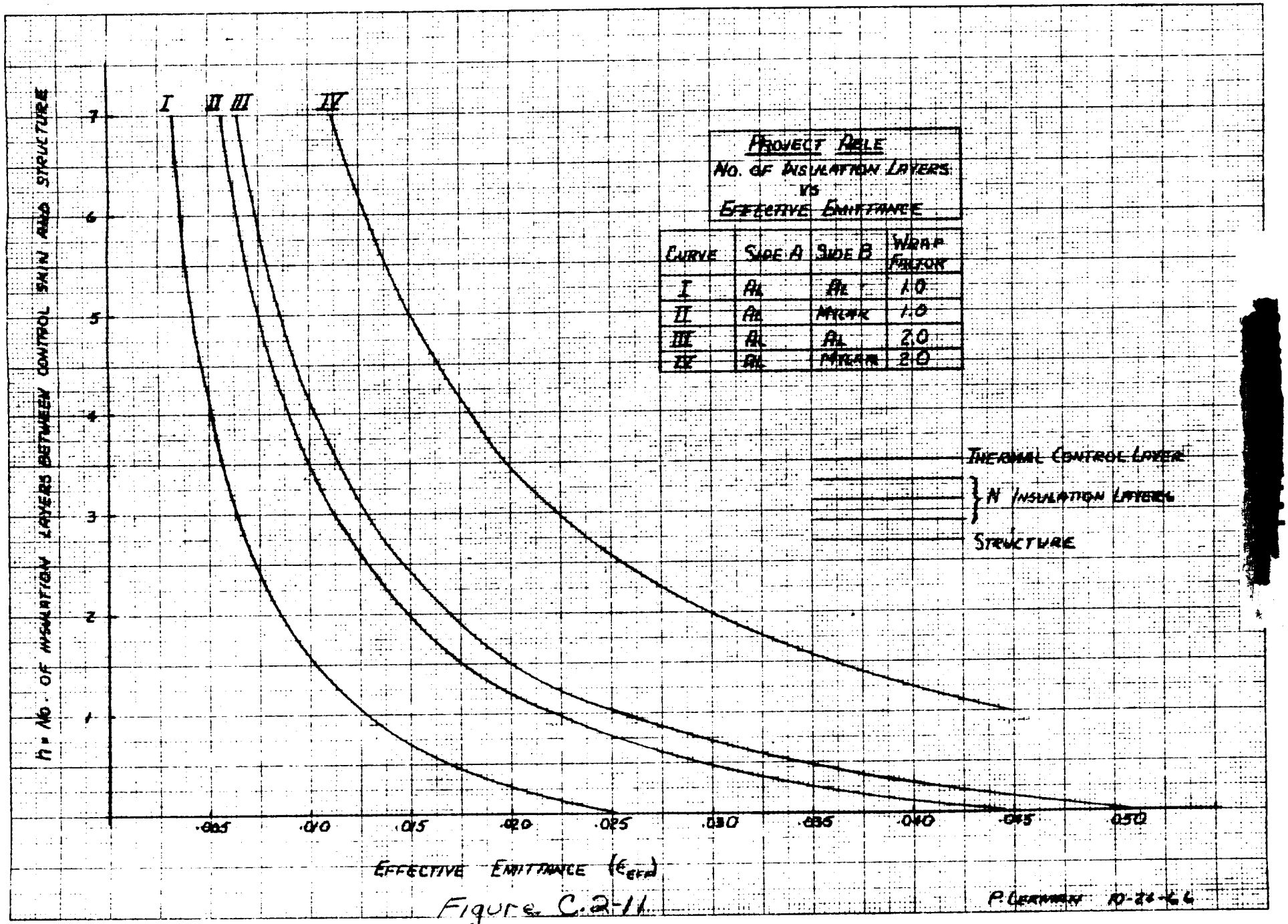
PROJECT RELE
NO. OF INSULATION LAYERS
VS
EFFECTIVE EMITTANCE
CURVE | SIDE A | SIDE B | WRAP FACTOR
I | AL | AL | 1.0
II | AL | MYLAR | 1.0
III | AL | AL | 2.0
IV | AL | MYLAR | 2.0
THERMAL CONTROL LAYER
N INSULATION LAYERS
STRUCTURE
I
II
III
IV
n = NO. OF INSULATION LAYERS BETWEEN CONTROL SKIN AND STRUCTURE
1
2
3
4
5
6
7
.005
.010
.015
.020
.025
.030
.035
.040
.045
.050
EFFECTIVE EMITTANCE (ϵ_{eff})
P. GERMAN 10-24-66

Figure C.2-11

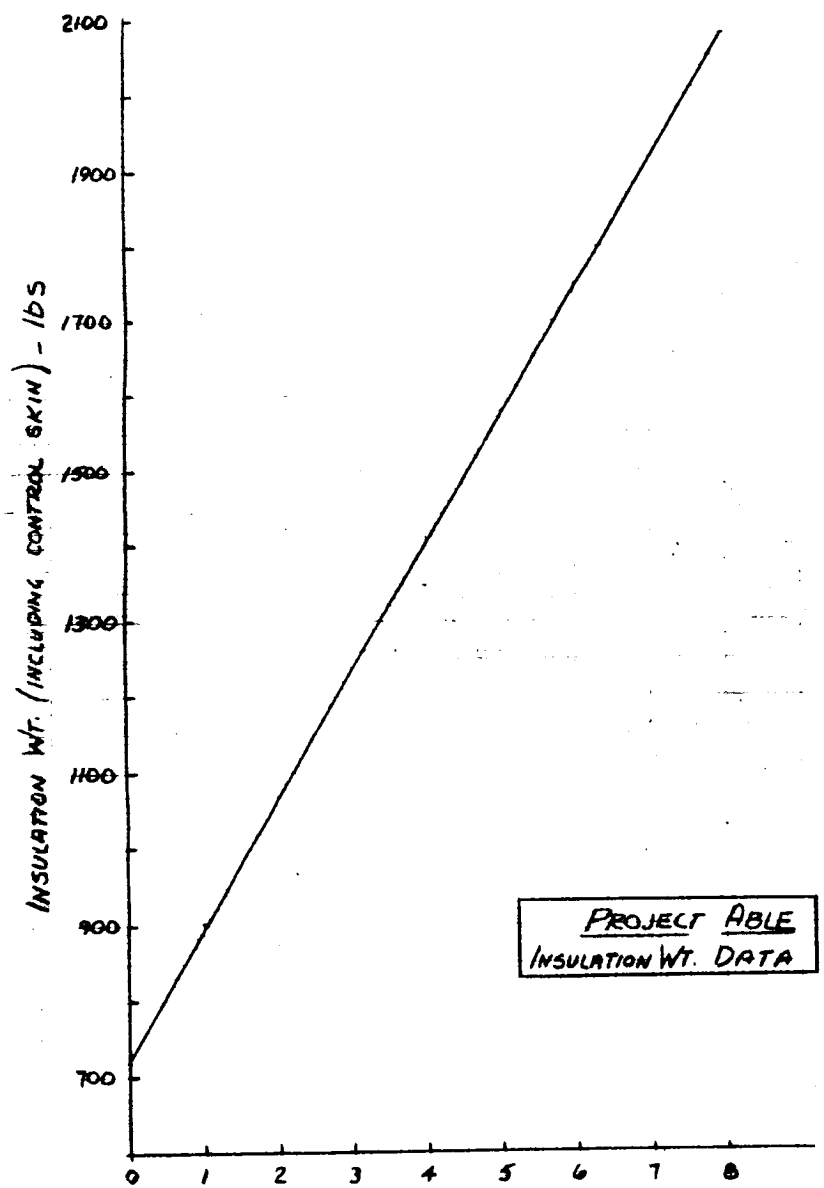

(a)

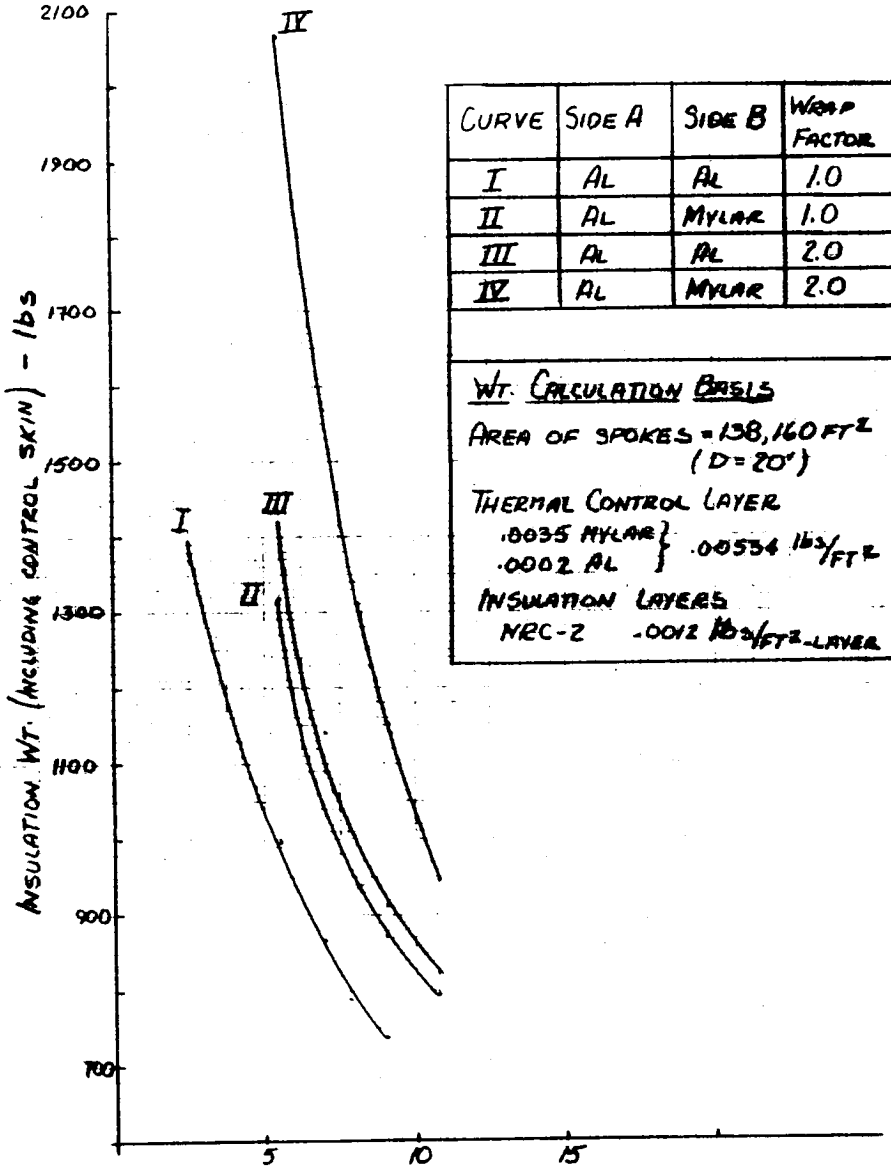

CURVE	SIDE A	SIDE B	WRAP FACTOR
I	AL	AL	1.0
II	AL	MYLAR	1.0
III	AL	AL	2.0
IV	AL	MYLAR	2.0

WT. CALCULATION BASIS

AREA OF SPOKES = 138,160 FT² (D = 20')

THERMAL CONTROL LAYER

.0035 MYLAR
.0002 AL } .00534 lbs/FT²

INSULATION LAYERS

MRC-2 .0012 lbs/FT²-LAYER

(b) P. LERMAN 10-26-66

Figure C.2-12

Aver

* Altitude in 1000 N

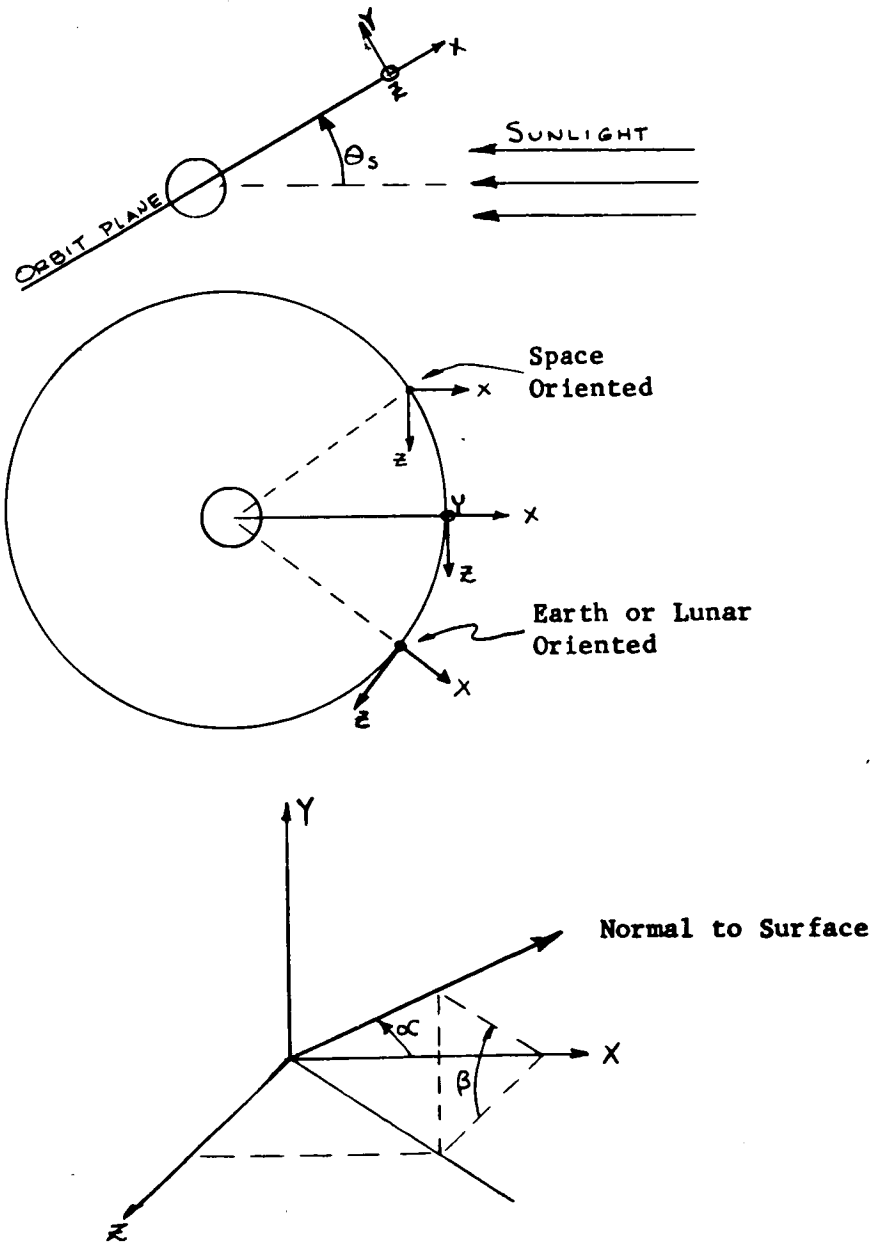

.5 *N.M. Earth Orbit - Ea

Inclination of Orbit to S

Surface Orientation		Incide in BTU
α	β	Solar Radiation
45°	0	137.820
	45	121.825
	90	99.382
	135	121.829
	180	137.823
	225	121.787
	270	99.320
	315	121.784
90°	0	104.443
	45	73.874
	90	0.058
	135	73.874
	180	104.443
	225	73.834
	270	0.
	315	73.833
135°	0	51.038
	45	35.031
	90	12.57
	135	35.02
	180	51.03
	225	35.01
	270	12.55
	315	35.01
0	-	140.50
180	-	17.76

[redacted]

ge Incident Radiation to Satellite Surfaces for One Orbit

M

rth Oriented lar Vector, θ_s= 0°		1.0* N.M. Earth Orbit - Earth Oriented Inclination of Orbit to Solar Vector, θ_s= 0°					2.0* N.M. Earth Orbit - Earth Oriented Inclination of Orbit to Solar Vector, θ_s= 0°					4.0* N.M. Earth Orbit - Earth Oriented Inclination of Orbit to Solar Vector, θ_s= 0°				
nt Radiation /HR-SQ.FT.		Surface Orientation		Incident Radiation in BTU/HR-SQ.FT.			Surface Orientation		Incident Radiation in BTU/HR-SQ.FT.			Surface Orientation		Incident Radiation in BTU/HR-SQ.FT.		
Albedo Radiation	Direct I-R Radiation	α	β	Solar Radiation	Albedo Radiation	Direct I-R Radiation	α	β	Solar Radiation	Albedo Radiation	Direct I-R Radiation	α	β	Solar Radiation	Albedo Radiation	Direct I-R Radiation
0.599	0.733	45°	0	140.137	0.046	0.056	45°	0	140.499	0.	0.	45°	0	140.502	0.	0.
0.591	0.734		45	122.365	0.044	0.056		45	122.654	0.	0.		45	122.658	0.	0.
0.582	0.735		90	99.383	0.042	0.056		90	99.384	0.	0.		90	99.388	0.	0.
0.590	0.734		135	122.369	0.044	0.056		135	122.658	0.	0.		135	122.662	0.	0.
0.599	0.733		180	140.141	0.046	0.056		180	140.502	0.	0.		180	140.507	0.	0.
0.591	0.734		225	122.326	0.044	0.056		225	122.614	0.	0.		225	122.619	0.	0.
0.582	0.735		270	99.321	0.042	0.056		270	99.323	0.	0.		270	99.326	0.	0.
0.590	0.734		315	122.322	0.044	0.056		315	122.611	0.	0.		315	122.614	0.	0.
11.330	13.861	90°	0	114.621	7.030	8.680	90°	0	124.661	3.404	4.269	90°	0	132.507	1.209	1.550
11.289	13.870		45	81.073	6.975	8.685		45	88.174	3.348	4.271		45	93.724	1.174	1.551
11.218	13.836		90	0.063	6.901	8.664		90	0.068	3.284	4.262		90	0.074	1.137	1.548
11.289	13.870		135	81.072	6.975	8.685		135	88.174	3.348	4.271		135	93.724	1.174	1.551
11.330	13.861		180	114.621	7.030	8.680		180	124.661	3.404	4.269		180	132.507	1.209	1.550
11.288	13.870		225	81.028	6.974	8.685		225	88.126	3.348	4.271		225	93.671	1.174	1.551
11.217	13.836		270	0.	6.900	8.664		270	0.	3.284	4.262		270	0.	1.137	1.548
11.288	13.870		315	81.028	6.974	8.685		315	88.126	3.348	4.271		315	93.672	1.174	1.551
30.582	37.444	135°	0	63.116	23.554	29.123	135°	0	77.662	15.407	19.419	135°	0	94.486	8.015	10.395
30.574	37.445		45	45.332	23.552	29.123		45	59.808	15.408	19.419		45	76.635	8.015	10.395
30.565	37.446		90	22.339	23.550	29.123		90	36.530	15.408	19.418		90	53.358	8.016	10.395
30.574	37.445		135	45.327	23.552	29.123		135	59.804	15.408	19.418		135	76.630	8.015	10.395
30.582	37.444		180	63.111	23.554	29.123		180	77.658	15.407	19.418		180	94.481	8.015	10.395
30.573	37.445		225	45.308	23.551	29.123		225	59.779	15.407	19.418		225	76.600	8.015	10.395
30.564	37.446		270	22.313	23.549	29.123		270	36.495	15.407	19.418		270	53.315	8.015	10.395
30.573	37.445		315	45.312	23.551	29.123		315	59.783	15.407	19.419		315	76.605	8.015	10.395
0.	0.	0	-	140.502	0.	0.	0	-	140.505	0.	0.	0	-	140.510	0.	0.
42.403	51.918	180	-	31.571	33.246	41.106	180	-	51.634	21.790	27.462	180	-	75.427	11.335	14.701

2

[redacted]

8.0*N.M. Earth Orbit - Earth Oriented

Inclination of Orbit to Solar Vector, θ_s = 0°

Surface Orientation		Incident Radiation in BTU/HR-SQ.FT.		
α	β	Solar Radiation	Albedo Radiation	Direct I-R Radiation
45°	0	140.510	0.	0.
	45	122.666	0.	0.
	90	99.396	0.	0.
	135	122.670	0.	0.
	180	140.515	0.	0.
	225	122.627	0.	0.
	270	99.334	0.	0.
	315	122.622	0.	0.
90°	0	137.243	0.312	0.409
	45	97.075	0.298	0.409
	90	0.079	0.284	0.408
	135	97.075	0.298	0.409
	180	137.243	0.312	0.409
	225	97.019	0.298	0.409
	270	0.	0.284	0.408
	315	97.019	0.298	0.409
135°	0	110.609	3.288	4.399
	45	92.760	3.288	4.399
	90	69.484	3.288	4.399
	135	92.756	3.288	4.399
	180	110.604	3.288	4.399
	225	92.720	3.288	4.399
	270	69.435	3.288	4.399
	315	92.725	3.288	4.399
0	-	140.521	0.	0.
180	-	98.228	4.650	6.222

19.1*N.M. Earth Orbit - Earth Oriented

Inclination of Orbit to Solar Vector, θ_s = 0°

Surface Orientation		Incident Radiation in BTU/HR-SQ.FT.		
α	β	Solar Radiation	Albedo Radiation	Direct I-R Radiation
45°	0	140.531	0.	0.
	45	122.687	0.	0.
	90	99.418	0.	0.
	135	122.692	0.	0.
	180	140.536	0.	0.
	225	122.648	0.	0.
	270	99.356	0.	0.
	315	122.643	0.	0.
90°	0	139.673	0.039	0.052
	45	98.794	0.037	0.052
	90	0.083	0.034	0.052
	135	98.794	0.037	0.052
	180	139.673	0.039	0.052
	225	98.735	0.037	0.052
	270	0.	0.034	0.052
	315	98.735	0.037	0.052
135°	0	125.328	0.821	1.134
	45	107.482	0.821	1.134
	90	84.207	0.821	1.134
	135	107.477	0.821	1.134
	180	125.323	0.821	1.134
	225	107.437	0.821	1.134
	270	84.151	0.821	1.134
	315	107.442	0.821	1.134
0	-	140.552	0.	0.
180	-	119.044	1.161	1.603

3

Table C.3-1

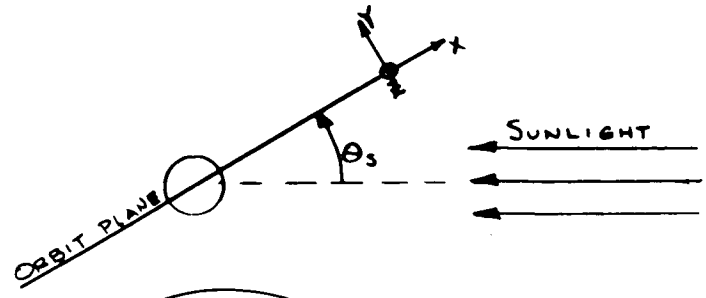

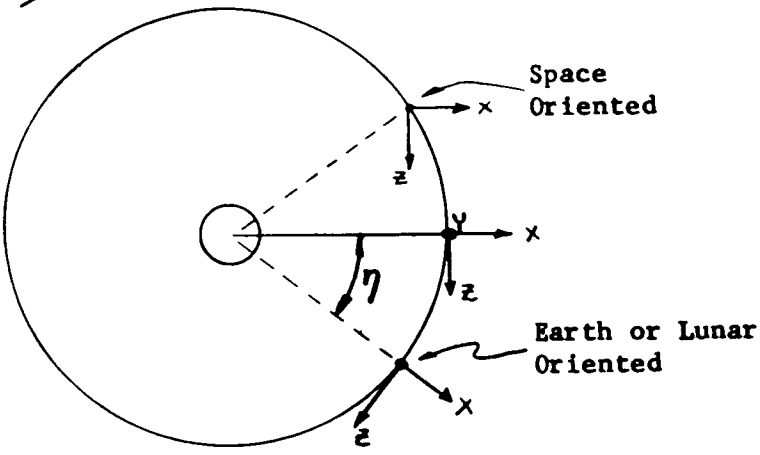

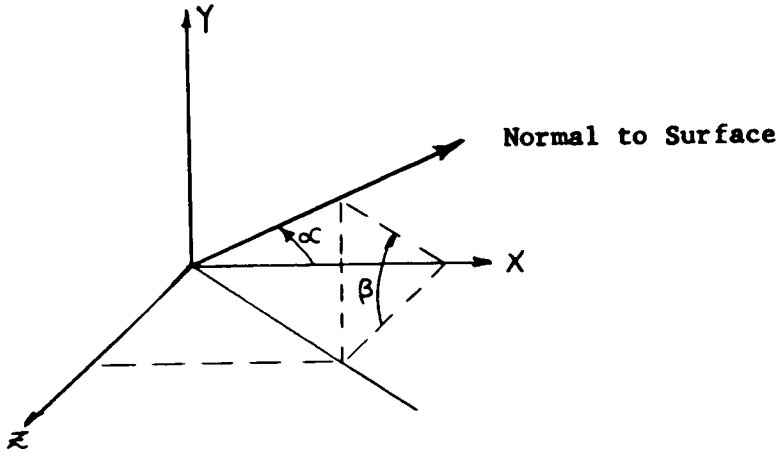

8,000 N.M. Earth Orbit

Inclination of Orbit

Surface Orientation		I i
α	β	So Radi
45°	0	3
	45	3
	90	3
	135	3
	180	3
	225	3
	270	3
	315	3
90°	0	
	45	
	90	
	135	
	180	
	225	
	270	
	315	
135°	0	
	45	
	90	
	135	
	180	
	225	
	270	
	315	
0	-	4
180	-	

INSTANTANEOUS INCIDENT RADIATION TO SATELLITE SURFACES FOR ONE ORBIT

- Earth Oriented -

to Solar Vector, θ_s= 0°

ncident Radiation n BTU/HR-SQ.FT.			Incident Radiation in BTU/HR-SQ.FT.			Incident Radiation in BTU/HR-SQ.FT.			Incident Radiation in BTU/HR-SQ.FT.			Incident Radiation in BTU/HR-SQ.FT.			Incider in BTU/
ar tion	Albedo Radiation	Direct I-R Radiation	Solar Radiation	Albedo Radiation	Direct I-R Radiation	Solar Radiation	Albedo Radiation	Direct I-R Radiation	Solar Radiation	Albedo Radiation	Direct I-R Radiation	Solar Radiation	Albedo Radiation	Direct I-R Radiation	Solar Radiation
3.97	0.	0.	0.	0.	0.	0.	0.	0.	0.	0.	0.	0.	0.	0.	0.
4.02	0.	0.	65.06	0.	0.	0.	0.	0.	0.	0.	0.	0.	0.	0.	0.
4.03	0.	0.	222.06	0.	0.	0.06	0.	0.	0.	0.	0.	0.	0.	0.	0.
4.01	0.	0.	379.01	0.	0.	222.00	0.	0.	0.	0.	0.	0.	0.	0.	0.
3.97	0.	0.	443.99	0.	0.	313.89	0.	0.	0.01	0.	0.	0.	0.	0.	0.
3.93	0.	0.	378.92	0.	0.	221.91	0.	0.	0.	0.	0.	0.	0.	0.	0.
3.91	0.	0.	221.93	0.	0.	0.	0.	0.	0.	0.	0.	0.	0.	0.	0.
3.93	0.	0.	64.98	0.	0.	0.	0.	0.	0.	0.	0.	0.	0.	0.	0.
0.00	0.80	0.41	0.	0.24	0.41	0.	0.00	0.41	0.	0.	0.41	0.	0.	0.41	0.
0.06	0.80	0.41	0.	0.34	0.41	0.	0.02	0.41	0.	0.	0.41	0.	0.	0.41	0.
0.09	0.80	0.41	0.09	0.57	0.41	0.09	0.16	0.41	0.09	0.00	0.41	0.09	0.	0.41	0.
0.06	0.80	0.41	222.06	0.82	0.41	313.95	0.38	0.41	221.97	0.02	0.41	94.53	0.	0.41	0.
0.	0.80	0.41	313.95	0.92	0.41	443.90	0.50	0.41	313.82	0.03	0.41	133.59	0.	0.41	0.
0.	0.80	0.41	221.93	0.82	0.41	313.82	0.38	0.41	221.84	0.02	0.41	94.40	0.	0.41	0.
0.	0.80	0.41	0.	0.57	0.41	0.	0.16	0.41	0.	0.00	0.41	0.	0.	0.41	0.
0.	0.80	0.41	0.	0.34	0.41	0.	0.02	0.41	0.	0.	0.41	0.	0.	0.41	0.
0.	9.19	4.40	0.	6.08	4.40	0.	1.56	4.40	0.	0.05	4.40	204.77	0.	4.40	0.
0.	9.19	4.40	0.	6.22	4.40	0.	1.66	4.40	65.03	0.05	4.40	232.49	0.	4.40	0.
0.	9.19	4.40	0.	6.56	4.40	0.06	1.92	4.40	221.96	0.07	4.40	299.30	0.	4.40	0.
0.	9.19	4.40	0.	6.91	4.40	221.99	2.17	4.40	378.86	0.08	4.40	366.08	0.	4.40	0.
0.	9.19	4.40	0.00	7.05	4.40	313.89	2.27	4.40	443.81	0.09	4.40	393.71	0.	4.40	0.
0.	9.19	4.40	0.	6.91	4.40	221.91	2.17	4.40	378.77	0.08	4.40	365.99	0.	4.40	0.
0.	9.19	4.40	0.	6.56	4.40	0.	1.92	4.40	221.84	0.07	4.40	299.18	0.	4.40	0.
0.	9.19	4.40	0.	6.22	4.40	0.	1.66	4.40	64.94	0.05	4.40	232.40	0.	4.40	0.
44.03	0.	0.	313.95	0.	0.	0.00	0.	0.	0.	0.	0.	0.	0.	0.	0.
0.	12.99	6.22	0.	9.28	6.22	0.	2.71	6.22	313.82	0.10	6.22	423.19	0.	6.22	0.
(η) ETA = 0°			(η) ETA = 45°			(η) ETA = 90°			(η) ETA = 135°			(η) Edge of Shadow ETA = 162.48°			(η)

2

[redacted]

t Radiation HR-SQ.FT.		Incident Radiation in BTU/HR-SQ.FT.			Incident Radiation in BTU/HR-SQ.FT.			Incident Radiation in BTU/HR-SQ.FT.			Incident Radiation in BTU/HR-SQ.FT.		
Albedo Radiation	Direct I-R Radiation	Solar Radiation	Albedo Radiation	Direct I-R Radiation	Solar Radiation	Albedo Radiation	Direct I-R Radiation	Solar Radiation	Albedo Radiation	Direct I-R Radiation	Solar Radiation	Albedo Radiation	Direct I-R Radiation
0.	0.	0.	0.	0.	0.00	0.	0.	313.89	0.	0.	443.99	0.	0.
0.	0.	0.	0.	0.	0.	0.	0.	221.99	0.	0.	379.01	0.	0.
0.	0.	0.	0.	0.	0.	0.	0.	0.06	0.	0.	222.05	0.	0.
0.	0.	0.	0.	0.	0.	0.	0.	0.	0.	0.	65.06	0.	0.
0.	0.	0.	0.	0.	0.	0.	0.	0.	0.	0.	0.	0.	0.
0.	0.	0.	0.	0.	0.	0.	0.	0.	0.	0.	64.97	0.	0.
0.	0.	0.	0.	0.	0.	0.	0.	0.	0.	0.	221.93	0.	0.
0.	0.	0.	0.	0.	0.	0.	0.	221.91	0.	0.	376.92	0.	0.
0.	0.41	133.59	0.	0.41	313.82	0.03	0.41	443.90	0.50	0.41	313.95	0.92	0.41
0.	0.41	94.52	0.	0.41	221.97	0.02	0.41	313.95	0.38	0.41	222.06	0.82	0.41
0.	0.41	0.09	0.	0.41	0.09	0.00	0.41	0.09	0.16	0.41	0.09	0.57	0.41
0.	0.41	0.	0.	0.41	0.	0.	0.41	0.	0.02	0.41	0.	0.34	0.41
0.	0.41	0.	0.	0.41	0.	0.	0.41	0.	0.	0.41	0.	0.24	0.41
0.	0.41	0.	0.	0.41	0.	0.	0.41	0.	0.02	0.41	0.	0.34	0.41
0.	0.41	0.	0.	0.41	0.	0.00	0.41	0.	0.16	0.41	0.	0.57	0.41
0.	0.41	94.40	0.	0.41	221.84	0.02	0.41	313.82	0.38	0.41	221.93	0.82	0.41
0.	4.40	393.71	0.	4.40	443.81	0.09	4.40	313.89	2.27	4.40	0.01	7.05	4.40
0.	4.40	366.08	0.	4.40	378.86	0.08	4.40	222.00	2.17	4.40	0.	6.91	4.40
0.	4.40	299.30	0.	4.40	221.97	0.07	4.40	0.06	1.92	4.40	0.	6.56	4.40
0.	4.40	232.49	0.	4.40	65.04	0.05	4.40	0.	1.66	4.40	0.	6.22	4.40
0.	4.40	204.78	0.	4.40	0.	0.05	4.40	0.	1.56	4.40	0.	6.08	4.40
0.	4.40	232.40	0.	4.40	64.95	0.05	4.40	0.	1.66	4.40	0.	6.22	4.40
0.	4.40	299.18	0.	4.40	221.84	0.07	4.40	0.	1.92	4.40	0.	6.56	4.40
0.	4.40	365.99	0.	4.40	378.77	0.08	4.40	221.91	2.17	4.40	0.	6.91	4.40
0.	0.	0.	0.	0.	0.	0.	0.	0.	0.	0.	313.95	0.	0.
0.	6.22	423.20	0.	6.22	313.82	0.10	6.22	0.00	2.71	6.22	0.	9.28	6.22
(η) ETA = 180°		Edge of Shadow (η) ETA = 197.52°			(η) ETA = 225°			(η) ETA = 270°			(η) ETA = 315°		

[redacted]

3

Table C.3-2

MINIMUM ALLOWABLE LOAD VS RADIATOR SYSTEM.

- RADIATOR AREA - 93 FT^2 (AREA FOR 2KW LOAD AT $Q_{ABS\ AVG}$ = 30 BTU/HR-FT^2 - NO WATER CONSUMPTION)
- MINIMUM ABSORBED RADIATION = 0 BTU/HR-FT^2

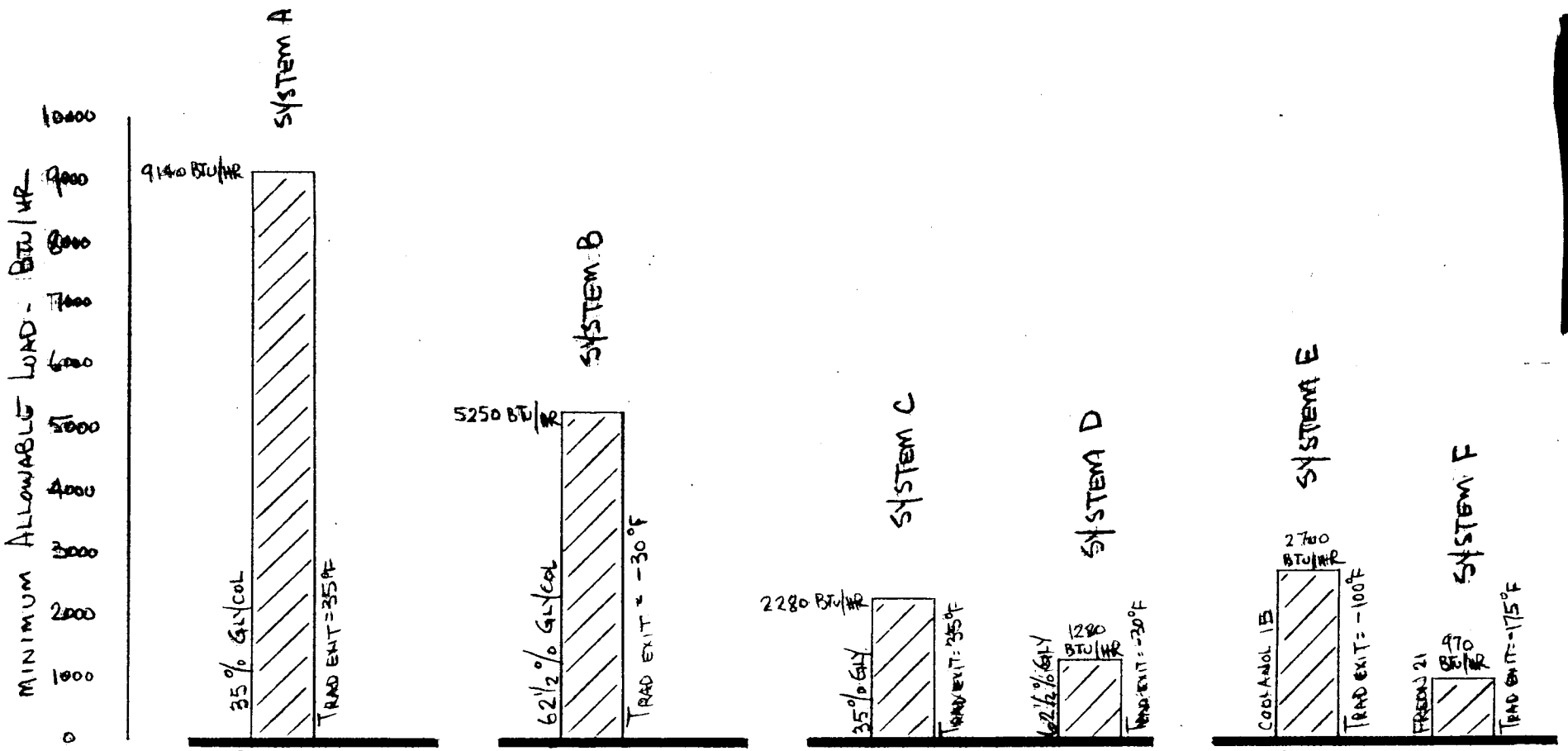

LR 9/2/66

Figure C.4-2

[redacted]

LEM ECS LOOP

WATER BOILERS REPLACED BY RADIATORS

62.5% GLYCOL
37.5% WATER
$WC_p = 163$ BTU/HR·°F

PUMP : $Q = 96$ BTU/HR
SUIT HX $Q_L = 535$ BTU/HR
$Q_S = 956$ BTU/HR
$W_{O_2} = 44.8$ LB/HR
LOW TEMP ELECT $Q = 300$ BTU/HR
CABIN $T = 75$ °F
$W_{O_2} = 650$ LB/HR
RH = 55%

LIOH $Q_L = 84$ BTU/HR } IN SUIT LOOP
$Q_S = 168$ BTU/HR }

RADIATORS : $\alpha_s = 0.18$
$\varepsilon = 0.90$
$\eta_f = 0.96$
TUBES ON 4" CENTERS

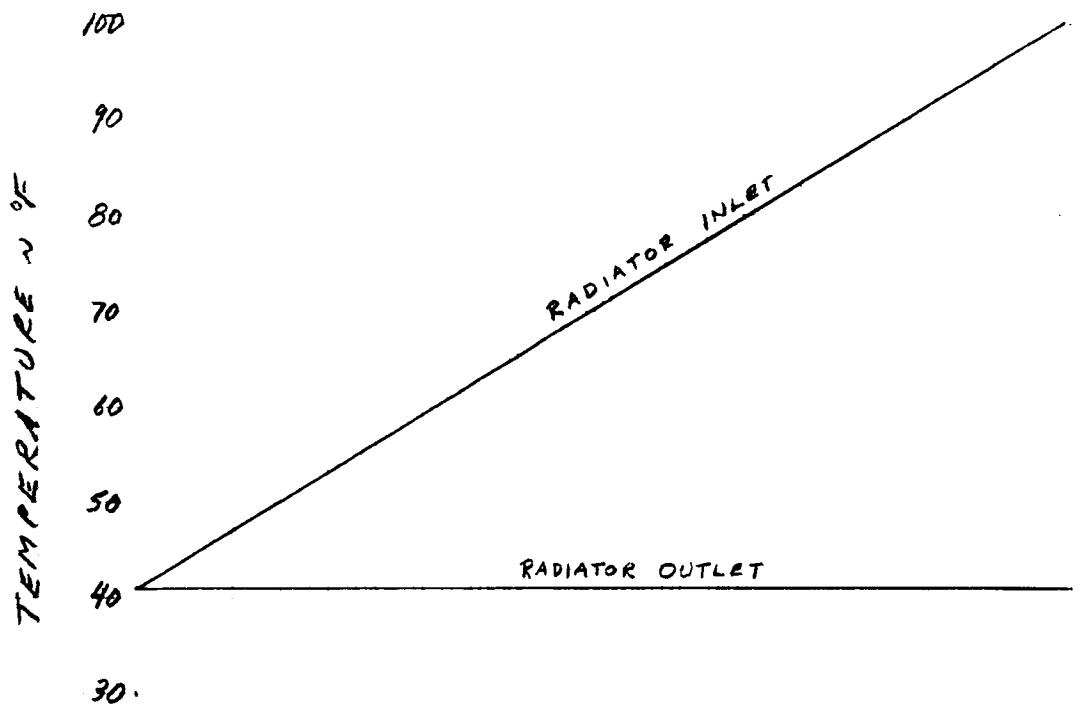

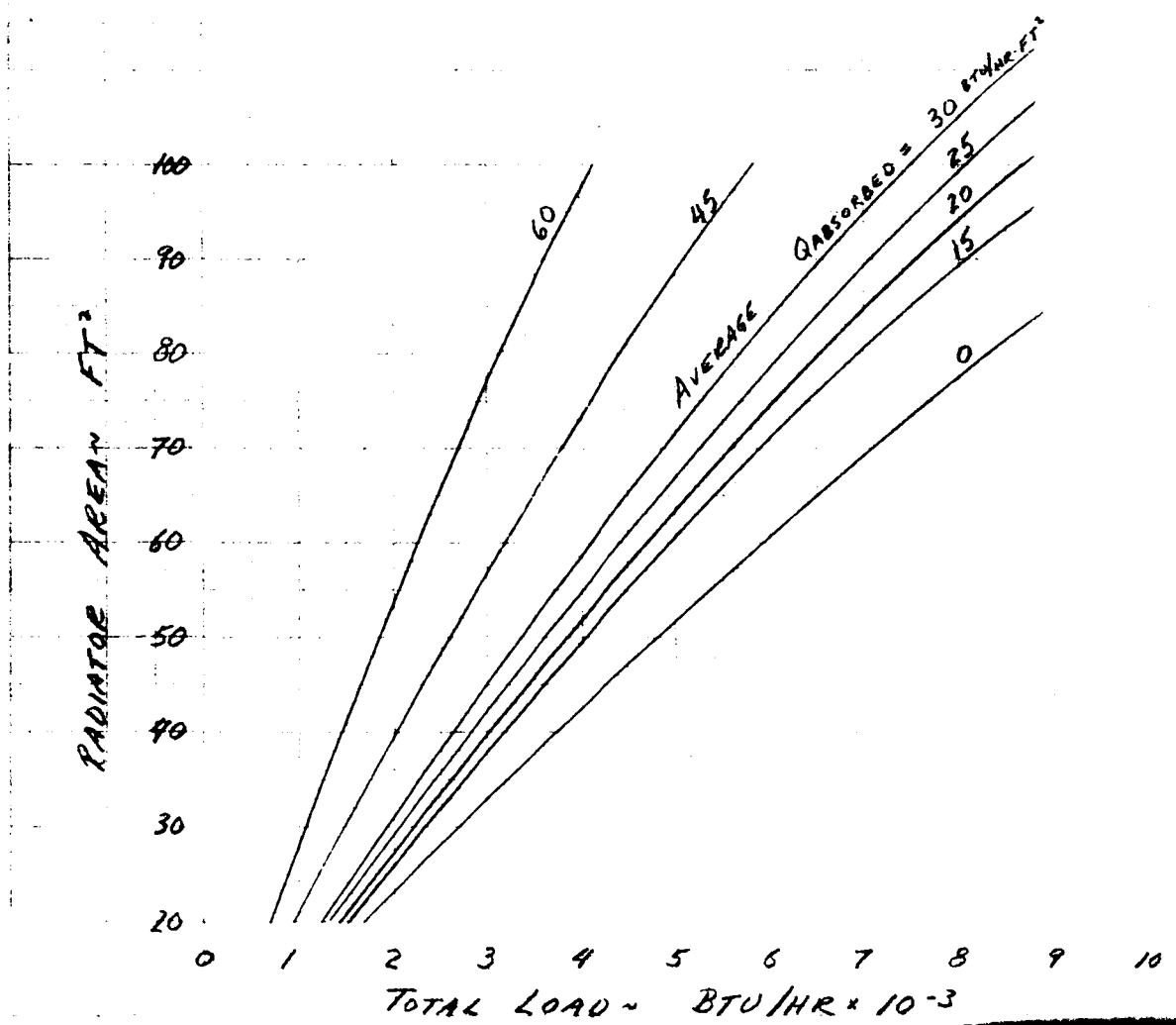

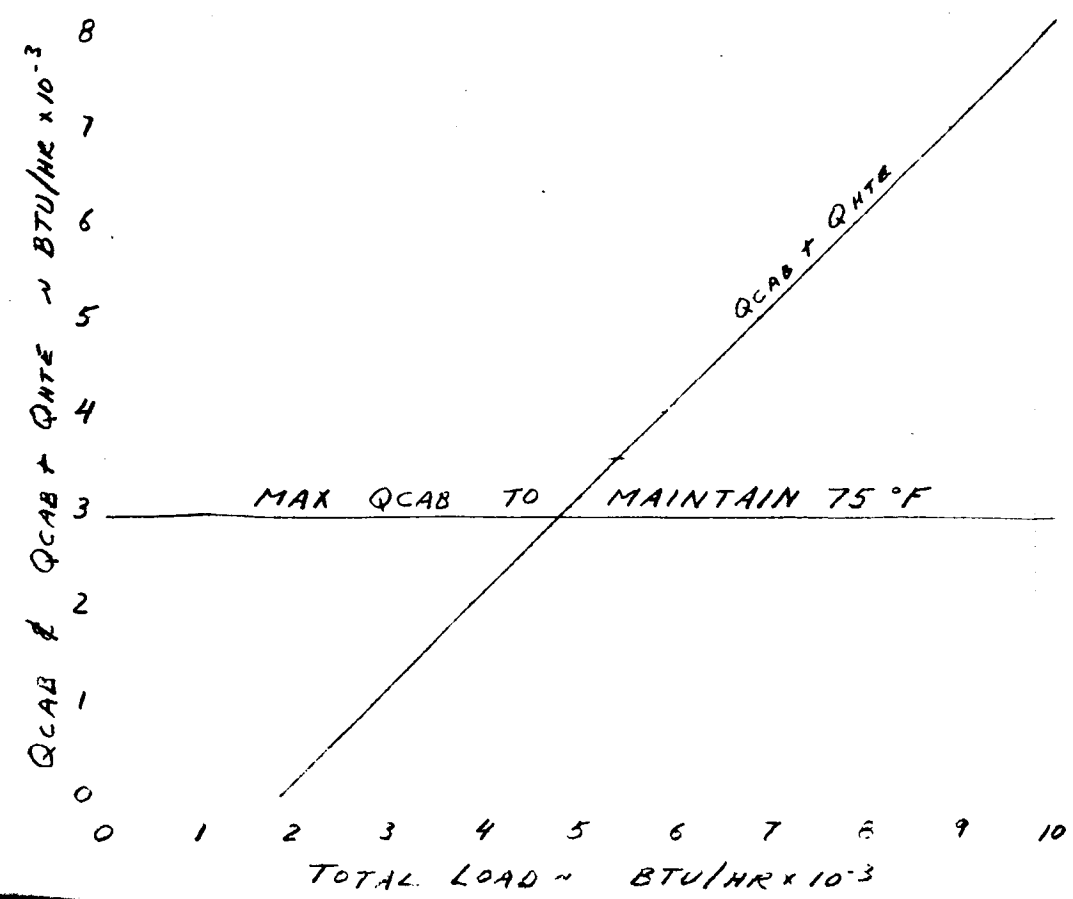

GAM
6-21-66

Figure C.4-1

[redacted]

[redacted]

FIGURE C.5-1
INFLATION SYSTEM HELIUM REQUIREMENT

- d = SPOKE/TORUS TUBE DIAMETER
- SKIN STRESS = 5000 PSI
- SKIN THICKNESS = .001 in
- INNER TORUS DIAMETER = 60 FT

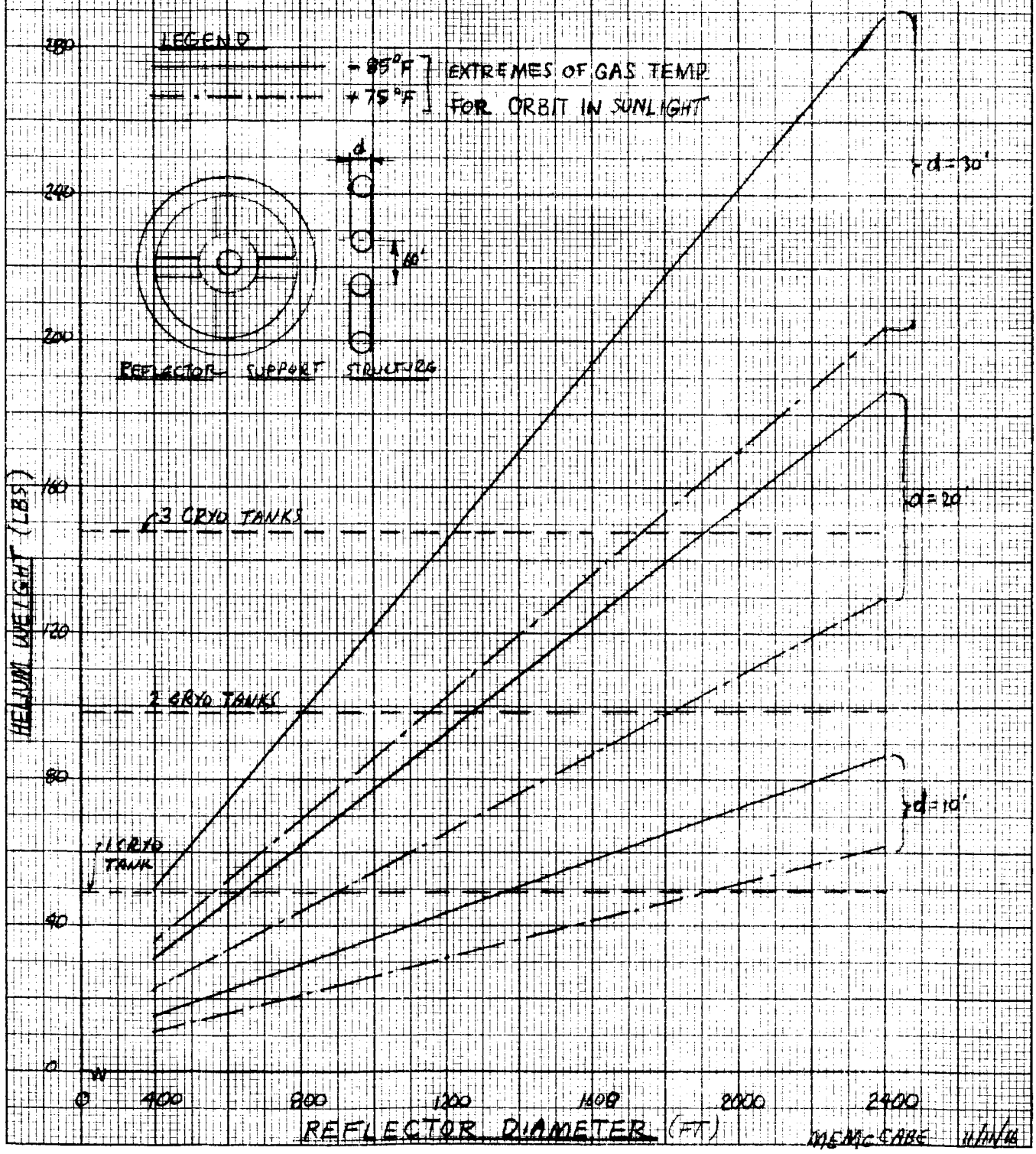

[redacted]

[redacted]

Figure C.5-2

CONFIGURATION A

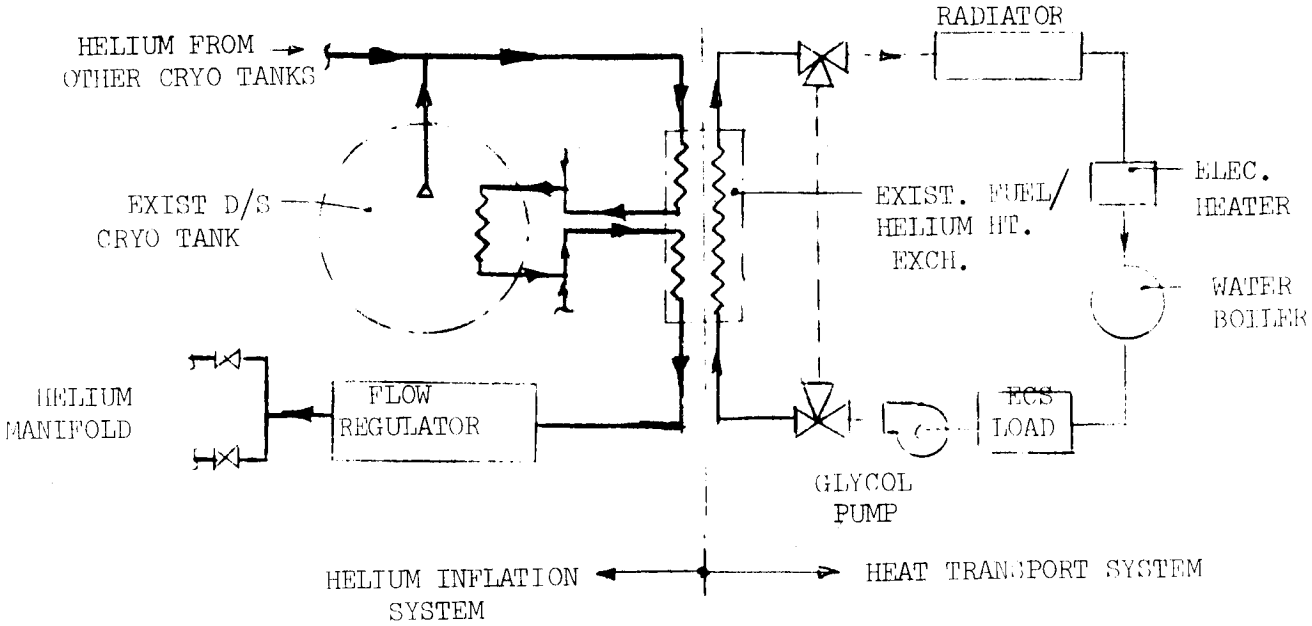

CONFIGURATION B

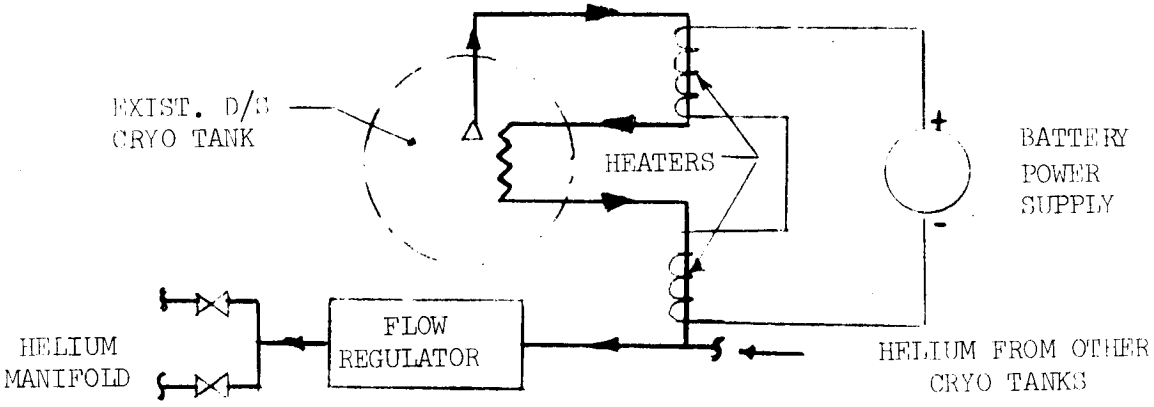

CONFIGURATIONS C & D

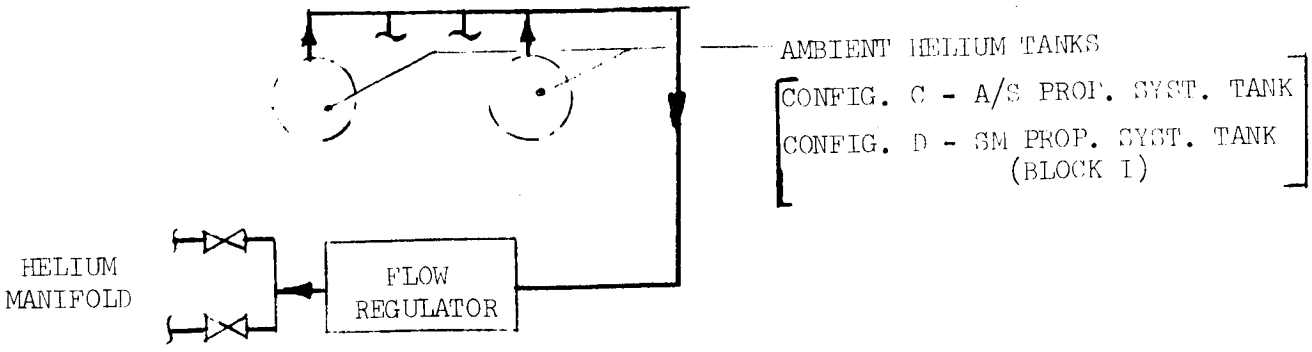

[redacted]

[redacted]

Figure C 5-3

CONFIGURATION WEIGHT COMPARISON

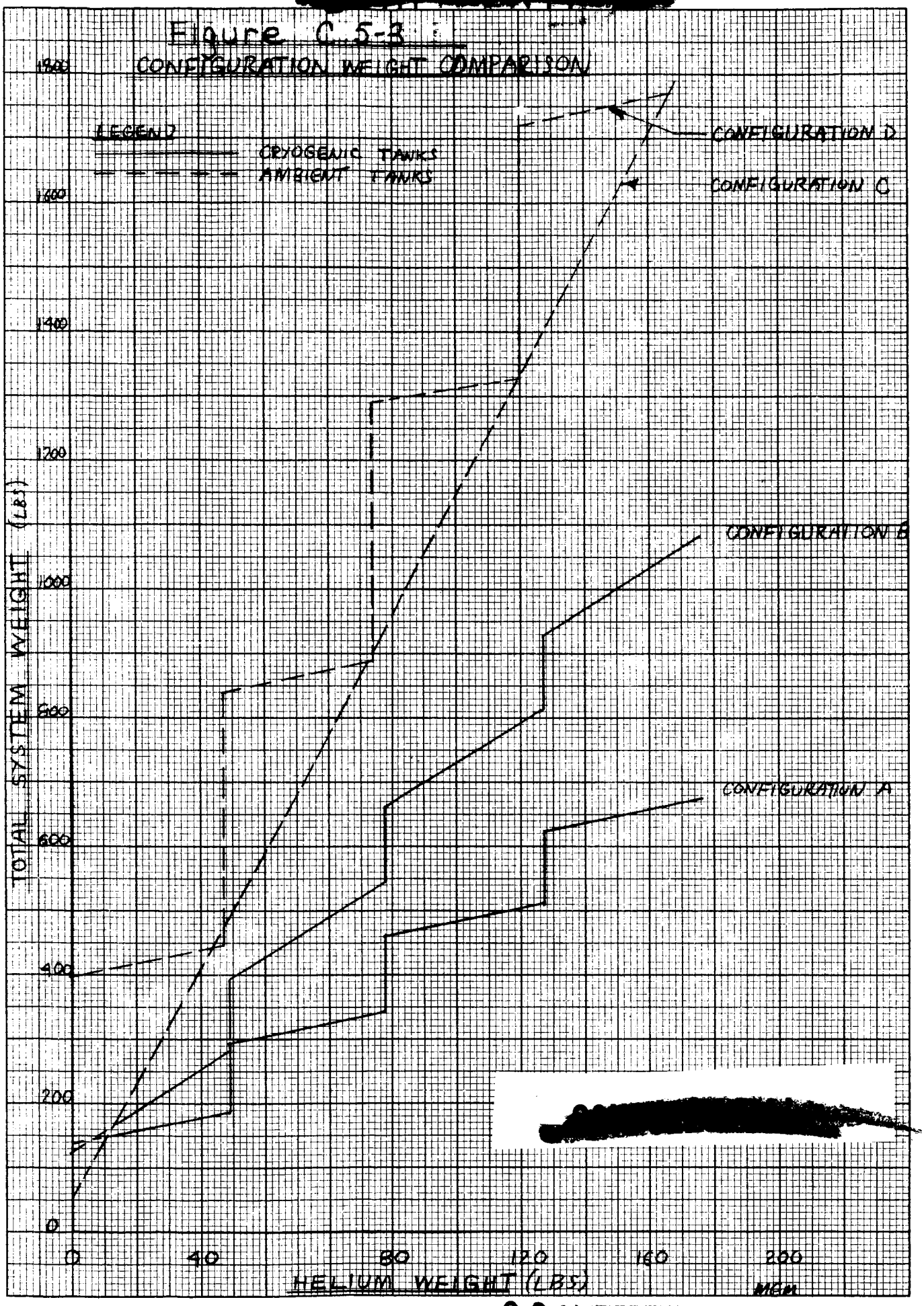

[redacted]

[redacted]

[redacted]

Figure C.5-4

- VOLUME = 1,800,000 FT³
- MINIMUM SKIN STRESS = 5000 psi
- TORUS/SPOKE CONFIGURATION

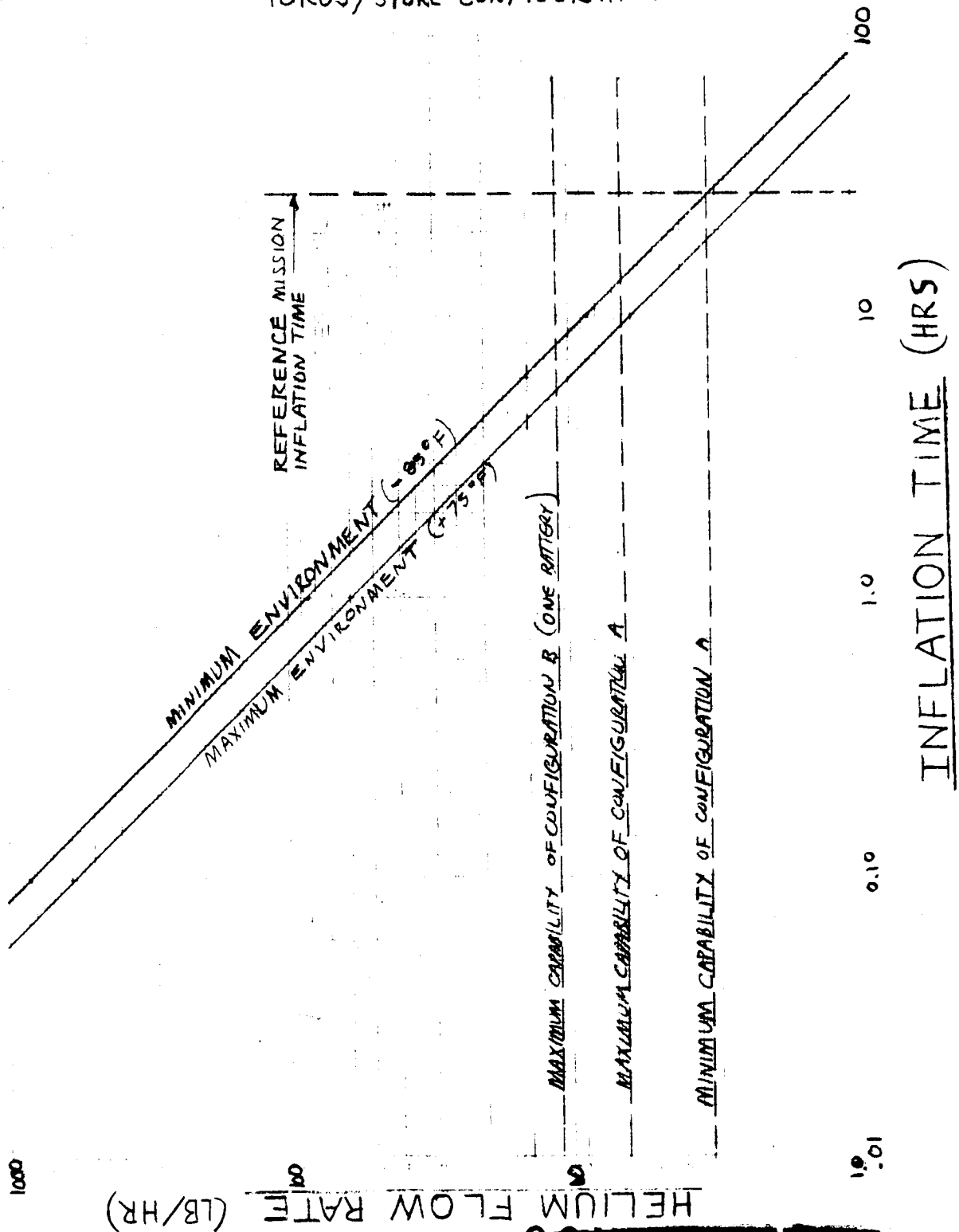

[redacted]